# Regional-to-local scale air quality modelling of the Republic of Ireland

# **Final report**

Distribution: FOR PUBLICATION

Circulation: Environmental Protection Agency (EPA, Ireland), UK

Centre for Ecology and Hydrology (UKCEH)

Project Title: Regional-to-local scale air quality modelling of the

Republic of Ireland

Report prepared for: Environmental Protection Agency (Ireland)

Report Status: Final

Report Reference: FM1297/T5.3

CERC Job Number: FM1297

Issue Version (Date): 1 (06/12/2022)

2 (05/05/2023) 3 (10/07/2023) 4 (19/12/2023)

Authors: Jenny Stocker, Kate Johnson, Christina Hood, Brian

Bien, Victoria Hamilton, Charlotte Aves, Rose Jackson

Reviewers: Kevin Delaney, Patrick Malone, Dermot Burke (EPA),

Massimo Vieno (UKCEH)

Cambridge Environmental Research Consultants (CERC)

Web: cerc.co.uk. Email: enquiries@cerc.co.uk. Tel: +44 (0)1223 357773.

Post: CERC, 3 Kings Parade, Cambridge, CB2 1SJ, UK.

This report is copyright © Cambridge Environmental Research Consultants Ltd.

### Contents

1	Executive summary	4
2	Introduction	6
3	Air quality standards	7
4	Air quality monitoring	8
	4.1 Automatic monitors	8
	4.2 Diffusion tubes	10
	4.3 Monitored exceedances of air quality limit and tar	rget values 10
5	Emissions Inventory	13
	5.1 MapEIre gridded emissions	13
	5.2 International emissions	14
	5.3 Road traffic emissions	15
	5.4 Temporal variability of emissions	18
	5.5 Spatial distribution of emissions	20
	5.6 Industrial emissions	23
	5.7 Detailed city modelling	25
6	Model descriptions & configuration	27
	6.1 Meteorological model	27
	6.2 Regional air quality model	28
	6.3 Street-scale air quality model	30
	6.4 Coupled system outputs	35
7	Meteorological modelling results	37
8	Model evaluation	40
	8.1 Model verification	40
	8.2 FAIRMODE metrics	54
	8.3 Temporal variations	59
	8.4 Proportions of regional and local pollution	63
	8.5 Sensitivity testing	65
9	Pollution maps	68
10	Discussion	80
11	References	83
App	ppendix A Diffusion tube location revisions	87
Арр	ppendix B FAIRMODE Model Performance Metrics	89

Appendix C Meteorological model evaluation	90
Appendix D Background monitor locations	93
Appendix E Supplementary model pollution maps	96
Appendix F Supplementary city model pollution maps	114



#### 1 Executive summary

#### Overview

- 1.1 Regional-to-local (street) scale air pollutant concentration modelling for Ireland has been undertaken for 2018 and 2019.
- 1.2 Modelled concentrations were compared to measurements. In general, model performance is good for both years at all site types (rural, background and traffic).
- 1.3 Predicted annual average and short-term concentrations of nitrogen dioxide (NO<sub>2</sub>), particulates with diameter less than 10  $\mu$ m (PM<sub>10</sub>), particulates with diameter less than 2.5  $\mu$ m (PM<sub>2.5</sub>) and ozone (O<sub>3</sub>) were compared to health-related Air Quality Standards Regulations 2011 (AQSR) thresholds.
- 1.4 Predicted exceedances of AQSR thresholds are generally associated with the major road network.

#### Modelling approach

- 1.5 Regional meteorological and chemical transport modelling for Ireland at 1 km × 1 km horizontal grid resolution and hourly temporal resolution was undertaken using the WRF meteorological model and the EMEP chemical transport model.
- 1.6 A Coupled system was used to link EMEP concentration outputs with local scale ADMS-Urban modelling of road traffic emissions and dispersion, avoiding double-counting local emissions. The system generated hourly concentrations at high spatial resolution (few metres) throughout Ireland. Strong pollutant concentration gradients that occur in the vicinity of heavily trafficked roads are resolved using this modelling approach.
- 1.7 Gridded emissions data from MapEIre were used as input to both EMEP and ADMS-Urban for all non-road traffic sectors.
- 1.8 Major and minor road traffic emissions were calculated using National Transport Authority traffic data and Five Cities Demand Management Study fleet information. Adjustments were applied to published NO<sub>X</sub> emissions factors to better represent realworld emissions.
- 1.9 A major industrial source emissions inventory was collated. These sources were modelled at coarse resolution in EMEP rather than explicitly within ADMS-Urban due to industrial source sector geometry simplifications in the regional model.
- 1.10 3D buildings datasets were generated for the five main cities: Dublin, Cork, Limerick, Galway and Waterford. The datasets were processed to derive street canyon and urban canopy parameters which: describe the urban morphology; and allow modelling of near-road air flow and pollutant dispersion in urban areas.
- 1.11 Detailed evaluation of modelled NO<sub>2</sub>, PM<sub>2.5</sub>, PM<sub>10</sub> and O<sub>3</sub> concentrations was carried out by comparison with measurements. The sensitivity of model outputs to model input parameters was tested.

#### Study outcomes

- 1.12 Street-scale modelling is necessary to identify areas of increased pollutant concentrations associated with the major road network.
- 1.13 The regional-to-local Coupled system configuration for Ireland meets the FAIRMODE model quality metrics for both annual average and short-term concentrations of NO<sub>2</sub>, PM<sub>2.5</sub>, PM<sub>10</sub> and O<sub>3</sub> for 2018 and 2019.

Page 4 of 132

CERC/FM1297

1.14 The Coupled system has adequate accuracy to assess compliance with AQSR thresholds. The evaluation suggests that there is some under-prediction by the system in terms of prediction of NO<sub>2</sub> concentrations at background locations in the less polluted urban areas.

#### **Data challenges**

- 1.15 Data capture was poor for some continuous monitoring sites, leading to no valid rural PM<sub>2.5</sub> concentration measurement availability in 2019. A data capture threshold of 50% was applied to continuous monitoring sites for inclusion in the evaluation.
- 1.16 Data capture from NO<sub>2</sub> diffusion tubes was also low, with some sites having as little as two months of data available.
- 1.17 Traffic models generate traffic flow data on simplified node-to-node geometries, whereas detailed real-world road locations are required for street-scale dispersion modelling. The process of assigning traffic flows to real-world geometries is time consuming.
- 1.18 Defining detailed and accurate street canyon properties across the full national major road network is challenging due to the large number of building footprints which require processing. Simplified approaches can be taken but may not capture individual site properties fully.
- 1.19 Industrial source data was supplied by the EPA but not used in the Coupled system due to challenges in matching initial emission height and dispersion between the regional and local models.

#### **Future directions**

- 1.20 The Coupled system could be used to investigate the effect of proposed regional and/or local emissions policy measures on ambient concentrations. The system is particularly suited for this application as it does not use measured concentration data for calibration.
- 1.21 The high-resolution mapped concentrations from the Coupled system could be used to calculate areas of exceedance of AQSR thresholds excluding road carriageways.
- 1.22 Additional data processing could be carried out to improve modelling of smaller urban areas by including buildings effects.
- 1.23 Suitable approaches for explicit modelling of industrial sources in the Coupled system require further investigation.

Page 5 of 132 CERC/FM1297



#### 2 Introduction

The Environmental Protection Agency (EPA) in Ireland commissioned Cambridge Environmental Research Consultants Ltd (CERC) to carry out regional-to-local scale air quality modelling of Ireland. The work builds on the Dublin air quality assessment completed by CERC in 2019. The UK Centre for Ecology and Hydrology have been sub-contracted by CERC to undertake the regional modelling aspects of the current study.

A state-of-the-art air quality modelling system has been used for this study, comprising the coupling of regional scale concentration modelling using the EMEP model [1], [2] and street-scale pollutant variations represented by the ADMS-Urban model [3], [4]. The result is a system that accounts for meteorological, chemical and dispersion processes at all the relevant spatial and temporal scales.

This exercise delivers baseline 2018 and 2019 air quality maps for Ireland for the health-related pollutants and metrics specified in the Irish Air Quality Standards Regulations (AQSR) [5]. Part of the motivation for this project is to provide evidence of the suitability of such a system for the assessment of Ireland's compliance with the EU Air Quality Directives [6] and other air quality guidelines such as those from the World Health Organisation [7].

This report describes the modelling system input data and assumptions, and presents the results of the modelling including evaluation against measured air pollutant concentrations and comparison against AQSR limit, target and objective values.

Section 3 summarises the Irish AQSR threshold values. The air quality monitoring data available for model evaluation are described in Section 4. Details of the emissions inventory used in the modelling are provided in Section 5. Model descriptions and configurations are described in Section 6 separately for the meteorological model, the regional air quality model and the street-scale air quality model; this section also summarises the outputs available from the Coupled system. Meteorological modelling results are presented in Section 7. Section 8 describes model evaluation of both the regional model and the Coupled system, and Section 9 presents example pollution maps. Project outcomes are discussed in Section 10 and references provided in Section 11. Supplementary information is provided in five appendices, specifically: additional information on diffusion tube locations (Appendix A); Forum for Air Quality Modelling (FAIRMODE) metric definitions (Appendix B); meteorological model evaluation (Appendix C); background monitor locations (Appendix D); additional regional (Appendix E) and city (Appendix F) pollution maps.

Page 6 of 132

#### 3 Air quality standards

The EU Ambient Air Quality and Cleaner Air for Europe (CAFE) Directive (2008/50/EC) [6] sets binding limits for concentrations of air pollutants, which take into account the effects of each pollutant on the health of those who are most sensitive to air quality. The Directive was transposed into Irish legislation by the Air Quality Standards Regulations 2011 [5]. The limit, target and values for nitrogen dioxide (NO<sub>2</sub>), particulate matter (PM<sub>2.5</sub> and PM<sub>10</sub>) and ozone (O<sub>3</sub>) are presented in Table 3.1. Note that the long-term objective for ozone has not been considered in this study.

**Table 3.1** – Air quality limits for NO<sub>2</sub>, PM<sub>2.5</sub>, PM<sub>10</sub> and O<sub>3</sub> as stated in the AQSR 2011 [5]; \*only one year considered.

Pollutant	Value (µg/m³)	Limit or target value?	Description						
NO <sub>2</sub>	200	Limit	Hourly mean not to be exceeded more than 18 times a calendar year (modelled as 99.79 <sup>th</sup> percentile)						
	40	Limit	Annual average						
DM	25	Limit	Stage 1: to be attained by 2015 Annual average						
PM <sub>2.5</sub>	20	Limit	Stage 2: to be attained by 2020 Annual average						
$PM_{10}$	50	Limit	24-hour mean not to be exceeded more than 35 times a calendar year (modelled as 90.41st percentile)						
	40	Limit	Annual average						
O <sub>3</sub>	120	Target	25 exceedances of the maximum daily running 8-hour mean within the year (modelled as 93.15 <sup>th</sup> percentile) averaged over 3 years*						

The short-term limits, i.e. those recorded hourly or over a 24 hour period, are specified in terms of the number of times during a year that a concentration recorded over a short period of time is permitted to exceed a specified value. For example, the concentration of  $NO_2$  measured as the average value recorded over a one-hour period is permitted to exceed the concentration of  $200~\mu g/m^3$  up to 18 times per year. Any additional exceedances during a one-year period would represent a breach of the limit.

It is convenient to model limits of this form in terms of the equivalent percentile concentration value. A percentile is the concentration below which lie a specified percentage of concentration measurements. For example, consider the  $98^{th}$  percentile of one-hour concentrations over a year. Taking all 8760 one-hour concentration values that occur in a year, the  $98^{th}$  percentile value is the concentration below which 98% of those concentrations lie. Or, in other words, it is the concentration exceeded by 2% (100-98) of those hours, that is, 175 hours per year. Taking the  $NO_2$  limit considered above, allowing 18 exceedances per year is equivalent to not exceeding for 8742 hours or for 99.79% of the year. This is therefore equivalent to the 99.79<sup>th</sup> percentile value.

It is important to note that modelling exceedances of short-term averages is generally less accurate than modelling annual averages.



#### 4 Air quality monitoring

The EPA measures air pollutant concentrations throughout Ireland. This section summarises the available measured air quality data used for model evaluation.

#### 4.1 Automatic monitors

The automatic monitors that are part of the National Ambient Air Quality Network [8] record hourly and daily pollutant concentrations. Table 4.1 summarises Irish automatic monitoring sites which record at least one of NO<sub>2</sub>, NO<sub>X</sub>, PM<sub>2.5</sub>, PM<sub>10</sub> and O<sub>3</sub> during 2018 and 2019. Only sites and pollutants where at least 50% of measurement periods (hourly or daily) have valid data have been included in the model evaluation. The table provides monitor names and locations, in addition to a site classification: rural, background or traffic, where traffic indicates locations near a road. Monitor inlet height information is also given; a height of 2.5 m has been assumed where this information has not been specified by the EPA. Monitor locations are shown in Figure 4.1. Information on real time air quality can be accessed at <a href="https://www.airquality.ie">www.airquality.ie</a>.

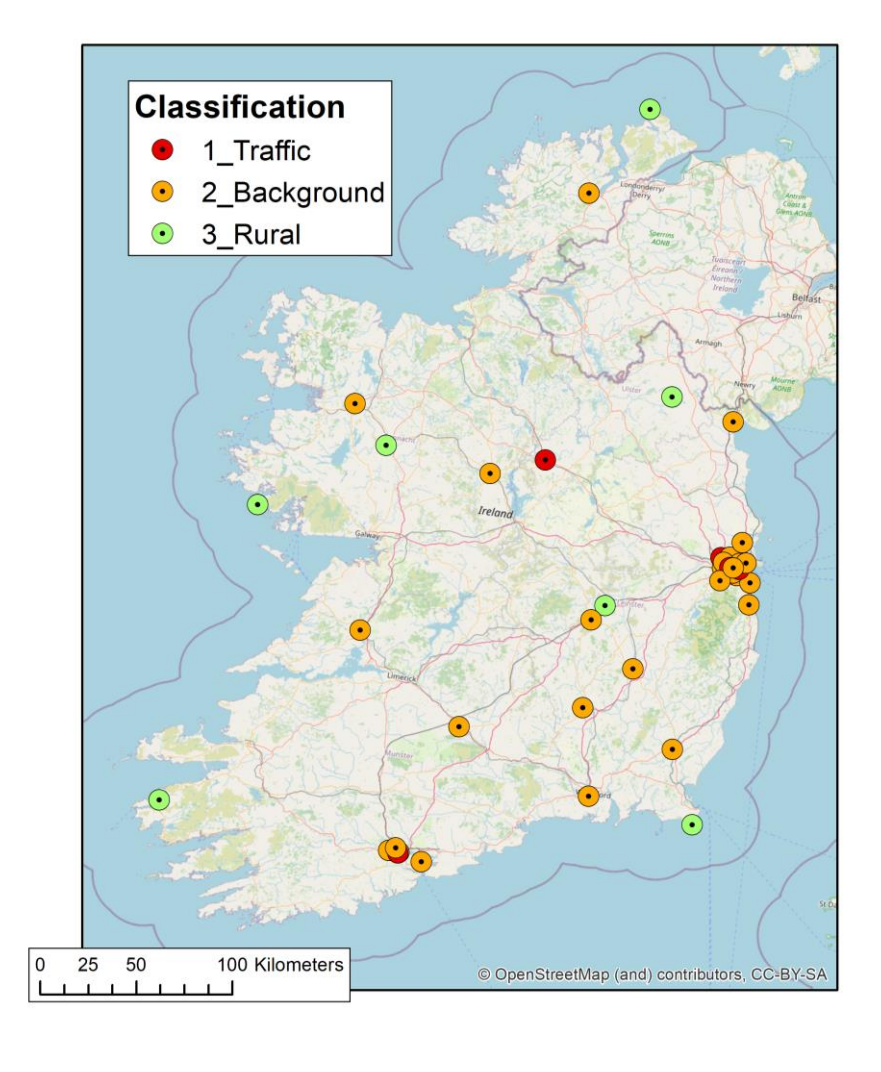


**Figure 4.1** – National Ambient Air Quality Network [8] continuous monitors locations, classified according to site type: rural, background or traffic. This includes all continuous monitors with valid data available for 2018 and/or 2019. Background map; © OpenStreetMap contributors <a href="https://www.openstreetmap.org/copyright">www.openstreetmap.org/copyright</a>.

 $\begin{tabular}{ll} \textbf{Table 4.1} - Continuous monitor summary: locations, type, inlet heights and pollutant measured; \\ & $^{$$$}$brackets indicate poor data capture ($< 50\% threshold used for model evaluation). \\ \end{tabular}$ 

							Pollut						
			m) ght	(	H in	dicate		rly a	nd D				')
	ou	4)	nt ( heiy alid			2018		ı		•	2019		
A	Location		Inlet height (m) (assumed height given in italics)	$NO_2$	$NO_{\rm X}$	${ m PM}_{10}$	PM <sub>2.5</sub>	$O_3$	$NO_2$	NOx	$PM_{10}$	PM <sub>2.5</sub>	$O_3$
Ballyfermot	Dublin	Background	2.5	Н	Н	D	(D)		Н	Н	D	D	
Bishopstown MTU	Cork	Background	2.5					(H)			D		Н
Blanchardstown	Dublin	Traffic	2.5	Н	Н	D			Н	Н	D		
Bray	Wicklow	Background	2.5				D	Н				D	Н
Brownes Road	Waterford	Background	2			(D)	(D)		Н	Н	D	D	
Carlow Town	Carlow	Background	3			(D)	(D)				D	D	
Carnsore	Wexford	Rural	2.5					(H)					Н
Castlebar	Mayo	Background	2.5	Н	Н	D		Н	Н	Н	D		Н
Claremorris	Mayo	Rural	2.3			D	D				D	(D)	
Clonskeagh	Dublin	Background	3.5					Н					Н
Cobh	Cork	Background	2.5			(D)	(D)				D	D	
Davitt Road	Dublin	Traffic	2.5	(H)	(H)	(D)	(D)		Н	Н	D	D	
Dun Laoghaire	Dublin	Background	2.5	Н	Н	D			Н	Н	(D)	(D)	
Dundalk	Louth	Background	2.5	Н	Н	D			Н	Н	D		
Emo	Laois	Rural	2.5	Н	Н			Н	Н	Н			Н
Ennis	Clare	Background	3			D	D				D	(D)	
Enniscorthy	Wexford	Background	2.5				(D)				D	D	
Finglas	Dublin	Background	5.5			(D)	D				D	D	
Heatherton Park	Cork	Background	1.5			D	D				D	D	
Kilkitt	Monaghan	Rural	3	Н	Н	D		Н	Н	Н	D		Н
Letterkenny	Donegal	Background	2.5								D	D	
Longford Town	Longford	Traffic	3				D					D	
Mace Head	Galway	Rural	2.5					Н					Н
Malin Head	Donegal	Rural	3					(H)					Н
Marino	Dublin	Background	2.5			(D)	D				D	D	
Phoenix Park	Dublin	Background	2.5			D	(D)				D	D	
Portlaoise	Laois	Background	3	Н	Н	D			Н	Н	(D)		
Rathmines	Dublin	Background	3.5	Н	Н	D	D	Н	Н	Н	D	D	Н
Ringsend	Dublin	Traffic	2.5	Н	Н	D	D		Н	Н	D	D	Н
Roscommon Town	Roscommon	Background	3			(D)	(D)				D	D	
Seville Lodge	Kilkenny	Background	2.5	Н	Н	(D)		Н	Н	Н	D		Н
South Link Road	Cork	Traffic	3.5	Н	Н	D		Н	Н		D		Н
St Annes Park	Dublin	Background	2.5			(D)	(D)				D	D	
St Johns Road	Dublin	Traffic	2	(H)	(H)	(D)	(D)		Н	Н	D	D	
Swords	Dublin	Background	2.5	Н	Н			Н	Н	Н			Н
Tallaght	Dublin	Background	2.5			D					D		
Tipperary Town	Tipperary	Background	2.5								D	D	
UCD Distillery Fields	Cork	Background	2.5	Н	Н		D	Н	Н			D	Н
Valentia	Kerry	Rural	5					Н					Н
Winetavern Street	Dublin	Background	2.5	Н	Η	D			Н	Н	D		



#### 4.2 Diffusion tubes

The EPA, in collaboration with city authorities, have deployed networks of NO<sub>2</sub> diffusion tubes within the five main cities: Dublin, Waterford, Limerick, Cork and Galway. Figure 4.2 a) to e) shows spatial deployment of diffusion tubes. All diffusion tube heights are assumed to be 2.3 m. Diffusion tube measurements were not taken for the full year; the number of months for which data was available ranged from 2 to 12. The EPA have provided monthly diffusion tube measurements for Dublin for 2018 and 2019; monthly diffusion tube data for the other four cities was only provided for 2019. Average monthly comparisons are presented in the evaluation (Section 8.1.1) but annualised<sup>1</sup> concentrations have been used to indicate measured exceedances (Table 4.2); both approaches include appropriate bias adjustment factors.

The Dublin diffusion tube network had different site locations in 2018 and 2019. Revised diffusion tube locations were provided for the Waterford and Cork networks during the project. Some additional revision of supplied diffusion tube locations was undertaken by the project team in order to ensure the monitors were located within street canyons where appropriate; details are provided in Appendix A.

#### 4.3 Monitored exceedances of air quality limit and target values

Table 4.2 presents a summary of the measured exceedances of the air quality limit values for 2018 and 2019. The quantity of diffusion tubes deployed in each city is also given. Note that this study has used a data capture threshold of 50% as a criterion for including monitors, whereas the EPA use a stricter threshold of 90%<sup>2</sup>. In summary:

#### • NO<sub>2</sub>

In Dublin there is one continuous monitor exceedance of the annual average limit value in 2019, as well as many diffusion tube exceedances in 2018 and 2019; there are also diffusion tube exceedances in Cork, but none in any of the other cities. None of the continuous monitors indicate an exceedance of the hourly limit value, although some hourly concentrations are recorded to be higher than the threshold (200  $\mu$ g/m³).

#### PM2.5

There are no monitored exceedances of the annual average AQSR PM<sub>2.5</sub> limit values.

#### • PM<sub>10</sub>

There are no monitored exceedances of the annual average AQSR  $PM_{10}$  limit values. None of the continuous monitors indicate an exceedance of the daily limit value although some daily concentrations are recorded to be higher than the threshold (50  $\mu$ g/m³).

#### • O<sub>3</sub>

There are some measured exceedances of the  $O_3$  target value in Galway and other more rural parts of the country. In addition, there are some maximum daily 8-hour rolling concentrations recorded to be higher than the threshold (120  $\mu g/m^3$ ) in Dublin and Cork.

.

<sup>&</sup>lt;sup>1</sup> Annualisation was performed by the EPA

<sup>&</sup>lt;sup>2</sup>https://www.epa.ie/publications/monitoring--assessment/air/Summary-data-tables-2018.pdf https://www.epa.ie/publications/monitoring--assessment/air/Summary-Data-Tables--2019.pdf

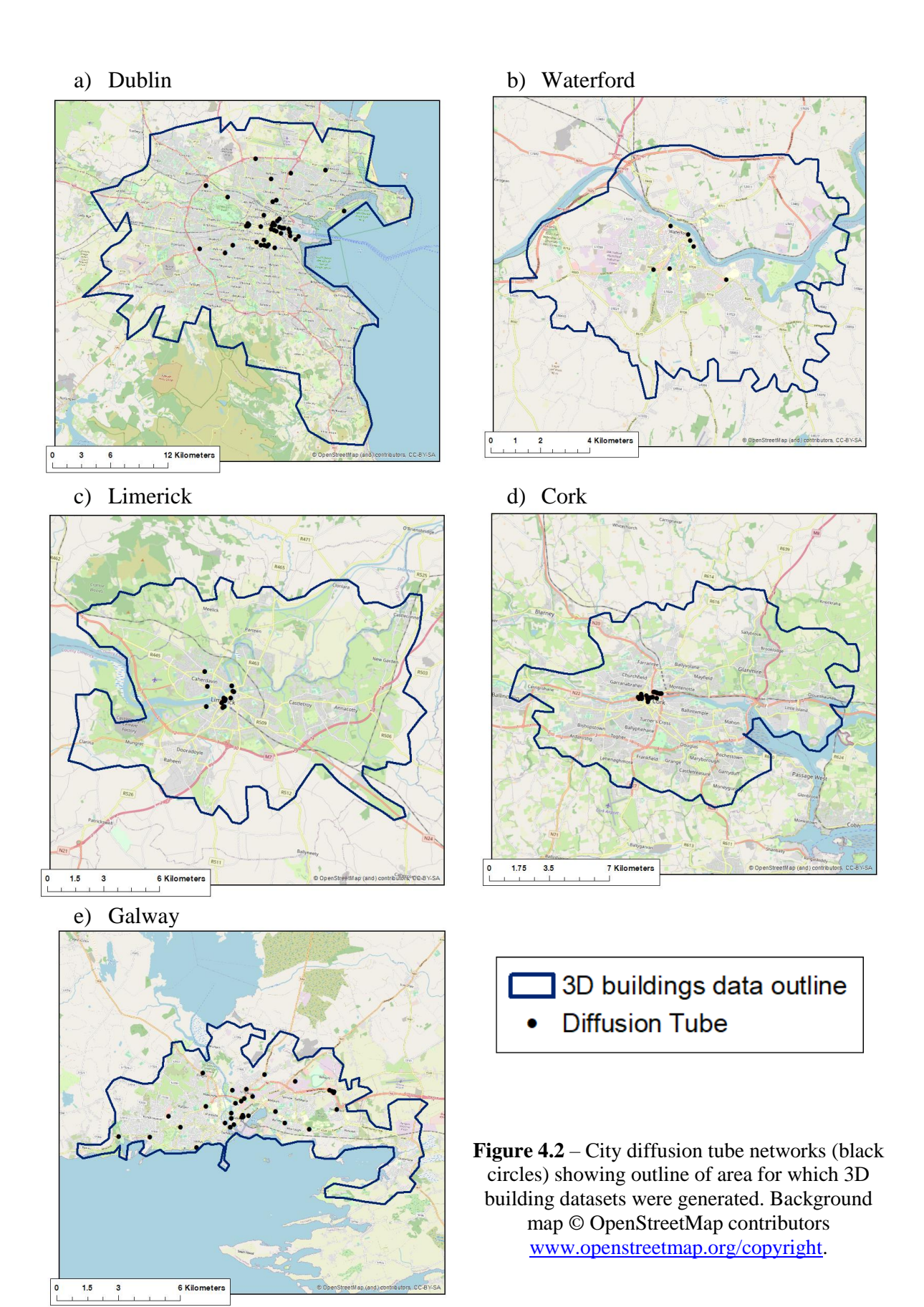


**Table 4.2** – Summary of the quantity of continuous monitors (CM) and measured air quality limit value exceedances for all pollutants and NO<sub>2</sub> diffusion tube (DT) quantity and annual exceedances, all diffusion tubes located at 2.3 m above ground; numbers in brackets indicate the quantity of monitors with at least one threshold exceedance.

										Pollutai	nt						
					NO <sub>2</sub>				PN	$I_{2.5}$			PN	$I_{10}$		(	<b>)</b> <sub>3</sub>
Location		Annual average (40 μg/m³)				> 18 hourly exceedances of 200 µg/m³		Annual average (25 μg/m³)		Annual average (20 μg/m³)			average g/m³)	> 35 daily exceedances of 50 µg/m³		> 25 maximum daily 8-hour rolling exceedances of 120 µg/m <sup>3</sup>	
		2018		2018		2018	2019	2018	2019	2018	2019	2018	2019	2018	2019	2018	2019
		$_{\rm CM}$	DT	CM	DT	20	20	20	20	20	20	20	20	20	20	20	50
Dublin	No. of monitors	7	26	9	21	9	9	9	9	9	9	8	8	8	8	3	3
	Exceed.	0	13	1	9	0(1)	0	0	0	0	0	0	0	0 (4)	0(8)	0(2)	0(3)
Waterford	No. of monitors	0	7	1	7	0	1	1	0	1	0	0	0	0	0	0	0
	Exceed.	0	0	0	0	0	0	0	0	0	0	0	0	0	0	0	0
Limerick	No. of monitors	0	14	0	14	0	0	0	0	0	0	0	0	0	0	0	0
	Exceed.	0	0	0	0	0	0	0	0	0	0	0	0	0	0	0	0
Cork	No. of monitors	2	19	0	19	2	0	3	3	3	3	1	1	1	1	3	3
	Exceed.	0	4	0	3	0	0	0	0	0	0	0	0	0	0(1)	0(3)	2 (3)
Galway	No. of monitors	0	26	0	19	0	0	0	0	0	0	0	0	0	0	1	1
	Exceed.	0	0	0	0	0	0	0	0	0	0	0	0	0	0	1	0(1)
Other	No. of monitors	6	0	6	0	6	6	7	7	7	7	6	6	6	6	8	8
	Exceed.	0	0	0	0	0(2)	0	0	0	0	0	0	0	0(2)	0 (4)	2 (6)	3 (6)

Page 12 of 132 CERC/FM1297



#### 5 Emissions Inventory

The emissions inventory is a key input for the modelling. The regional air quality model requires estimates of emissions from Ireland, the UK and mainland Europe, and the local model requires road traffic and industrial<sup>3</sup> emissions data.

Irish emissions data are broadly categorised according to gridded and explicit emissions, where the gridded data are primarily derived from the MapEIre project deliverables [9] and explicit road and industrial source datasets have been provided by the EPA, the Irish National Transport Authority (NTA) and Dublin City Council. Derivation of road traffic emission rates from activity data (flows and speeds) combined with fleet composition information and emissions factors have replaced the MapEIre traffic emissions estimates, whereas emissions from all other sectors within Ireland are taken from the MapEIre dataset.

UK emissions data for the EMEP model are derived from the UK National Atmospheric Emissions Inventory (NAEI) [10] and mainland European emissions are from the European Monitoring and Evaluation Programme (EMEP) inventory [11].

Section 5.1 describes the MapEIre emissions dataset used for non-road gridded emissions within Ireland. Section 5.2 summarises the regional emissions used outside Ireland. Detailed road traffic emissions calculations are described in Section 5.3. The temporal variation profiles applied to annual emissions totals to obtain hourly emissions are presented in Section 5.4. The distribution of 2D gridded emissions into 3D for modelling is described in Section 5.5. Information about industrial emissions is given in Section 5.6

#### 5.1 MapElre gridded emissions

The MapEIre project developed a detailed emissions model for Ireland. Inventories for 2015, 2016 and 2019 have been collated, with the most recent year used for the current study. The emissions cover Ireland at 1 km<sup>2</sup> resolution using the TM65 Irish Grid coordinate system, with 138 NFR (Nomenclature For Reporting) source sectors and 32 pollutants. The 138 NFR sectors have been assigned to 16 aggregated GNFR (Gridded Nomenclature for Reporting) sectors with associated labels A to P (first two columns, Table 5.1).

The MapEIre gridded emissions are used as input to EMEP, which, for this application, was run at 1 km² resolution. However, EMEP requires SNAP (Selected Nomenclature for Air Pollution) sectors, so it was necessary to assign the GNFR emissions to SNAP sectors; the relationship assumed between the two emissions reporting categorisations is shown in Table 5.1. The coordinate system used by EMEP is a polar stereographic projection⁴, and therefore it was also necessary to re-grid the MapEIre data into this coordinate system. One consequence of converting datasets between grids in different coordinate systems at similar spatial resolutions is that the resultant dataset will undergo spatial smoothing, with fewer extreme values compared to the original dataset.

-

<sup>&</sup>lt;sup>3</sup> Industrial emissions were collated for use in the study, but were not modelled explicitly due to discrepancies between the vertical distribution of emissions assumed in the EMEP configuration and real-world industrial source release heights. Further details are provided in Section 5.6.

<sup>&</sup>lt;sup>4</sup> https://www.emep.int/grid/projinterpol.pdf

**Table 5.1** – Relationship between GNFR and SNAP sector definitions (presented in order of SNAP 1 to 11); note that the GNFR 'B\_Industry' classification does not allow for separation between SNAP 3 and SNAP 4, hence all 'B\_industry' emissions were allocated to SNAP 3 because: SNAP 3 was found to be dominant in the UK NAEI; and identical properties are routinely assigned to SNAP 3 and 4.

GN		SNAP						
	pEIre category)		IEP category)					
ID	Sector	ID	Sector					
Α	Public power	1	Combustion in energy production and transformation					
C	Other stationary combustion	2	Combustion in commercial, institutional, residential and agriculture					
В	Industry	3	Combustion in industry					
-	-	4	Production Processes					
D	Fugitive	5	Extraction and distribution of fossil fuels					
Е	Solvents	6	Solvent use					
F	Road transport	7	Road transport					
G	Shipping (domestic and international)	8	Other transport and mobile machinery					
H	Aviation (domestic and international) Off road transport	0	Other transport and mobile machinery					
J	Waste	9	Waste treatment and disposal					
K	Agriculture (livestock)		wase treatment and disposar					
L	Agriculture (other)	10	Agriculture, forestry and land use change					
Q	Land use change and forestry							
N	Natural	11	Nature					
О	Aviation cruise	-	Emissions from the cruise phase of flights. These emissions are allocated evenly over the Irish grid and do not represent release location. They are assumed to be released at heights which do not directly affect near-ground air quality.					
P	International shipping	-	International shipping emissions allocated to Ireland. The EMEP model uses a different dataset for international shipping emissions.					

#### 5.2 International emissions

UK emissions data for the EMEP model are derived from the UK National Atmospheric Emissions Inventory (NAEI) [10], re-gridded to the model grid. Mainland European emissions for the outer model domain are obtained from the European Monitoring and Evaluation Programme (EMEP) inventory [11].

UK NAEI data was also used for domestic and international shipping in a 10 km buffer over sea, with EMEP Centre on Emission Inventories and Projections (CEIP) emissions for remaining international shipping emissions. There is uncertainty over whether this dataset incorporates domestic shipping emissions for all countries. MapEIre shipping emissions were used around the Irish coastline for areas outside the NAEI extent.



#### 5.3 Road traffic emissions

Two sources of traffic data have been used for this project, referred to in the following descriptions as the NTA dataset (Section 5.3.1) and the Prime 2 dataset (Section 5.3.2). These datasets were processed to generate major and minor road traffic emissions datasets (Sections 5.3.3 and 5.3.4, respectively). Figure 5.1 provides a flow chart indicating the required data processing steps.

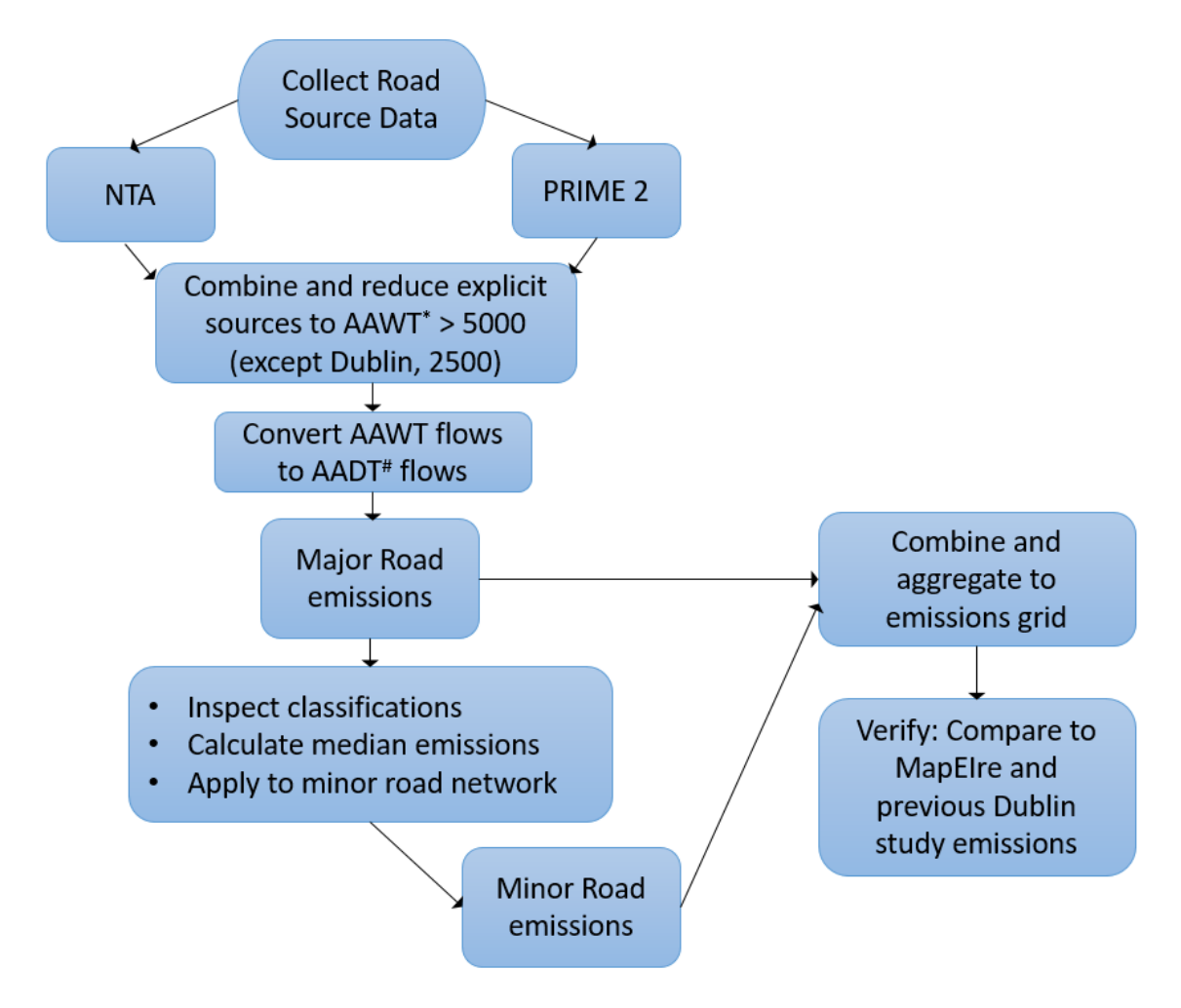


**Figure 5.1** – Road source emissions processing steps; \*Annual Average Weekday Traffic (AAWT), \*Annual Average Daily Traffic (AADT).

#### 5.3.1. National Transport Authority dataset

The NTA provided traffic data from their strategic transport planning tool - Regional Modelling System. This model generates multiple traffic parameters associated with each road included in the network, for example flows split by periods (AM peak, PM peak and inter-peak), and congestion data. Roads within the network were assigned into five geographical regions. Table 5.2 summarises the regions in terms of: the region name and associated acronym; the largest city included within the region; and the region extent.

When initially supplied for use in this air quality modelling study, the data for each region was provided with straight line node-to-node link geometries. However, in order to accurately map air pollutant concentrations at street-scale resolution, it was necessary to assign the road traffic emissions to accurate source locations. Traffic model outputs were then mapped to Prime 2



road network dataset records (refer to Section 5.3.2). Traffic information was consolidated to include Annual Average Weekday Totals (AAWTs), split by vehicle type. Average speed data was also included.

**Table 5.2** – Summary of the NTA Regional Modelling System model regions.

Region		City included in region	Region extent (km²)			
Name	Acronym	City included in region	Region extent (km )			
East Regional Model	ERM	Dublin	15 000			
Mid West Regional Model	MWRM	Limerick	9 500			
South East Regional Model	SERM	Waterford	9 000			
South West Regional Model	SWRM	Cork	11 000			
West Regional Model	WRM	Galway	19 500			

#### 5.3.2. Prime 2 dataset

The full Prime 2<sup>5</sup> geodatabase for Ireland was provided by the EPA. This dataset is maintained by Ordnance Survey Ireland (OSI) and contains over 50 million attributed objects represented as either a point, line or polygon. Each object has a FORM and FUNCTION classification which describe the physical form (e.g. building) and its use (e.g. residential, hospital, church etc.) respectively. There are over 1000 different function types recorded in Prime 2. NTA used the Prime 2 WAY datasets as the basis for mapping the NTA link-based traffic data to real-world geometries.

The NTA provided datasets of '1-to-1' and '1-to-Many' joins of the NTA data to Prime 2. The datasets were used to categorise the roads by FORM and FUNCTION (further information on these characteristics is provided in Section 6.3.4) and were also used to create a subset of the roads not explicitly modelled, required for the minor road calculations.

#### 5.3.3. Major road traffic emissions processing

AAWT thresholds of 2500 for Dublin and 5000 for the other four cities were used to determine the sub-set of explicitly modelled roads; the exception to this was in the vicinity of continuous monitors, where all roads within the NTA network roads were included within 750 m of the monitor locations. Emissions from all Prime 2 roads not included in the major road dataset were included in the minor road emissions dataset, aggregated to an emissions grid for modelling (Section 5.3.4). Multiple iterations of traffic flow datasets were generated in order to resolve issues with road extents and other inconsistencies.

Initial traffic data processing steps included:

- Defining geographical areas for each NTA model region;
- Combining links for all regions together, removing any duplicates where links overlapped two regions;
- Removing spatially duplicated links, so road centreline links represent total 2-way flows, where appropriate; and
- Calculating traffic flows in AAWT format.

The traffic data was linked to the Prime 2 datasets allowing a separation of the complete Prime 2 dataset into major and minor roads. CERC performed some additional processing, such as

-

<sup>&</sup>lt;sup>5</sup> https://www.osi.ie/wp-content/uploads/2018/07/PRIME2-Client-Documentation-Concepts-V-02.6.pdf

simplifying vertices to a suitable resolution for local dispersion modelling. Initial estimates of road carriageway widths were calculated using the Prime 2 dataset FORM and FUNCTION definitions; in urban areas, these widths were subsequently constrained by calculated street canyon (building-to-building) extents.

An AAWT to Annual Average Daily Totals (AADT) conversion factor was calculated from the time varying flow data based on traffic counts, as described in Section 5.4.1.

As vehicle types and ages strongly influence emissions, detailed traffic fleet information is required in order to convert traffic activity data (flows, speeds) into road source emission rates. For this study, different fleet profiles were applied to each region of Ireland. The fleet calculations were based on monitoring data taken from the Five Cities Demand Management Study<sup>6</sup>. The raw data provided a split of traffic into different vehicle classes with the year of manufacture. The year of manufacture was used to assign the vehicle engine Euro class. Additional information was required in order to further categorise vehicles into more detailed vehicle types, such as individual HGV weight classes. Supplementary information was taken from vehicle splits used within the UK Emission Factor Toolkit<sup>7</sup> fleet data for Northern Ireland. CERC's Emissions Inventory Toolkit, EMIT<sup>8</sup>, was used to perform the road traffic emissions calculations, including adjustments to account for real-world NO<sub>X</sub> emissions following the method described in [12].

#### 5.3.4. Minor road traffic emissions processing

Following calculation of major road emission rates, a summary of the range of emissions of each pollutant was made through inspection of the FORM and FUNCTION classifications.

The major roads showed that certain emission rate bin ranges were most common for all road type combinations. The median value for each classification was therefore used as an estimate for the emission rate on minor roads of the same classification (Figure 5.2). There were exceptions where the minor road classification did not match any major road classification, assumptions were therefore made for these cases, which are:

- Some extremely minor / non-road classifications were ignored (e.g. ford, tow path);
- Reclassified FORM IDs (e.g. Link Roads) to Single carriageways;
- Reclassified Fifth and lower class roads as Fourth Class; and
- On-Ramp and Off-Ramp classifications were grouped together.

Following road-by-road assignment of minor road emission rates, emissions were aggregated onto the model emissions grid. A number of checks were made to validate the magnitude of the minor road emissions. These included comparing the newly calculated minor road emission rates to those used for a previous project modelling Dublin [13]. In addition, the total major plus minor road emission rates were aggregated and compared to the emissions supplied from MapEIre for category F\_Road Transport. The minor road emissions were then included in the 3D grid source.

\_

<sup>&</sup>lt;sup>6</sup> <u>https://www.gov.ie/en/publication/63517-publication-of-five-cities-demand-management-study-phase-1-report-and-toolkits/</u>

<sup>&</sup>lt;sup>7</sup> https://laqm.defra.gov.uk/air-quality/air-quality-assessment/emissions-factors-toolkit/

<sup>8</sup> https://www.cerc.co.uk/EMIT



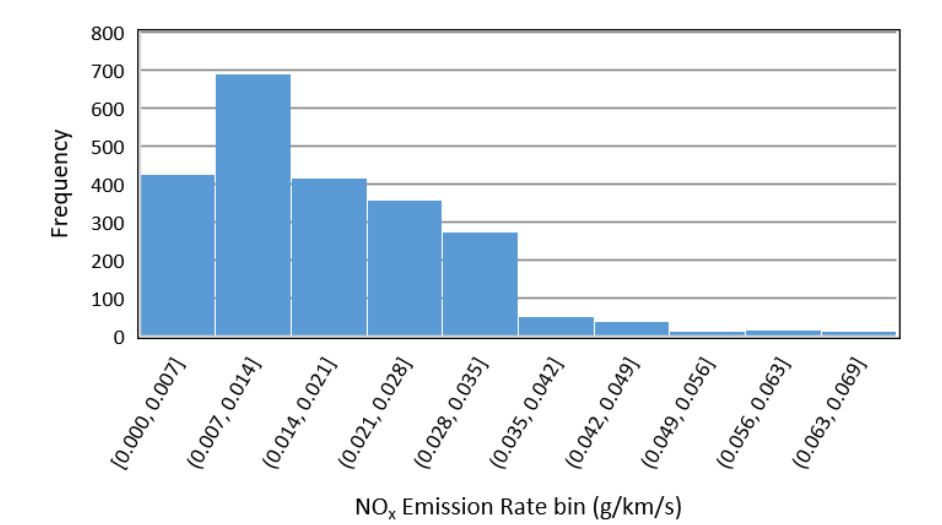


**Figure 5.2** – Example distribution of NO<sub>X</sub> emission rate on major roads, for a single carriageway First Class road.

#### 5.4 Temporal variability of emissions

#### 5.4.1. Traffic

Monitored traffic flow data is available from the TII website<sup>9</sup>. The road types on which vehicle counts are recorded by TII include the national primary road network (motorways and other major roads) and national secondary roads, in addition to some less busy roads. CERC downloaded all available hourly traffic count data for a week in mid-January 2019, a week in mid-May 2019 and a week in mid-October 2019, in order to represent typical term-time conditions.

The hourly traffic flows were subsequently averaged over all sites and all weeks to provide an average profile by hour and day of the week (summing to  $7 \times 24 = 168$  hours). This profile has been applied to all road sources, the profiles for each day are shown in Figure 5.3.

Figure 5.4 compares the average traffic for each of January, May and October over all traffic counts, on a daily basis. This dataset has been used to estimate a conversion factor from the TII National Transport model AAWT values to AADT values, by calculating the average weekday flow as a proportion of all flow, over a full 7-day week. The resultant factor for converting AAWT to AADT was 0.936.

<sup>&</sup>lt;sup>9</sup> https://trafficdata.tii.ie/publicmultinodemap.asp



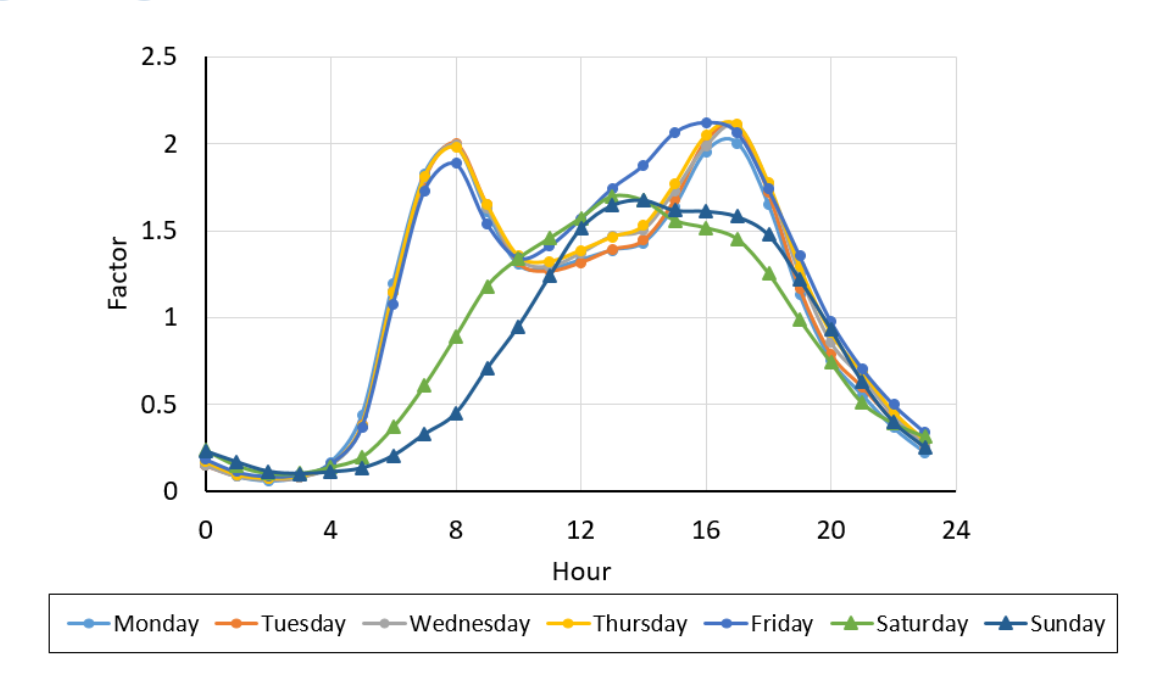


Figure 5.3 – Daily road traffic diurnal profiles derived from TII data.

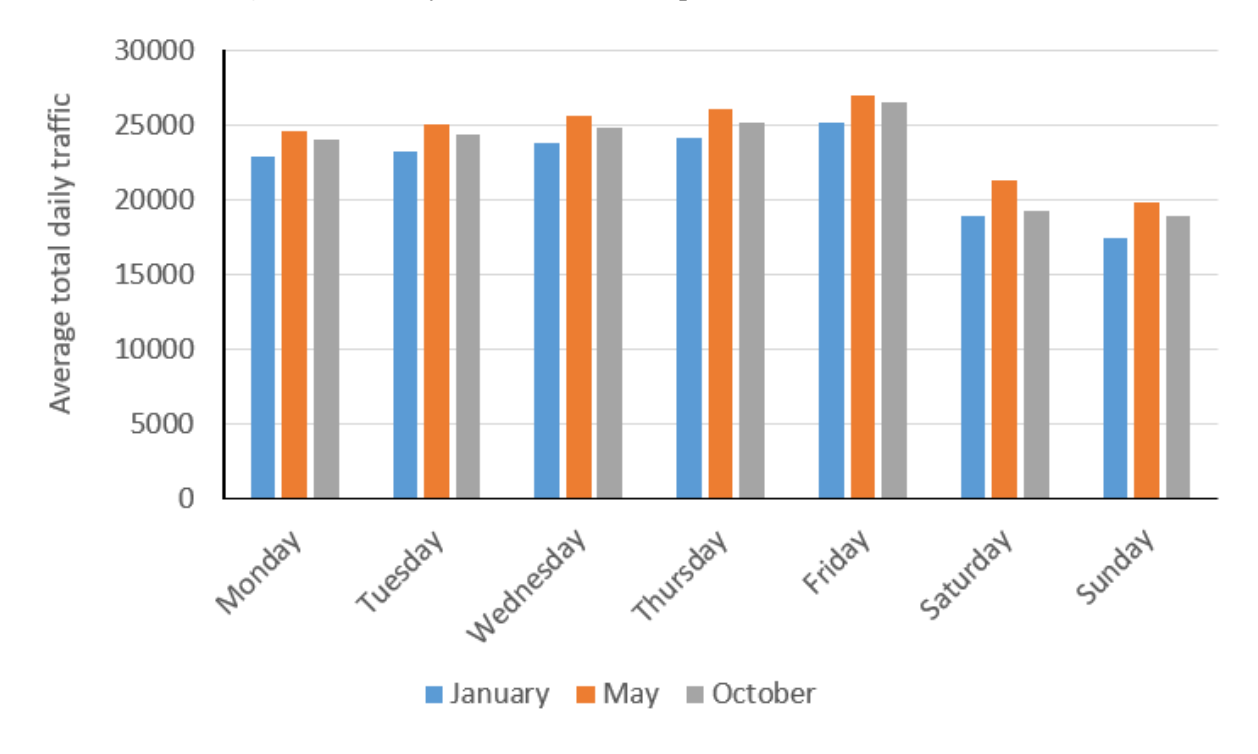


Figure 5.4 – Average total daily traffic counts for January, May and October calculated from TII data.

#### 5.4.2. Non-traffic

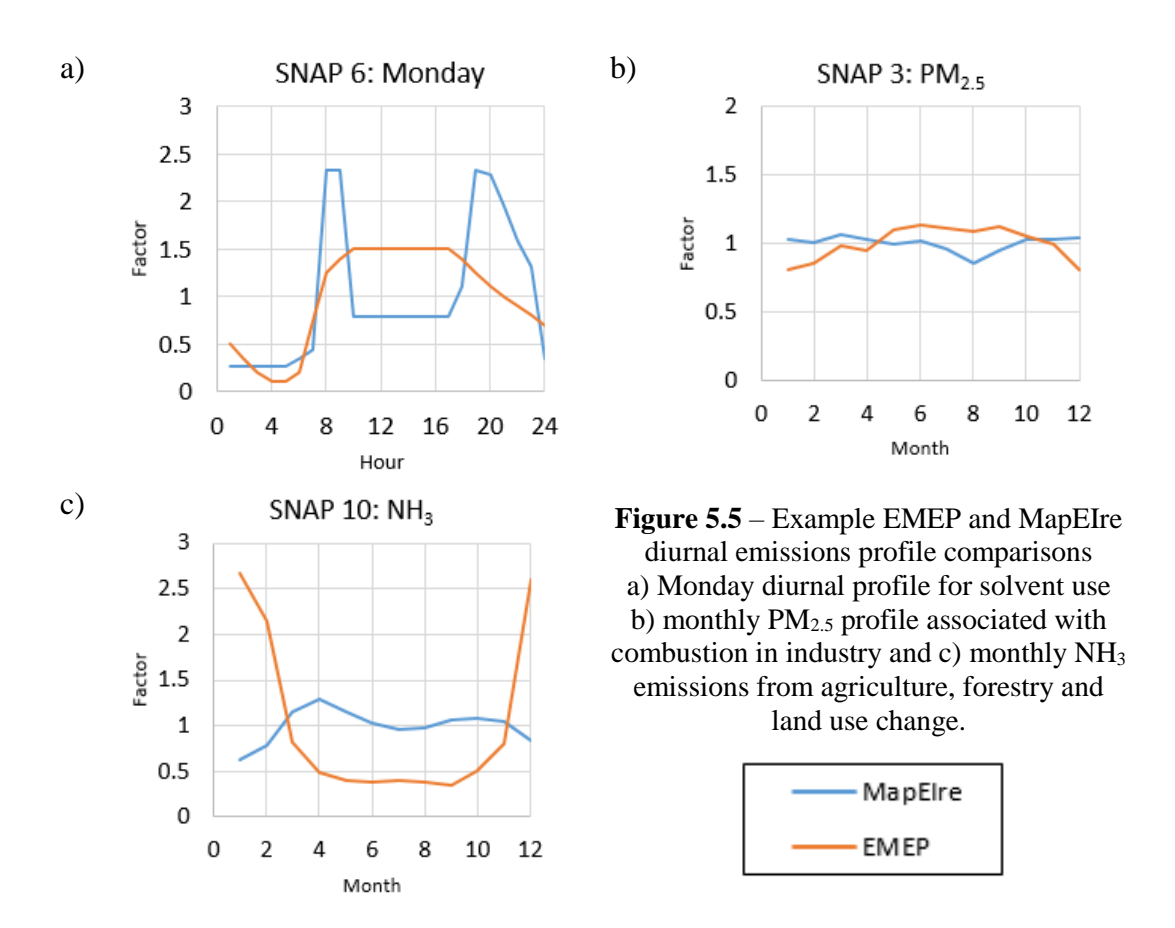
\_

MapEIre provides separate hourly, daily and monthly temporal profiles for each NFR sector. NFR profiles have been combined to generate GNFR profiles on a pollutant-by-pollutant basis using weighting factors corresponding to sector emissions totals. NFR annual emissions totals are available to download from the EPA's UNECE $^{10}$  reporting.

<sup>10</sup> https://www.epa.ie/publications/monitoring--assessment/climate-change/air-emissions/Annex-I-IE-IIR-2022.xlsx

The EMEP model incorporates standard temporal profiles defining hourly, daily and monthly emissions variations for each SNAP emissions sector, categorised by pollutant and country for daily and monthly profiles. These default temporal profiles are derived from TNO-MACC data published in 2011 [14] for all source types apart from traffic. For traffic, default time-variation emissions profiles are taken from INERIS [15], for different countries.

The project team intended to use MapEIre temporal profiles in place of the default EMEP profiles for this project. However, a detailed intercomparison between the MapEIre and EMEP profiles highlighted possible issues with the MapEIre profiles for some sectors; examples are shown in Figure 5.5. Consequently, the decision was made to model using the default EMEP profiles for all non-traffic sectors.



#### 5.5 Spatial distribution of emissions

Anthropogenic emissions data are typically supplied as 2D grids. For regional modelling they must be distributed vertically into the layers of the 3D grid. EMEP incorporates standard vertical distribution factors based on published calculations for each source sector [16], derived from analysis using European point source characteristics and meteorology in the SMOKE emissions pre-processor [17]. It is important to model industrial emissions at appropriate heights in a 3D grid model, representing both physical release height and initial plume rise due to buoyancy, in order to prevent excessive local ground-level concentrations from these sectors.

The surface layer of UKCEH's implementation of WRF and EMEP has a depth of 45 m. This helps to represent well-mixed concentrations across mixed terrain for deposition calculations. However, it can also under-estimate the concentrations resulting from anthropogenic emissions

which are, in practice, generated closer to the ground, such as traffic and domestic combustion. Within the Coupled system, 3D gridded emissions for local modelling were modified to bring surface emissions closer to the ground, by adding a grid layer of 10 m depth and assigning emissions from domestic combustion (SNAP sector 2), solvent use (SNAP sector 6), traffic (SNAP sector 7), agriculture (SNAP sector 10) and natural sources (SNAP sector 11) to this new surface layer. In order to limit the size of the resulting 3D grid files, the top 3 layers of the EMEP emissions distribution (above 324 m) were also combined for local modelling, this only affects emissions from power generation (SNAP sector 1) and waste (SNAP sector 9). These alterations are depicted in Table 5.3.

Table 5.3 – Vertical distribution of gridded emissions by SNAP sectors as used in EMEP and CERC local modelling. Shading indicates layers including a

significant proportion of emissions for a particular sector.

Height (m)	SNAF	1	SNAF	2	SNAF	3	SNAP		SNAF		SNAF		SNAP	<b>?</b> 7	SNAF	8	SNAF	9	SNAF	<b>P</b> 10	SNAF	11
	EMEP	CERC	EMEP	CERC	EMEP	CERC	EMEP	CERC	EMEP	CERC	EMEP	CERC	EMEP	CERC	EMEP	CERC	EMEP	CERC	EMEP	CERC	EMEP	CERC
781 - 1106	15		0		0		0		0		0		0		0		0		0		0	
522-781	30	85	0	0	0	0	0	0	0	0	0	0	0	0	0	0	0	2	0	0	0	0
324 - 522	40		0		0		0		0		0		0		0		2		0		0	
184 - 324	14.7 5	14.7 5	0	0	3	3	10	10	30	30	0	0	0	0	0	0	57	57	0	0	0	0
92 - 184	0.25	0.25	0	0	75	75	70	70	60	60	0	0	0	0	0	0	41	41	0	0	0	0
45 - 92	0	0	0	0	16	16	15	15	8	8	0	0	0	0	0	0	0	0	0	0	0	0
10 - 45	0	0	100	0	6	6	5	5	2	2	100	0	100	0	100	100	0	0	100	0	100	0
0 - 10	U	0	100	100	6	0	3	0	<i>L</i>	0	100	100	100	100	100	0	U	0	100	100	100	100

Page 22 of 132 CERC/FM1297



#### 5.6 Industrial emissions

The industrial source data are based on two data sources provided by the Irish EPA:

- A. A spreadsheet of 2019 national industrial emission point sources<sup>11</sup>; and
- B. The industrial emission monitoring reports<sup>12</sup>.

Figure 5.6 shows the location of all industrial sources included in the emission inventory.

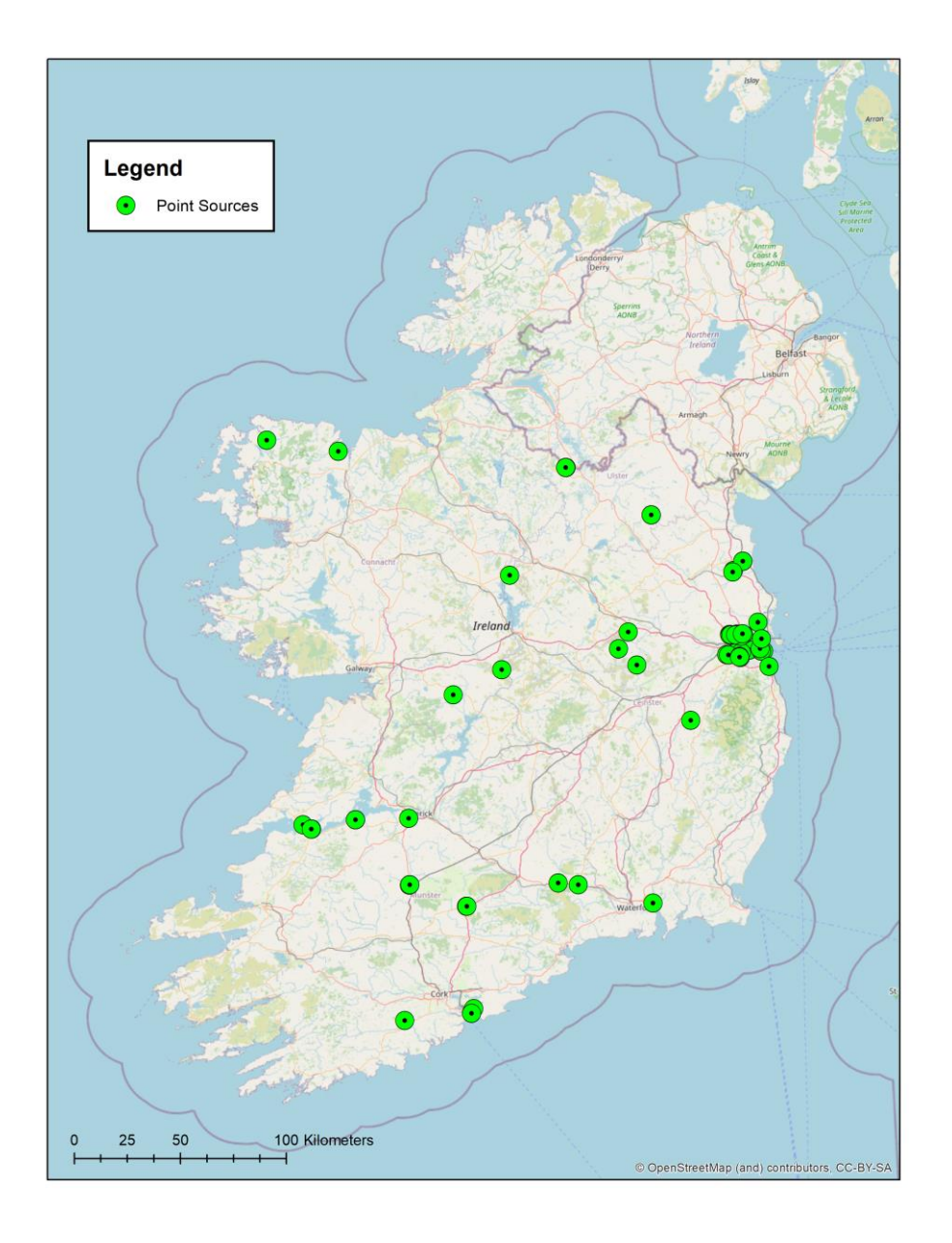


**Figure 5.6** – Industrial point sources included in the inventory.

-

<sup>&</sup>lt;sup>11</sup> Supplied by the Irish EPA to CERC on 6/7/21

<sup>&</sup>lt;sup>12</sup> Supplied by the Irish EPA to CERC on 5/7/21

Default parameters are used to characterise emissions and release properties for sources where stack data are missing. The assumptions used are consistent with previous work for the Irish EPA, i.e. the 2015 and 2017 Dublin modelling project [12]; assumptions are summarised in Table 5.4. Total  $NO_X$ ,  $PM_{2.5}$  and  $PM_{10}$  emissions from all explicit industrial sources included within Ireland are given in Table 5.5. By default,  $NO_2$  emissions are taken to be 5% of  $NO_X$  emissions. VOC emissions were not provided.

**Table 5.4** – Assumptions made when estimating missing parameters.

Parameter	Data Source (reference letter from list above)	Notes
Location	Data source A.	
HEIGHT	Data source A.	
EXITTEMP	Data source B.	Default 200 °C
EXITVEL	Data source B.	Default 15 m/s
DIAMETER	Data source B.	If no data available, or if monitoring report data is averaged, use data source A
Emissions	Data sources A. and B.	Emissions from data source B are used, in preference. If data source A values are used, they are proportionally distributed between the sources based on data source B. If PM emissions are taken from the data source B, $PM_{2.5}$ is calculated equal to $PM_{10}$ .

**Table 5.5** – Total emission rates over the model domain.

Pollutant	Emission rate (tonnes/yr)
$NO_X$	14 564
$PM_{2.5}$	345
$PM_{10}$	409

The fixed vertical distribution applied to industrial emissions in the regional model, described in Section 5.5, may not match the more detailed stack parameters and time-varying plume rise which would be applied in the local model when modelling these emissions explicitly. Mismatched emissions between the local and regional models could lead to artefacts in concentration contours, so the industrial emissions have not been modelled explicitly in the local model.

More investigation of the Irish industrial stack parameters and typical initial plume rise calculated by ADMS-Urban would be needed in order to develop corresponding modified vertical profiles for EMEP to allow explicit modelling of industrial emissions in the local modelling. However, the Coupled system methodology only includes the influence of locally modelled explicit source emissions within a maximum of 2 cells distance from the output location, 2 km in the current configuration. For industrial sources with elevated releases and substantial plume rise, there may not be a substantial impact on near-ground concentrations within this distance. Hence the simplification of only modelling industrial emissions as gridded sources may not significantly influence the modelling outputs.



#### 5.7 Detailed city modelling

Although it was not possible to model all urban features in detail due to the large domain considered for this study, near-source features have been added in some locations where concentrations are high, specifically tunnel portals (Section 5.7.1) and Heuston station in Dublin (Section 5.7.2).

#### 5.7.1. Tunnel portals

Over 140 road tunnels have been identified in Ireland. Project resources did not allow all these to be accounted for explicitly, but tunnel portals have been modelled at three locations within the model domain (Figure 5.7). For each location, the emissions from the road tunnel are considered to occur at the tunnel portals where the traffic leaves the tunnel. The effects of emissions from the traffic in the tunnels impact on concentrations outside the tunnel; air pollutant concentrations are not calculated within the tunnel.

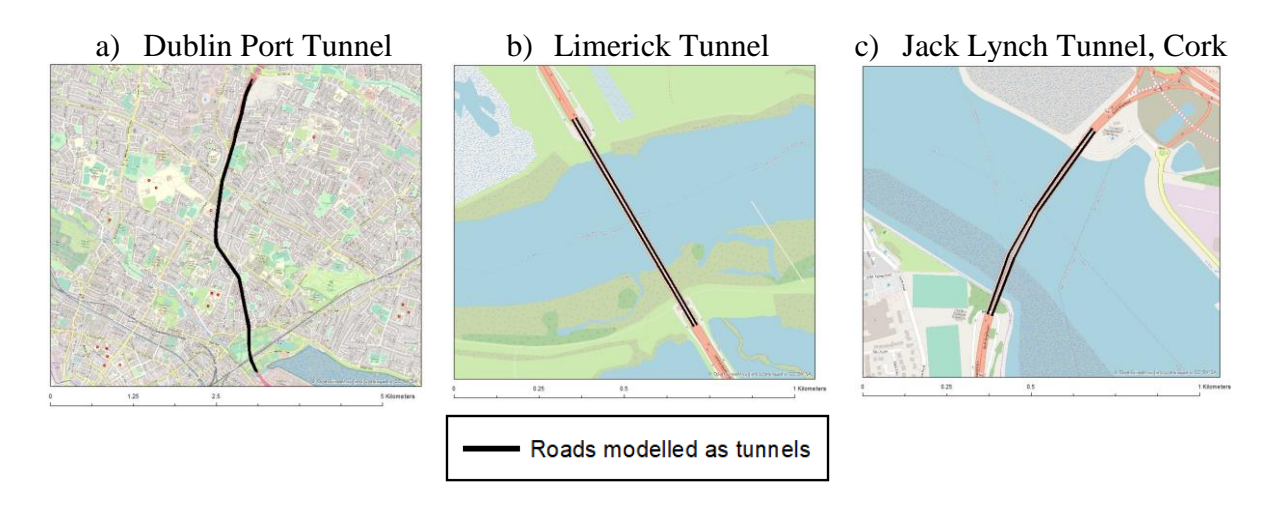


**Figure 5.7** – Sections of the major roads which have been modelled as tunnel sources a) Dublin, b) Limerick and c) Cork. © OpenStreetMap contributors <a href="https://www.openstreetmap.org/copyright">www.openstreetmap.org/copyright</a>.

#### 5.7.2. Heuston station

Heuston railway station in Dublin has been modelled explicitly in this study. It has been represented as a volume source over the location of the uncovered section of the station with a depth of 3 m (Figure 5.8). The MapEIre emission rates for the rail sector in the grid square of interest have been used, specifically:  $1.5 \text{ t/yr NO}_x$ ,  $0.04 \text{ t/yr PM}_{2.5}$ , and  $0.04 \text{ t/yr PM}_{10}$ .

Diurnal profiles have been applied to the volume source representing the station emissions; profiles were calculated using the daily and hourly MapEIre profiles for the rail sector.

A continuous monitor and several diffusion tubes are located to the south of the station, on St John's Road. The validation results at these locations improve when the station is modelled explicitly, rather than spreading the rail emission throughout the grid cell.

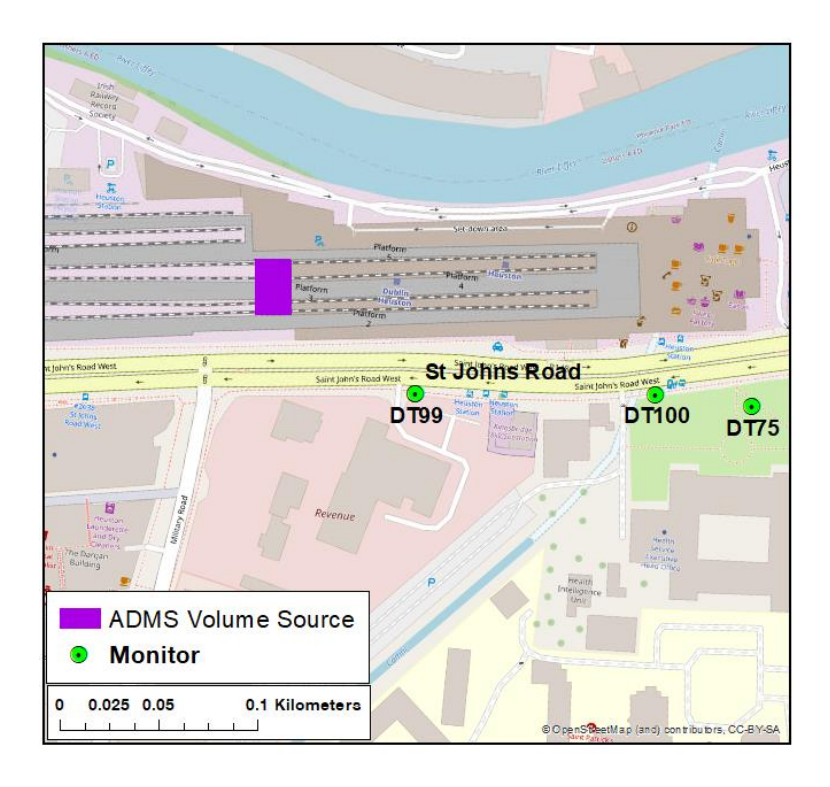


**Figure 5.8** – Modelling configuration for Heuston railway station. The continuous monitor, St John's Road, is at the same location as diffusion tube DT99. Diffusion tubes DT100 and DT75 can also be seen.



#### 6 Model descriptions & configuration

The coupled regional-to-local scale air quality modelling system used for this study comprises three models:

- Weather, Research and Forecasting (WRF) model (Section 6.1);
- European Monitoring and Evaluation Programme (EMEP) model (Section 6.2); and
- ADMS-Urban model (Section 6.3).

These models are linked by a group of scripts and utilities which coordinate data extraction from the regional components and input to the local model, alongside combining the outputs for final concentrations.

Brief model descriptions are provided below; for further information relating to the component models, please refer to the model documentation (referenced within each section).

#### 6.1 Meteorological model

The WRF model [18] is used extensively worldwide for meteorological modelling studies on global, continental and regional scales. The model generates hourly estimates of wind speed and direction, temperature, humidity, surface heat flux and other meteorological parameters; the model assimilates meteorological measurements to improve performance. The model is usually configured to run within multiple nested domains, with the inner domain grid as fine as  $1 \text{ km} \times 1 \text{ km}$  resolution. Meteorological datasets generated by WRF can be used to drive dispersion calculations within EMEP and ADMS-Urban.

For the current project, UKCEH ran WRF version 4.1.1 in 4 domains, the outermost covering all of Europe at 27 km  $\times$  27 km grid resolution, two intermediate domains covering the UK and Ireland at 9 km and 3 km, and an innermost domain covering the Republic of Ireland at 1 km  $\times$  1 km resolution (Figure 6.1). The model runs with 21 vertical layers, with a surface layer depth of approximately 45 m.

UKCEH use NCEP Final Analysis (GFS-FNL) global meteorological model data at 1-degree spatial resolution and hourly temporal resolution [19] to drive the outermost WRF domain. Land use data based on MODIS satellite imagery [20] is used to define surface properties, in combination with the NOAH land-surface model [21]. The Yonsei University (YSU) boundary layer scheme represents turbulent mixing in the lower atmosphere [22]. The updated Purdue Lin microphysics scheme [23] accounts for atmospheric processes involving water, affecting precipitation and cloud predictions. Convective mixing, cloud and precipitation processes are modelled explicitly in the  $1 \text{ km} \times 1 \text{ km}$  grid resolution domain; the Kain-Fritsch parameterisation [24] is used for convective features smaller than grid scale, primarily in the outer domain. The RRTM [25] and Dudhia [26] parameterisations are used for longwave and shortwave radiation calculations, respectively.



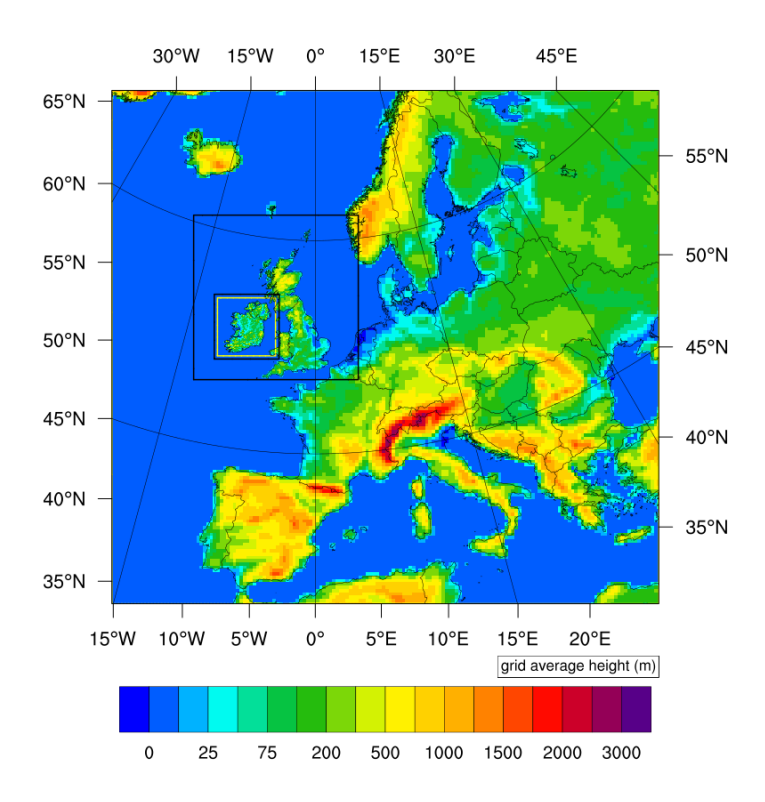


**Figure 6.1** – Extent of domains used in the UKCEH WRF modelling. The outermost domain (full map extent) covers Europe at 27x27 km resolution, the intermediate domains at 9x9 km and 3x3 km resolution cover the UK and Ireland, while the innermost domain (yellow outline) covers Northern Ireland and the Republic of Ireland at 1 km ×1 km resolution.

#### 6.1.1. Meteorological model outputs

The meteorological parameter outputs from WRF that are used in the Coupled system for local dispersion modelling are:

- Horizontal wind speed components at 10 m above ground level;
- Temperature at 2 m above ground level;
- Surface sensible heat flux (influences atmospheric stability);
- Incoming solar radiation (may influence daytime atmospheric stability and chemistry processes); and
- Boundary layer height.

Additional variables and attributes relating to coordinate system definition, grid cell locations and model output timesteps are also required in the files.

#### 6.2 Regional air quality model

The European Monitoring and Evaluation Programme (EMEP) model [1] was developed as part of the work of the Meteorological Synthesizing Centre-West (MSC-West), hosted by the Norwegian Meteorological Institute. EMEP is used within Europe for modelling transboundary pollutant fluxes and calculating source-receptor matrices that contain the contribution of emissions in any European country to concentrations in any other country [27]. UKCEH use and have contributed to development of the EMEP model for fine resolution UK modelling [28]. UKCEH have modelled the interaction of long-range transport and local emissions in secondary particulate concentrations for Defra (UK Department for Environment, Food & Rural Affairs) [2].

UKCEH have run EMEP version rv3.6 for this project, driven by WRF meteorological model data described in Section 6.1. EMEP is run with two nested domains at  $27 \text{ km} \times 27 \text{ km}$  and  $1 \text{ km} \times 1 \text{ km}$  which match the outermost and innermost WRF domains. The model can be used to predict concentrations of pollutants at rural, suburban background and urban background locations. However, due to its relatively coarse resolution within urban areas, the model is not suitable for use in predicting air pollutant concentrations in near-road environments.

Emissions data for the outer European domain are taken from the EMEP inventory [11], while emissions for Ireland have been updated as described in Section 5. 2D annual emissions data are distributed temporally and vertically as described in Sections 5.4 and 5.5.

EMEP uses standardised vertical profiles of concentrations as boundary conditions for the outer European domain, with a modification to O<sub>3</sub> concentrations on the western boundary based on monthly measurements at Mace Head to represent Atlantic air conditions. Biogenic emissions from Saharan dust, volcanoes, road wind-blown dust, sea salt formation and volatile organic compounds from vegetation (bVOCs) are included in the EMEP model [1]. Daily biomass burning emissions are taken from the FINN inventory [29].

#### 6.2.1. Regional air quality model outputs

The gridded concentration outputs from EMEP that are used in the Coupled system for local dispersion modelling are:

- Nitric Oxide (NO);
- Nitrogen Dioxide (NO<sub>2</sub>);
- Ozone  $(O_3)$ ;
- Total fine particulate matter (PM<sub>2.5</sub>);
- Total particulate matter (PM<sub>10</sub>); and
- Sulphur Dioxide (SO<sub>2</sub>).

Additional variables and attributes relating to coordinate system definition, grid cell locations and model output timesteps are also required in the files. Regional concentrations of ammonia (NH<sub>3</sub>), fine and coarse nitrate (NO<sub>3</sub><sup>-</sup>) are also available in the files.

The EMEP output files can include two types of concentration output: 3D variables, which represent mean concentrations throughout a grid cell; and surface variables, which adjust grid cell concentrations from the centre of the lowest layer of the grid towards the ground surface by taking into account the effects of deposition. This adjustment is particularly important for  $O_3$ , where deposition to vegetation reduces surface concentrations by around 8% on average. In general, the Coupled system works with the 3D cell centre concentrations, which match the assumptions made in the local modelling, but for  $O_3$  the surface concentrations have been used as being more representative of conditions at typical monitoring heights. In addition, the total  $PM_{2.5}$  from EMEP in the Coupled system has been calculated as the sum of primary and secondary dry  $PM_{2.5}$ , 27% of coarse nitrate (i.e. nitrate particles with diameters in the range 2.5 to  $10 \mu g/m^3$ ), and a contribution from particle-bound water appropriate to typical surface measurement conditions, as recommended by  $EMEP^{13}$ .

<sup>13</sup> https://emep.int/mscw/mscw\_moddata.html



#### 6.3 Street-scale air quality model

The ADMS-Urban model ([3], [4]) has been used extensively to model air quality in cities throughout the world ([30], [31], [32]). For the current Ireland study, it been used as the local modelling component of the Coupled system ([33], [12]).

In addition to emissions data, the model requires a number of input parameters and datasets. In particular, in order to better account for the influence of the urban built environment on dispersion processes, urban morphological datasets are used by the model. Specifically, 'urban canopy' datasets quantify overall building density and 'street canyon' datasets describe building dimensions in near-road environments. These urban datasets are derived from digital 3D buildings datasets using GIS tools [34].

Model settings are described in Section 6.3.1. Section 6.3.2 provides details of the 3D buildings datasets for the five largest urban areas within the model domain (Dublin, Cork, Limerick, Waterford and Galway). The urban canopy and street canyon datasets are described in Sections 6.3.3 and 6.3.4, respectively. Model outputs are discussed in Section 6.4.

#### 6.3.1. ADMS-Urban model settings

In stand-alone local air quality modelling it is possible to take account of the variation in surface roughness by specifying values for the surface roughness at the location of the meteorological measurements and the dispersion site separately. When modelling with the Coupled system, the modelled WRF meteorological data is aligned with the meteorological site surface roughness.

The current version of Coupled system does not allow for spatial variations in dispersion site surface roughness and minimum Monin-Obukhov length. Table 6.1 summarises the spatially homogeneous values applied for the current study. Sensitivity testing in relation to the specified value of the minimum Monin-Obukhov length has been performed, results are presented in Section 8.5.

**Table 6.1** – Model settings.

Parameter	Value Used
Dispersion site surface roughness (m)	0.5
Meteorological site surface roughness (m)	0.1
Minimum Monin-Obukhov length (m)	30
Chemistry	Generic reaction scheme with night time chemistry
Model output receptor spacing along roads (m)	15
Daylight saving time included	Yes

ADMS-Urban includes the Generic Reaction Set atmospheric chemistry scheme [3]. The scheme has seven reactions which are significant for the concentrations of nitrogen oxides and ozone, including reactions which are parameterisations of the large number of reactions involving a wide range of Volatile Organic Compounds (VOCs). In addition, an eighth reaction has been included within ADMS-Urban for the situation when high concentrations of nitric oxide (NO) can convert to nitrogen dioxide (NO<sub>2</sub>) using molecular oxygen.

When modelling with the intention of creating a contour plot of calculated concentrations, attention needs to be given to the resolution of the output points. A high output point resolution is required in the vicinity of road sources where concentration gradients are high. It is possible in ADMS-Urban to specify the along-road spacing of receptor points, at each of these locations a number of receptors are aligned across the road to capture the high gradients.

Times entered into the model are in local solar time, daylight saving times changes the relationship between the local solar time and clock time during the daylight savings period. In order to ensure the diurnal profiles entered into the model are applied at the correct solar times, the model adjusts the emissions correctly during this period. Note, that the methods for applying this feature in the regional and local models are not entirely consistent.

#### 6.3.2. 3D buildings data for Dublin, Cork, Limerick, Waterford and Galway

3D buildings data are required to calculate the street canyon and urban canopy parameters which are used as input to ADMS-Urban. 3D buildings data were unavailable for use in this project, thus it was necessary to develop a method to generate a suitable dataset; details are provided below. Street canyons and urban canopy flow are only modelled within the five major urban areas in Ireland i.e. Dublin, Cork, Limerick, Waterford and Galway, thus the requirement for 3D buildings data was limited to these regions.

2D building outline data was downloaded from Open Street Map [35]. Building height estimates were required in order to add a vertical dimension to the 2D dataset. Building heights were derived from LiDAR surface and terrain data [36], which were available at 2 m resolution. LiDAR data was unavailable for large areas within Cork and Waterford; Local Climate Zone (LCZ) data [37] was used in these locations (available at 100 m resolution), assigning building heights based on parameter values associated with each LCZ type (as given in Table 1 of [37]). Figure 6.2 shows example 3D buildings in Limerick.

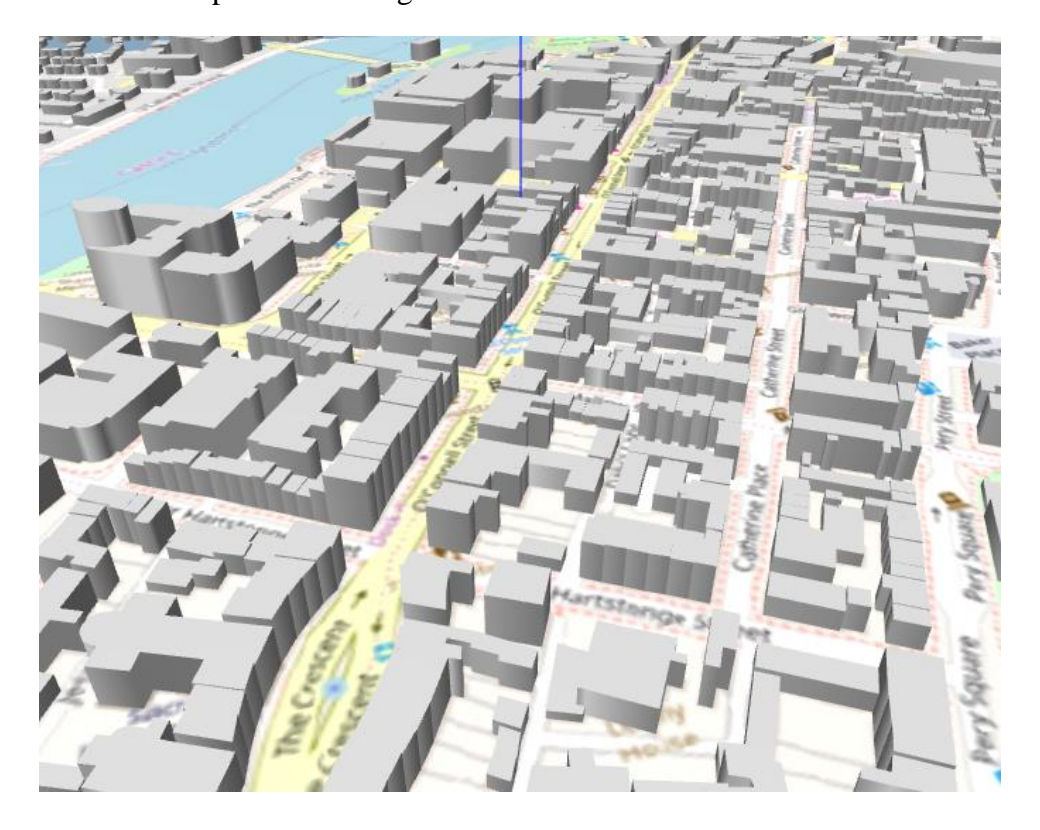


**Figure 6.2** – Example 3D buildings in Limerick, derived from 2D dataset (Open Map data copyrighted OpenStreetMap contributors and available from <a href="https://www.openstreetmap.org">https://www.openstreetmap.org</a>) and Lidar data, viewed in the ADMS Mapper. Background map; © OpenStreetMap contributors <a href="https://www.openstreetmap.org/copyright">www.openstreetmap.org/copyright</a>.



#### 6.3.3. Urban canopy datasets

Urban canopy datasets are used to represent the neighbourhood scale distribution of flow parameters due to variations in urban structures. The parameters that describe the urban morphology, derived from the 3D buildings dataset, are summarised in Table 6.2. Figure 6.3 provides a graphical explanation how these  $\lambda_P$  and  $\lambda_F$  parameters are derived from 3D buildings datasets for a particular neighbourhood. For this study, these parameters have been calculated at a grid resolution of 1 km<sup>2</sup>. Specifically, for each grid cell,  $\lambda_P$  is calculated as the ratio of the sum of the plan area ( $A_P$ ) occupied by buildings to the total area of the grid cell ( $A_T$ ). The spatial distribution of  $\lambda_P$  over the urban area of Cork is shown in Figure 6.4. Calculations of  $\lambda_F$  are performed for a subset of wind directions (e.g. every 90° or 45°). For each grid cell,  $\lambda_F$  is calculated as the ratio of the total frontal area ( $A_F$ ) of buildings perpendicular to the wind direction to total plan area within the cell. Although  $\lambda_F$  is wind direction dependent, for the majority of building configurations, there is little variation.

The initial urban canopy flow formulation is described in [38], with evaluation. The current formulation with minor extensions is defined in [3].

**Table 6.2** – Data included in the urban canopy input for each grid cell.

Parameter	Description
Lambda P (λ <sub>P</sub> )	A measure of building coverage at ground level
Lambda F (λ <sub>F</sub> )	A measure of building frontage for particular wind directions

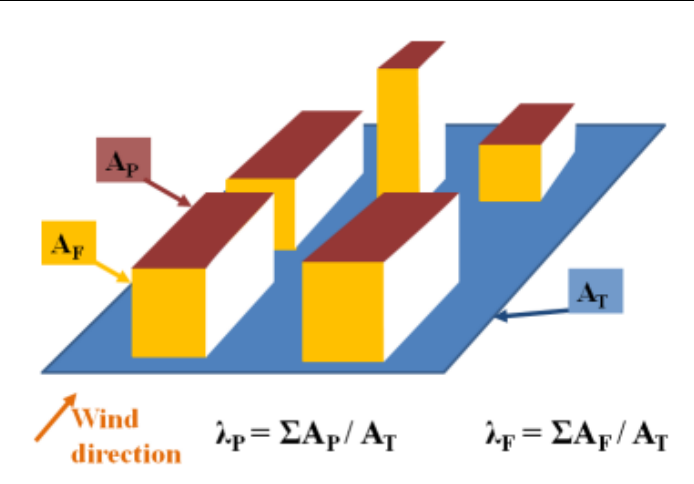


**Figure 6.3** – Illustration of  $\lambda_P$  and  $\lambda_F$  for a schematic urban neighbourhood.

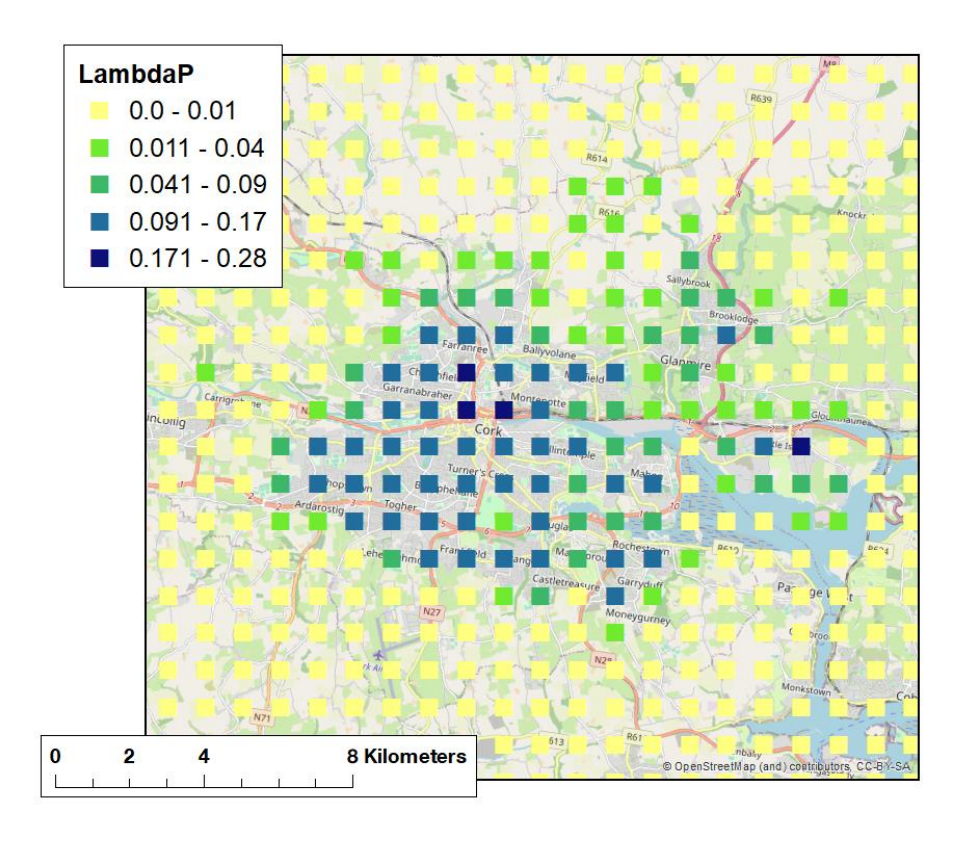


**Figure 6.4** – Variation in  $\lambda_P$  across the region modelled for Cork. Background map; © OpenStreetMap contributors www.openstreetmap.org/copyright.

#### 6.3.4. Road source dimension datasets

Street canyon and road carriageway width parameters are required for each road within the major road emissions dataset. The street canyon data derived from the 3D buildings dataset includes:

- Average canyon width;
- Canyon porosity; and
- Average, minimum and maximum building height.

These parameters are required for both sides of the road because street canyon parameters are commonly asymmetric with respect to the digital definition of the road centreline. Note that street canyon data was derived using a subset of the 3D buildings data, up to 100 m from each road. The justification for this approach is that building facades in excess of 100 m from the road centreline will have minimal impact on road source dispersion. A description and evaluation of the ADMS-Urban street canyon model has been published in the literature [39].

Road carriageway widths are not supplied as road attributes within the Prime 2 dataset. Therefore the Prime 2 FUNCTION and FORM attributes have been used to estimate road widths. Table 6.3 provides the full list of FORM and FUNCTION parameters within the dataset; any FUNCTION ID can go with any FORM ID, although some combinations are more common than others. It was found that there were 48 individual combinations of these parameters, and an estimate of road width for each combination was made. The validity of the estimates was checked by measuring a subset of roads in each description category using Google Earth. The most frequent combinations of FORM and FUNCTION are given in Table 6.4 with the estimated road widths for that combination.



**Table 6.3** – Road data FORM and FUNCTION descriptions.

ID	FORM	ID	FUNCTION
122	Dual Carriageway	177	Fifth Class
212	Lane	179	First Class
215	Level Crossing	191	Fourth Class
246	Motorway	266	Main Road
281	Pedestrian Zone	409	Second Class
330	Roundabout	475	Third Class
362	Single Carriageway	659	Motorway On-ramp
369	Sliproad	660	Motorway Off-ramp
411	Motorway Toll Plaza	661	National Road On-ramp
492	Link Road	662	National Road Off-ramp
654	National Road Toll Plaza	667	Third Class (Access Only)
655	Regional Road Toll Plaza	669	Sixth Class (Managed)

**Table 6.4** – Example road widths for the most common FORM and FUNCTION combinations.

Percentage of roads in inventory	FORM	FUNCTION	Estimated width (m)
43	Single Carriageway	First Class	8.70
43	Single Carriageway	Second Class	7.25
34	Single Carriageway	Third Class	7.25
25	Single Carriageway	Main Road	8.70
16	Motorway	Main Road	10.77
8	Dual Carriageway	Main Road	7.36
7	Roundabout	Second Class	5.65
5	Dual Carriageway	Second Class	4.46
5	Roundabout	Main Road	7.88
4	Roundabout	First Class	7.88
3	Roundabout	Third Class	5.65
3	Single Carriageway	Fourth Class	7.25

Road carriageway widths are assumed to be symmetric in relation to the road centreline. A two-tier approach has been used to estimate road width, specifically:

- The road width is first estimated using road description FORM and FUNCTION parameters; and
- Secondly a correction is applied derived from the canyon geometries (where available) to ensure that the road carriageway width remains within the canyon.

Figure 6.5 provides a 2D illustration of calculated road carriageway (light blue) and street canyon (pink) extents, for a neighbourhood in Dublin. A single background monitoring site is shown (green circle). The canyons to the north of the domain shown have been calculated by the tools to be asymmetric, which is correct because the road is adjacent to a stretch of water (the River Liffey).

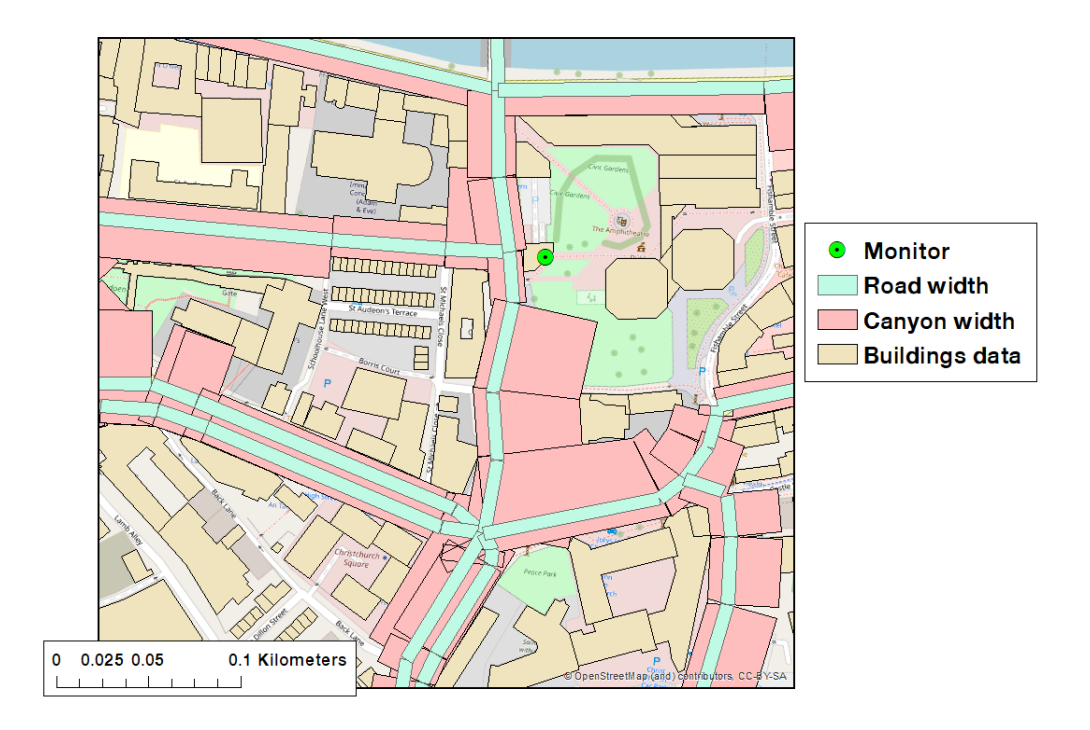


**Figure 6.5** – Example monitor showing modelled road and canyon widths and available buildings outlines in the vicinity of the road sources (neighbourhood in Dublin). Background map; © OpenStreetMap contributors <a href="www.openstreetmap.org/copyright">www.openstreetmap.org/copyright</a>.

#### 6.4 Coupled system outputs

There are two types of system runs:

- 1. **Receptor run**, a fast calculation that gives concentrations at specified discrete locations. This model run generates hourly modelled pollutant concentration time series at continuous monitor and diffusion tube locations, for comparison with measurements.
- 2. **Contour run**, a longer calculation that gives concentrations over a defined domain using high resolution output receptors. *This model run generates hourly modelled pollutant concentration on a grid covering Ireland, for generating pollution maps*.

System output files are in netCDF format. For the contour run, the receptor locations are on a variable resolution grid to resolve concentration gradients near road sources. All calculations generate concentrations for multiple pollutants<sup>14</sup>, e.g. NO<sub>x</sub>, NO<sub>2</sub>, O<sub>3</sub>, PM<sub>2.5</sub> and PM<sub>10</sub>.

A number of post-processing tools have been used to convert the raw output datasets into the metrics for evaluation as well as for comparison with AQSR limit and target values.

Modelling pollutant concentrations over Ireland at high spatial and temporal resolution takes a large amount of computational resources and generates 1.05 terabytes of raw model output data per year. In order to facilitate data processing and ensure relatively short run times (few days), the Ireland domain has been divided into seven sub-domains, as shown in Figure 6.6. Model outputs have been re-combined for the purpose of evaluation and mapping. Two sub-domains cover parts of Northern Ireland, however explicit road emissions were only modelled within the Republic of Ireland, thus output concentration maps have been cropped at the border with Northern Ireland.

<sup>14</sup> Other pollutants can be modelled where emissions are available and appropriate chemical mechanisms are accounted for in the component models.

\_

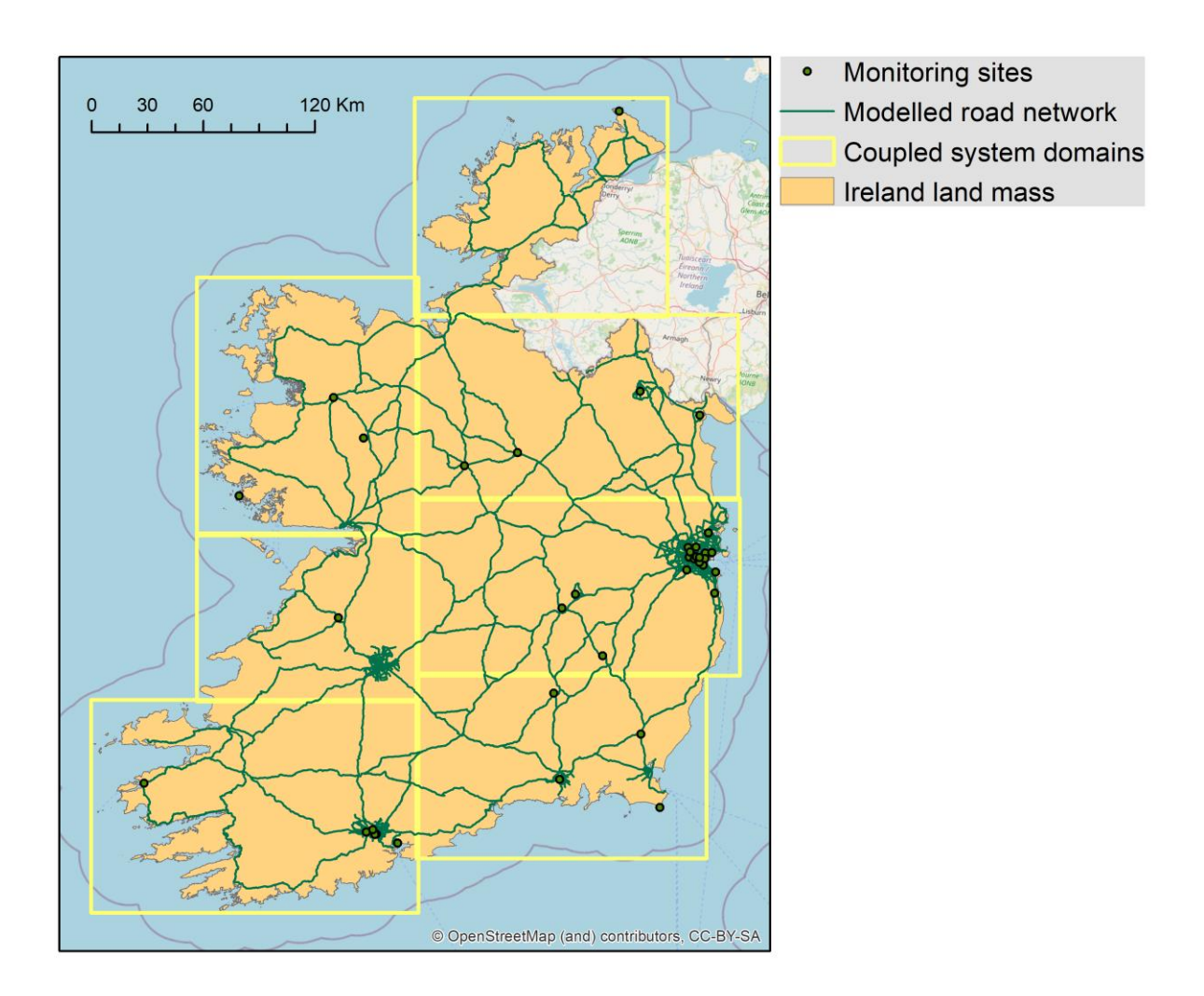


**Figure 6.6** – Modelling sub-domains, shown by yellow rectangles, alongside the explicitly modelled road network and continuous monitoring site locations.



#### 7 Meteorological modelling results

The WRF regional meteorological model results were evaluated against meteorological measurements at Met Éireann sites in Ireland, before their use in the EMEP regional chemical-transport model and for local modelling in the Coupled system. Full results were reported to the EPA in April 2019, while a summary is given here and further plots in Appendix C.

R software and the OpenAir package were used to process the modelled and measured data and produce statistical and graphical comparisons. Statistical metrics for each parameter were compared with suggested benchmark values from the FAIRMODE initiative<sup>15</sup>, themselves based on typical performance values identified by studies for the US Environmental Protection Agency.

In general, the evaluation results show good performance for the WRF model configuration for the Republic of Ireland, with most statistical metrics within the benchmark values, both for individual sites and over all sites, with similar performance in both modelled years, as shown in Table 7.1. There is a model tendency for small positive bias in wind direction and small negative bias in temperature. Spatial plots of the bias values show that there may be greater uncertainty in the model wind speed values for coastal measurement sites, which could relate to the representation of the coastline at 1 km resolution or to uncertainties in the modelling of marine conditions. However, overall the performance of the meteorological data is adequate for use in the regional and local air quality modelling.

**Table 7.1** – Statistical metrics and benchmark values, with values missing benchmark thresholds in italics. Gross Error: mean magnitude of difference between model and measurement <sup>16</sup>; IoA: Index of Agreement.

Parameter	Metric	Benchmark	2018	2019
Wind speed	RMSE	< 2	1.71	1.69
Wind speed (m/s)	Bias	$< \pm 0.5$	-0.45	-0.41
(111/8)	IoA	≥ 0.6	0.73	0.73
Wind	Gross Error	< 30	23.19	22.22
direction (°)	Bias	< ± 10	11.72	11.04
	Gross Error	< 2	1.17	1.15
Temperature	Bias	$< \pm 0.5$	-0.51	-0.60
	IoA	≥ 0.8	0.86	0.84

Frequency scatter plots for hourly wind speed and temperature over all measurement sites are shown in Figure 7.1. Different scales are used for the different years due to higher maximum measured temperature and wind speed values in 2018. Otherwise model performance is broadly consistent between the two years. The hourly values are fairly well clustered around the 1:1 line and within the factor of two lines. The slight model tendency to underestimate measured temperature is visible in the plot. Equivalent plots for each site in 2019 are shown in Appendix C, which continue to show generally good performance.

<sup>&</sup>lt;sup>15</sup> Suggested statistical benchmarks for meteorological mesoscale model evaluation - Table A2.3: 'The Application of models under the European Union's Air Quality Directive' <a href="https://www.eea.europa.eu/publications/fairmode">https://www.eea.europa.eu/publications/fairmode</a>

<sup>&</sup>lt;sup>16</sup> Gross Error defined as  $\frac{1}{n}\sum_{i=1}^{n}|M_i-O_i|$  where is the number of valid pairs of modelled and observed values and  $M_i/O_i$  represent modelled / observed values for the  $i^{th}$  data point respectively.

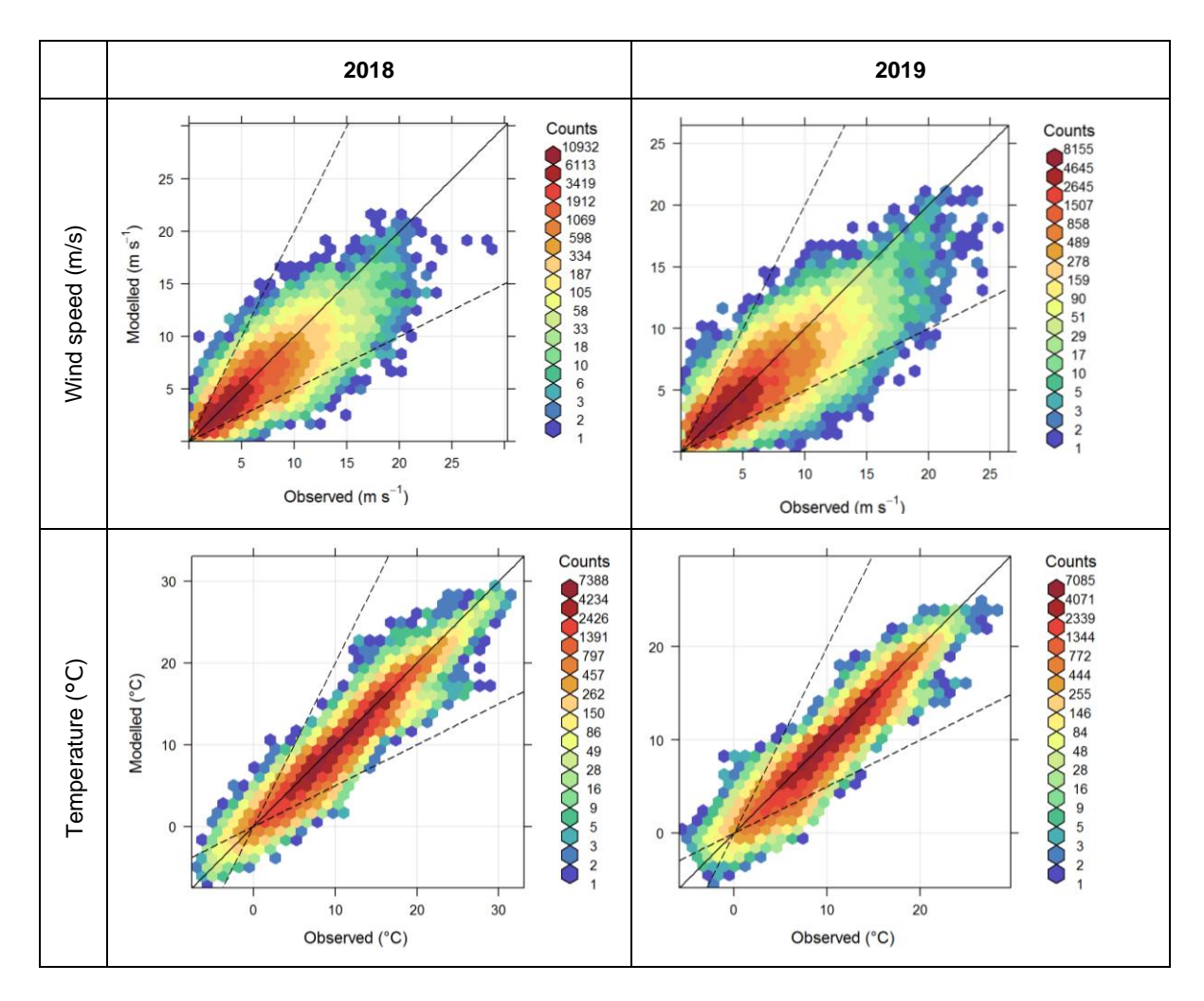


**Figure 7.1** – Frequency scatter plots of hourly modelled and measured wind speed for wind speed (upper row) and temperature (lower row) for 2018 (left column) and 2019 (right column). In these plots the colour indicates the frequency of points in each area of the graph. The solid line indicates a 1:1 relationship between modelled and observed, while the dashed lines show factor of 2 relationships.

The spatial plot of mean bias in wind speed presented in Figure 7.2 shows greater modelled underpredictions of wind speed at coastal measurement sites, where measured wind speeds tend to be higher. An equivalent plot for temperature mean bias, given in Appendix C Figure C.3, does not show any clear spatial pattern.

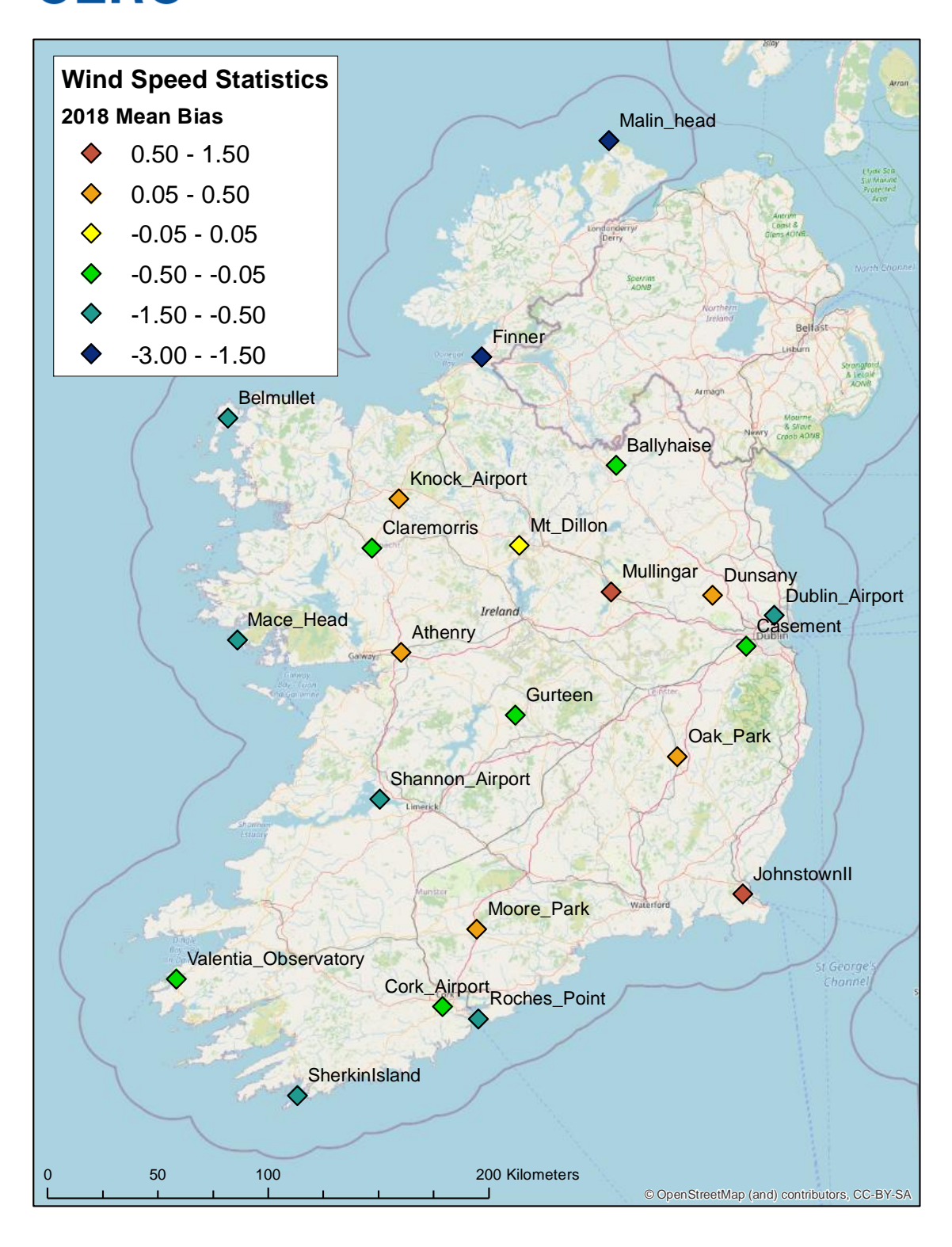


**Figure 7.2** – Spatial plot of mean bias in wind speed at each of the measurement sites, with bias shown in coloured diamonds at the measurement locations. Background map: © OpenStreetMap contributors <a href="https://www.openstreetmap.org/copyright">www.openstreetmap.org/copyright</a>.



#### 8 Model evaluation

There are multiple stages involved in checking that the modelling system generates pollutant concentrations that are representative of real-world ambient air quality. Direct comparisons between the pollution levels recorded by monitoring equipment (Section 4) and modelled concentrations allows quantification of model accuracy at a range of locations. In addition to evaluating annual average concentrations, it is important to consider how the model is performing on an hour-by-hour basis by calculating statistics; average temporal variations such as daily and monthly patterns are also of interest. A range of model evaluation plots and statistics generated by CERC's Model Evaluation Toolkit [40] are presented in Section 8.1 with examples of temporal variations presented in Section 8.3.

FAIRMODE [41] have developed an approach to the evaluation of air quality models that allows for measurement uncertainty, which varies according to pollutant. In future, these FAIRMODE model performance metrics are likely to be required as part of the QA/QC process of e-reporting of air quality model results to the European Environment Agency, so modelling system results must satisfy the relevant criteria. FAIRMODE target plots and related metrics are presented in Section 8.2. Model outputs relate to model inputs, and consequently the sensitivity of modelled concentrations to model inputs have been considered throughout the project, for instance in terms of configuration options for the 3D representation of gridded emissions. Section 8.5 presents the outcome of example sensitivity testing.

Policy makers need to know where pollution originates. Therefore, it is important to quantify the relative proportion of concentrations that arise from long-range pollutant transport, regional sources and local sources. This is a non-trivial exercise when modelling over a large domain such as Ireland due to the influence of non-linear chemistry processes. Some quantification of relative contributions is presented in Section 8.4.

In all these evaluations, it is important to note that the modelling system has not been calibrated by using measured data as input or in post-processing adjustments. In addition, running and evaluating two consecutive years provides confidence that the results are repeatable for other years.

#### 8.1 Model verification

Model verification results are presented separately for 2018 and 2019, for  $NO_2$ ,  $PM_{2.5}$ ,  $PM_{10}$  and  $O_3$  in Sections 8.1.1, 8.1.2, 8.1.3 and 8.1.4, respectively. The majority of results relate to comparisons of modelled concentrations with continuous monitor measurements, but comparisons against diffusion tube measurements are also provided for  $NO_2$ .

For the continuous monitor comparisons, statistics calculated include:

- The number of valid observations:
- The observed and modelled mean concentrations;
- The normalised mean square error (NMSE), a positive number for which a value closest to zero is best;
- The correlation coefficient (R), which varies between 0 (worst) and 1 (best);
- The fraction of modelled values within a factor of two of the observed (Fac2), which varies between 0 (worst) and 1 (best); and
- The fractional bias (Fb), which can be either positive or negative, with zero being the best value.

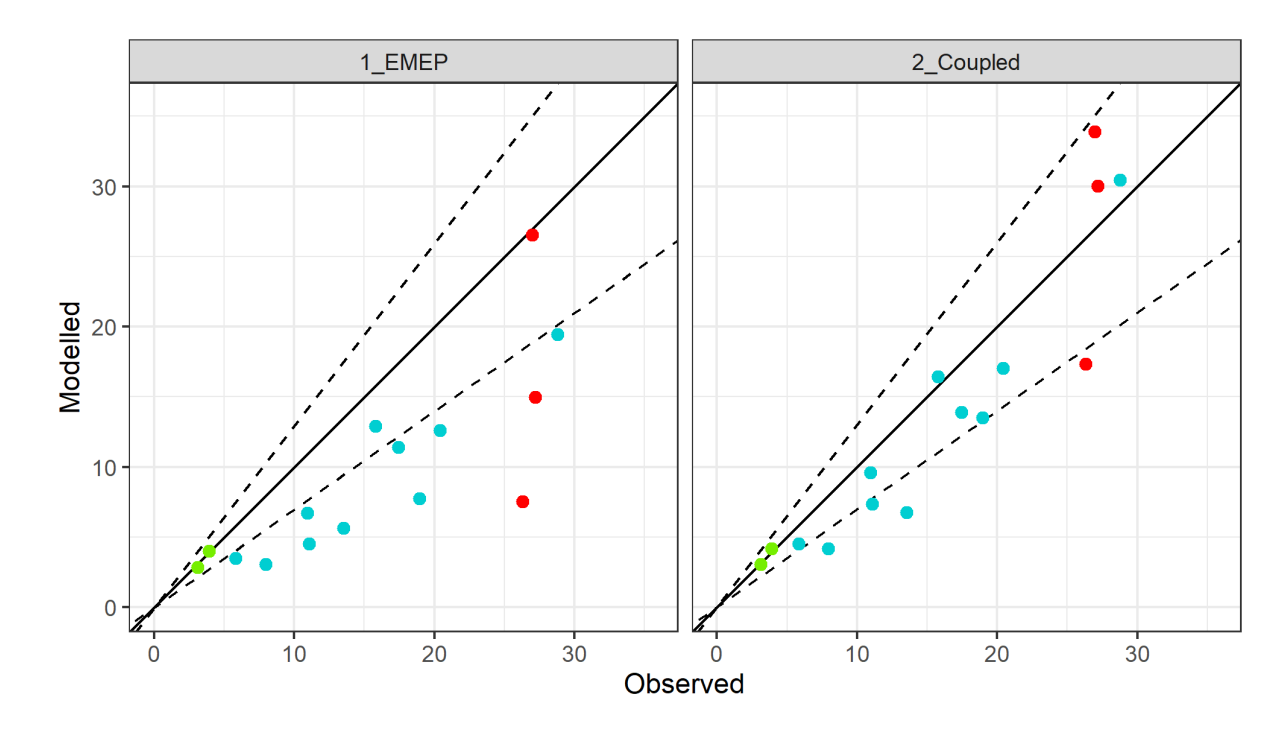
The averaging times over which statistics are calculated correspond to the air quality standards averaging time associated with each pollutant i.e. hourly, daily and maximum daily 8-hour rolling averages for NO<sub>2</sub>, particulates and O<sub>3</sub>, respectively. Scatter plots comparing modelled and observed concentrations are presented for both annual average and, where relevant, high percentile short-term average metrics. The plots include a 1:1 line that relates to ideal model performance, in addition to lines indicating the modelling uncertainty data quality objectives from Schedule 1 of the AQSR [5].

Concentrations as calculated solely by the regional model are presented alongside those calculated by the Coupled system. The coarser  $1 \text{ km} \times 1 \text{ km}$  resolution modelled concentrations from EMEP can differ significantly from the Coupled system street-scale resolution concentrations in locations where dispersion and chemistry processes associated with major road sources strongly influence pollution levels (e.g. at traffic monitors). The magnitude of the differences between the models varies according to the pollutant.

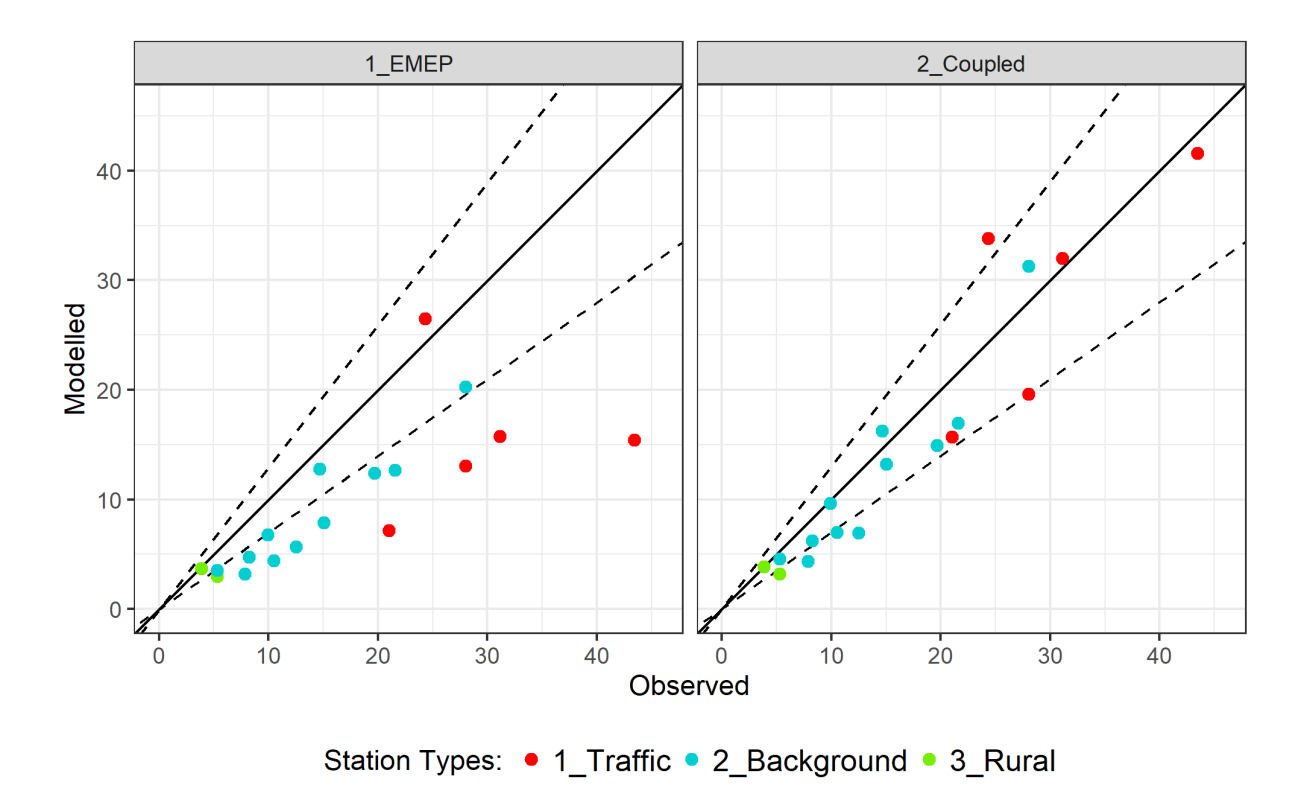
#### 8.1.1. NO<sub>2</sub>

Figures 8.1 and 8.2 show the annual average scatter plots for NO<sub>2</sub> for 2018 and 2019, respectively, for all continuous monitors with sufficient data capture (>50%); Tables 8.1 and 8.2 present statistics corresponding to hourly average concentration values. Scatter plots demonstrating the models' abilities in terms of predicting high concentrations corresponding to the 99.79<sup>th</sup> percentile of NO<sub>2</sub> hourly concentrations are shown in Figures 8.3 and 8.4.

Overall, the Coupled system generates good predictions of  $NO_2$  concentration at all continuous monitor sites in terms of both annual average and 99.79<sup>th</sup> percentile. From a spatial perspective, the highest concentrations are recorded at the traffic stations due to influences from nearby roads. Consequently, the regional model EMEP generally under-predicts in those locations because it is not designed to predict near-road concentrations. There is also a tendency for the Coupled system to under-predict at some background sites, specifically those corresponding to the lowest measured mean concentrations, away from the five main cities (specifically Brownes Road, Castlebar, Dundalk, Portlaoise and Seville Lodge). There is likely to be a number of contributory factors, as discussed further in the sensitivity testing described in Section 8.5 and Appendix D. Agreement at the two rural monitors is good on average for 2018, but one site shows model under-prediction for 2019. In terms of evaluation of hourly concentrations, the number of points within a factor of two of the observed are high ( $\geq$ 0.60) for background and traffic sites for the Coupled system, and NMSE values are low, particularly for the traffic stations ( $\leq$ 0.68).



Station Types: • 1\_Traffic • 2\_Background • 3\_Rural Figure 8.1 – 2018 NO<sub>2</sub> scatter plot of modelled versus measured annual average concentration (μg/m³) at continuous monitors, points coloured by site type with ±30% modelling uncertainty lines shown;



EMEP (left) and Coupled system (right).

**Figure 8.2** – 2019 NO<sub>2</sub> scatter plot of modelled versus measured annual average concentration (μg/m³) at continuous monitors, points coloured by site type with ±30% modelling uncertainty lines shown; EMEP (left) and Coupled system (right).

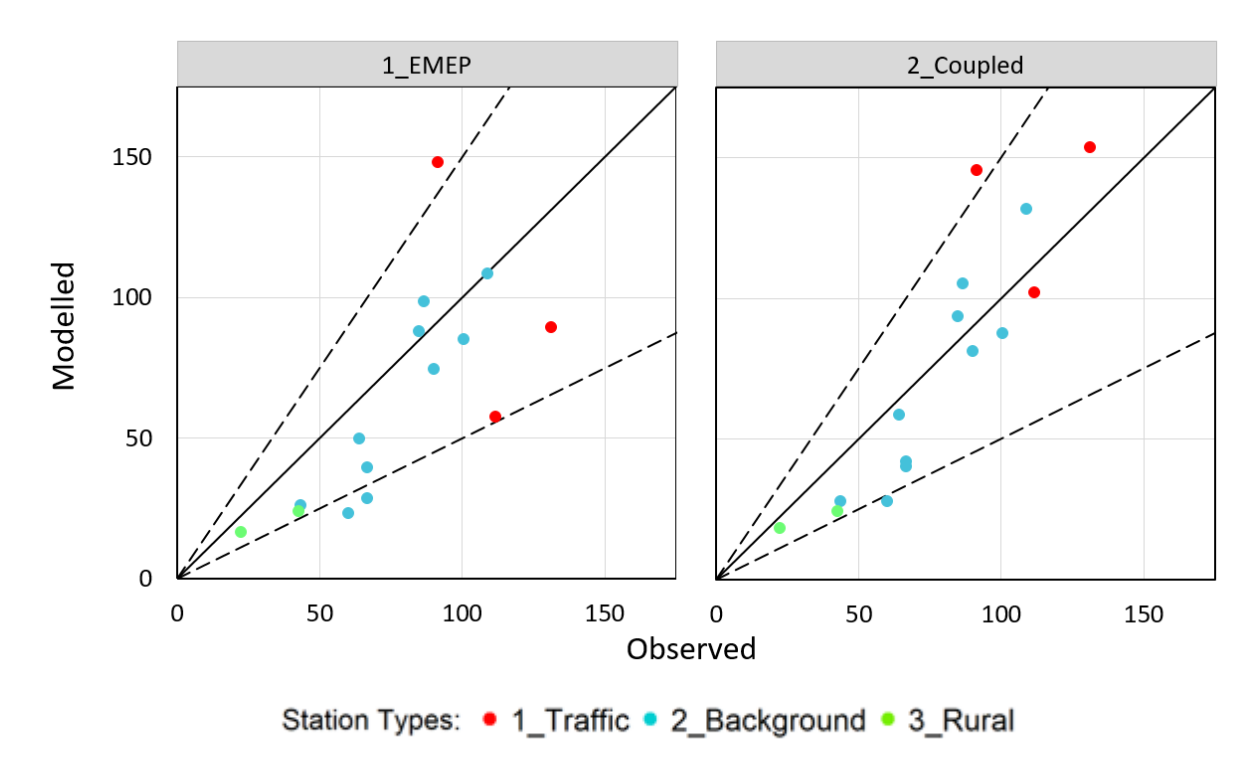


**Figure 8.3** – 2018 NO<sub>2</sub> scatter plot of modelled versus measured 99.79<sup>th</sup> percentile of hourly average concentration ( $\mu$ g/m³) at continuous monitors, points coloured by site type with  $\pm 50\%$  modelling uncertainty lines shown; EMEP (left) and Coupled system (right).

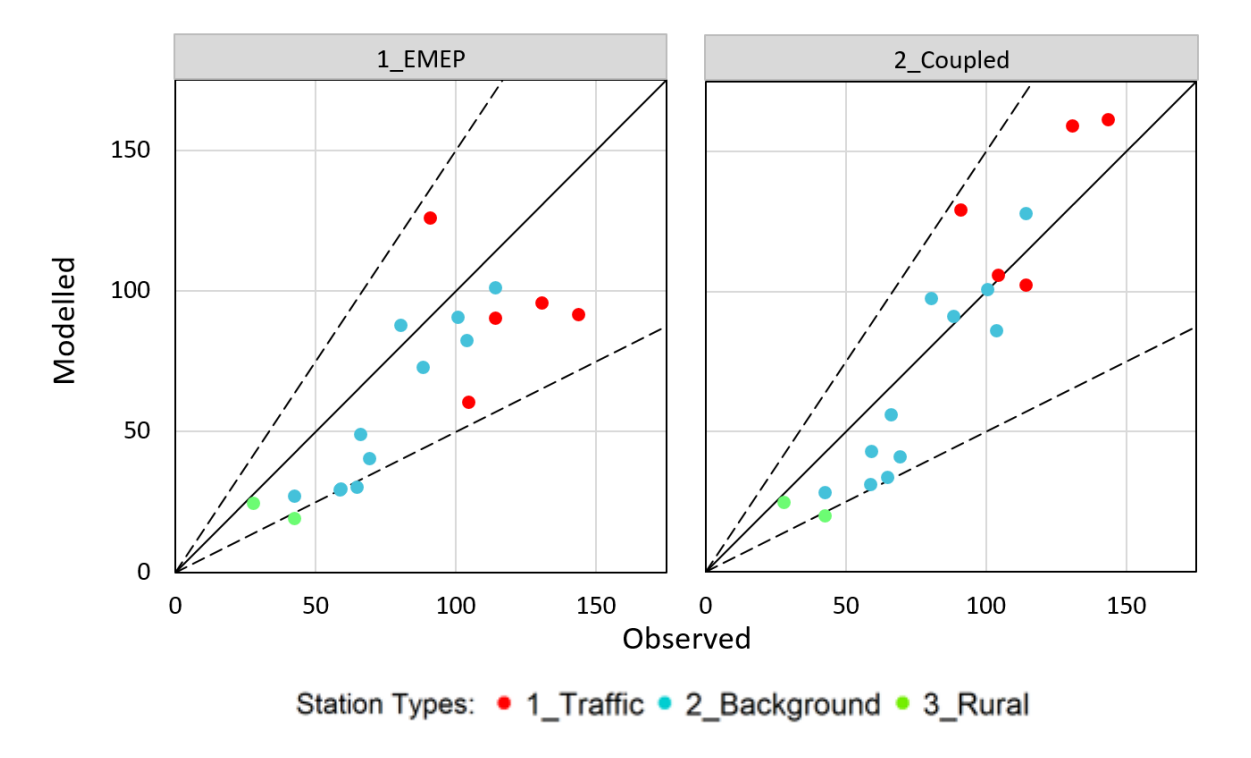


**Figure 8.4** – 2019 NO<sub>2</sub> scatter plot of modelled versus measured 99.79<sup>th</sup> percentile of hourly average concentration (μg/m³) at continuous monitors, points coloured by site type with ±50% modelling uncertainty lines shown; EMEP (left) and Coupled system (right).

**Table 8.1** – 2018 NO<sub>2</sub> model evaluation statistics, hourly average, by site type.

Station type	No. of	Model	Mean (µ	Mean (μg/m³)		R	Fac2	Fb
Station type	valid obs.	Model	Monitored	Modelled	NMSE	K	r ac2	ГD
Rural	15047	EMEP	EMEP 3.5	3.4	1.39	0.43	0.57	-0.03
Kurai	13047	Coupled		3.6	1.36	0.42	0.57	0.02
Daalramaund	82358	EMEP	15.1	8.8	1.37	0.63	0.50	-0.53
Background	82338	Coupled		12.4	0.80	0.68	0.66	-0.19
Traffic 20429	20420	EMEP	26.9	17.5	1.30	0.37	0.52	-0.42
	20429	Coupled	26.8	27.9	0.68	0.51	0.60	0.04

**Table 8.2** – 2019 NO<sub>2</sub> model evaluation statistics, hourly average, by site type.

Ctation towns	No. of	Model	Mean (μg/m³)		NMSE	ъ	Eas?	Fb
Station type	valid obs.	Model	Monitored	Modelled	NWISE	R	Fac2	Fb
Dumo1	16267	EMEP	1.6	3.3	1.80	0.37	0.50	-0.32
Rural	10207	Coupled	4.6	3.5	1.67	0.38	0.51	-0.26
Doolsonound	88403	EMEP	14.1	8.7	1.23	0.69	0.53	-0.47
Background	88403	Coupled		12.1	0.79	0.71	0.67	-0.15
Traffic 415	41590	EMEP	20.6	15.5	1.41	0.48	0.42	-0.63
	41389	Coupled	29.6	28.4	0.52	0.64	0.67	-0.04

Diffusion tubes are a less accurate method for recording  $NO_2$  concentrations and are only able to demonstrate monthly variation in concentrations. However, they are useful for providing indicative measured concentrations at hotspot locations for comparison with modelled values. The diffusion tube deployment in the five main cities in Ireland had relatively poor data capture, with some locations delivering as little as two months of data. Consequently, following bias correction of measured data, only directly corresponding temporal periods were compared during the evaluation process (as opposed to using annualised diffusion tube data for comparison with annual average modelled concentrations). In addition, two anomalously low diffusion tube measurements were removed from the dataset prior to calculation of period-average concentrations: North Wall 4 (DT90), with a value of 1.3  $\mu$ g/m³ measured during the period 31/01/2018 to 08/03/2018, and Bus Aras Environs 3 (Amien St. Upper, DT93) with a value of 0.7  $\mu$ g/m³ measured during the period 01/08/2018 to 30/08/2018.

Figures 8.5 and 8.6 show the period average scatter plots for NO<sub>2</sub> for 2018 and 2019, respectively, corresponding to values recorded on the diffusion tube networks. Monthly data was provided for Dublin for both years, but monthly data for the other four cities has only been supplied for 2019. Data capture ranged between 3 and 12 months of the year for the deployment of diffusion tubes in Dublin for 2018 and between 3 and 7 months for 2019. Data capture for 2019 for Cork, Limerick, Galway and Waterford was 4 to 8 months, 3 to 7 months, 2 to 11 months and 4 to 6 months, respectively.

The agreement between Coupled system modelled concentrations and diffusion tube measurements for Dublin for 2018 is good, with only 3 sites outside the modelling uncertainty criteria of  $\pm 30\%$ . However, with many measurements being available for periods substantially smaller than a year, there could be justification for applying slightly larger modelling uncertainty percentages. EMEP results have been included in the evaluation to provide context to the Coupled system concentrations, by quantifying the background contribution. This comparison shows the benefit of explicit road modelling for representing near-road concentrations.



The agreement for 2019 is not as good as for 2018 for Dublin, with the Coupled model underpredicting concentrations at some sites. In terms of the other cities:

#### Cork

Moderately high concentrations are measured, with two sites exceeding the  $40 \mu g/m^3$  limit as a period average. Model generally under-predicts concentrations.

#### Waterford

Measured concentrations are low in Waterford (less than 25  $\mu$ g/m³). The model underpredicts, with minimum values of approximately 50% of the measured concentration.

#### Limerick

Measured concentrations are less than 30  $\mu g/m^3$ , and the model has a tendency to underpredict.

#### Galway

Here inspection of monitor locations highlighted that a number of the monitors were adjacent to roads that were not included explicitly in the major road emissions inventory. These sites correspond to the results indicated by green crosses in Figure 8.6. Model performance is better for the remaining sites that have some roads in close proximity, but as for the other cities, there is some under-prediction.

A number of factors will contribute to the under-prediction of modelled NO<sub>2</sub> concentrations, although it is difficult to explain why agreement is worse for 2019. In general, the restriction that only roads with AAWT above 5000 vehicles per day have been modelled explicitly will contribute to model under-prediction. CERC highlighted that the model results would be improved if as many NTA traffic model roads as possible were included in the vicinity of the continuous monitors. In contrast, higher resolution road network data was not requested in the vicinity of the diffusion tubes, which will contribute to the under-prediction of modelled concentrations. For sites located in smaller towns and the outskirts of major cities, the issue with the lack of spatial variation of the atmospheric stability parameter, minimum Monin-Obukhov length, may contribute to the under-prediction in modelled concentrations (see Section 8.5). There is additionally some uncertainty associated with the placement of some of the diffusion tubes. It would be possible to review the pollution maps to identify whether the model predicts any concentrations similar to those recorded by the diffusion tubes.

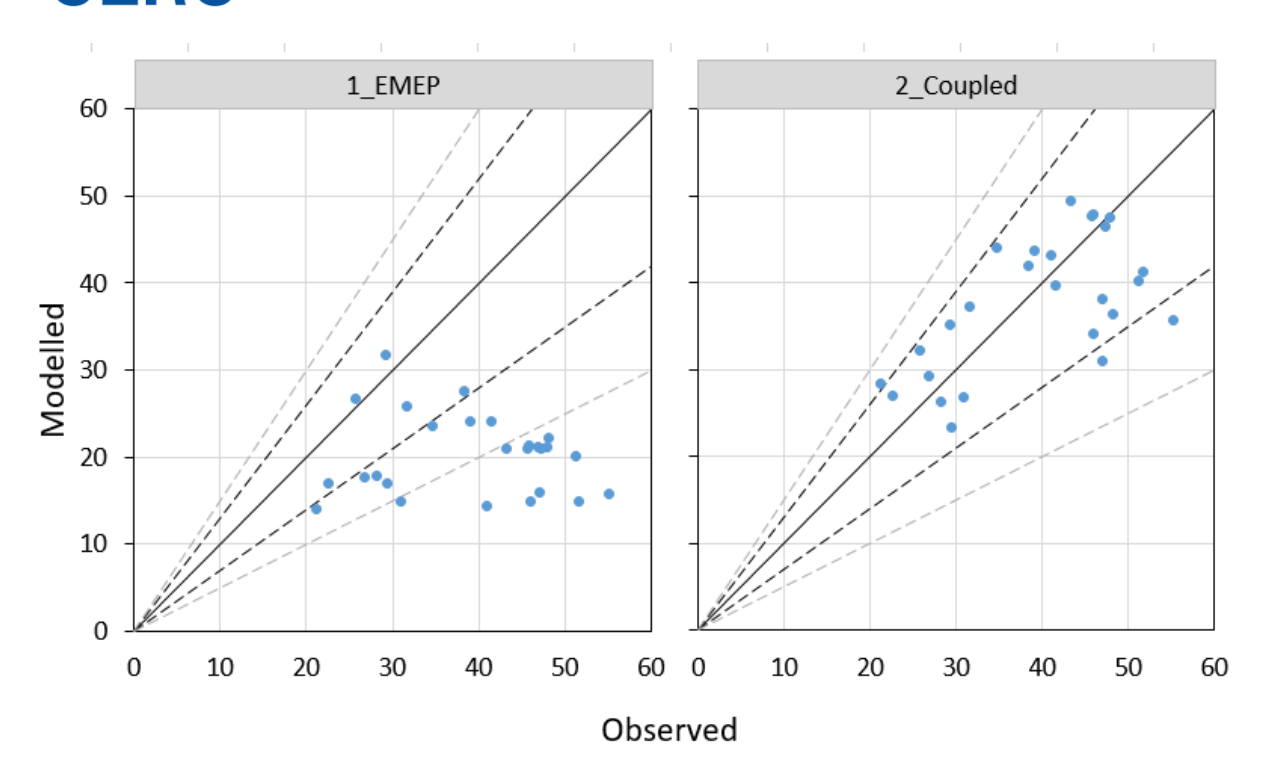


**Figure 8.5** – 2018 NO<sub>2</sub> scatter plot of modelled versus measured diffusion tube period average concentration ( $\mu$ g/m³), for Dublin sites only with  $\pm 30\%$  and  $\pm 50\%$  modelling uncertainty lines shown; EMEP (left) and Coupled system (right).

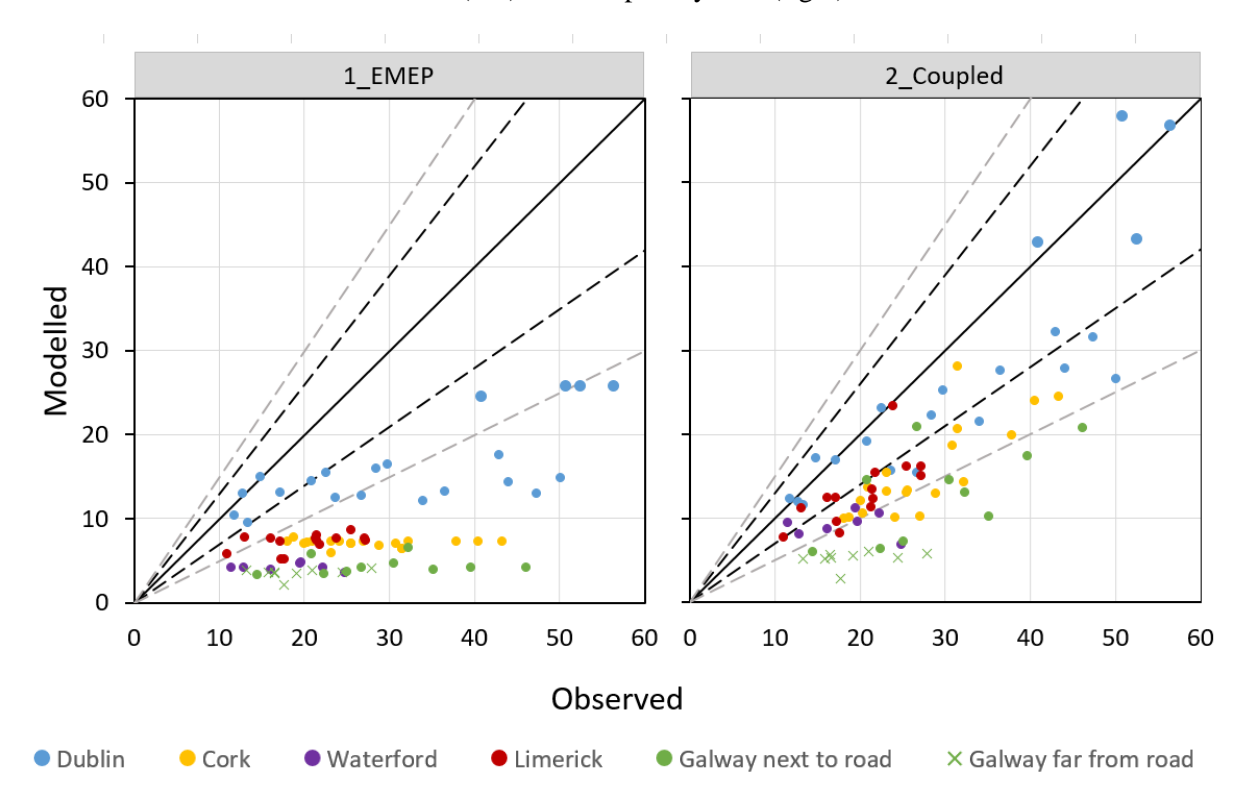


**Figure 8.6** – 2019 NO<sub>2</sub> scatter plot of modelled versus measured diffusion tube period average concentrations ( $\mu$ g/m³), with points coloured by site location with  $\pm$ 30% and  $\pm$ 50% modelling uncertainty lines shown; EMEP (left) and Coupled system (right).



#### 8.1.2. PM<sub>2.5</sub>

Figures 8.7 and 8.8 show the annual average scatter plots for  $PM_{2.5}$  for 2018 and 2019, respectively, for all continuous monitors with sufficient data capture (>50%). This data capture threshold resulted in no rural measurement sites for 2019. Tables 8.3 and 8.4 present statistics corresponding to daily average concentration values.

There are proportionally smaller differences between  $PM_{2.5}$  concentrations predicted by the EMEP and the Coupled system compared to  $NO_2$  because the majority of  $PM_{2.5}$  arises from regional and long-range atmospheric pollutant transport and chemistry, i.e. roadside increments of  $PM_{2.5}$  are relatively small, approximately 1-2  $\mu g/m^3$ . There is a slight negative bias in the Coupled system results, although this is less than 24% and 16% for both years at the background and traffic stations respectively. The number of points within a factor of two of the observed is over 79% for background sites and over 80% for traffic sites for both years for the Coupled system.

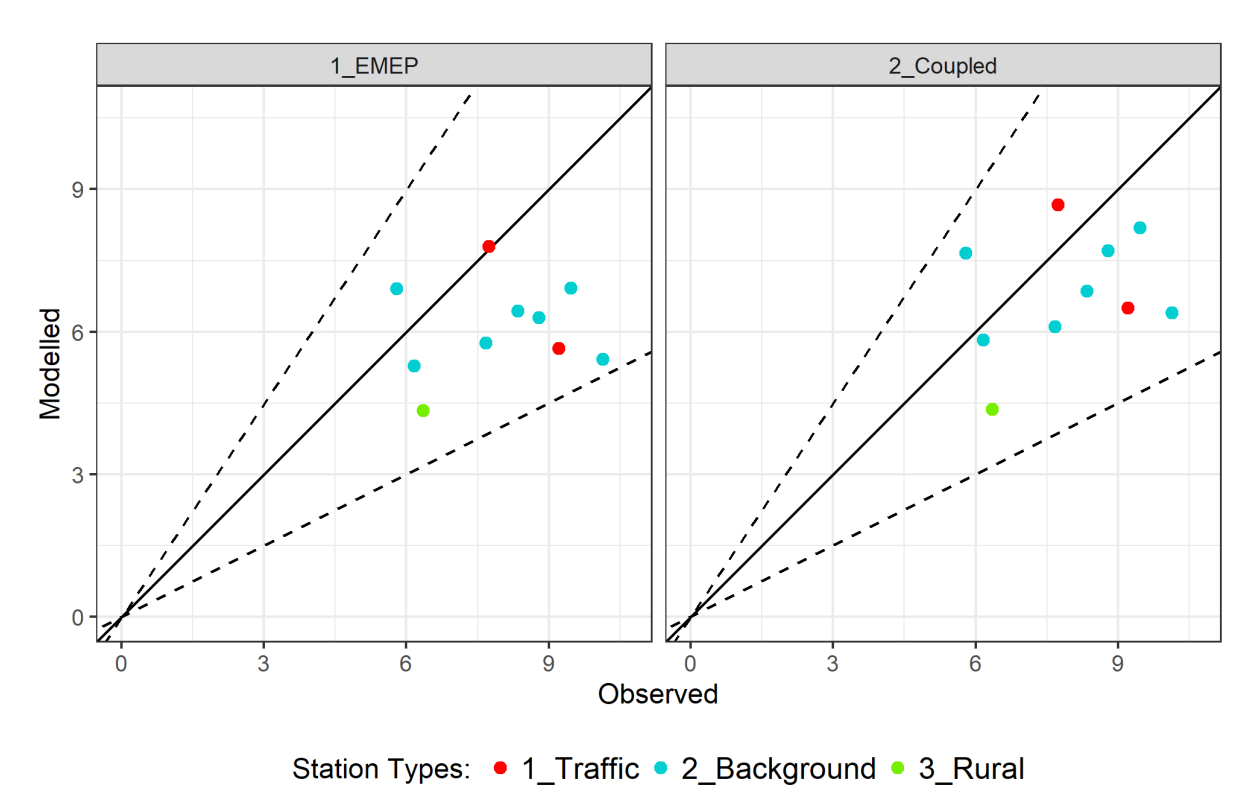


**Figure 8.7** – 2018 PM<sub>2.5</sub> scatter plot of modelled versus measured annual average concentration ( $\mu$ g/m³) at continuous monitors, points coloured by site type with  $\pm 50\%$  modelling uncertainty lines shown; EMEP (left) and Coupled system (right).

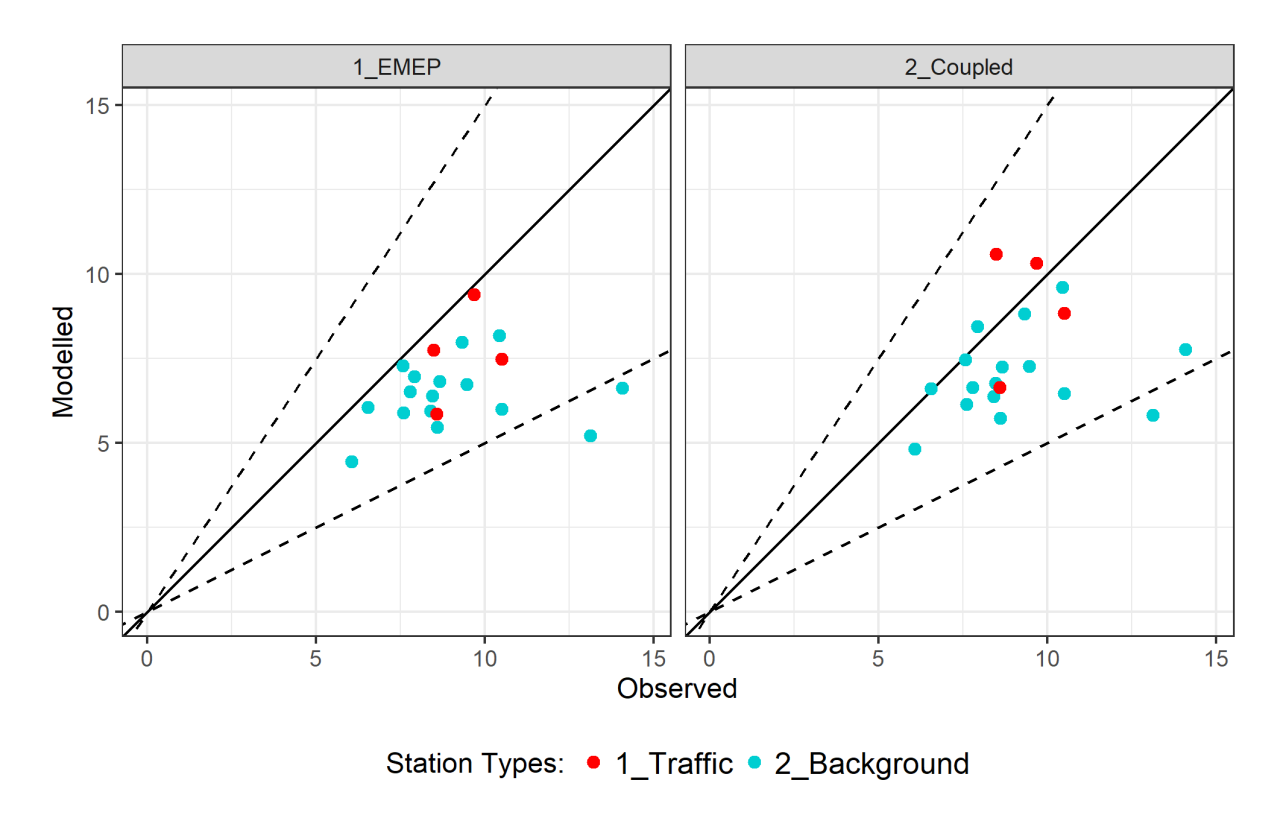


**Figure 8.8** – 2019 PM<sub>2.5</sub> scatter plot of modelled versus measured annual average concentration ( $\mu$ g/m³) at continuous monitors, points coloured by site type with  $\pm 50\%$  modelling uncertainty lines shown; EMEP (left) and Coupled system (right).

**Table 8.3** – 2018 PM<sub>2.5</sub> model evaluation statistics, daily average, by site type

No. of		Model	Mean (µ	ug/m³)	NMSE	R	Fac2	Fb
Station type	valid obs.	Model	Monitored	Modelled	MMSE	K	rac2	LD
Dame 1	260	EMEP	6.2	4.3	0.48	0.76	0.65	-0.38
Rural	360	Coupled	6.3	4.4	0.47	0.76	0.66	-0.37
D1 1	22.45	EMEP	8.1	6.2	0.74	0.52	0.73	-0.27
Background	2245	Coupled		7.0	0.59	0.54	0.80	-0.14
True CC' - 5.5.4	551	EMEP	0.6	6.5	0.69	0.56	0.74	-0.28
Traffic	554	Coupled	8.6	7.3	0.55	0.58	0.80	-0.16

Table 8.4 – 2019 PM<sub>2.5</sub> model evaluation statistics, daily average, by site type

Station type	No. of	Model	Mean (µ	Mean (μg/m³)		R	Fac2	Fb
Station type	valid obs.	Model	Monitored	Modelled	NMSE	N	rac2	FD
Durol	<b>n</b> /o	EMEP	n/a	-	-	-	-	-
Kurai	Rural n/a	Coupled	II/a	-	-	-	-	-
Daalramaund	5225	EMEP	9.0	6.5	0.87	0.66	0.74	-0.33
Background	5335	Coupled		7.1	0.74	0.67	0.79	-0.24
Traffic 1358	1250	EMEP	9.3	7.7	0.39	0.81	0.85	-0.19
	1338	Coupled		9.2	0.31	0.80	0.87	-0.01

#### 8.1.3. PM<sub>10</sub>

Figures 8.9 and 8.10 show the annual average scatter plots for  $PM_{10}$  for 2018 and 2019, respectively. All sites displayed correspond to continuous monitors with data capture >50%. Scatter plots demonstrating the models' abilities in terms of predicting high concentrations corresponding to the 90.41<sup>st</sup> percentile of  $PM_{10}$  daily concentrations are shown in Figures 8.11 and 8.12. Tables 8.5 and 8.6 present statistics corresponding to 24-hour average concentration values.

The magnitude of differences between  $PM_{10}$  concentrations predicted by EMEP and the Coupled system are larger than for  $PM_{2.5}$  at traffic sites because road traffic emits coarse fraction particles from the non-exhaust processes of brake, tyre and road wear, in addition to generating suspended particulates. The contribution of these road source emissions to total  $PM_{10}$  concentrations is more accurately modelled in the Coupled system compared to EMEP. However, as for  $PM_{2.5}$ , the majority of  $PM_{10}$  arises from regional and long-range atmospheric pollutant transport and chemistry. Roadside increments of  $PM_{10}$  range from 1.6-2.7  $\mu g/m^3$  over the two years, with the smaller value corresponding to 2018, where data for fewer sites was available for analysis. The Coupled system results have a near-zero mean bias for traffic sites in 2019, along with a relatively high percentage of points within a factor of two of the observed for both years (80%). Correlations are generally low for  $PM_{10}$ , although values are better in 2019 compared to 2018 (0.61 and 0.44 at traffic sites, respectively). The low correlation can be explained by the lack of granularity of local  $PM_{10}$  emissions sources within the emissions inventory e.g. construction sites and cooking sources.

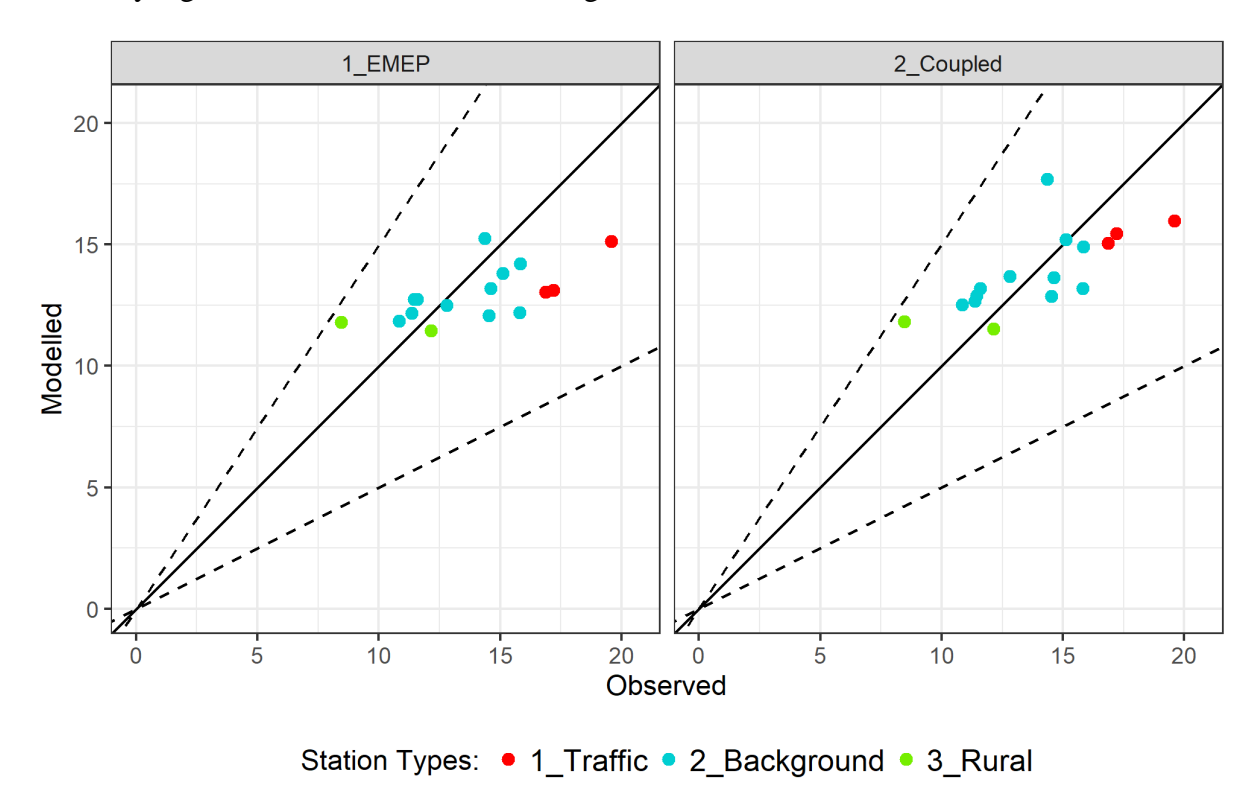


**Figure 8.9** – 2018 PM<sub>10</sub> scatter plot of modelled versus measured annual average concentration ( $\mu$ g/m³) at continuous monitors, points coloured by site type with  $\pm 50\%$  modelling uncertainty lines shown; EMEP (left) and Coupled system (right).

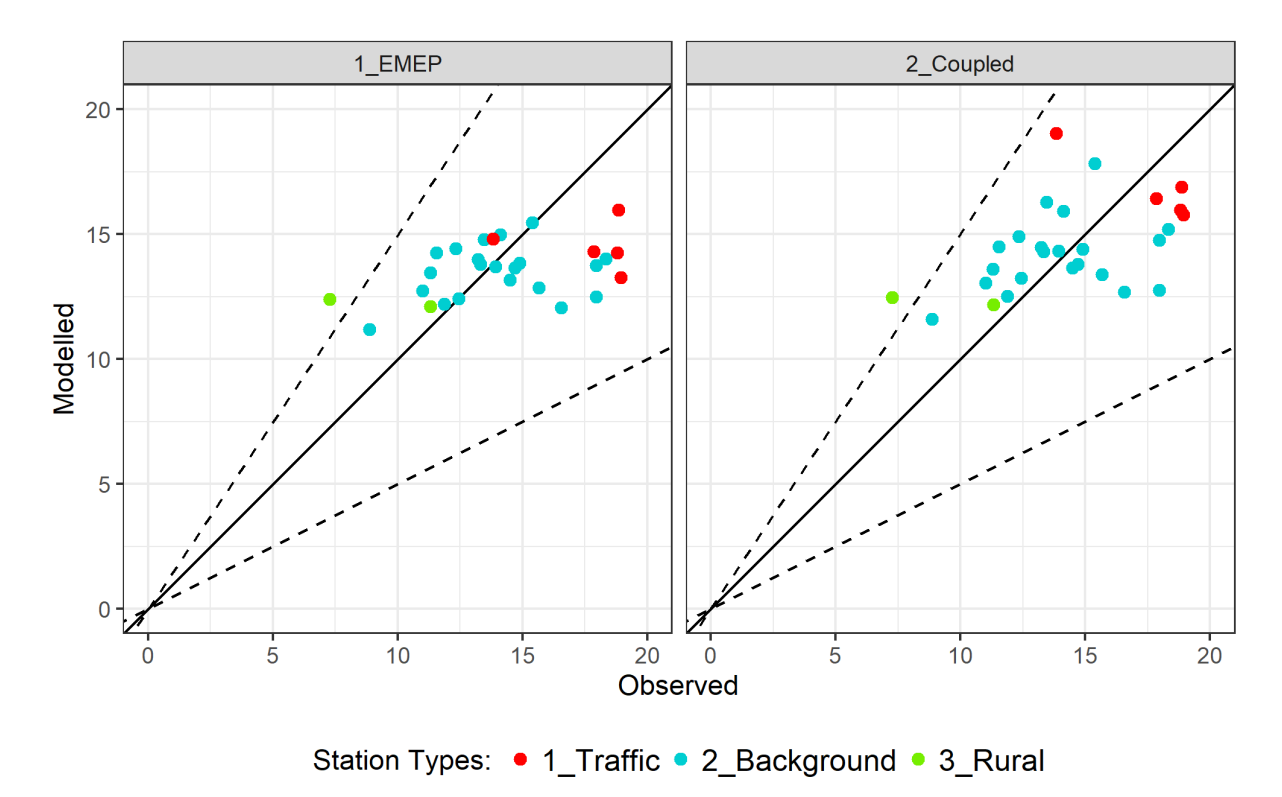


**Figure 8.10** – 2019 PM<sub>10</sub> scatter plot of modelled versus measured annual average concentration ( $\mu$ g/m³) at continuous monitors, points coloured by site type with  $\pm 50\%$  modelling uncertainty lines shown; EMEP (left) and Coupled system (right).

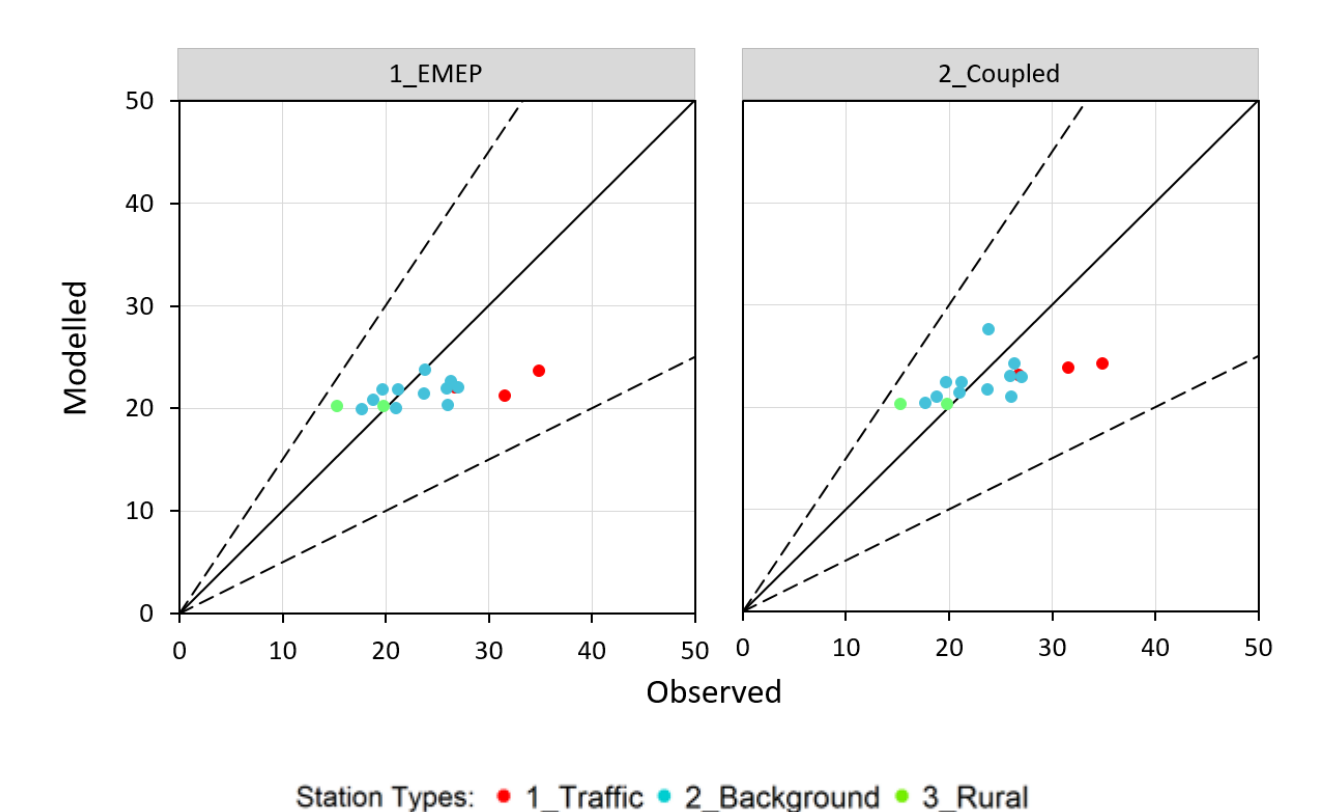
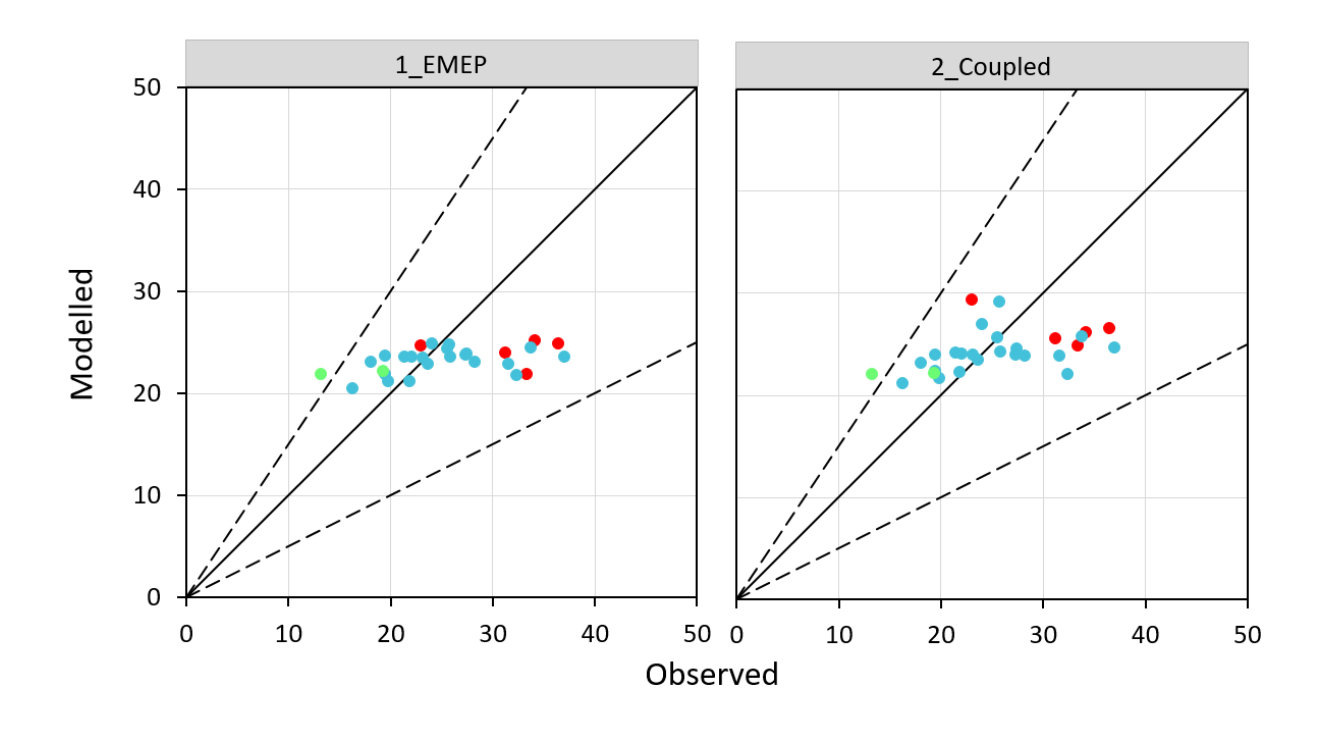


**Figure 8.11** – 2018 PM<sub>10</sub> scatter plot of modelled versus measured 90.41<sup>st</sup> percentile daily average concentration ( $\mu$ g/m³) at continuous monitors, points coloured by site type with  $\pm$ 50% modelling uncertainty lines shown; EMEP (left) and Coupled system (right).



Station Types: • 1\_Traffic • 2\_Background • 3\_Rural

**Figure 8.12** – 2019 PM<sub>10</sub> scatter plot of modelled versus measured 90.41<sup>st</sup> percentile daily average concentration ( $\mu$ g/m³) at continuous monitors, points coloured by site type with  $\pm$ 50% modelling uncertainty lines shown; EMEP (left) and Coupled system (right).

**Table 8.5** – 2018  $PM_{10}$  model evaluation statistics, daily average, by site type.

Station type	No. of	Model	Mean (µ	Mean (μg/m³)		R	Fac2	Fb
Station type	valid obs.	Model	Monitored	Modelled	NMSE	IX.	rac2	FD
Dumo1	Rural 706	EMEP	10.2	11.6	0.35	0.44	0.76	0.12
Kurai		Coupled	10.3	11.7	0.35	0.44	0.77	0.12
Dealronound	2592	EMEP	13.4	13.0	0.31	0.45	0.83	-0.03
Background	3583	Coupled		13.9	0.29	0.47	0.83	0.03
TD 66" 1000	1022	EMEP	17.0	13.7	0.40	0.38	0.76	-0.26
Traffic	1033	Coupled	17.8	15.5	0.29	0.44	0.84	-0.14

**Table 8.6** – 2019  $PM_{10}$  model evaluation statistics, daily average, by site type.

Station tyme	No. of	Model Mean		ug/m³)	NMSE	R	Fac2	Fb
Station type	valid obs.	Model	Monitored	Modelled	MMSE	K	rac2	ΓU
Dumo1	604	EMEP	EMEP 9.2	12.3	0.45	0.56	0.66	0.28
Rural	694	Coupled		12.3	0.45	0.56	0.66	0.29
Daalsananad	7044	EMEP	14.0	13.6	0.38	0.56	0.83	-0.03
Background	7044	Coupled		14.2	0.36	0.57	0.84	0.02
T fC: . 1.000	1660	EMEP	17.6	14.5	0.39	0.61	0.80	-0.19
Traffic	1660	Coupled	17.6	16.9	0.31	0.61	0.84	-0.04



#### 8.1.4. O<sub>3</sub>

Scatter plots demonstrating the models' abilities for predicting high concentrations corresponding to the  $93.15^{th}$  percentile of maximum daily 8-hour rolling  $O_3$  concentrations are shown in Figures 8.13 and 8.14. All sites displayed correspond to continuous monitors with data capture >50%. Tables 8.7 and 8.8 present statistics corresponding to maximum daily 8-hour rolling average concentrations.

Differences between O<sub>3</sub> concentrations predicted by EMEP and the Coupled system are small because O<sub>3</sub> is not a directly emitted pollutant. The spatial and temporal variations of O<sub>3</sub> are a result of complex atmospheric chemistry processes which occur both at the regional scale, modelled by EMEP, and as part of fast NO<sub>X</sub> chemistry, which occurs within metres of road sources and is modelled by ADMS-Urban. The dominant near-road NO<sub>X</sub> chemical reaction (titration of O<sub>3</sub> by NO) results in a reduction of O<sub>3</sub> in roadside environments compared to rural locations. Consequently, the Coupled system predicts slightly lower traffic and background O<sub>3</sub> concentrations compared to EMEP. The scatter plots and statistics indicate good agreement between modelled and measured O<sub>3</sub>, with over 90% of modelled values within a factor of two of the observed at all locations for the Coupled system. Overall however, Tables 8.7 and 8.8 indicate that there is a positive bias in modelled concentrations, although this is relatively small in rural areas, where O<sub>3</sub> concentrations are highest (fractional biases of 0.06 and 0.03 for the Coupled system for 2018 and 2019 respectively). Poorer agreement at background and traffic sites, and less variability in the modelled concentrations compared to measurements, may relate to emissions inventory inaccuracies (NO<sub>X</sub> and VOC).

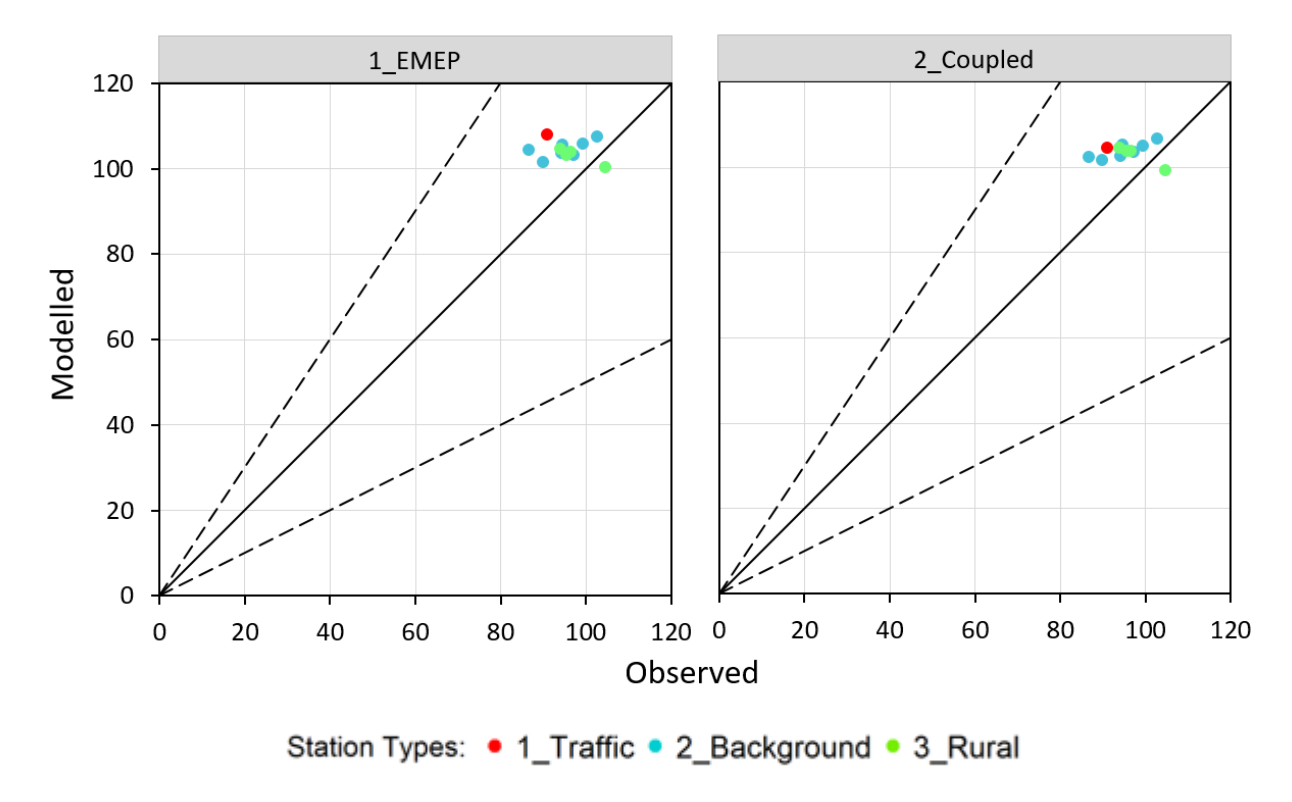


**Figure 8.13** – 2018  $O_3$  scatter plot of modelled versus measured 93.15<sup>th</sup> percentile of daily maximum 8-hourly rolling average concentration ( $\mu g/m^3$ ) at continuous monitors, points coloured by site type with  $\pm 50\%$  modelling uncertainty lines shown; EMEP (left) and Coupled system (right).

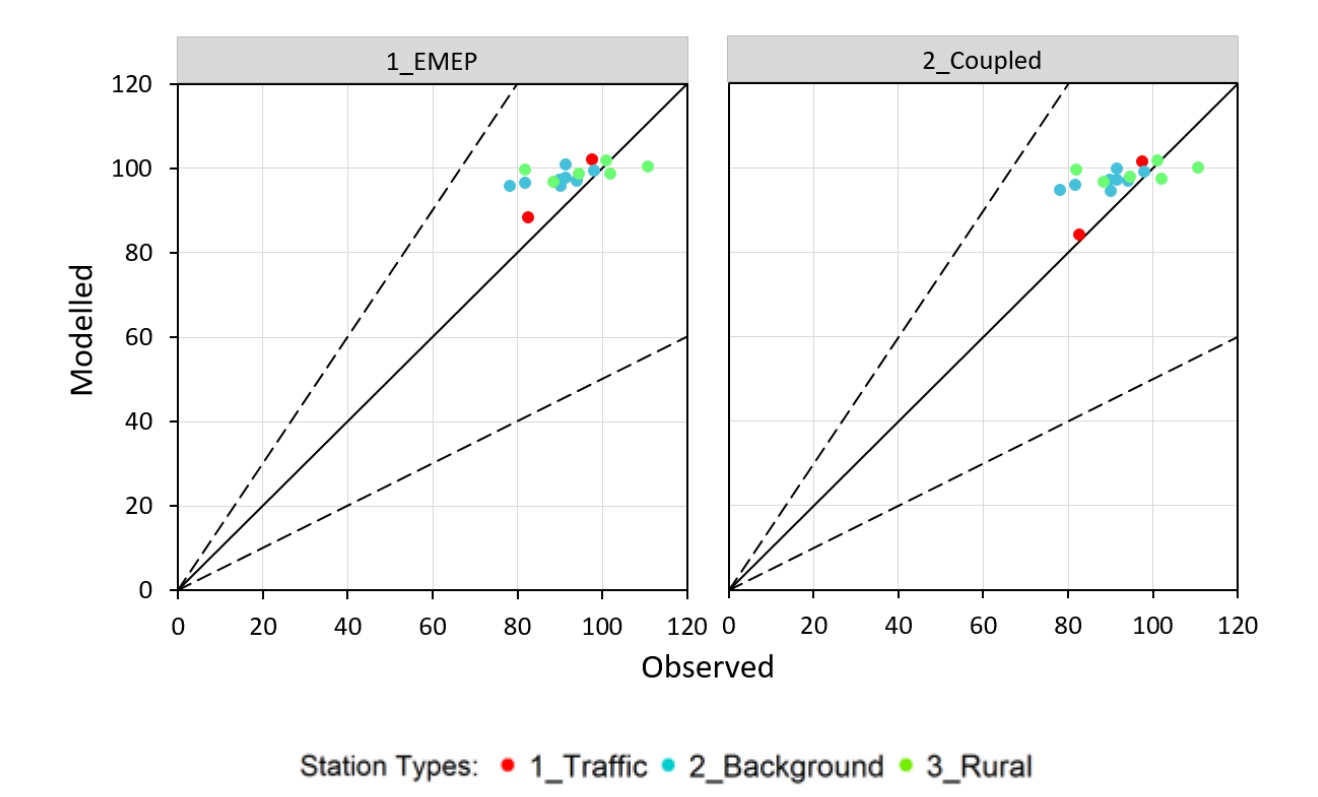


**Figure 8.14** – 2019  $O_3$  scatter plot of modelled versus measured 93.15<sup>th</sup> percentile of daily maximum 8-hourly rolling average concentration ( $\mu g/m^3$ ) at continuous monitors, points coloured by site type with  $\pm 50\%$  modelling uncertainty lines shown; EMEP (left) and Coupled system (right).

**Table 8.7** – 2018 O<sub>3</sub> model evaluation statistics, maximum daily 8-hour rolling average, by site type.

No. of		Model	Mean (µ	ug/m³)	NMSE	R	Fac2	Fb
Station type	valid obs.	Model	Monitored	Modelled	MINISE	K	rac2	гu
Daniel 1	1 1407	EMEP	74.0	80.3	0.03	0.74	1.00	0.07
Rural	1407	Coupled	74.9	79.9	0.03	0.74	1.00	0.06
D1 1	2410	EMEP	69.2	79.9	0.04	0.78	0.99	0.14
Background	2410	Coupled		78.7	0.04	0.78	1.00	0.13
Traction 202	202	EMEP	567	81.3	0.18	0.73	0.84	0.36
Traffic	292	Coupled	56.7	76.5	0.13	0.77	0.91	0.30

**Table 8.8** – 2019 O<sub>3</sub> model evaluation statistics, maximum daily 8-hour rolling average, by site type.

Station type	No. of	Model	Mean (µ		NMSE	R	Fac2	Fb
Station type	valid obs.	Model	Monitored	Modelled	NIVISE	N	rac2	ΓD
Duro1	2105	EMEP	75.4	78.6	0.03	0.72	1.00	0.04
Kurai	Rural 2105	Coupled	73.4	78.1	0.03	0.72	1.00	0.03
Do alsonoun d	2742	EMEP	65.7	76.3	0.05	0.72	0.98	0.15
Background	2742	Coupled		75.1	0.05	0.73	0.98	0.13
Traffic 599	500	EMEP	60.0	73.1	0.11	0.55	0.92	0.18
	399	Coupled	60.9	68.5	0.10	0.56	0.93	0.12



#### 8.2 FAIRMODE metrics

FAIRMODE Target plots and associated metrics are presented separately for 2018 and 2019, for  $NO_2$ ,  $PM_{2.5}$ ,  $PM_{10}$  and  $O_3$  in Sections 8.2.1, 8.2.2, 8.2.3 and 8.2.4, respectively. Target plot metric definitions are given in Appendix B. In summary, modelling system outputs satisfy the Model Quality Objective (MQO) if the Model Quality Indicator (MQI) is less than or equal to unity. There are two MQIs, one relates to short-term metrics (hourly / daily / maximum daily 8-hour) and the other is an annual metric. For a modelling system that calculates short-term as well as annual concentrations, both metrics must be satisfied. The annual metric is usually more stringent.

Of note is that all stations are included in the FAIRMODE metric calculations. Satisfying the MQO for rural, background and traffic stations indicates that the system performs sufficiently well at all spatial scales, from regional to roadside.

The Target plot diagrams are generated in CERC's Model Evaluation Toolkit using formulation and parameters consistent with the most recent implementation within the Delta Tool (Version 7.0, April 2022).

#### 8.2.1. NO<sub>2</sub>

Figures 8.15 and 8.16 show the Target plots for 2018 and 2019 for NO<sub>2</sub>, and the associated hourly and annual MQI values are presented in Table 8.9. The Coupled system comfortably achieves the objectives for both years. The regional model passes the hourly criteria but fails the annual metric. Annual metric evaluates variation between sites, whereas the hourly metric gives weighting in terms of hour-by-hour performance/correlation. For pollutants with strong diurnal variations (e.g. NO<sub>2</sub>, O<sub>3</sub>), if the model correctly represents the diurnal variation, but not the overall magnitude, then the MQI\_HD may be lower than MQI\_YR.

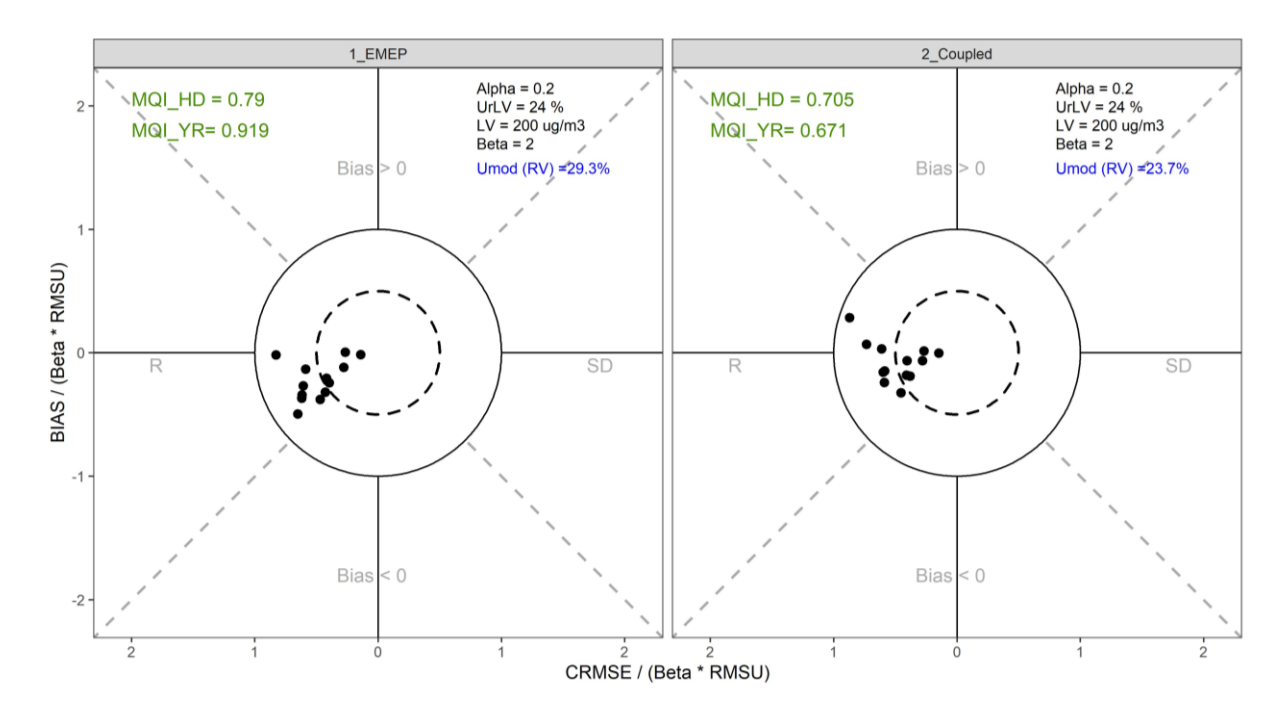


Figure 8.15 – 2018 NO<sub>2</sub> FAIRMODE Target plot (all stations).



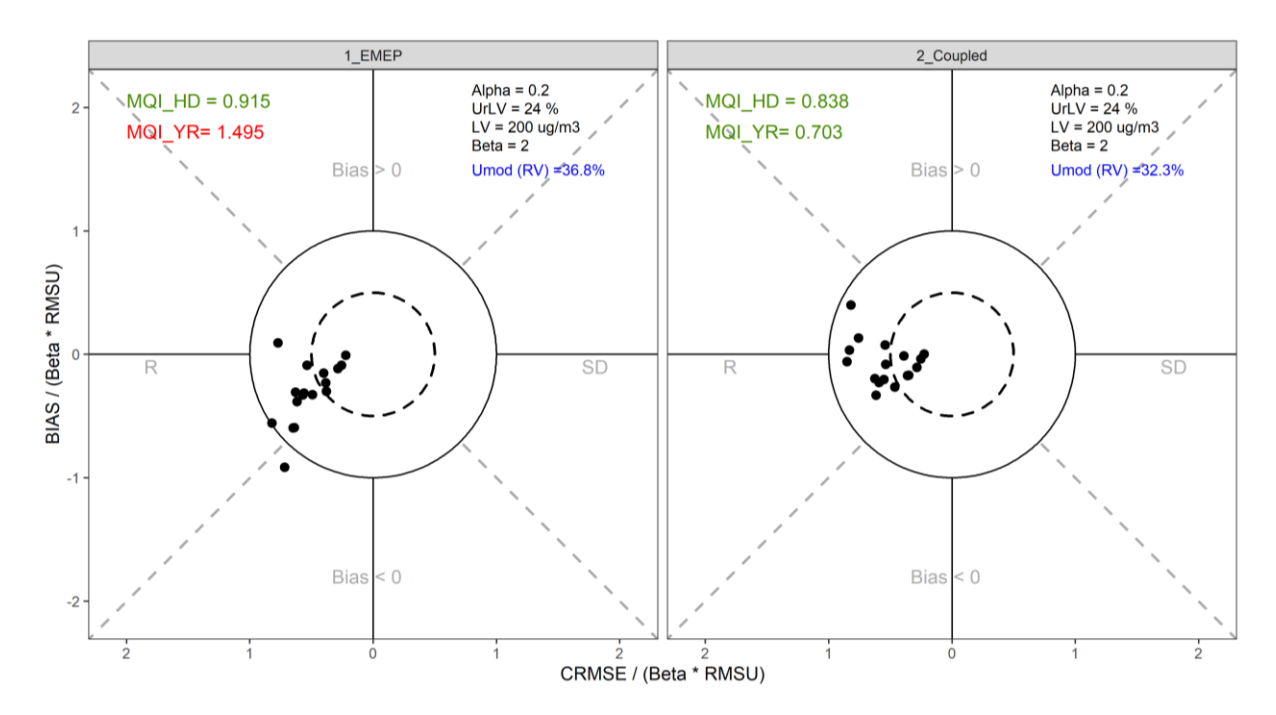


Figure 8.16 – 2019 NO<sub>2</sub> FAIRMODE Target plot (all stations).

**Table 8.9** – NO<sub>2</sub> Model Quality Indicators (all stations).

Station type	Model	MQI_HD	MQI_YR
2018	EMEP	0.79	0.919
2018	Coupled	0.705	0.671
2019	EMEP	0.915	1.495
2019	Coupled	0.838	0.703

#### 8.2.2. PM<sub>2.5</sub>

Figures 8.17 and 8.18 show the Target plots for 2018 and 2019 for  $PM_{2.5}$ , and the associated daily and annual MQIs are presented in Table 8.10. Both EMEP and the Coupled system easily achieve the objectives for both years. This is in part because the uncertainty associated with  $PM_{2.5}$  measurements is relatively high, which through the definition of the evaluation metrics makes the criteria more easily satisfied than for  $NO_2$ , where the relative measurement uncertainty is lower.



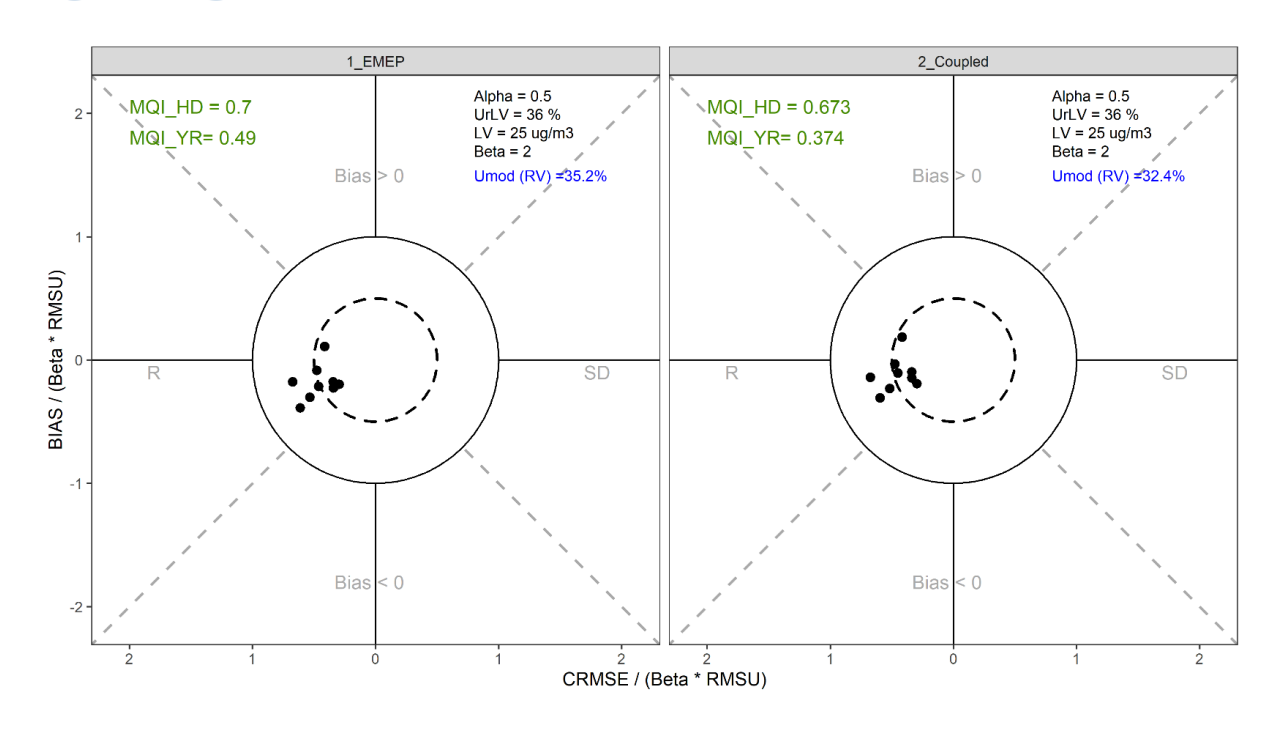


**Figure 8.17** – 2018 PM<sub>2.5</sub> FAIRMODE Target plot (all stations).

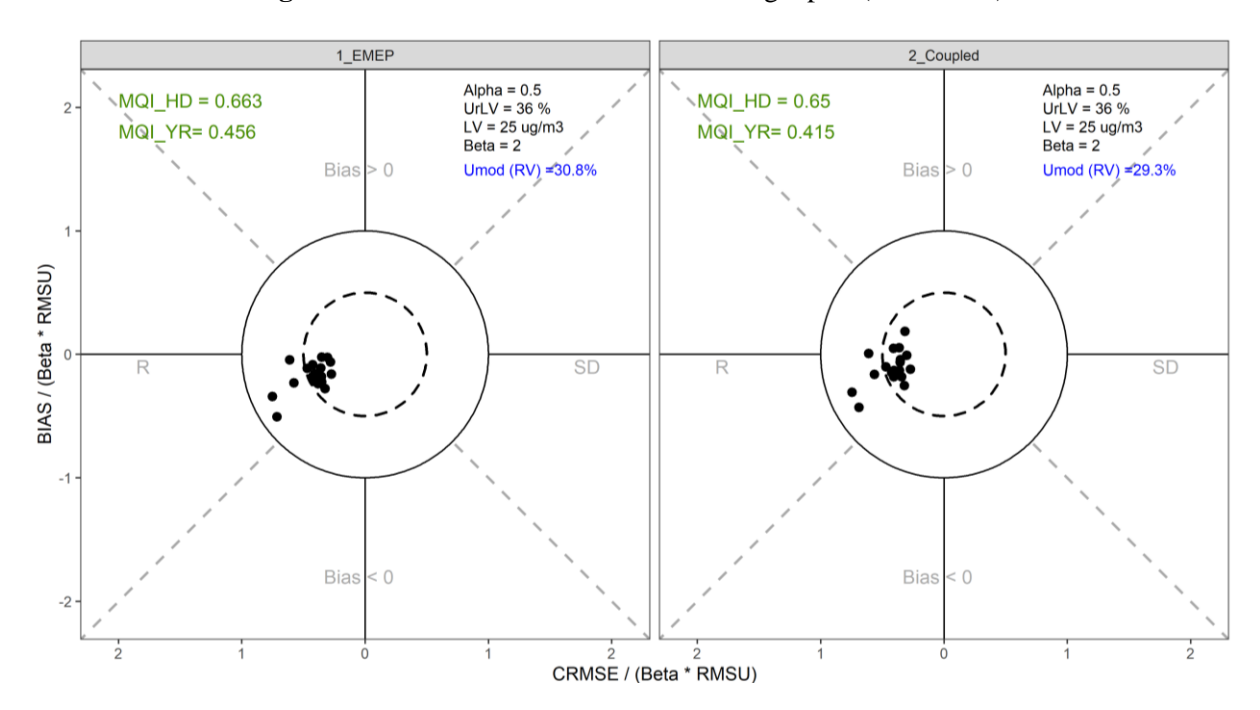


**Figure 8.18** – 2019 PM<sub>2.5</sub> FAIRMODE Target plot (all stations).

**Table 8.10** – PM<sub>2.5</sub> Model Quality Indicators (all stations).

Station type	Model	MQI_HD	MQI_YR
2018	EMEP	0.70	0.49
2018	Coupled	0.673	0.374
2019	EMEP	0.663	0.456
2019	Coupled	0.650	0.415



#### 8.2.3. PM<sub>10</sub>

Figures 8.19 and 8.20 show the Target plots for 2018 and 2019 for  $PM_{10}$ , and the associated daily and annual MQIs are presented in Table 8.11. As for  $PM_{2.5}$ , EMEP and the Coupled system achieve the objectives for both years by a substantial margin and again this is in part because the uncertainty associated with  $PM_{10}$  measurements is relatively high, making the criteria relatively easy to satisfy.

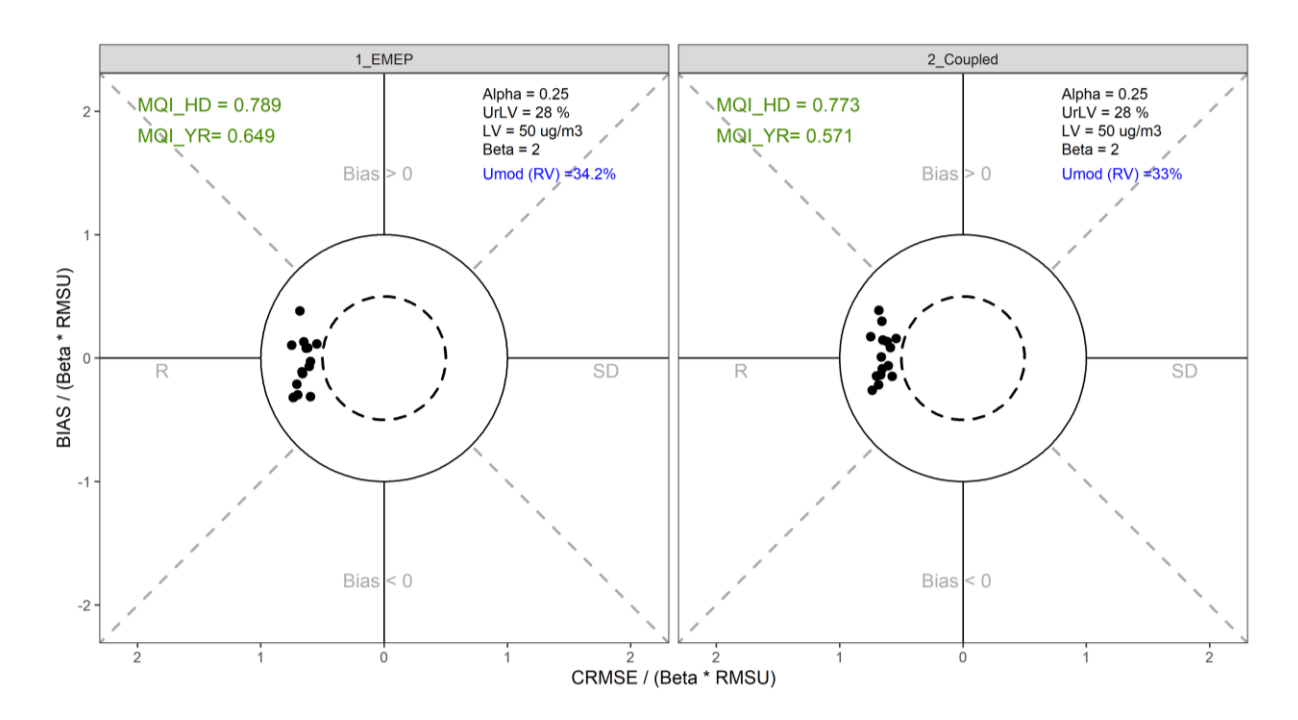


**Figure 8.19** – 2018 PM<sub>10</sub> FAIRMODE Target plot (all stations).

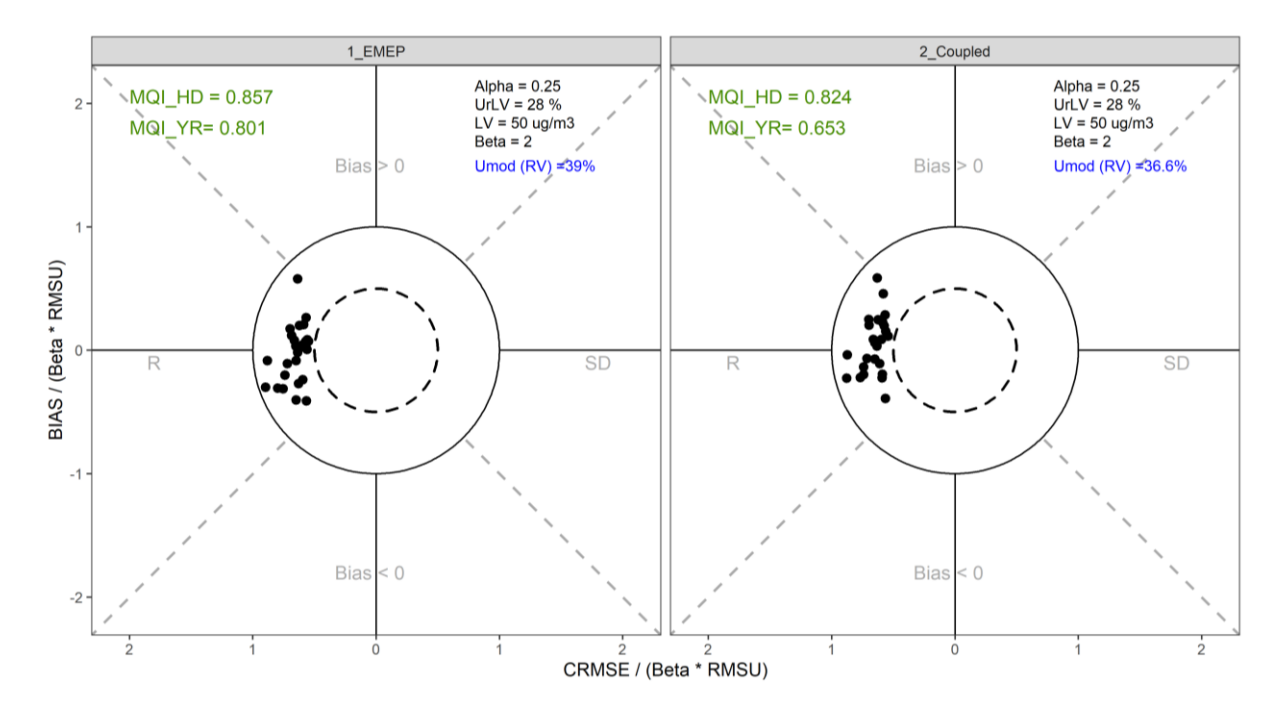


**Figure 8.20** – 2019 PM<sub>10</sub> FAIRMODE Target plot (all stations).



**Table 8.11** – PM<sub>10</sub> Model Quality Indicators (all stations).

Station type	Model	MQI_HD	MQI_YR
2018	EMEP	0.789	0.649
2018	Coupled	0.773	0.571
2019	EMEP	0.857	0.801
2019	Coupled	0.824	0.653

#### 8.2.4. O<sub>3</sub>

Figures 8.21 and 8.22 show the Target plots for 2018 and 2019 for O<sub>3</sub>, and the associated maximum daily 8-hour rolling and annual MQIs are presented in Table 8.12. The regional model and Coupled system both achieve the objectives for both years.

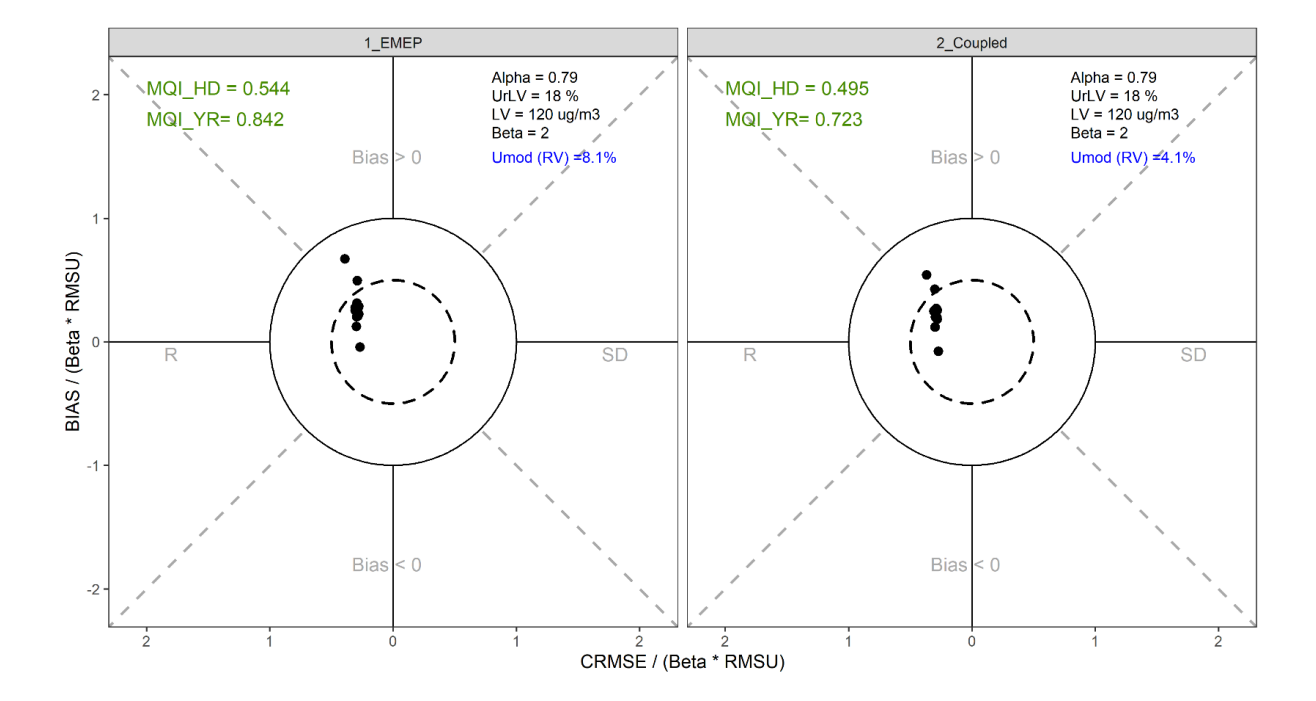


**Figure 8.21** – 2018 FAIRMODE O<sub>3</sub> Target plot (all stations).



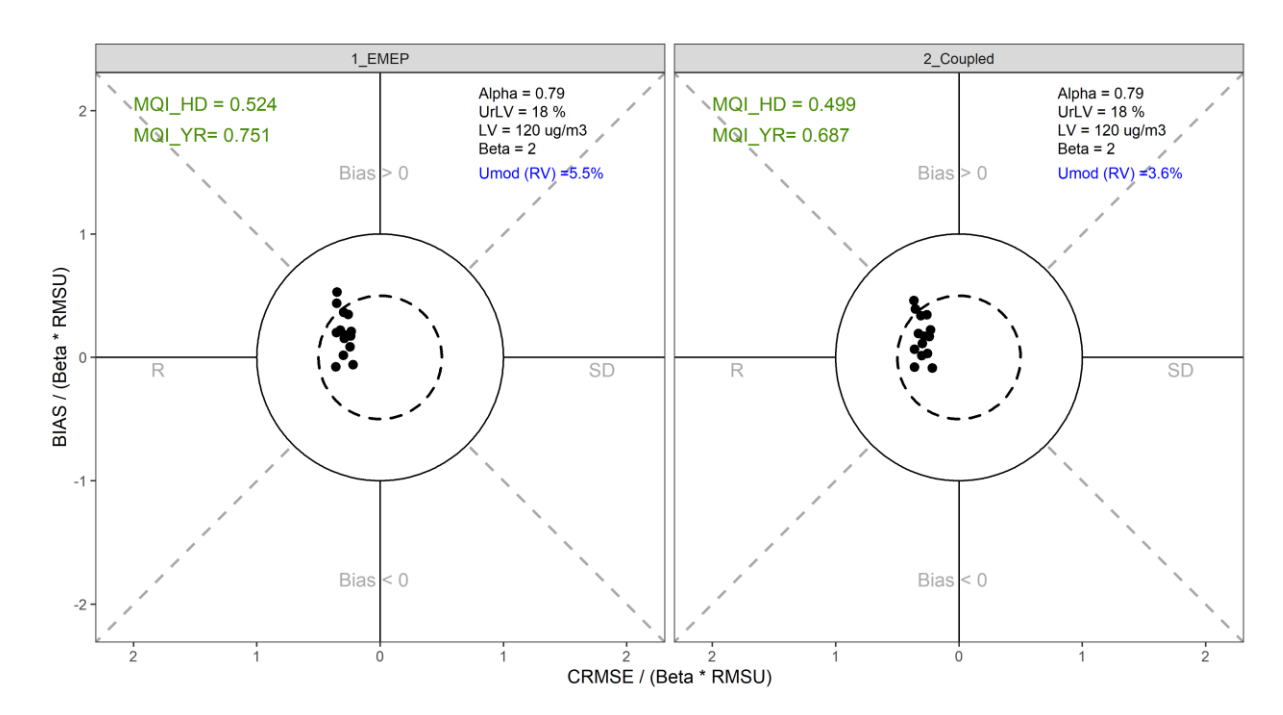


Figure 8.22 – 2019 FAIRMODE O<sub>3</sub> Target plot (all stations).

**Table 8.12** – O<sub>3</sub> Model Quality Indicators (all stations).

Station type	Model	MQI_HD	MQI_YR		
2018	EMEP	0.544	0.842		
	Coupled	0.495	0.723		
2019	EMEP	0.524	0.751		
	Coupled	0.499	0.687		

#### 8.3 Temporal variations

The Model Evaluation Toolkit generates a series of time variation plots<sup>17</sup> which allow supplementary model performance assessment, beyond the metrics defined in the AQSR. Some example comparisons of time variations are presented in this section.

 $NO_X$  concentration evaluations were omitted from earlier analyses because  $NO_X$  is not included in the AQSR as a human health air pollutant. However, evaluation of  $NO_X$  performance can be informative because ambient  $NO_X$  has a relatively short pollutant lifetime in the atmosphere, i.e. on the regional scale  $NO_X$  is converted into other species, such as ammonium nitrate. However, at the urban scale,  $NO_X$  remains approximately invariant with regard to chemical reactions and concentrations are dominated by local emissions. Thus,  $NO_X$  acts as a useful pollutant for evaluating model performance in terms of city-scale dispersion (as opposed to chemistry) processes.

<sup>&</sup>lt;sup>17</sup> These are generated using the OpenAir package within R software [43]

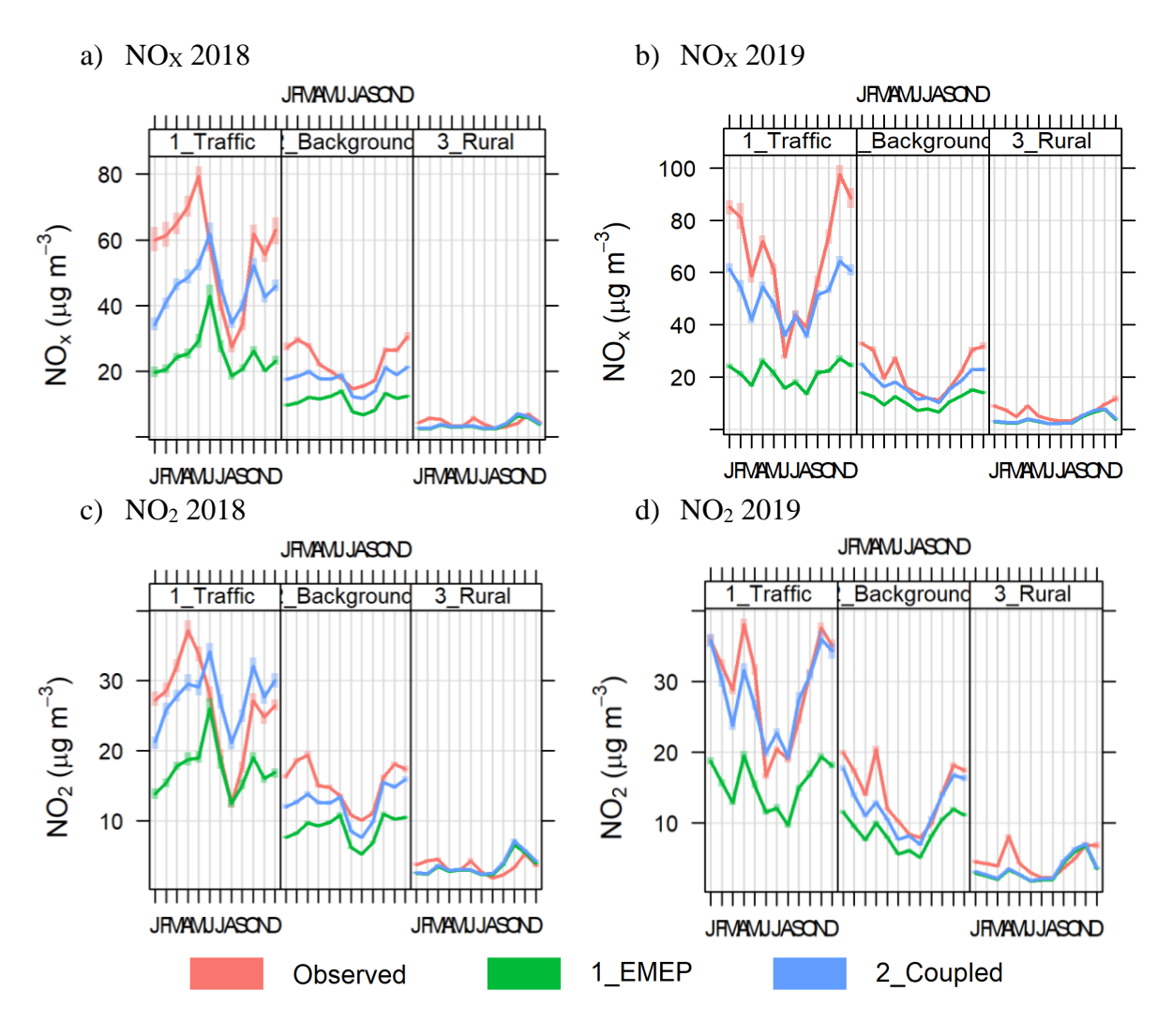


**Figure 8.23** – Comparisons of observed, regional model (EMEP) and Coupled system monthly concentrations variations (all stations): a) NO<sub>X</sub> 2018, b) NO<sub>X</sub> 2019, c) NO<sub>2</sub> 2018 and d) NO<sub>2</sub> 2019; **note differing scales between years for NO<sub>X</sub>, with higher concentrations in 2019.** 

Figure 8.23 compares monthly modelled and observed  $NO_X$  and  $NO_2$  concentrations for 2018 and 2019. The Coupled system  $NO_X$  concentrations broadly follow the measured monthly variations, with some under-prediction of  $NO_X$  during the colder months of the year. Considering specifically the higher concentration traffic sites, of note is the difference in monthly  $NO_X$  concentration variations between 2018 and 2019. The overall trend is for lower concentrations in the summer months and higher in the winter, however concentrations are generally lower but remain elevated until later in the year in 2018 compared to 2019. This monthly variation is primarily due to monthly variations in meteorological conditions and the Coupled system replicates this variation, indicating that the modelling system responds well to concentration changes that are a result of atmospheric conditions. The  $NO_2$  concentrations predicted by the Coupled system at the traffic sites also compare well with measurements, particularly for 2019. It is also clear how the monthly average  $NO_2$  concentration variations relate closely to  $NO_X$  variations.

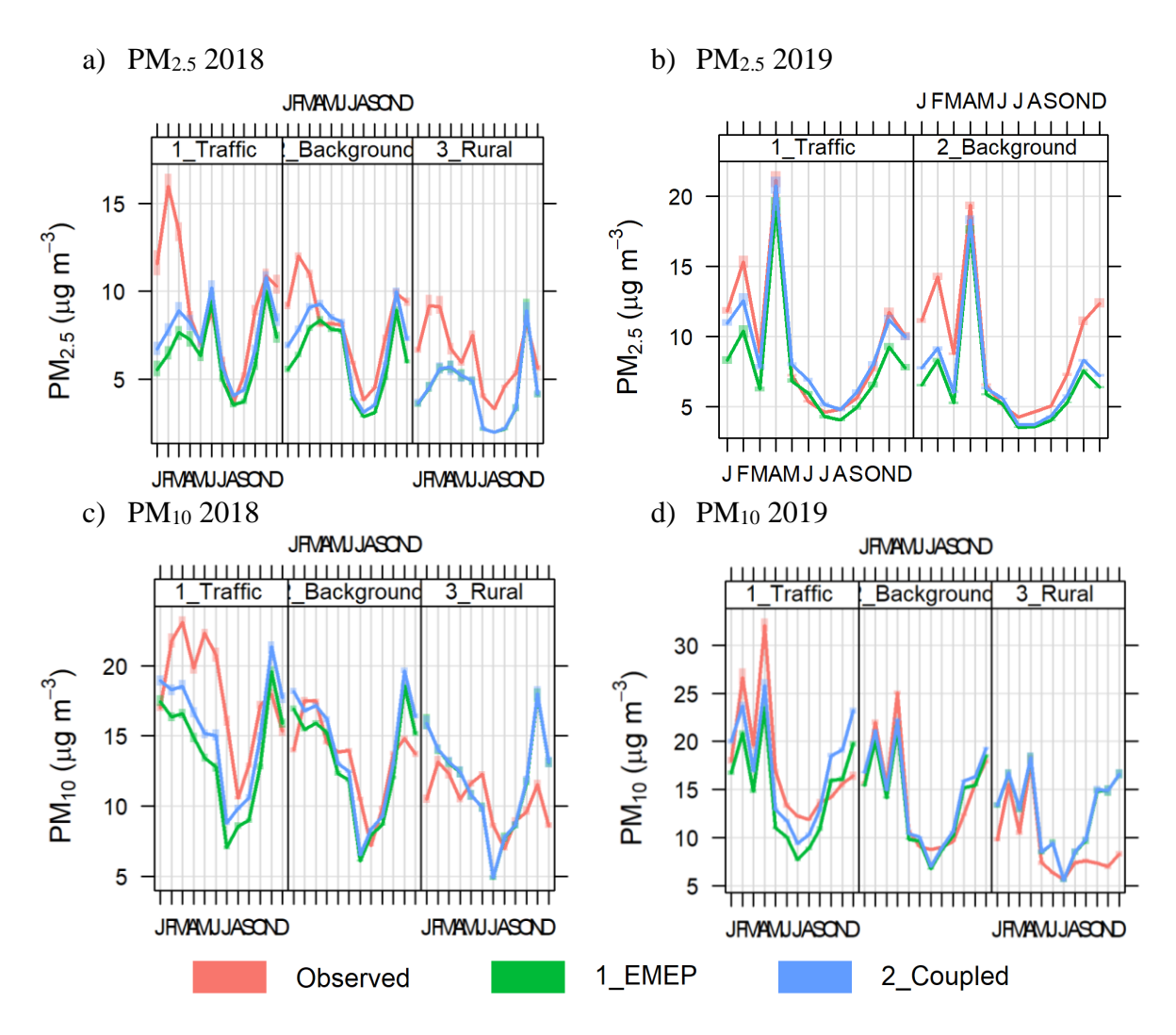


**Figure 8.24** – Comparisons of observed, regional model (EMEP) and Coupled system monthly concentrations variations (all stations): a) PM<sub>2.5</sub> 2018, b) PM<sub>2.5</sub> 2019, c) PM<sub>10</sub> 2018 and d) PM<sub>10</sub> 2019; **note differing scales between years.** 

Figure 8.24 presents corresponding monthly variation plots for PM<sub>2.5</sub> and PM<sub>10</sub> for 2018 and 2019. As for NO<sub>X</sub> and NO<sub>2</sub>, there is a similarity between PM<sub>2.5</sub> and PM<sub>10</sub> monthly variations, but there is a large difference in terms of the inter-annual profiles. Again, this can be explained in terms of the influence of meteorological conditions on concentrations. The 2019 April peak in PM concentrations was also apparent in the NO<sub>X</sub> and NO<sub>2</sub> profiles, which again supports the influence of meteorological conditions on pollutant concentrations. In the UK, there was a period of low wind speeds and pollutant import from continental Europe in April 2019 which led to very high particulate concentrations across much of the UK [42]; some of the same conditions may have occurred in Ireland during this period. The Coupled system generally compares well with observations for both pollutants for 2019, although, as for NO<sub>X</sub>, there is some under-prediction of PM<sub>2.5</sub> in the colder, earlier months of the year at the background sites. Similarly, for 2018, the model under-predicts PM<sub>2.5</sub> at the start of the year, and has the same trend for PM10 at traffic sites only.

Figure 8.25 shows the observed and Coupled system modelled diurnal concentration variations at the Dun Laoghaire background continuous monitor in Dublin for NO<sub>X</sub> and NO<sub>2</sub> in 2018 and 2019. The 2019 observed variation is relatively well matched for both pollutants, with small

under-predictions for night time NO<sub>X</sub> and midday NO<sub>2</sub>. In 2018, the observed mean concentrations are higher and this change is not matched by the Coupled system. The Dun Laoghaire monitoring site shows a sharp peak in concentrations in August 2018, which may be distorting the diurnal profiles; there is a flatter monthly profile in 2019.

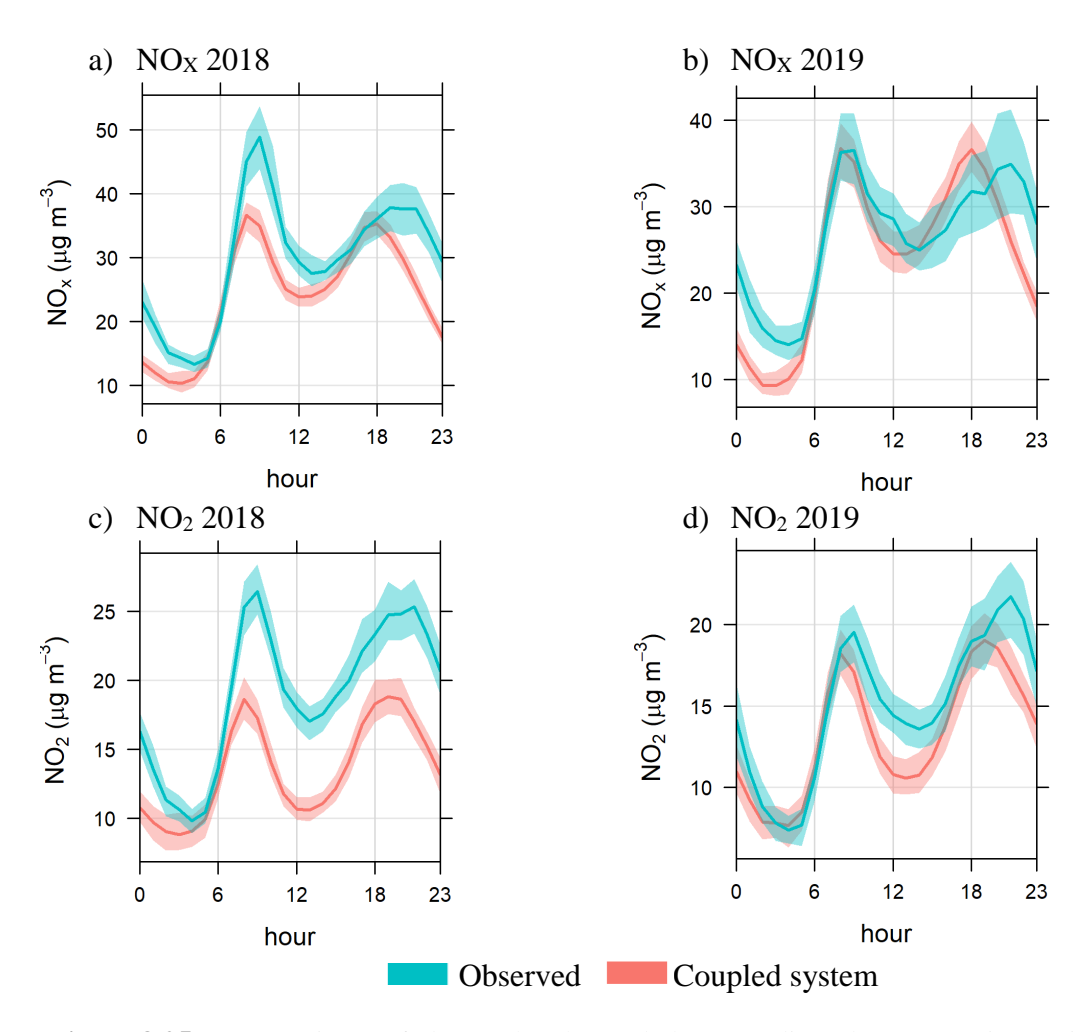


**Figure 8.25** – Comparisons of observed and Coupled system diurnal concentration variations, Dun Laoghaire continuous monitor: a) NO<sub>X</sub> 2018, b) NO<sub>X</sub> 2019, c) NO<sub>2</sub> 2018 and d) NO<sub>2</sub> 2019; **note different colour convention from monthly plots and slightly different vertical scales between years.** 

Figure 8.26 compares average diurnal observed and modelled (Coupled system) concentration variations of NO<sub>X</sub> and NO<sub>2</sub> at the Winetavern Street background continuous monitor in central Dublin. For NO<sub>X</sub>, the Coupled system matches the morning peak and midday concentrations well but overpredicts the evening concentrations in both years. For NO<sub>2</sub> the peak morning and evening concentrations are somewhat overpredicted in both years, while the overnight and midday concentrations are better matched. Winetavern Street has three lanes of traffic, two running northwards and one southwards. Thus, there may be asymmetric traffic flow patterns between morning and evening peak times that are not reflected in the standardised time-variation profile used in the modelling (described in Section 5.4.1).

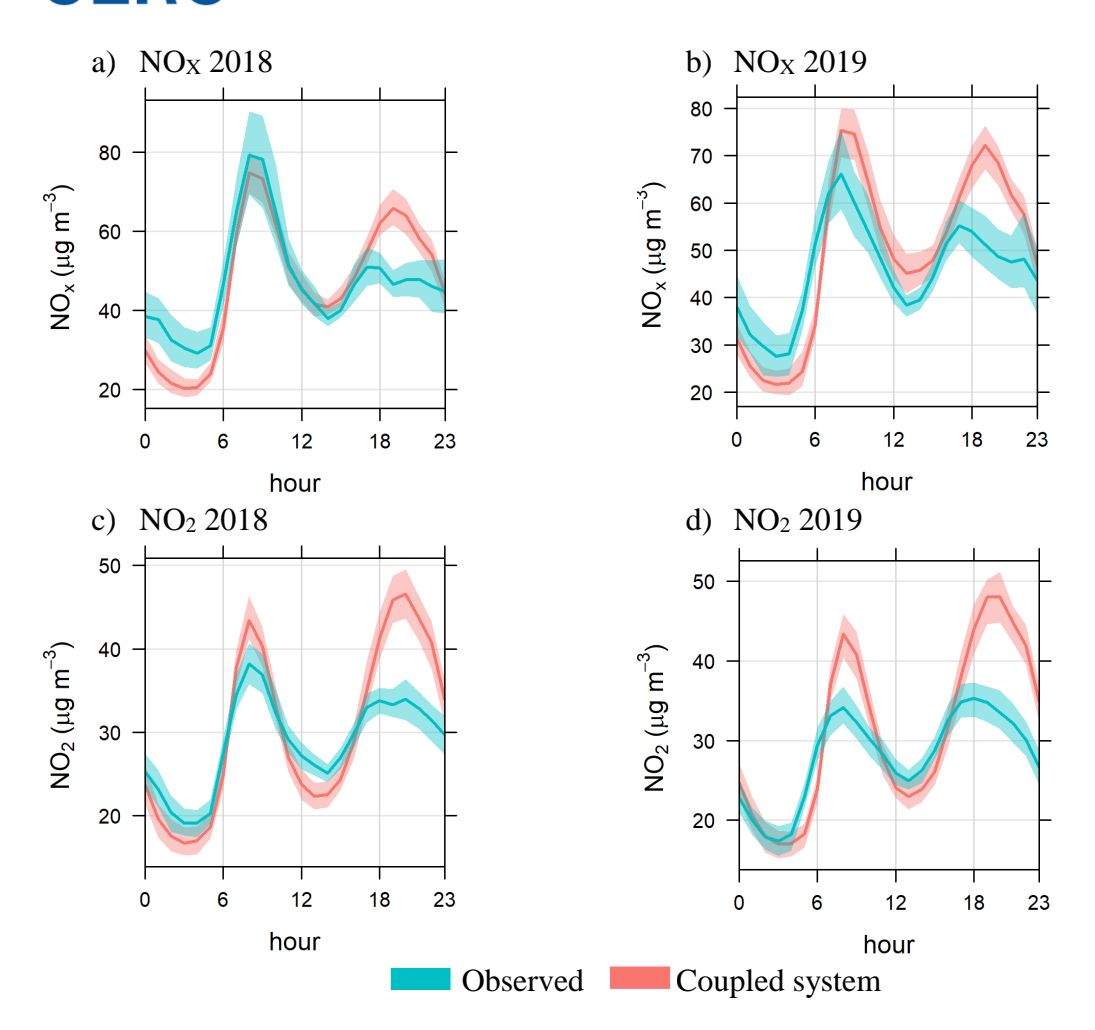


**Figure 8.26** – Comparisons of observed and Coupled system diurnal concentrations variations, Winetavern street monitor: a) NO<sub>X</sub> 2018, b) NO<sub>X</sub> 2019, c) NO<sub>2</sub> 2018 and d) NO<sub>2</sub> 2019; **note different colour convention from monthly plots and slightly different vertical scales between years.** 

#### 8.4 Proportions of regional and local pollution

In order to propose possible pollutant mitigation options, it is important to consider pollution origins. Of the pollutants of interest for this study, particulate ( $PM_{10}$  and  $PM_{2.5}$ ) and  $O_3$  concentrations are dominated by regional scale emissions, chemistry and transport processes.  $NO_X$  and  $NO_2$  concentrations are dependent on local emissions and are affected by urban chemistry and dispersion processes.

The Coupled system allows quantification of the relative proportion of pollutant concentrations that arise from long-range pollutant transport, regional sources and local sources. It is non-trivial to undertake formal source apportionment calculations for the full non-linear Coupled system. Consequently, this task was not undertaken for the current study, although a selection of PM<sub>2.5</sub> source apportionment results from the regional modelling is presented in Section 8.4.

2018 and 2019 annual average measured rural, background and traffic concentrations have been compared to those modelled by EMEP and by the Coupled system, with background and traffic concentrations calculated separately for Dublin and non-Dublin locations. Figure 8.27 presents results for NO<sub>X</sub>, NO<sub>2</sub> and O<sub>3</sub>, while Figure 8.28 presents the corresponding results for PM<sub>2.5</sub>

and  $PM_{10}$ . These calculations have been performed for the continuous monitor network. Some sub-categories have no sites e.g. rural  $PM_{2.5}$  for 2019, and some have only one. Trends in pollutant concentrations are more robust for combinations of site location and pollutant where more sites are used in the calculation of the modelled or measured value.

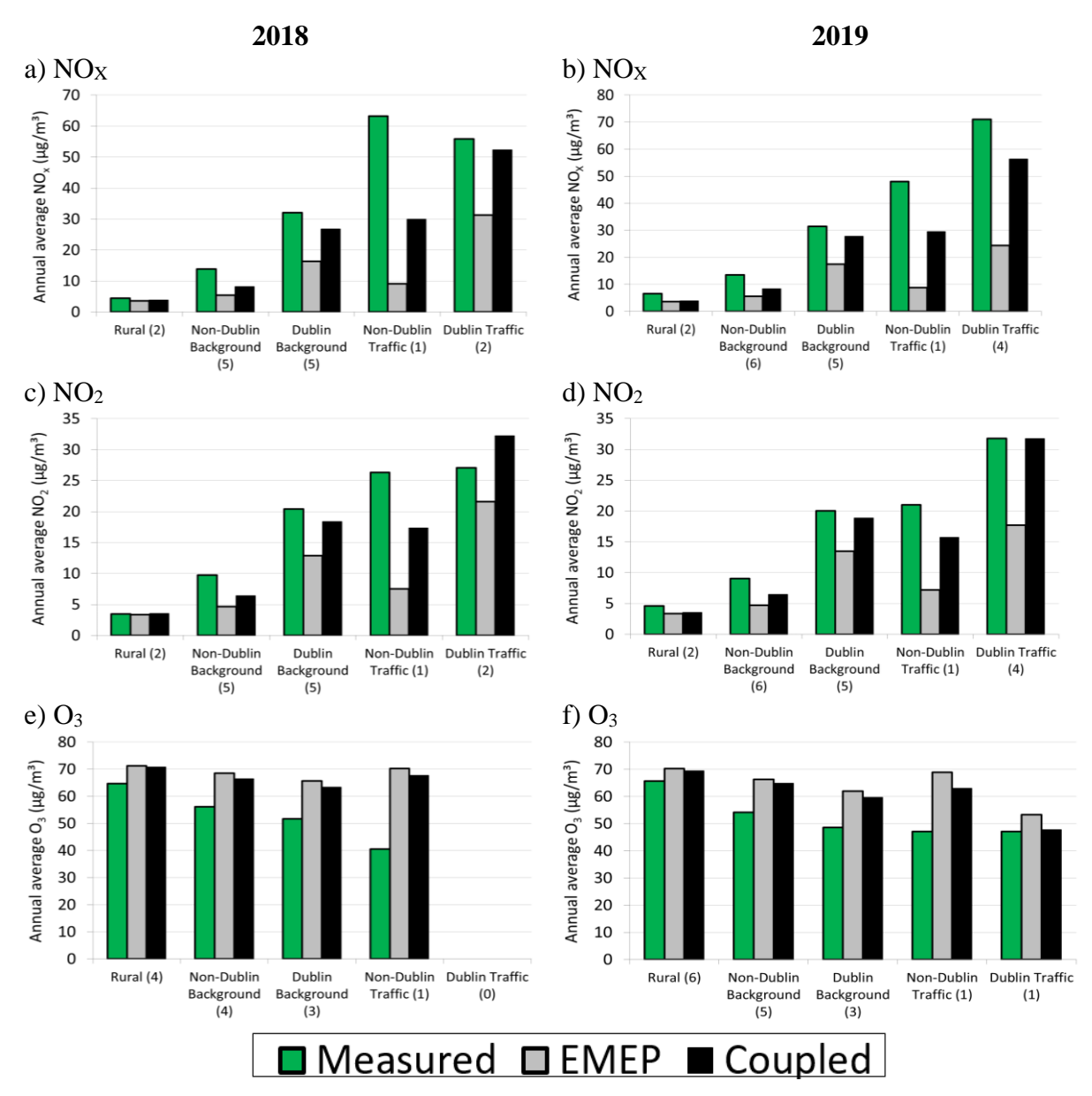


**Figure 8.27** – Comparison of measured and modelled rural, background and traffic gaseous pollutant concentrations (μg/m³), showing Dublin and non-Dublin background and traffic locations separately: a) NO<sub>x</sub> 2018, b) NO<sub>x</sub> 2019, c) NO<sub>2</sub> 2018, d) NO<sub>2</sub> 2019, e) O<sub>3</sub> 2018 and f) O<sub>3</sub> 2019.

Figure 8.27 shows large rural to background and background to traffic concentration differences for NO<sub>X</sub> and NO<sub>2</sub>. Also, this plot highlights the poorer air quality in Dublin at both traffic and background sites compared to the other cities; however as there is only one non-Dublin traffic site, these values may not be widely representative. O<sub>3</sub> concentrations vary less between locations, with a general trend of lower concentrations in the traffic areas.

Figure 8.28 presents the corresponding concentrations for  $PM_{2.5}$  and  $PM_{10}$ . As for  $O_3$ , particulate concentrations vary less with location than  $NO_X$  and  $NO_2$ . The modelling indicates that  $PM_{2.5}$  concentrations outside Dublin are lower than within Dublin. The measurements do

not demonstrate a clearly corresponding trend, for example the Dublin traffic concentration is slightly lower than the Dublin background concentration in 2018. These results are not conclusive because there are relatively few sites (i.e. one) included in some of the concentration bins. A possible explanation for the relatively high measured concentrations in background areas is inaccurate representation of domestic solid fuel burning in the MapEIre emissions inventory, used as input into the modelling system. Coupled system predictions and measurements follow broadly the same trend for PM<sub>10</sub>, although there is some under-prediction by the model at traffic sites, which may be explained by the lack of construction and other coarse particulate emissions sources in the inventory, which are more likely to occur adjacent to major roads rather than in residential areas.

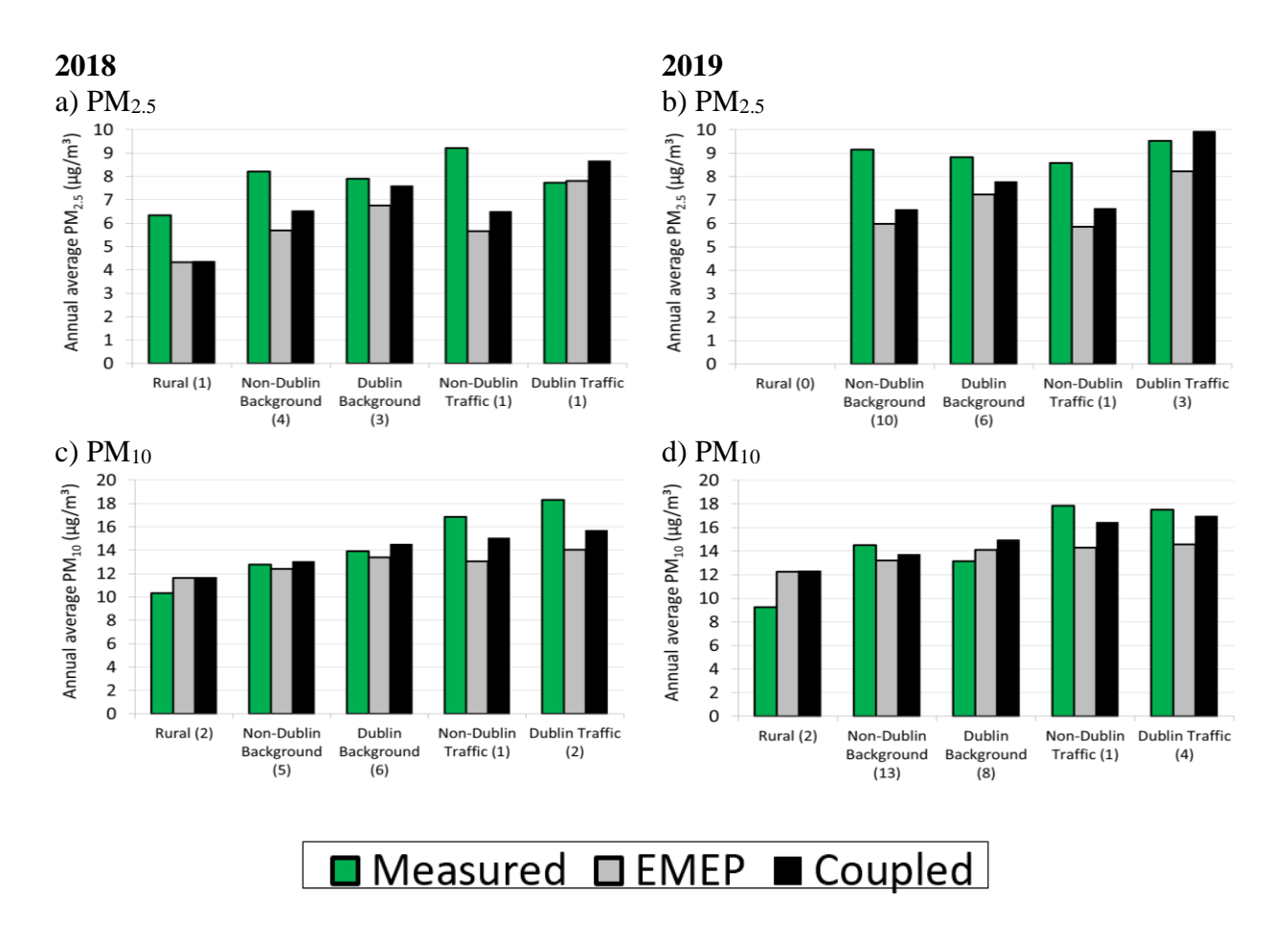


**Figure 8.28** – Comparison of measured and modelled rural, background and traffic particulate air quality levels, showing Dublin and non-Dublin background and traffic locations separately: a)  $PM_{2.5}$  2018, b)  $PM_{2.5}$  2019, c)  $PM_{10}$  2018 and d)  $PM_{10}$  2019.

#### 8.5 Sensitivity testing

Sensitivity testing is an important part of any air quality modelling study. This section presents results of some testing that has been carried out in order to investigate possible causes for the under-prediction of modelled NO<sub>2</sub> at some suburban locations.

The local model uses a minimum Monin-Obukhov length parameter to allow for the effect of heat production in cities, which may not be well represented by the meteorological data. The Monin-Obukhov length provides a measure of atmospheric stability. In very stable conditions in a rural area its value would typically be 2 to 20 m, whereas in urban areas, there is a

significant amount of heat generated from buildings and traffic, which warms the air above the town/city and is associated with larger values of Monin-Obukhov length. For large urban areas this is known as the urban heat island and this heating has the effect of preventing the atmosphere from ever becoming very stable. A typical minimum Monin-Obukhov length for urban areas is 30 m.

Atmospheric stability conditions influence dispersion. There is less dispersion in stable conditions, which means that for ground-level emissions sources such as road traffic, ground-level concentrations resulting from the dispersion of primary emissions are higher in stable conditions compared to neutral and convective conditions. The converse is true for elevated sources, which have a comparatively lower impact at ground level in stable conditions. For the current version of the Coupled system where the regional model is linked to ADMS-Urban<sup>18</sup>, it is not possible to enter spatially varying values of the minimum Monin-Obukhov length. A uniform value of 30 m has been used throughout the domain for all model runs apart from those presented in this section. In some rural and suburban locations a value of 30 m may be too high, leading to an under-prediction of concentrations.

The evaluation has been re-run for both years using a minimum Monin-Obukhov length of 10 m throughout the domain. The site type categorisation used in this sensitivity testing differs from elsewhere in the evaluation because sites have been categorised according to 'suburban' and 'urban' rather than 'background' and 'traffic'. This is because the minimum Monin-Obukhov length parameter relates to area type rather than vicinity to road.

The outcome of the intercomparison is consistent between years. At suburban and urban locations where road source dispersion influences modelled concentrations, concentrations of all pollutants increase when a lower value of minimum Monin-Obukhov length is used, apart from for O<sub>3</sub> where there is a slight decrease in concentrations due to the influence of NO<sub>x</sub> chemistry. Differences are most noticeable for NO<sub>x</sub> and NO<sub>2</sub> because of their strong dependence on primary emissions. Figure 8.29 shows the NO<sub>2</sub> scatter plot for 2019, and Table 8.13 presents the corresponding statistics, grouped by site type. The small increase in concentrations at suburban sites has the effect of reducing the magnitude of model bias from -0.22 to -0.16 for 2019; corresponding statistics for 2018 are -0.24 and -0.20.

The outcome of this sensitivity testing is that using a uniform urban value of the minimum Monin-Obukov length is likely to be contributing to the under-prediction of NO<sub>2</sub> at some suburban locations, but it is not the only factor.

\_

<sup>&</sup>lt;sup>18</sup> The next release version of the system will allow this feature.

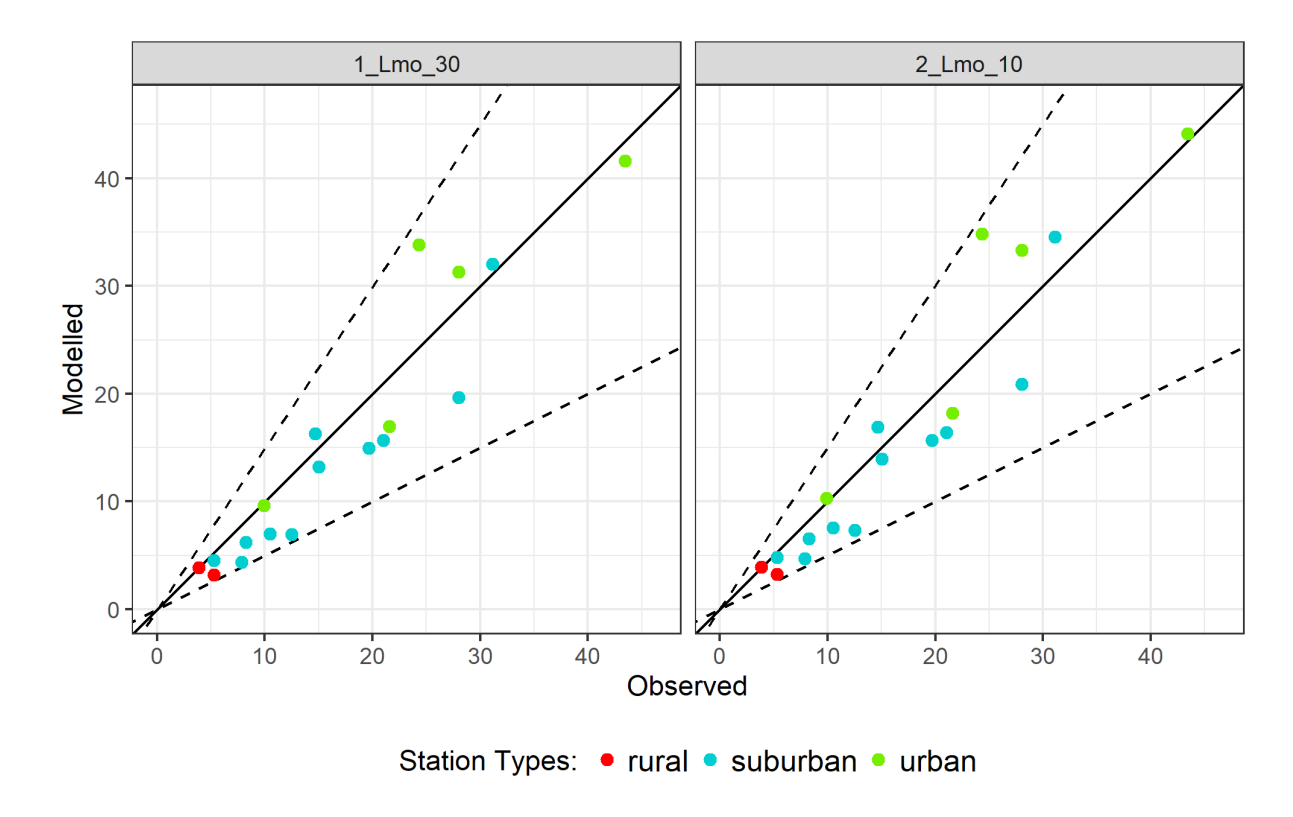


**Figure 8.29** – 2019 NO<sub>2</sub> scatter plot of Coupled system modelled versus measured annual average concentrations ( $\mu g/m^3$ ) at continuous monitors, points coloured by site type with  $\pm 50\%$  modelling uncertainty lines shown, showing sensitivity testing of minimum Monin-Obukhov length: MinLmo 30 m (left) as used in the base model runs compared to MinLmo 10 m (right).

**Table 8.13** – 2019 NO<sub>2</sub> model evaluation statistics, comparing minimum Monin-Obukhov lengths 10 and 30 m, by site type; results in bold indicate those corresponding to the most suitable value of minimum Monin-Obukhov length for the station type.

		Minimum	Mean (µ	ug/m³)				
Station type	No. of valid obs.	Monin- Obukhov length (m)	Monitored	Modelled	NMSE	R	Fac2	Fb
Rural	16267	10	4.6	3.6	1.67	0.38	0.51	-0.25
		30		3.5	1.67	0.38	0.51	-0.26
Suburban	87884	10	15.9	13.5	0.93	0.70	0.65	-0.16
		30		12.8	0.82	0.72	0.66	-0.22
Urban	42108	10	25.6	28.4	0.65	0.66	0.68	0.10
		30		26.8	0.53	0.68	0.69	0.05



#### 9 Pollution maps

The model evaluation process provides evidence to justify the use of a particular air quality model configuration for generating air pollution maps for a range of policy and research applications. In terms of modelled output:

- The Coupled system calculates hourly pollutant concentration predictions at any receptor location within the model domain. In order to generate pollution maps, model output points are specified as a variable grid, with higher output point resolution in the vicinity of explicitly modelled roads in order to resolve near-road pollutant concentration gradients. Output points can be placed at any vertical height.
- EMEP pollutant concentrations are calculated at 1 km × 1 km horizontal grid resolution, with a height corresponding to the midpoints of each vertical layer (Table 5.3). Concentrations are also calculated at the surface.

Pollution maps can be generated for all AQSR metrics (Table 3.1), although for this study the O<sub>3</sub> maps relate to a single year rather than the 3-year average specified in the metric definition. The regional model and Coupled system maps are presented in slightly different ways. The majority of EMEP maps include pollutant concentrations over sea and land, and parts of Northern Ireland are shown; this is because the regional model domain extends beyond Ireland. Conversely, as the output domain for the Coupled system is restricted to Ireland, the high-resolution pollution maps are presented for Ireland only. EMEP and Coupled system maps are presented using matching colour scales for each pollutant metric. All pollutant concentration maps relate to near-ground concentrations (receptor height taken as zero).

The EMEP and Coupled system pollution maps look broadly similar when compared at the national level. This is because the Coupled system uses the regional model concentrations to represent background pollution levels for sub-km resolution dispersion and chemistry calculations. To demonstrate this, Figure 9.1 compares EMEP and Coupled system national air quality  $NO_2$  annual average concentration maps for 2019, and also Dublin maps for the same period for both models. Figure 9.1 a) and b) compare the national level concentrations. The figures look similar, although the Coupled system predicts higher peak concentrations in the cities. Figure 9.1 c) and d) compare EMEP and Coupled system concentrations for Dublin. The pollution maps differ significantly in this area, with the Coupled system showing much higher near-road concentrations, and the regional model output clearly resolved to 1 km  $\times$  1 km grid cells. Overall, Figure 9.1 demonstrates the smooth transition between regional and local scales in the modelling. Only Coupled system pollution maps are presented in this section; corresponding regional model maps for both 2018 and 2019 are included in Appendix E.

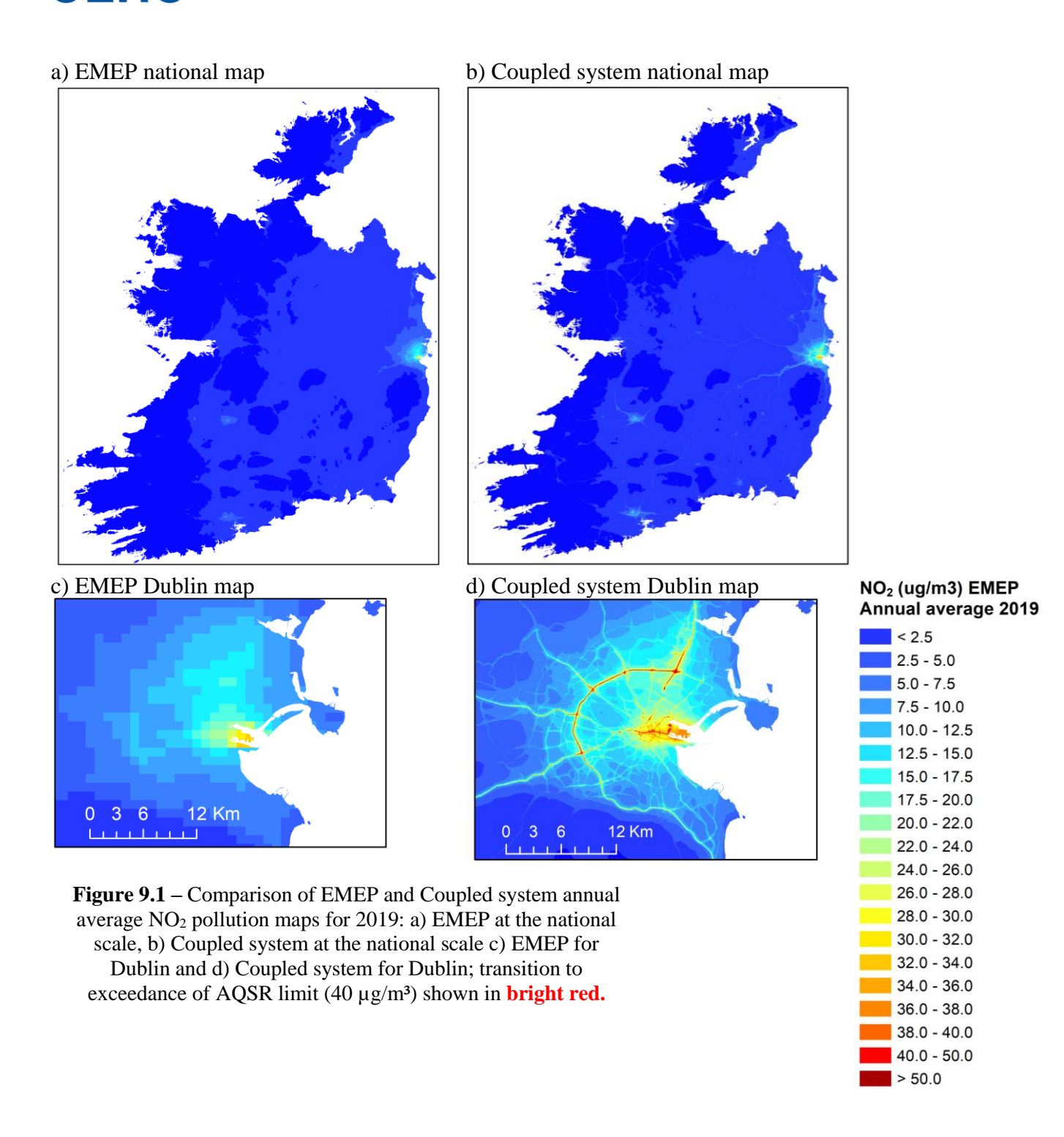
Example pollution maps generated by the Coupled system include insets with higher-resolution shown for the five main cities. Pollution maps for NO<sub>2</sub>, PM<sub>2.5</sub>, PM<sub>10</sub> and O<sub>3</sub> for 2019 corresponding to all AQSR metrics are shown in Sections 9.1.1 and 9.1.3 to 9.1.5 respectively. Equivalent maps for 2018, which are very similar for most metrics, are presented in Appendix E. Section 9.1.2 provides some PM<sub>2.5</sub> component results from the regional model, for 2019. A full set of high-resolution concentration map files have been provided to the EPA for further exploration of the results, including a subset of city maps which are also presented in Appendix F for reference.

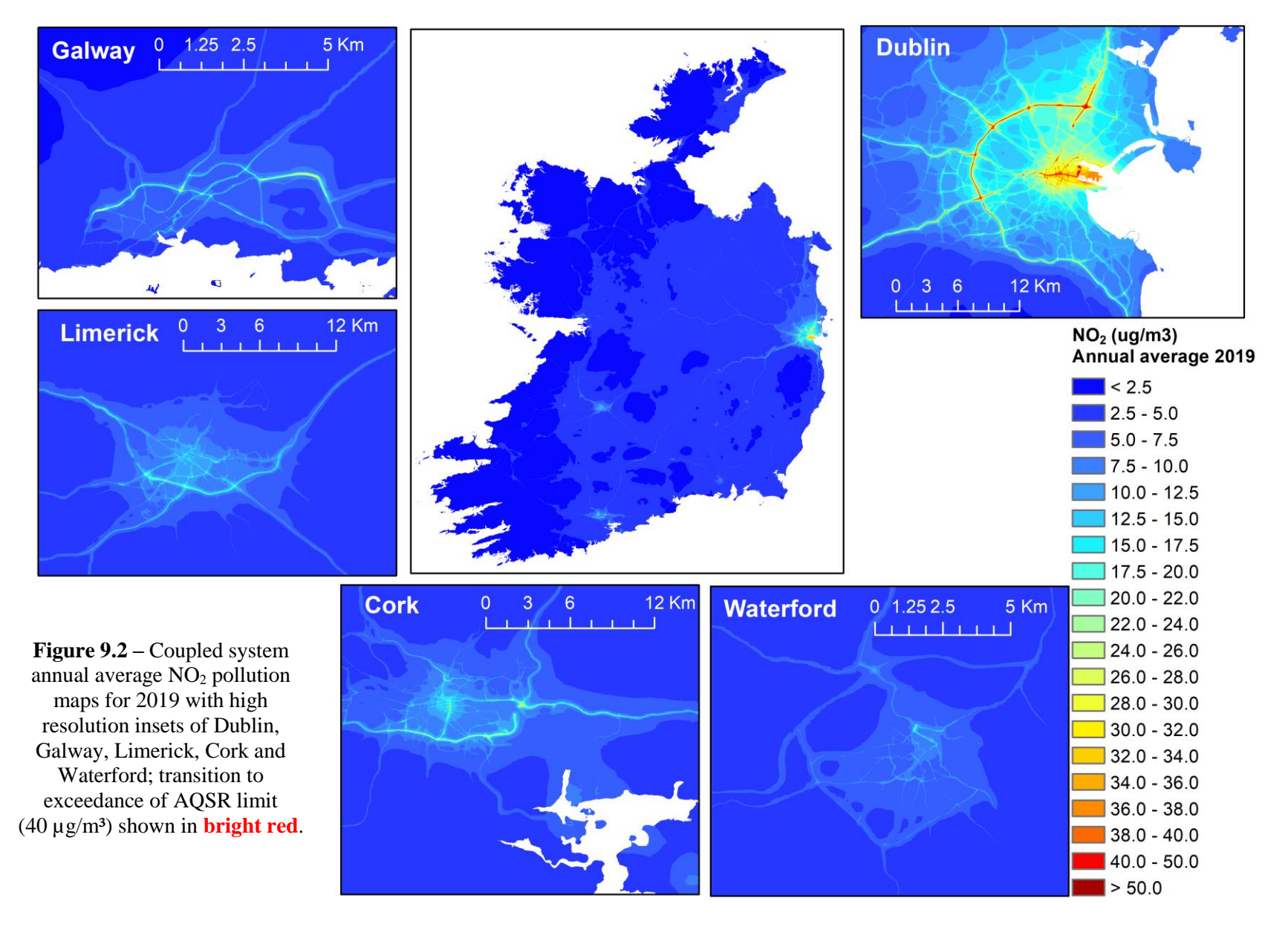


#### 9.1.1. Regional-to-local scale NO<sub>2</sub>

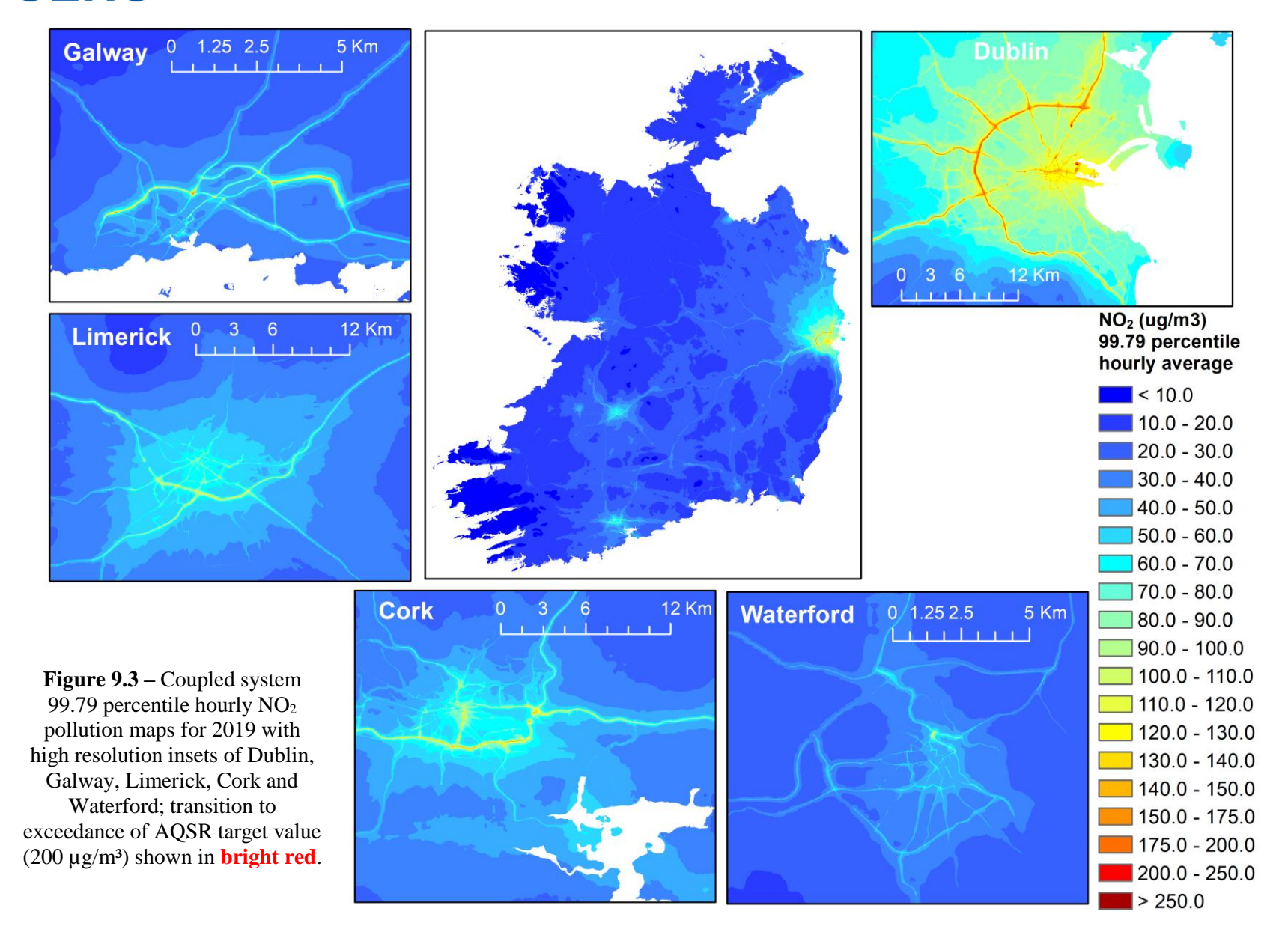
Figure 9.2 presents a Coupled system annual average NO<sub>2</sub> pollution map for 2019. The model predicts small areas of exceedance of the annual average limit value associated with the busiest roads in Dublin and the portals of road tunnels. A formal calculation of areas of exceedance would require exclusion of road carriageway areas, where the limit values do not apply. This calculation has not been carried out.

Figure 9.3 shows the Coupled system maps of the  $99.79^{th}$  percentile of modelled hourly  $NO_2$  concentrations, corresponding to 18 exceedances of the  $200\,\mu\text{g/m}^3$  AQSR limit value. The Coupled system predicts exceedances associated with major roads and Dublin Port tunnel portals. Again, a formal calculation of areas of exceedance would require exclusion of road carriageway areas, where the limit values do not apply; this calculation has not been carried out.





Page 71 of 132 CERC/FM1297





### 9.1.2. Regional scale PM<sub>2.5</sub>

PM<sub>2.5</sub> concentrations are dominated by regional emissions, dispersion and chemistry. PM<sub>2.5</sub> is made up of both directly emitted primary components and secondary components formed through chemical processes from gaseous precursors. Secondary components, include both inorganic and organic species, while secondary organic species are typically further separated into those from anthropogenic and biogenic precursors. The EMEP regional model is able to output PM<sub>2.5</sub> components, which provide an indication of the relative contributions of each component to total PM<sub>2.5</sub>.

As discussed in Section 6.2.1, PM<sub>2.5</sub> measurements include small amounts of water and coarse nitrate (secondary inorganic), so PM<sub>2.5</sub> measurements are compared to the sum of modelled primary and secondary dry PM<sub>2.5</sub>, 27% coarse nitrate, and a contribution from particle-bound water appropriate to typical surface measurement conditions. Figure 9.4 presents the annual average spatial distribution of these components for 2019, specifically: dry PM<sub>2.5</sub>, particle bound water PM<sub>2.5</sub>, 27% coarse nitrate and total PM<sub>2.5</sub>. Both the water and coarse nitrate components are small within the Republic of Ireland, less than 1 μg/m³. The water component is linked to secondary inorganic aerosol (SIA) formation (Figure 9.5), which explains the eastwest gradient, relating to the influence of anthropogenic emissions sources from Northern Ireland, GB and continental Europe. Coarse nitrate concentrations relate to total nitrate, sea salt and dust, and have a smaller relative magnitude of spatial variation. Total PM<sub>2.5</sub> has a slightly stronger east-west concentration gradient compared to dry PM<sub>2.5</sub> due to the inclusion of the water and coarse nitrate components, and values are correspondingly higher in the east of the domain.

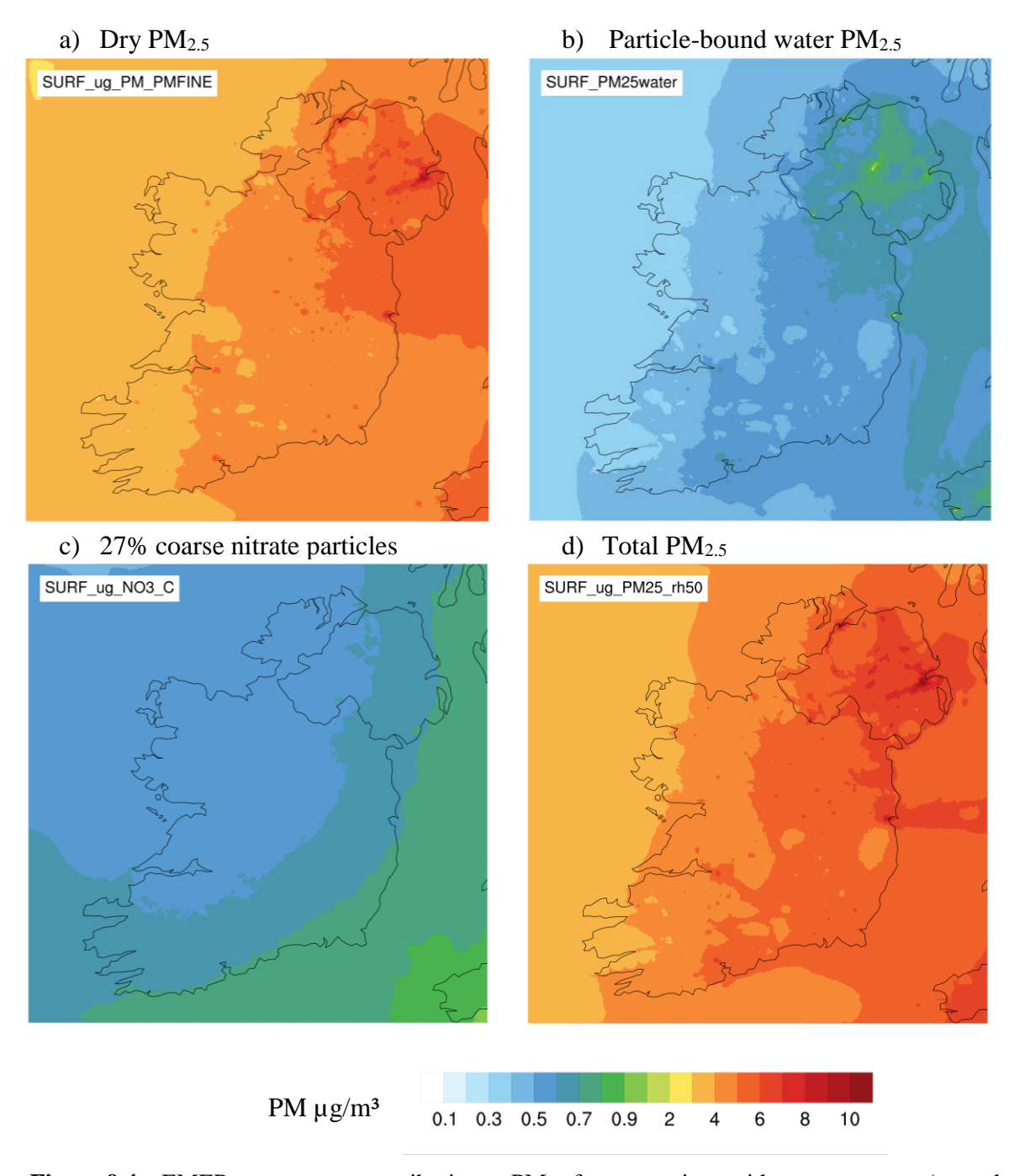
The dominant fine particulate (diameter less than  $2.5\,\mu m$ ) components that relate to anthropogenic activities are: primary emissions, nitrates, sulphates and ammonium. Gaseous ammonia neutralises gaseous nitric acid (HNO<sub>3</sub>, formed by oxidation of NO<sub>X</sub>) and gaseous sulphuric acid (H<sub>2</sub>SO<sub>4</sub>, formed by the oxidation of SO<sub>2</sub>) to form aerosol ammonium compounds. The dominant SIA components are therefore ammonium nitrate (NH<sub>4</sub>NO<sub>3</sub>) and ammonium sulphate ((NH<sub>4</sub>)<sub>2</sub>SO<sub>4</sub>). Without anthropogenic releases of NO<sub>X</sub> and SO<sub>2</sub>, SIA formation will be limited, even with high ammonia concentrations.

Figure 9.5 presents the annual average spatial distribution of  $PM_{2.5}$  components directly related to anthropogenic activities for 2019. Primary  $PM_{2.5}$  is highest in urban areas due to the density of combustion source emissions in these locations, with concentrations noticeably higher in Belfast compared to Dublin. The remaining three secondary inorganic aerosol components demonstrate the east-west gradient seen previously for particle-bound water. In terms of magnitudes, nitrate is the largest component contributing between 1 and 2  $\mu$ g/m³ to total  $PM_{2.5}$  over a large part of the Republic of Ireland, and exceeding primary  $PM_{2.5}$  everywhere apart from the central urban areas of Dublin (and Belfast); sulphate is smaller in magnitude than ammonium. Other  $PM_{2.5}$  components include natural dust, secondary organic aerosols and sea salt.

#### 9.1.3. Regional-to-local scale PM<sub>2.5</sub>

Figure 9.6 presents annual average  $PM_{2.5}$  pollution maps for 2019 for the Coupled system. There are very small regions of modelled exceedance of the AQSR limit value of  $20 \,\mu g/m^3$  associated with the Dublin Port tunnel portals. Modelled concentrations above the WHO  $10 \,\mu g/m^3$  guideline are seen in Dublin city centre and in the vicinity of major roads. System

outputs also show the background pattern of concentrations above the 5  $\mu$ g/m<sup>3</sup> WHO guideline in eastern Ireland from the regional model (refer to Figure E.9 in the Appendix).



**Figure 9.4** – EMEP components contributing to  $PM_{2.5}$  for comparison with measurements (annual average, 2019)

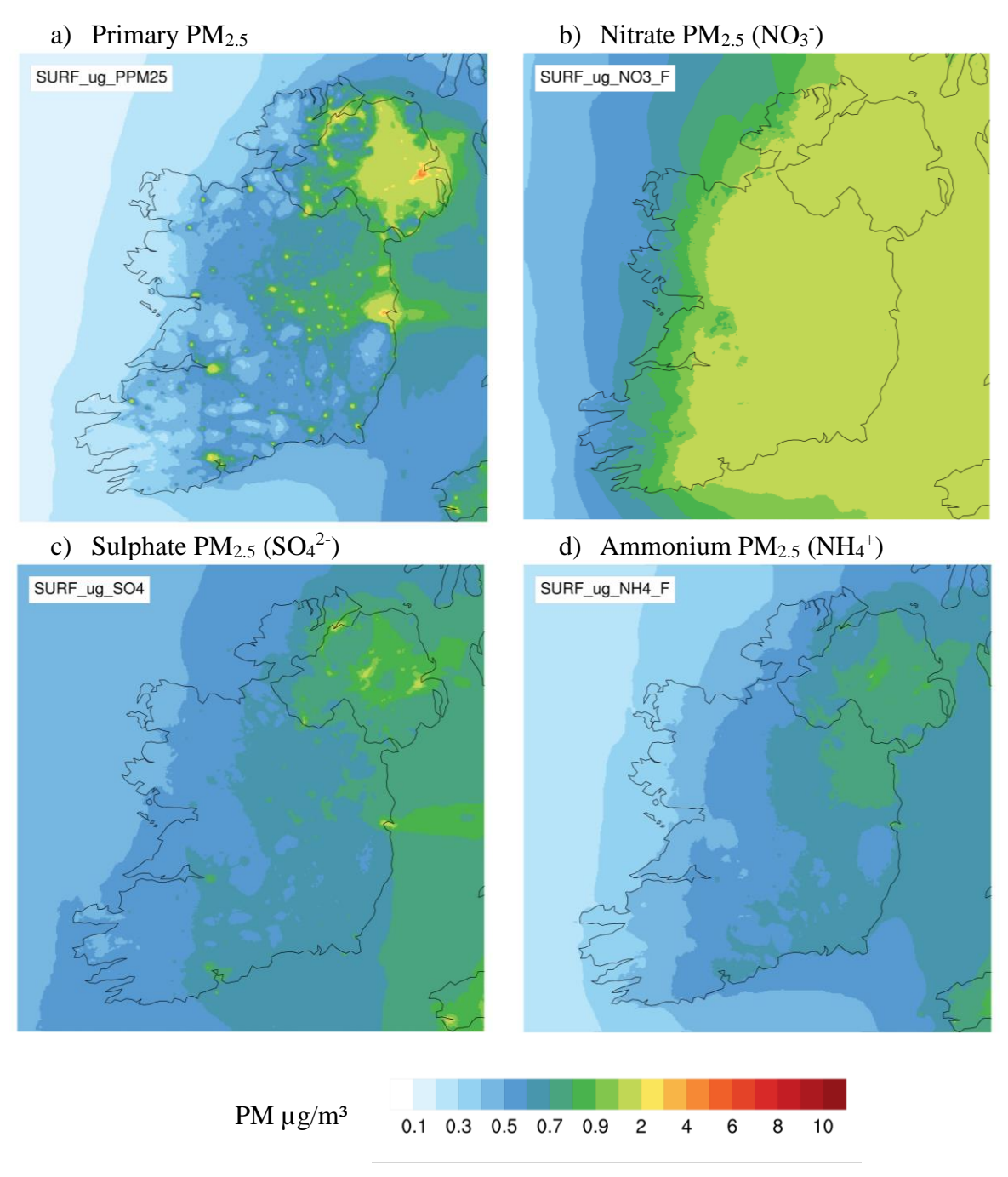
### 9.1.4. Regional-to-local scale PM<sub>10</sub>

Figure 9.7 presents annual average  $PM_{10}$  Coupled system pollution maps for 2019. There are small areas of modelled exceedance of the annual average  $PM_{10}$  limit value (40  $\mu g/m^3$ ) associated with the Dublin Port tunnel portals.

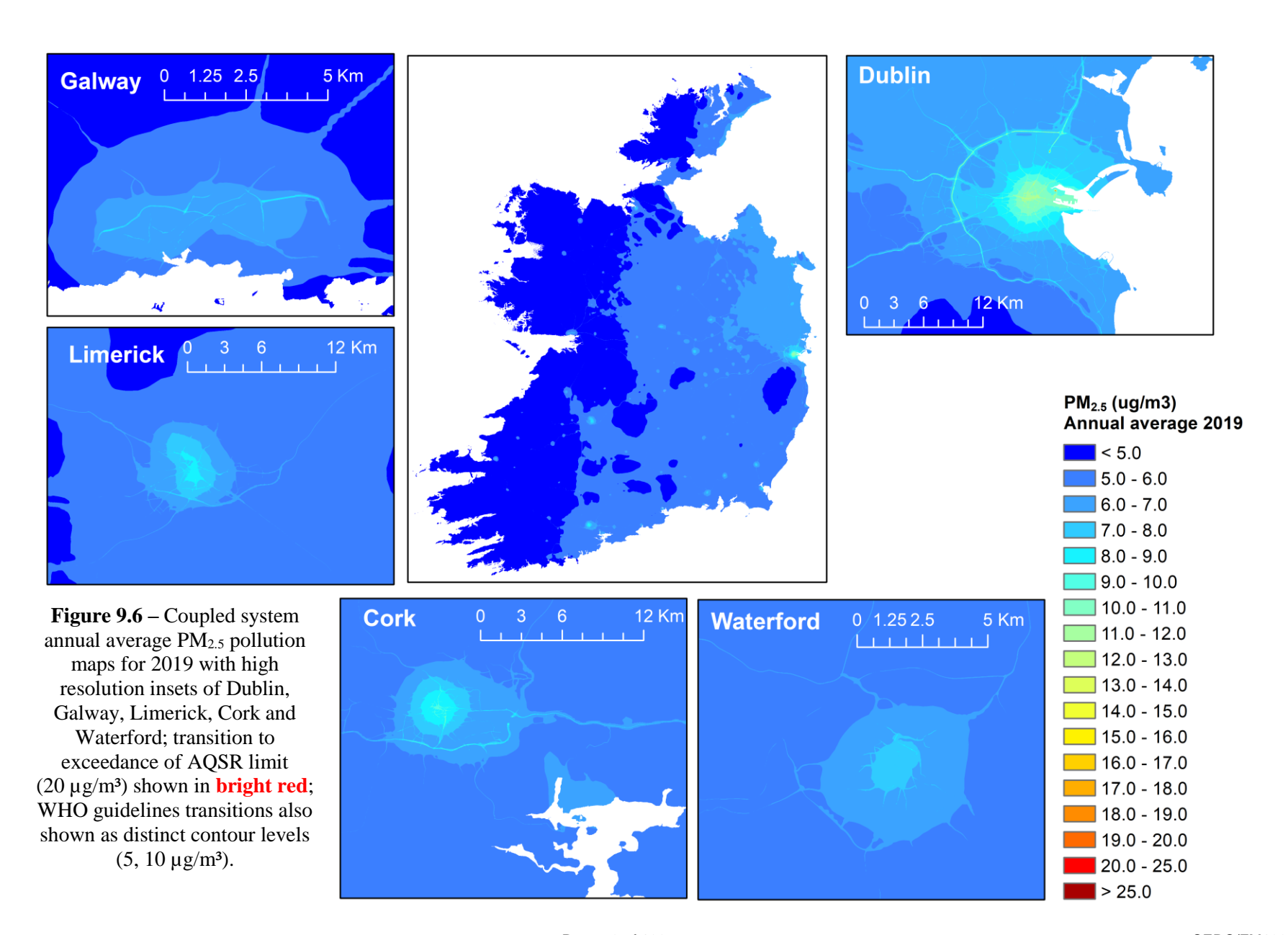
Figure 9.8 shows Coupled system modelled  $90.41^{th}$  percentile of daily average  $PM_{10}$  concentrations for 2019. Again, the system predicts exceedances in small areas associated with Dublin Port tunnel portals. A formal calculation of areas of exceedance in line with the AQSR would require exclusion of road carriageway areas.

### 9.1.5. Regional-to-local scale O<sub>3</sub>

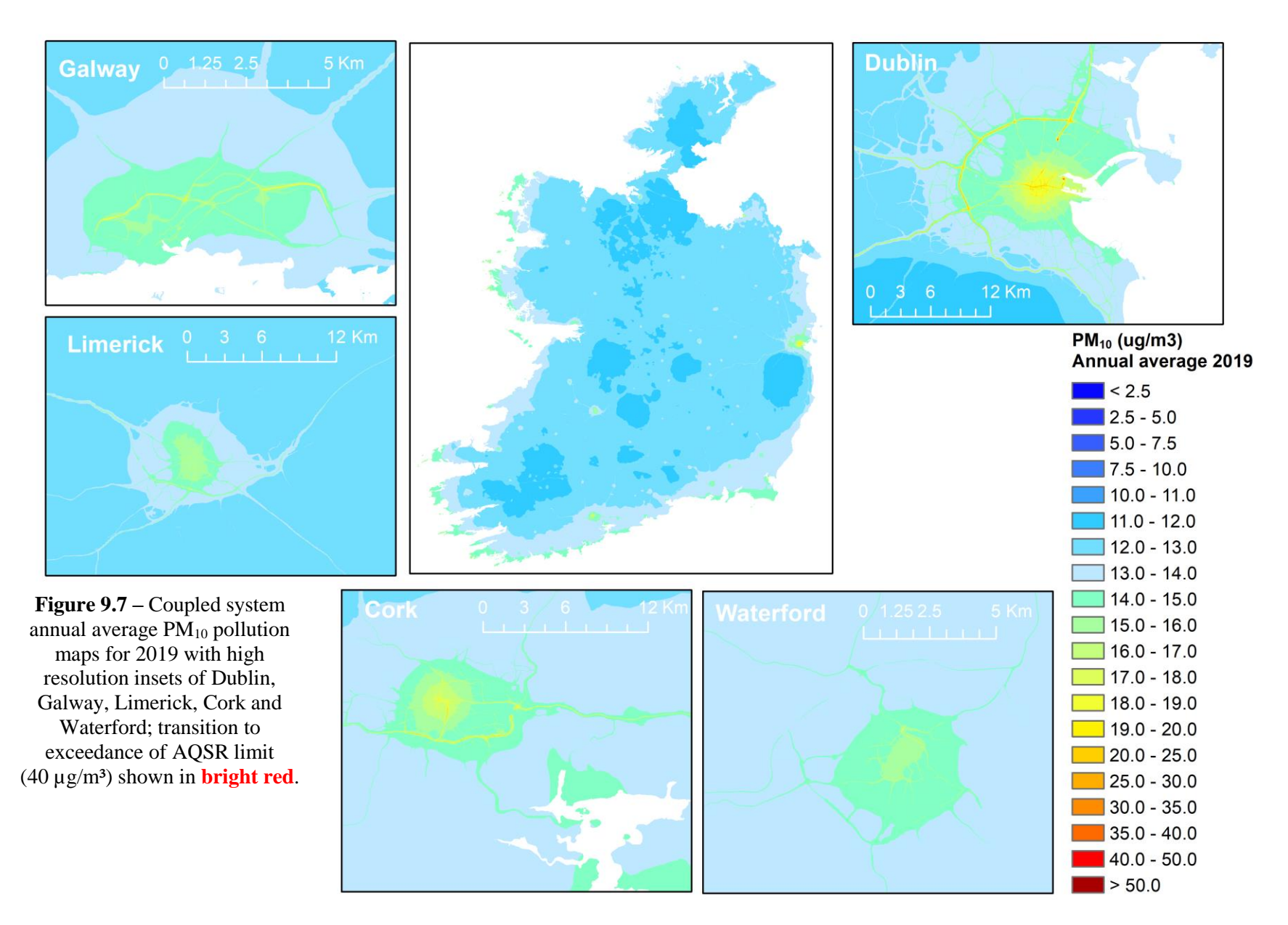
Figure 9.9 shows the Coupled system modelled  $O_3$  pollution maps for 2019 corresponding to the 93.15<sup>th</sup> percentile of maximum daily 8-hour rolling concentrations. The 93.15<sup>th</sup> percentile values do not exceed the 120  $\mu$ g/m<sup>3</sup> target value.



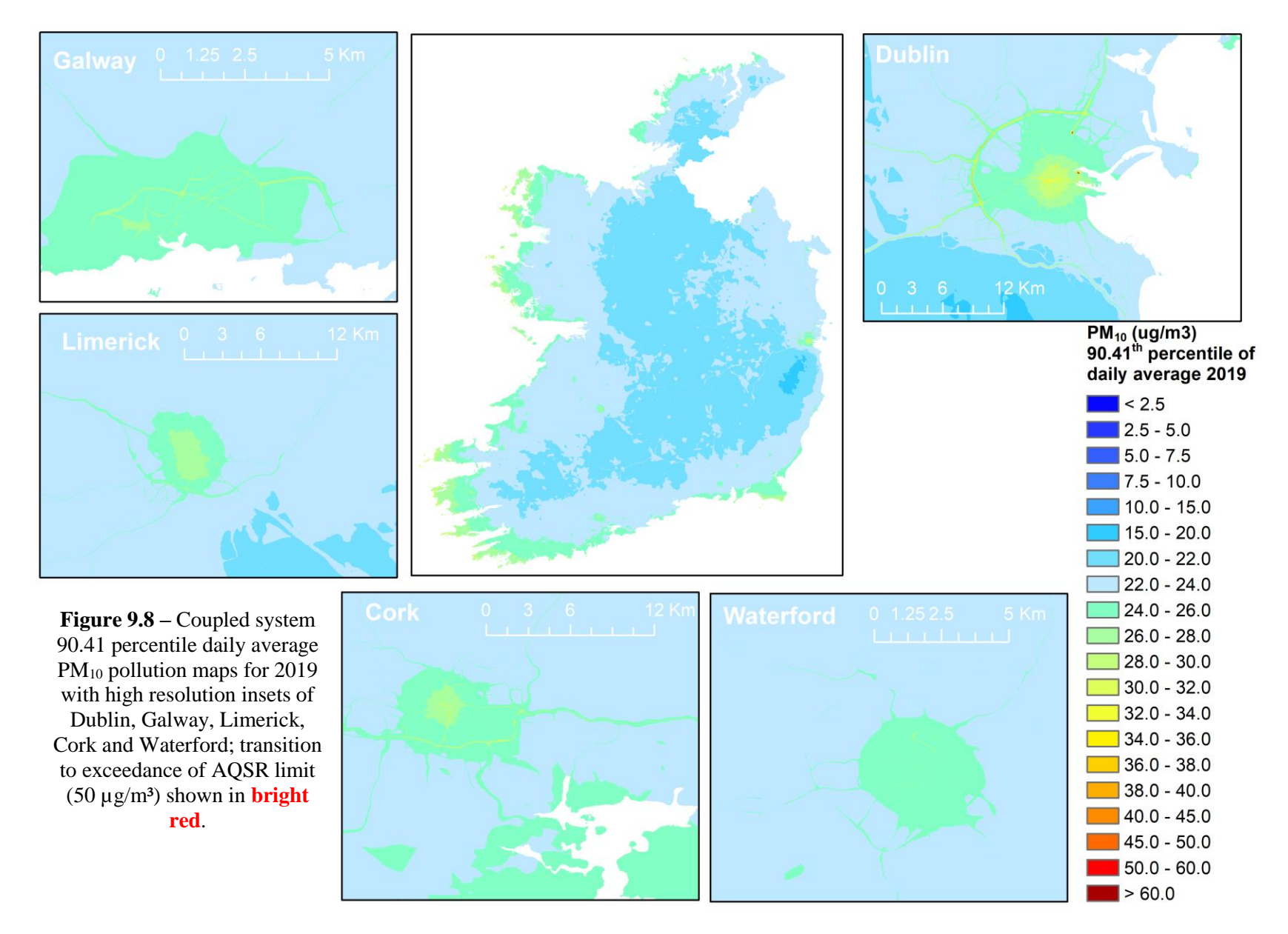
**Figure 9.5** – EMEP dry PM<sub>2.5</sub> components relating to anthropogenic activities (annual average, 2019)



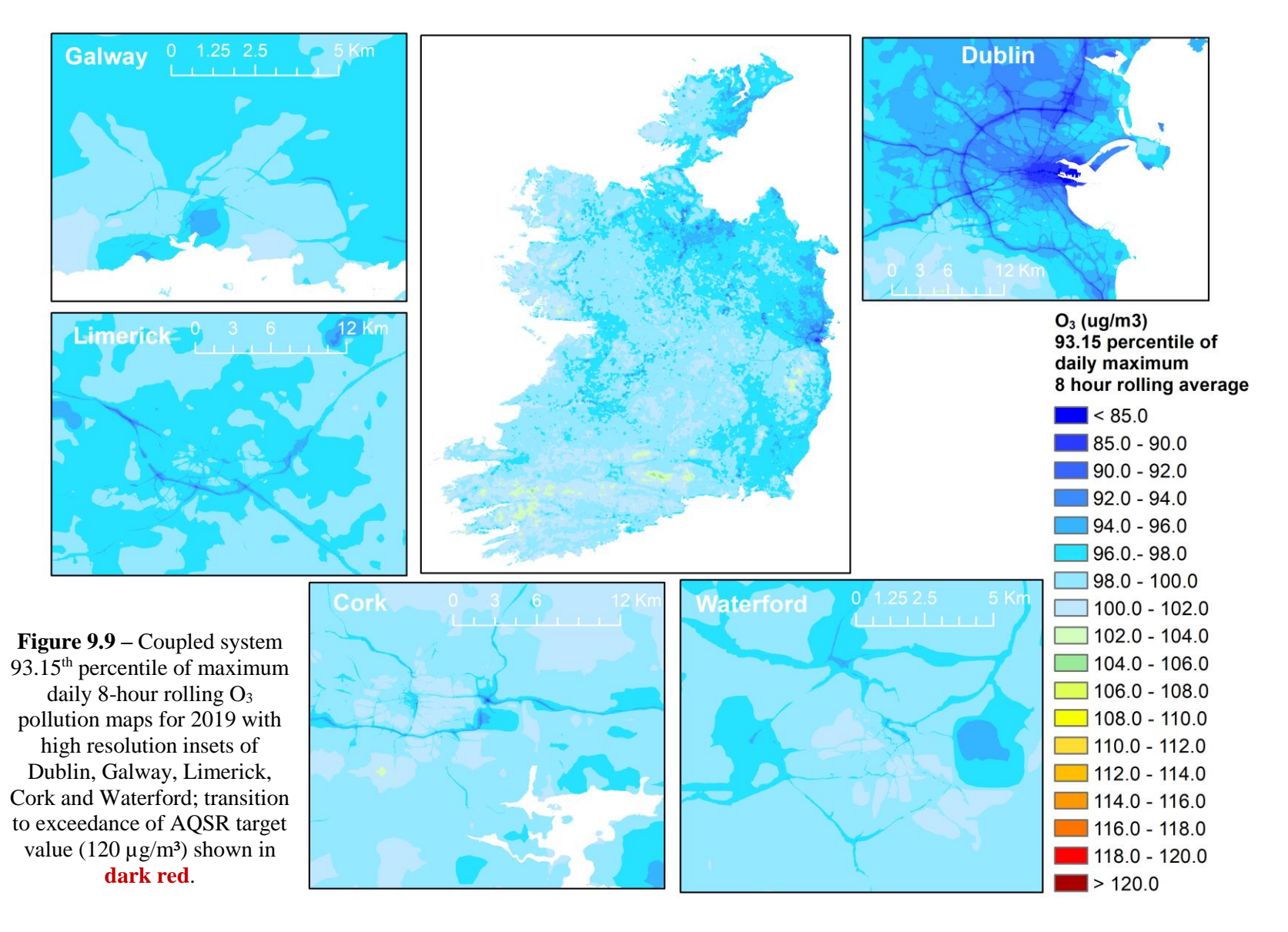
Page 76 of 132 CERC/FM1297



Page 77 of 132 CERC/FM1297



Page 78 of 132 CERC/FM1297



Page 79 of 132 CERC/FM1297

#### 10 Discussion

A modelling system that couples the regional scale EMEP chemical transport model to the street-scale ADMS-Urban quasi-Gaussian dispersion model has successfully been configured and run for Ireland. This modelling system generates regional-to-local scale predictions of ambient NO<sub>2</sub>, PM<sub>2.5</sub>, PM<sub>10</sub> and O<sub>3</sub> concentrations at hourly temporal resolution over the full domain. The mesoscale meteorological model WRF has been used to generate hourly, 1 km  $\times$  1 km resolution datasets of meteorological parameters required as input to the regional and local modelling components of the system.

Model evaluation and pollution maps have focused on all health-related Irish AQSR NO<sub>2</sub>, PM<sub>2.5</sub>, PM<sub>10</sub> and O<sub>3</sub> concentration metrics with associated limit and target values. Modelling has been performed for 2018 and 2019.

Ireland's five largest cities (Dublin, Cork, Limerick, Galway and Waterford) have been modelled in greater detail compared to smaller urban areas and rural locations. 3D buildings datasets have been generated for the five major cities to allow the system to account for the influence of urban morphology on dispersion processes, through the modelling of urban canopy flows and street canyons.

There are challenges associated with modelling such a large domain at high resolution. It is necessary to use tools to automatically generate the datasets used as input to the modelling (for instance, street canyon properties) and to make some broad assumptions (such as in relation to road carriageway widths). Whilst this is normal practice when generating datasets for input to air quality models, it is important to note that there will be parts of the domain where the model may not exactly represent the real world. Measurements are used to check that the model is performing sufficiently well at specific locations.

An industrial emissions inventory was collated for inclusion in the Coupled system. However, there is an incompatibility between explicit industrial source heights and the assumptions associated with the vertical distribution of industrial emissions in the EMEP model. In order to avoid runtime issues associated with grid disaggregation, the industrial source emissions were not modelled explicitly in the final version of the model runs, i.e. these emissions were modelled in EMEP not in ADMS-Urban.

Meteorological model performance has been evaluated through comparison of modelled wind speed, wind direction and temperature parameters against measurements recorded at 22 Met Éireann synoptic stations located throughout Ireland. Despite a small positive bias in wind direction and small negative bias in temperature, the meteorological data is sufficiently accurate for use in the regional and local air quality modelling.

The accuracy of modelled air pollutant concentrations has been extensively evaluated by comparison against measurements from the national network of continuous air quality monitors run by the Irish Environmental Protection Agency. Available measurement data include hourly concentrations of NO<sub>X</sub>, NO<sub>2</sub> and O<sub>3</sub> and daily concentrations of PM<sub>2.5</sub> and PM<sub>10</sub> recorded at rural, background and traffic sites (40 sites), in addition to monthly average NO<sub>2</sub> readings from diffusion tubes deployed in the five main cities (92 and 80 sites for 2018 and 2019, respectively). A range of evaluation graphs and statistics have been calculated, including

FAIRMODE target plots, which present summary metrics including consideration of measurement uncertainty.

This project has demonstrated that the EMEP-ADMS-Urban Coupled system can be used to generate national maps of modelled air pollutant concentrations that satisfy the FAIRMODE model quality objectives for both 2018 and 2019. Thus, the modelling system could be used to demonstrate compliance with the EU AQD.

Pollution maps associated with all Irish AQSR limit and target values have been generated. The pollution maps presented in the current report include insets showing pollutant concentration contours in the five main cities. High resolution concentration map files have also been provided to the EPA for further exploration. Formal calculations of areas in exceedance of AQSR limit or target areas would require road carriageways to be excluded.

The results from the Coupled system are not calibrated using measurements. Consequently, the system can be used for emissions scenario testing, as may be required when considering air pollutant mitigation options as part of air quality plans.

The dependence of model performance on model inputs has been tested throughout the study, and the model configuration has been revised as a result. For example, the vertical distribution of emissions has been adjusted in the local model compared to the regional model due to the latter having a relatively large lowest grid height (45 m), which is unrepresentative of some emissions sources e.g. traffic. Results from one sensitivity test relating to atmospheric stability presented in the report indicates that model results are relatively insensitive to this particular parameter.

The Coupled system model configuration for Ireland demonstrates generally good performance, with consistent model outcomes for 2018 and 2019. Specific aspects of modelled results are summarised for each pollutant in turn.

### $NO_2$

The system generates relatively accurate predictions of the higher NO<sub>2</sub> concentrations, which relate to near-road monitored concentrations. Coupled system biases are small at the traffic sites (5% or less).

There is some under-prediction of NO<sub>2</sub> at a subset of background sites that are located in small towns. Sensitivity testing and site investigations have highlighted a number of contributory factors, including:

- not accounting for urban canopy or street canyon effects;
- not explicitly modelling adjacent car parks or fire stations; and
- the modelling of a spatially homogeneous minimum Monin-Obukov length throughout Ireland.

On an hourly basis, Coupled system statistics that quantify the temporal variability of modelled concentrations show good performance, allowing for the fact that average temporal profiles have been used as input to the system. For roadside sites, these statistics include correlation values over 0.5 and 60% of modelled hourly concentrations within a factor of two of the observed.

Model performance is consistent between the annual average and the hourly metric.

Comparison of modelled period-averaged NO<sub>2</sub> concentrations to diffusion tube measurements was challenging due to uncertainty surrounding exact passive sampler locations, in addition to relatively poor data capture associated with the measurements. Agreement between modelled and measured values is good for 2018 (Dublin only), but the model generally under-predicts for 2019.

#### PM<sub>2.5</sub>

Allowing for the complexity associated with modelling PM<sub>2.5</sub> in terms of the generation of secondary particles, model performance is generally good, with a slight negative bias (16% and 1% for 2018 and 2019, respectively).

On an hourly basis, model performance is better for 2019 than 2018, with correlation values of 0.58 for 2018 and 0.80 for 2019 and number of points within a factor of two of the observed 80% (2018) and 87% (2019) for the Coupled system predictions at traffic sites.

#### $PM_{10}$

 $PM_{10}$  concentrations are accurately predicted by the model, both in terms of the annual average and the  $90.41^{st}$  percentile metric.

As for  $PM_{2.5}$ , on an hourly basis, model performance is better for 2019 than 2018, with corresponding correlations being 0.44 for 2018 and 0.61 for 2019 and number of points within a factor of two of the observed 84% for both years for the Coupled system predictions at traffic sites.

#### $O_3$

The modelling system provides an accurate prediction of the relevant O<sub>3</sub> metric for all sites.

### 11 References

- 1. Simpson, D., Benedictow, A., Berge, H., Bergström, R., Emberson, L. D., Fagerli, H., Flechard, C. R., Hayman, G. D., Gauss, M., Jonson, J. E., Jenkin, M. E., Nyíri, A., Richter, C., Semeena, V. S., Tsyro, S., Tuovinen, J.-P., Valdebenito, Á., Wind, P (2012) The EMEP MSC-W chemical transport model technical description. *Atmospheric Chemistry and Physics*, **12**, 7825-7865. DOI: 10.5194/acp-12-7825-2012.
- 2. Vieno, M., Heal, M. R., Hallsworth, S., Famulari, D., Doherty, R. M., Dore, A. J., Tang, Y. S., Braban, C. F., Leaver, D., Sutton, M. A., and Reis, S. (2014) The role of long-range transport and domestic emissions in determining atmospheric secondary inorganic particle concentrations across the UK. *Atmospheric Chemistry and Physics*, **14**, 8435-8447. DOI: 10.5194/acp-14-8435-2014.
- 3. Owen, B., Edmunds, H.A., Carruthers, D.J. and Singles, R.J. (2000). Prediction of total oxides of nitrogen and nitrogen dioxide concentrations in a large urban area using a new generation urban scale dispersion model with integral chemistry model. *Atmospheric Environment*, **34(3)**, 397-406. DOI: 10.1016/S1352-2310(99)00332-5.
- 4. CERC (2022). *ADMS-Urban Technical Specification*. <u>www.cerc.co.uk/TechSpecs</u> (accessed November 2022).
- 5. Air Quality Standards Regulations 2011 (S.I. No. 180/2011), Iris Oifigiúil.
- 6. UNION, P. (2008) Directive 2008/50/EC of the European Parliament and of the Council of 21 May 2008 on ambient air quality and cleaner air for Europe. *Official Journal of the European Union*, **152**, 1–44.
- 7. World Health Organization. (2021). WHO global air quality guidelines: particulate matter (PM2.5 and PM10), ozone, nitrogen dioxide, sulfur dioxide and carbon monoxide. <a href="https://apps.who.int/iris/handle/10665/345329">https://apps.who.int/iris/handle/10665/345329</a> (accessed November 2022).
- 8. National Ambient Air Quality Monitoring Programme 2017-2022 Environmental Protection Agency, November 2017. <a href="https://www.epa.ie/publications/monitoring--assessment/air/National-Ambient-Air-Quality-Monitoring-Programme-2017-2022.pdf">https://www.epa.ie/publications/monitoring--assessment/air/National-Ambient-Air-Quality-Monitoring-Programme-2017-2022.pdf</a> (accessed November 2022).
- 9. MapEire Project: https://projects.au.dk/mapeire/ (accessed November 2022).
- 10. UK National Atmospheric Emissions Inventory <a href="https://naei.beis.gov.uk/">https://naei.beis.gov.uk/</a> (accessed November 2022).
- 11. EMEP Centre for Emission Inventories and Projections (CEIP) <a href="https://www.ceip.at/">https://www.ceip.at/</a> (accessed October 2022).
- 12. Hood, C., MacKenzie, I., Stocker, J., Johnson, K., Carruthers, D., Vieno, M., Doherty, R. (2018) Air quality simulations for London using a coupled regional-to-local modelling system. *Atmospheric Chemistry and Physics*, **18**, 11221-11245, DOI: 10.5194/acp-18-11221-2018.

- 13. CERC (2019) Report to Irish EPA: Urban air quality modelling of Dublin <a href="https://www.epa.ie/publications/monitoring--assessment/air/Technical\_report\_NO2\_modelling\_Dublin.pdf">https://www.epa.ie/publications/monitoring--assessment/air/Technical\_report\_NO2\_modelling\_Dublin.pdf</a>.
- 14. Denier van der Gon, H., Hendriks, C., Kuenen, J., Segers, A., Visschedijk, A. (2011) Description of current temporal emission patterns and sensitivity of predicted AQ for temporal emission patterns. EU FP7 MACC deliverable report D\_D-EMIS\_1.3.
- 15. Menut, L., Goussebaile, A., Bessagnet, B., Khvorostiyanov, D., Ung, A. (2012) Impact of realistic hourly emissions profiles on air pollutants concentrations modelled with CHIMERE. *Atmospheric Environment*, **49**, 233-244. DOI: 10.1016/j.atmosenv.2011.11.057.
- 16. Bieser, J., Aulinger, A., Matthias, V., Quante, M., Denier van der Gon, H. A. C. (2011) Vertical emission profiles for Europe based on plume rise calculations. *Environmental Pollution*, **159**(10), 2935-2946. DOI: 10.1016/j.envpol.2011.04.030.
- 17. SMOKE model, University of North Carolina Institute for the Environment, <a href="https://www.cmascenter.org/smoke/">https://www.cmascenter.org/smoke/</a> (accessed October 2022).
- 18. Skamarock, W. C. et al. (2019) A Description of the Advanced Research WRF Model Version 4 (No. NCAR/TN-556+STR). DOI: 10.5065/1dfh-6p97.
- National Centres for Environmental Prediction/National Weather Service/NOAA/U.S.
   Department of Commerce (2000, updated daily). NCEP FNL Operational Model Global Tropospheric Analyses, continuing from July 1999. Research Data Archive at the National Center for Atmospheric Research, Computational and Information Systems Laboratory. DOI: 10.5065/D6M043C6.
- 20. Friedl, M. A., Sulla-Menashe, D., Tan, B., Schneider, A., Ramankutty, N., Sibley, A., Huang, X. M. (2010) MODIS Collection 5 global land cover: Algorithm refinements and characterization of new datasets. *Remote Sensing of Environment*, **114**, 168-182. DOI: 10.1016/j.rse.2009.08.016.
- 21. Tewari, M., Chen, F., Wang, W., Dudhia, J., LeMone, M. A., Mitchell, K., Ek, M., Gayno, G., Wegiel, J., Cuenca. R. H. (2004) Implementation and verification of the unified NOAH land surface model in the WRF model. *20th conference on weather analysis and forecasting/16th conference on numerical weather prediction 2004*, **1115(6)**, 2165-2170.
- 22. Hong, S.-Y., Noh, Y., Dudhia, J. (2006) A new vertical diffusion package with an explicit treatment of entrainment processes. *Monthly Weather Review*, **134**, 2318–2341. DOI: 10.1175/MWR3199.1.
- 23. Chen, S.-H., Sun, W.-Y. (2002) A one-dimensional time dependent cloud model. *Journal of the Meteorological Society of Japan*, **80(1)**, 99–118. DOI: 10.2151/jmsj.80.99.
- 24. Kain, J. S. (2004) The Kain–Fritsch convective parameterization: An update. *Journal of Applied Meteorology*, **43**, 170–181. DOI: 10.1175/1520-0450(2004)043%3C0170:TKCPAU%3E2.0.CO;2.
- 25. Mlawer, E. J., Taubman, S. J., Brown, P. D., Iacono, M. J., Clough, S. A. (1997) Radiative transfer for inhomogeneous atmospheres: RRTM, a validated correlated–k

- model for the longwave. *Journal of Geophysical Research*, **102**, 16663–16682. DOI: 10.1029/97JD00237.
- 26. Dudhia, J. (1989) Numerical study of convection observed during the Winter Monsoon Experiment using a mesoscale two–dimensional model. *Journal of the Atmospheric Sciences*, **46**, 3077–3107. DOI: 10.1175/1520-469(1989)046<3077:NSOCOD>2.0.CO;2.
- 27. EMEP/MSC-W, EMEP/CCC, EMEP/CEIP, EMEP/CIAM, CCE/UBA, CIEMAT, TNO (2022) Transboundary particulate matter, photo-oxidants, acidifying and eutrophying components, EMEP status report 1/2022. September 29 2022, ISSN 1504-6192, available from <a href="https://emep.int/publ/reports/2022/EMEP\_Status\_Report\_1\_2022.pdf">https://emep.int/publ/reports/2022/EMEP\_Status\_Report\_1\_2022.pdf</a> (accessed October 2022).
- 28. Vieno, M., Dore, A. J., Stevenson, D. S., Doherty, R., Heal, M. R., Reis, S., Hallsworth, S., Tarrason, L., Wind, P., Fowler, D., Simpson, D., Sutton, M. A. (2010) Modelling surface ozone during the 2003 heat-wave in the UK. *Atmospheric Chemistry and Physics*, **10**, 7963-7978 DOI: 10.5194/acp-10-7963-2010.
- 29. Wiedinmyer, C., Akagi, S. K., Yokelson, R. J., Emmons, L. K., Al-Saadi, J. A., Orlandi, J. J., Soja, A. J. (2011) The Fire Inventory from NCAR (FINN): a high resolution global model to estimate the emissions from open burning. *Geoscientific Model Development*, **4**, 625-641. DOI: 10.5194/gmd-4-625-2011.
- 30. Zhong, J., Hood, C., Johnson, K., Stocker, J., Handley, J., Wolstencroft, M., Mazzeo, A., Cai, X., Bloss, W.J. (2021) Using task farming to optimise a street-scale resolution air quality model of the West Midlands (UK). *Atmosphere*, **12(8)**, 983. DOI: 10.3390/atmos12080983.
- 31. Lao, J., Teixidó, O. (2011) Air quality model for Barcelona. Air Pollution, 19, 25-36.
- 32. Biggart, M., Stocker, J., Doherty, R.M., Wild, O., Hollaway, M., Carruthers, D., Li, J., Zhang, Q., Wu, R., Kotthaus, S., Grimmond, S. (2020) Street-scale air quality modelling for Beijing during a winter 2016 measurement campaign. *Atmospheric Chemistry and Physics*, **20**(5), 2755-2780. DOI: 10.5194/acp-20-2755-2020.
- 33. Stocker, J., Hood, C., Carruthers, D., McHugh, C. (2012) ADMS–Urban: Developments in modelling dispersion from the city scale to the local scale. *International Journal of Environment and Pollution*, **50(1)**, 308.
- 34. Jackson, M., Hood, C., Johnson, C., Johnson, K. (2016) Calculation of urban morphology parameterisations for London for use with the ADMS-urban dispersion model. *International Journal of Advanced Remote Sensing and GIS*, **5(4)**, 1678-87.
- 35. Open Street Maps 2D building outline data. OpenStreetMap contributors. (2015) Planet dump [Data file from 18<sup>th</sup> May 2021]. Retrieved from <a href="https://planet.openstreetmap.org">https://planet.openstreetmap.org</a>.
- 36. Lidar data for Dublin, Waterford, Galway, Limerick and Cork supplied by the Flood Risk Management Section of the Office of Public Works (<a href="https://www.opw.ie">https://www.opw.ie</a>).
- 37. Demuzere, M., Bechtel, B., Middel, A., Mills, G. (2019) Mapping Europe into local climate zones. *PloS one*, **14(4)**, p.e0214474. DOI: 10.1371/journal.pone.0214474.

- 38. Hood, C., Carruthers, D., Seaton, M., Stocker, J., Johnson, K. (2014) Urban canopy flow field and advanced street canyon modelling in ADMS-Urban. *Proc. 16<sup>th</sup> International Conference on Harmonisation within Atmospheric Dispersion Modelling for Regulatory* Purposes, Varna, Bulgaria, September 2014. <a href="https://www.harmo.org/Conferences/Proceedings/\_Varna/publishedSections/H16-067-Hood-EA.pdf">https://www.harmo.org/Conferences/Proceedings/\_Varna/publishedSections/H16-067-Hood-EA.pdf</a> (accessed October 2022).
- 39. Hood, C., Stocker, J., Seaton, M., Johnson, K., O'Neill, J., Thorne, L., Carruthers, D. (2021) Comprehensive evaluation of an advanced street canyon air pollution model. *Journal of the Air & Waste Management Association*, **71**(2), 247–267. DOI: 10.1080/10962247.2020.1803158.
- 40. Stidworthy, A., Carruthers, D., Stocker, J., Balis, D., Katragkou, E. and Kukkonen, J., (2013) Myair toolkit for model evaluation. 15<sup>th</sup> International Conference on Harmonisation within Atmospheric Dispersion Modelling for Regulatory Purposes, Madrid, Spain.
- 41. The Forum for Air Quality Modelling (FAIRMODE) <a href="https://fairmode.jrc.ec.europa.eu">https://fairmode.jrc.ec.europa.eu</a> (accessed November 2022).
- 42. Defra (2020) Air Pollution in the UK 2019 Full Report. Available from <a href="https://uk-air.defra.gov.uk/library/annualreport/index">https://uk-air.defra.gov.uk/library/annualreport/index</a> (accessed December 2022).
- 43. Carslaw, D. C. and Ropkins, K. (2012) OpenAir --- an R package for air quality data analysis. *Environmental Modelling & Software*. **27-28**, 52-61.

### **Appendix A Diffusion tube location revisions**

Each diffusion tube located outside of a street canyon was assessed. This included those located outside of both the street canyon and the modelled road, and those located within a modelled road. Diffusion tubes with revised locations are summarised in Table A.1. Initially, if possible, the location of diffusion tube was confirmed visually. For example, DT59 could be seen attached to a lamppost within the street canyon, Figure A.1(ai), so its location was adjusted accordingly, as shown in, Figure A.1(aii).

Considering diffusion tubes that were located outside of both the street canyon and the road; first it was determined whether it was possible to be at the location specified, for example tubes cannot be located inside a building. In other instances, it was found that the diffusion tube location and canyon width both required revision. For example, for DT30, shown in Figure A.1(bi), it can be seen that the diffusion tube cannot be located within the buildings and that the buildings are not offset from the road. From this information, it was clear that the canyon must extend to the buildings and the diffusion tube must be within the canyon. As shown in Figure A.1(bii), the canyon was extended to the buildings and the diffusion tube was moved along a line perpendicular to road centreline from the originally supplied location to be within the canyon. Those tube locations that were a significant distance outside of a canyon were unchanged.

Considering diffusion tubes that were located within a road; it was determined whether it was possible to be located within a road, for example on an island. If there was nowhere the diffusion tube could be located within the road, the diffusion tube was moved along a line perpendicular to the centre of the road to be in the canyon, on the road/canyon edge. For instance, for DT94, Figure A.1(ci), it can be seen that there is nothing in the centre of the road that could possibly have a diffusion tube attached, so the location was revised, as shown in Figure A.1(cii).

**Table A.1** – Summary of DT location revisions.

Location	Site	Summary of revision		
Dublin	DT102	Moved outside road to canyon edge		
	DT94	Moved outside road to canyon edge		
	DT93	Moved from outside canyon to within canyon and canyon width_L (15001ERM) increased from 0 m to 10 m		
	DT75	Moved from outside canyon to within canyon, known location		
	DT76	Moved outside road to canyon edge		
Limerick	DT59	Moved from outside canyon to within canyon, known location		
	DT55	Moved outside road to canyon edge		
Cork	DT16	Moved outside road to canyon edge		
	DT5	Moved along road, known location		
	DT2	Moved outside road to canyon edge		
	DT20	Moved outside road to canyon edge		
Galway	DT42	Moved from outside canyon to within canyon		
	DT30	Moved from outside to within canyon and canyon width_R (1206WRM) increased from 5.54 m to 10.54 m		

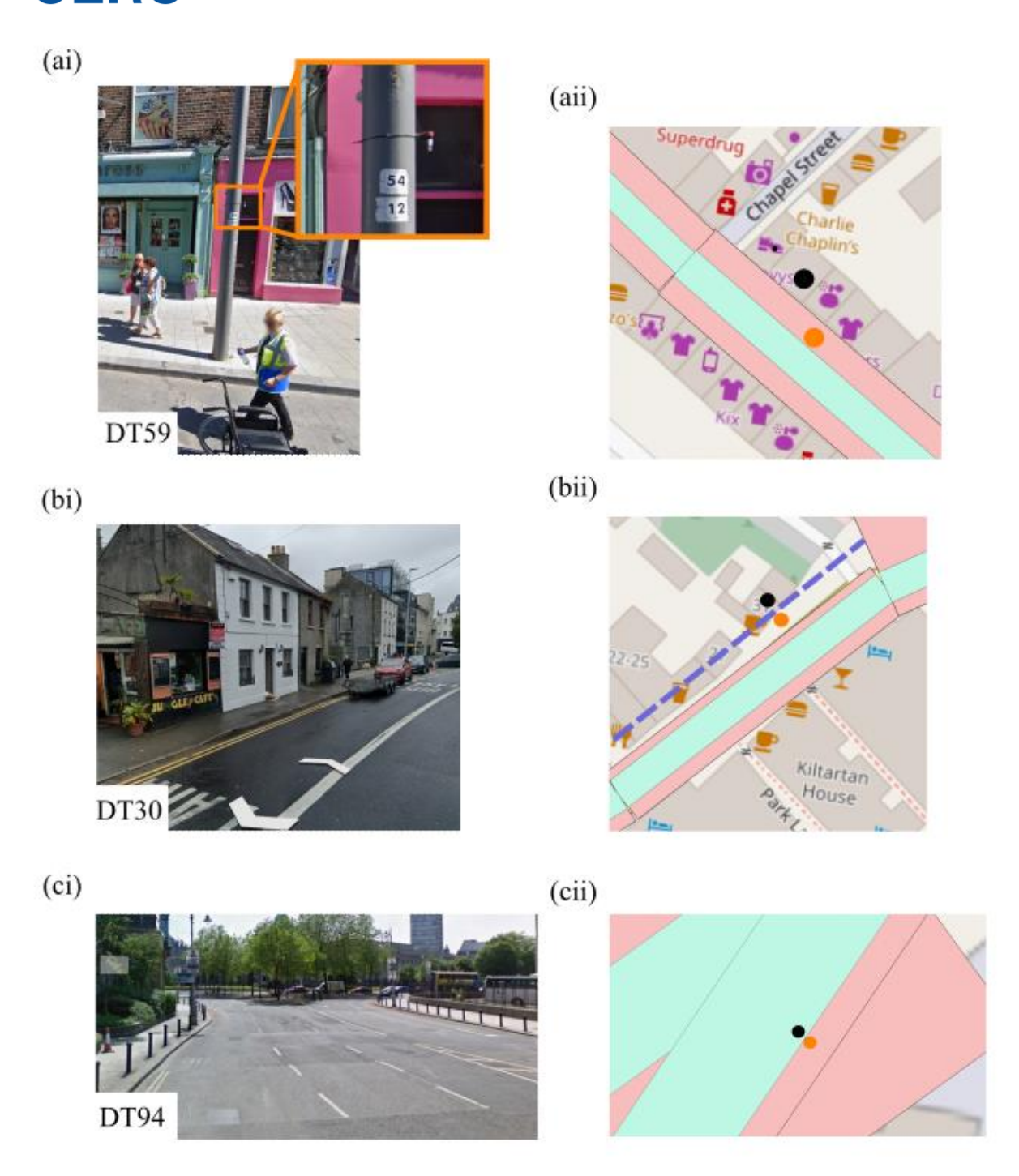


**Figure A.1** – Examples of diffusion tubes with revised locations. A black circle indicates the original location and an orange circle indicates the revised location, new canyon dimensions are shown by a blue dashed line. Map data ©2022 Google. Background map; © OpenStreetMap contributors <a href="https://www.openstreetmap.org/copyright">www.openstreetmap.org/copyright</a>.

### **Appendix B FAIRMODE Model Performance Metrics**

Table B.1 summarises the FAIRMODE model performance metrics.

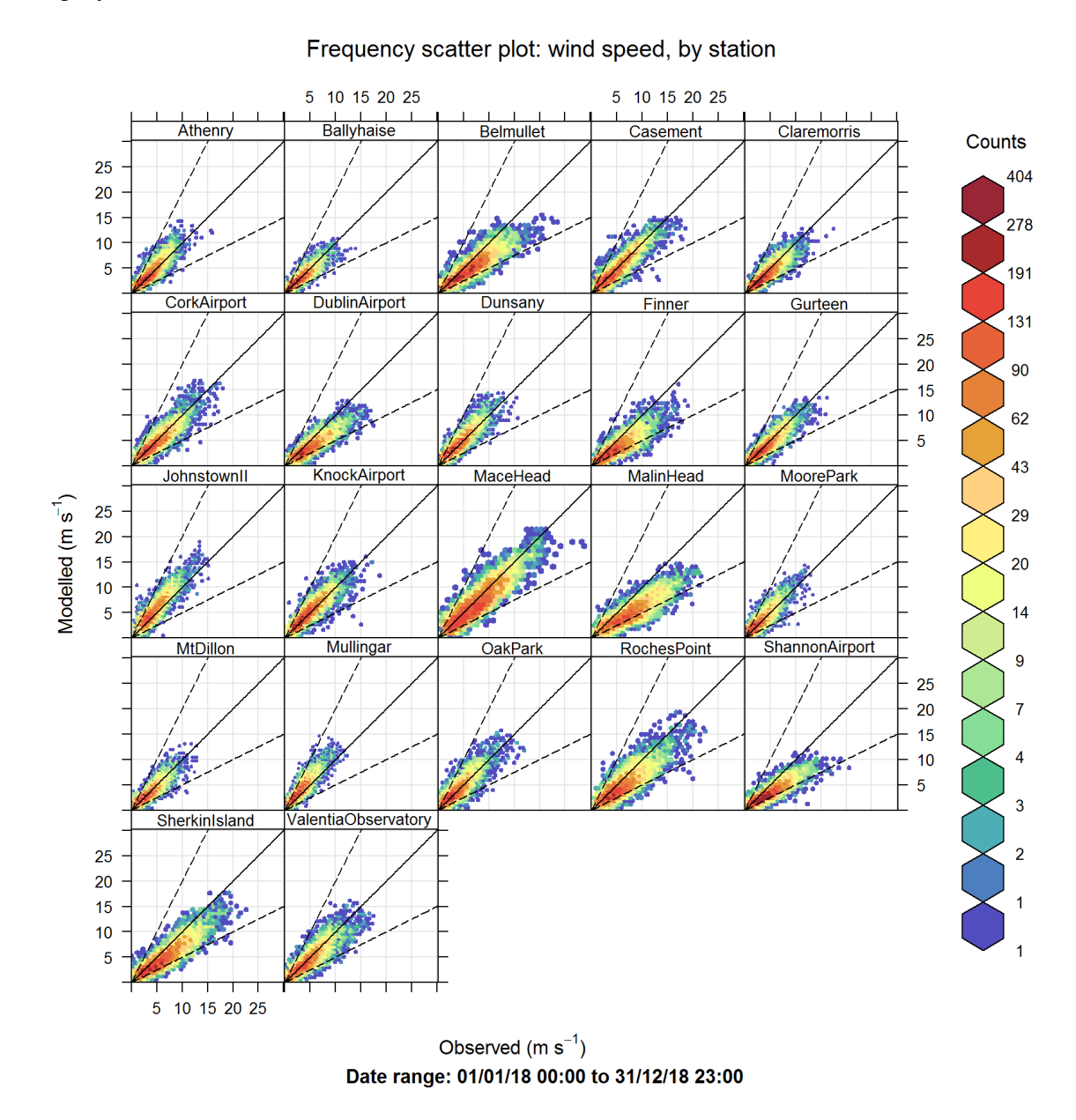
Table B.1 – FAIRMODE model performance metrics.

Name	Title	Purpose	Mathematical definition
MQI	Modelling Quality Indicator	Describes the difference between observed and modelled values, normalised by the measurement uncertainty and a scaling factor. $\beta$ is taken to be 2.	$\frac{\text{RMSE}}{\beta \times \text{RMSU}}$
MQI <sub>90</sub> or MQI_HD	Modelling Quality Objective for hourly / daily / maximum daily 8- hour means	Criterion for the value of the MQI. FAIRMODE considers model performance to be good if MQI_HD ≤ 1. The ideal value is 0.	90 <sup>th</sup> percentile of all valid values of the MQI
MQI <sub>annual</sub>	Modelling Quality Indicator for annual means	Mean bias between modelled and observed annual averaged concentrations normalised by the expanded measurement uncertainty of the mean concentration.	$\frac{ \bar{O} - \bar{M} }{\beta \times UOmean}$
MQI <sub>annual 90</sub> or MQI_YR	Modelling Quality Objective for annual means	Criterion for the value of the MQI <sub>annual</sub> . FAIRMODE considers model performance to be good if MQI <sub>annual 90</sub> $\leq$ 1. The ideal value is 0.	90 <sup>th</sup> percentile of all valid values of the MQI <sub>annual</sub>
Umod(RV)	Model uncertainty, expressed as a percentage	The value of Umod(RV) shown on the target plot is the 90th percentile of the individual Umod(RV) values for each station.  Umod(RV) is zero when $RMSE \leq RMSU$ .	



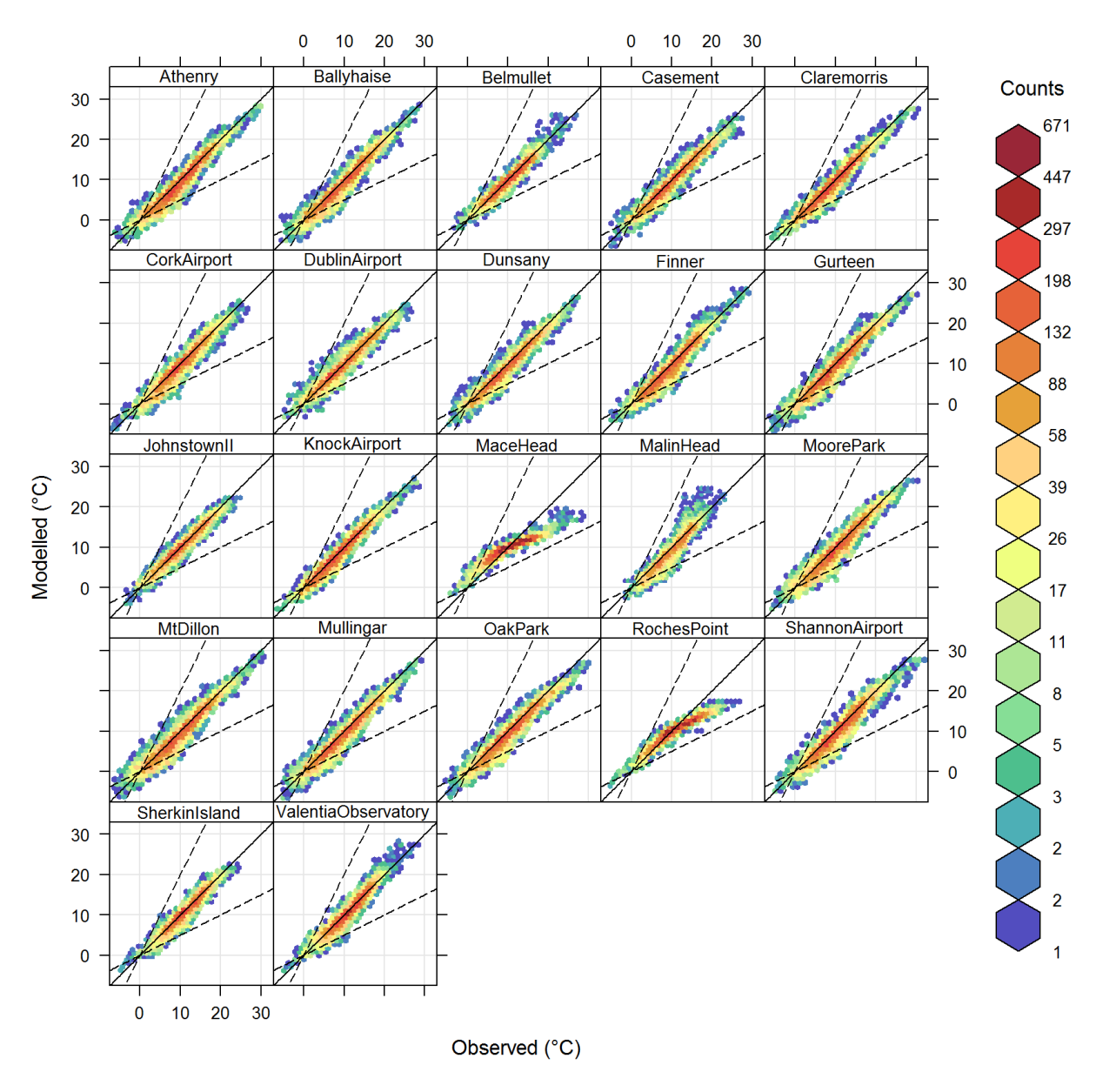
### Appendix C Meteorological model evaluation

Figure C.1 shows frequency scatter plots of hourly modelled and measured wind direction values at each measurement site in 2018. The highest measured wind speeds are found at coastal locations such as Mace Head and Malin Head. Equivalent plots for modelled and measured temperature are shown in Figure C.2. These show some sites where the model is predicting overly maritime temperatures, with lower maximum modelled temperatures than measured. This can happen when the cell containing the modelled location has a dominant land use category of sea.



**Figure C.1** – Frequency scatter plots showing hourly modelled and measured wind speed at each measurement site for 2018. Colours indicate the density of points in each area of the graph.

Page 90 of 132



**Figure C.2** – Frequency scatter plots showing hourly modelled and measured temperature at each measurement site for 2018. Colours indicate the density of points in each area of the graph.

The map in Figure C.3 shows no clear spatial pattern in model mean bias for temperature.

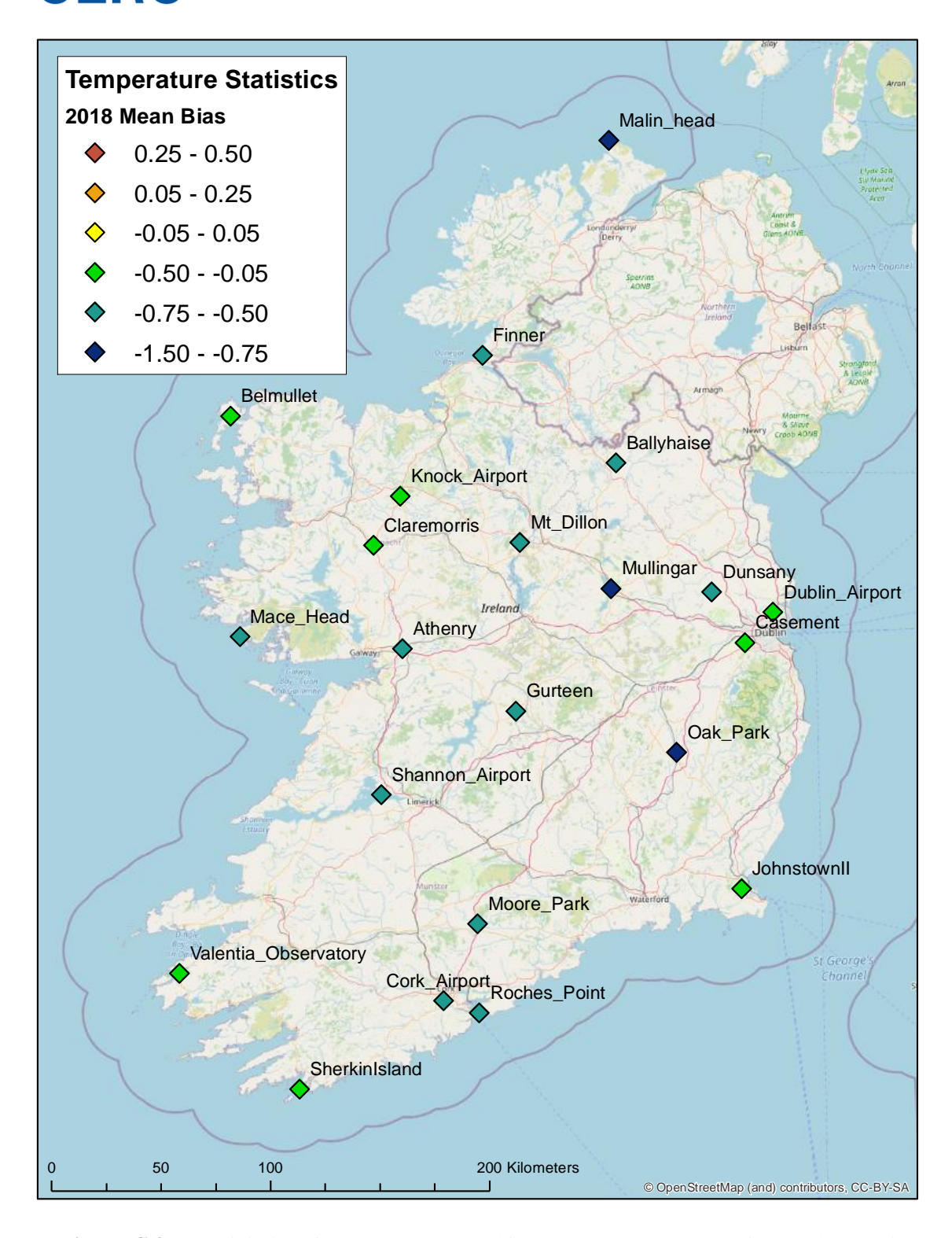


**Figure C.3** – Spatial plot of temperature mean bias at each measurement site. Background map: © OpenStreetMap contributors <a href="https://www.openstreetmap.org/copyright">www.openstreetmap.org/copyright</a>.



### Appendix D Background monitor locations

An explanation for the under-prediction of modelled NO<sub>2</sub> concentrations at selected background continuous monitors has been undertaken (refer to average scatter plots and statistics in Section 8.1.1, and summary in Table D.1 below). The locations of the five sites of particular interest are shown in Figure D.1. The first point to note is that all the background sites are located away from the five main cities. This means that urban canopy and street canyon effects have not been accounted for at these sites.

Tables D.2 and D.3 summarise these monitors in terms of their site locations and particular features. In most cases, the monitors are located away from explicitly modelled roads but all are in, or adjacent to, car parks or fire stations. Specific activity in the vicinity of these monitors, such as parking emissions and accelerating fire engines, has not been modelled explicitly, which will also contribute to the under-prediction of modelled NO<sub>2</sub> concentrations.



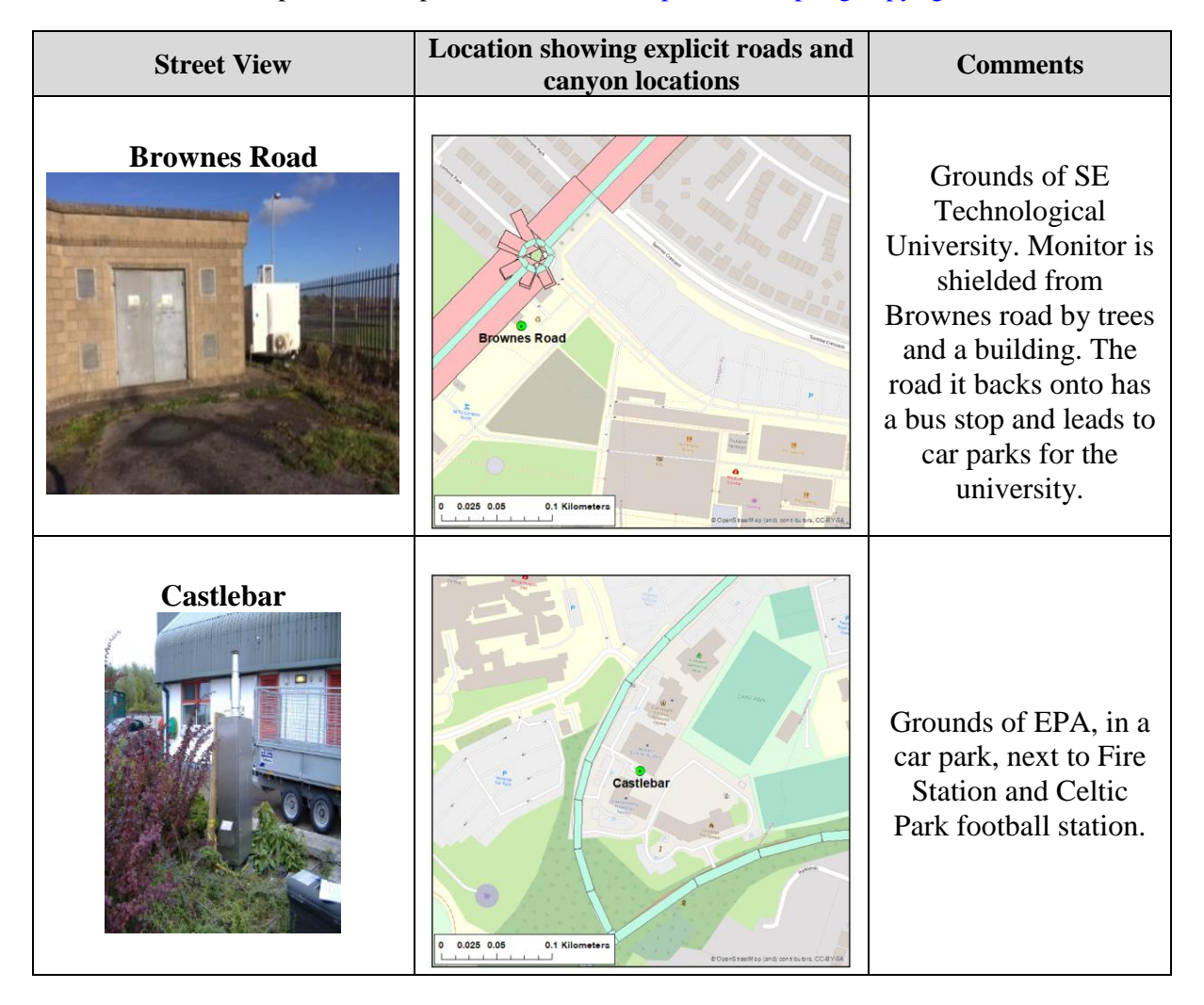
**Figure D.1** – Ireland map showing the locations of the five background sites where the Coupled system is under-predicting. © OpenStreetMap contributors <a href="www.openstreetmap.org/copyright">www.openstreetmap.org/copyright</a>.



**Table D.1** – Summary of observed and modelled annual average NO<sub>2</sub> concentrations for the five background sites where the Coupled system is under-predicting.

Location	Monitor Name	Town	2018 Annual average NO <sub>2</sub> (μg/m³)		2019 Annual average NO <sub>2</sub> (μg/m³)	
		population	Observed	Modelled	Observed	Modelled
Waterford	Brownes Road	53,500	n/a	n/a	8.2	6.2
Mayo	Castlebar	12,000	8.0	4.2	7.8	4.4
Louth	Dundalk	39,000	13.5	6.7	12.5	7.0
Laois	Portlaoise	22,000	11.1	7.3	10.5	7.0
Kilkenny	Seville Lodge	26,500	5.8	4.5	5.3	4.6

**Table D.2** – Details of selected background monitoring sites not located in any of the five main cities. © OpenStreetMap contributors <a href="www.openstreetmap.org/copyright">www.openstreetmap.org/copyright</a>.





 $\begin{table linear length=0.50cm} \textbf{Table D.3} - \textbf{Details of selected background monitoring sites not located in any of the five main cities.} \\ \hline & \textcircled{OpenStreetMap contributors } \underline{www.openstreetmap.org/copyright.} \\ \end{table}$ 

Street View	Location showing explicit roads and canyon locations	Comments	
Dundalk	Dundalk  Dundalk  Count restraction (one burn CCSYG)	Dundalk fire station grounds.	
Portlaoise	Portlaoise  0 0.025 0.05 0.1 Kilometers  8 Continuities land considers. CCSYGA	Grounds of a fire station. Nearest roads included, but activity in surrounding car parks not modelled.	
Seville Lodge	Seville Lodge  Seville Lodge  Seville Lodge  Seville Lodge	Car park of EPA Inspectorate.	



### **Appendix E Supplementary model pollution maps**

Figures E.1 to E.6 present the 2018 regional model EMEP pollution maps for  $NO_2$ ,  $PM_{2.5}$ ,  $PM_{10}$  and  $O_3$  for all AQSR metrics; figures E.7 to E.12 show the corresponding maps for 2019. The 2018 coupled system maps corresponding to Figures 9.2 to 9.9 are presented in Figures E.13 to E.18.

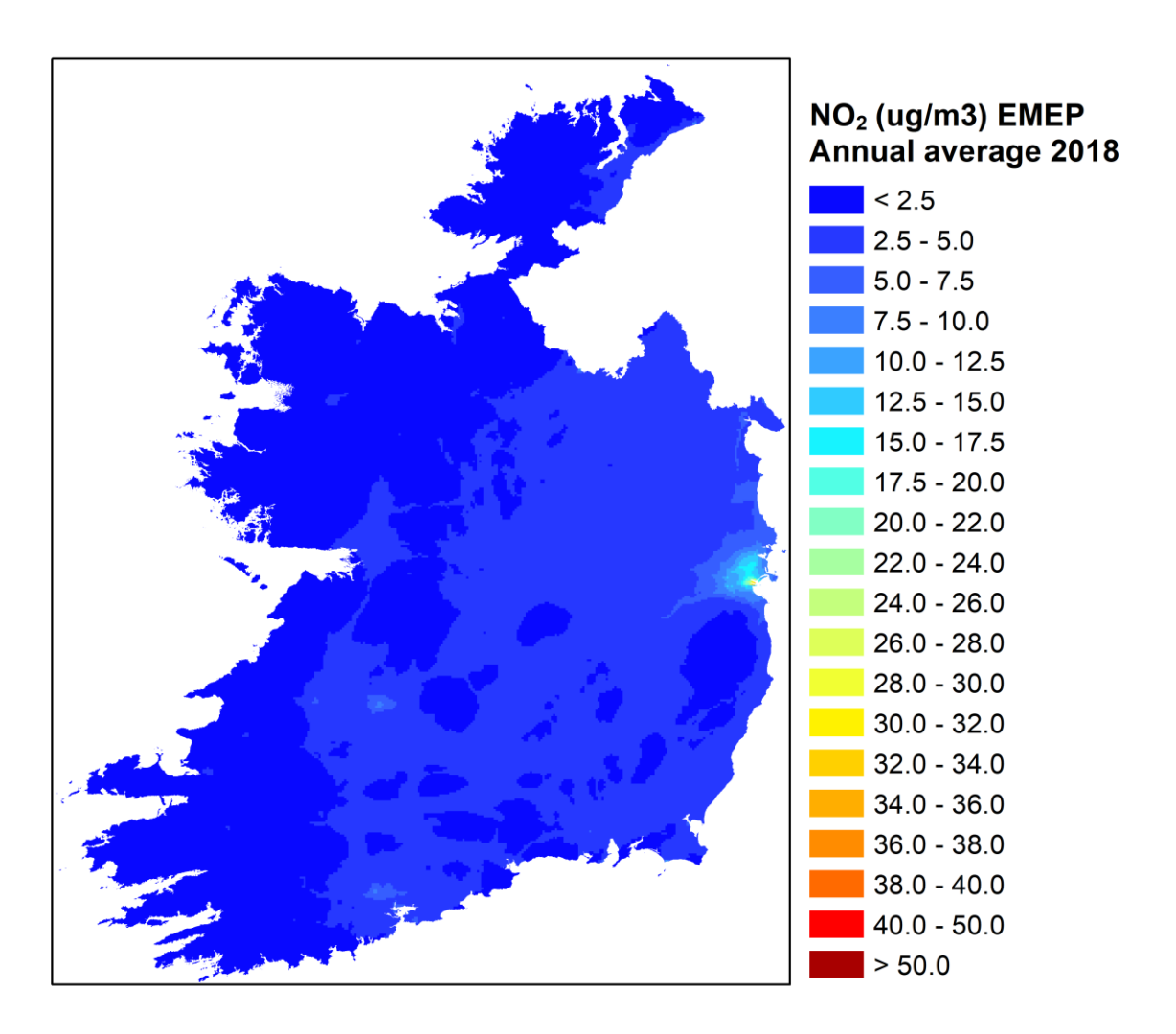


**Figure E.1** – Regional model (EMEP) annual average NO<sub>2</sub> pollution map for 2018; transition to exceedance of AQSR limit (40 μg/m³) shown in **bright red**.

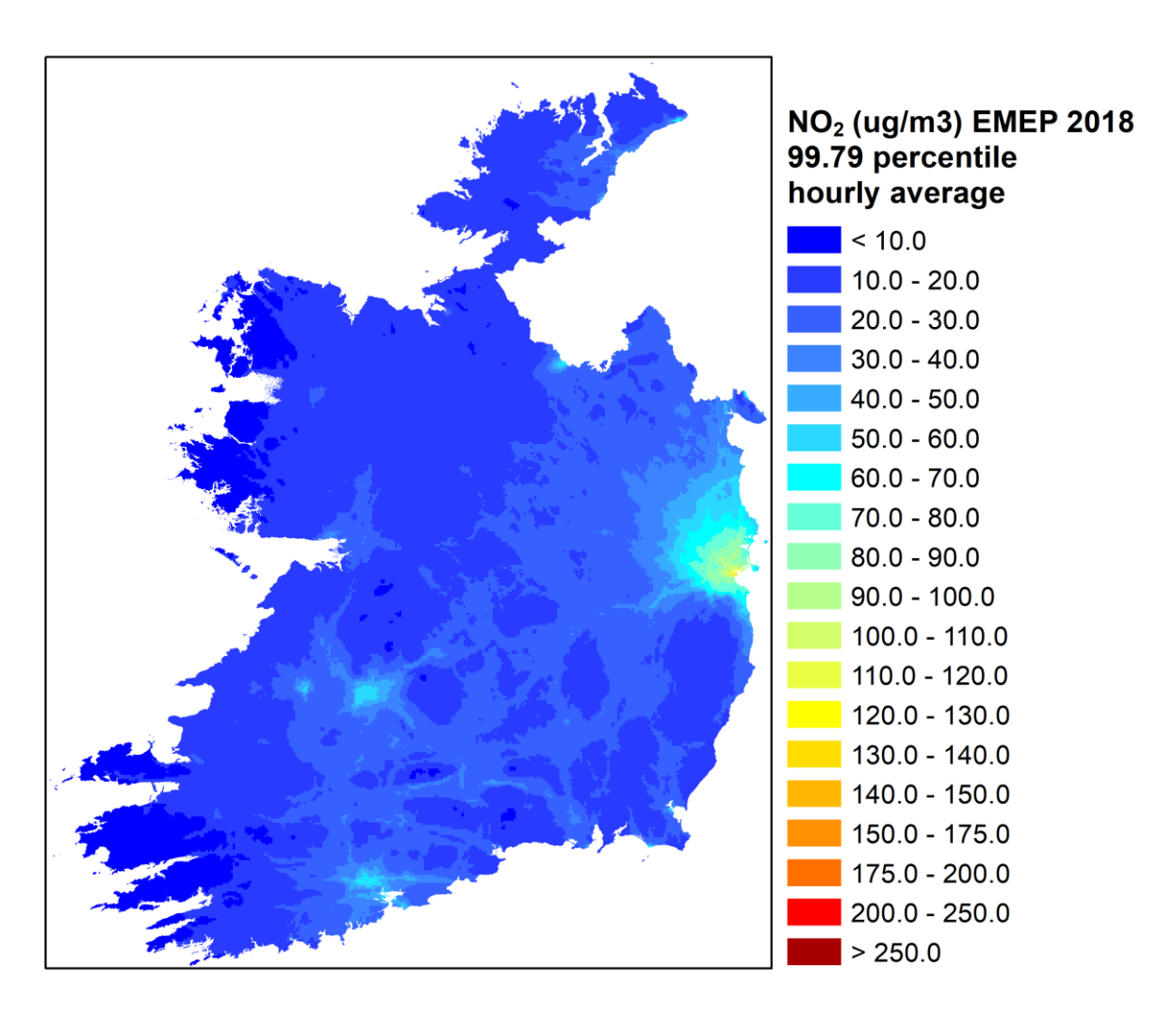


**Figure E.2** – Regional model (EMEP) 99.79<sup>th</sup> percentile hourly NO<sub>2</sub> pollution map for 2018; transition to exceedance of AQSR limit (200 μg/m³) shown in **bright red**.

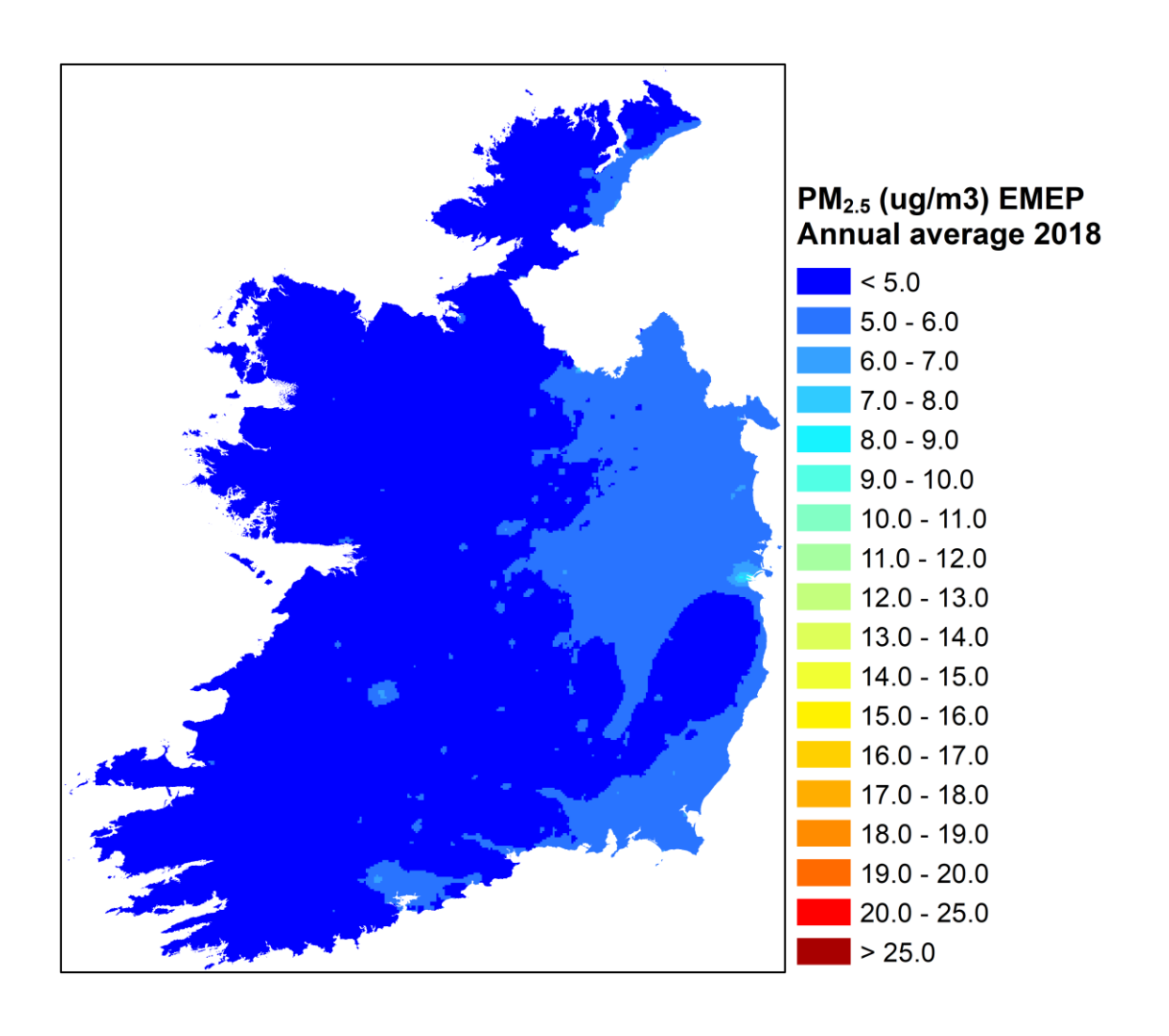


**Figure E.3** – Regional model (EMEP) annual average  $PM_{2.5}$  pollution map for 2018; transition to exceedance of AQSR limit (20  $\mu$ g/m³) shown in **bright red**; WHO guidelines transitions also shown as distinct contour levels (5, 10  $\mu$ g/m³).

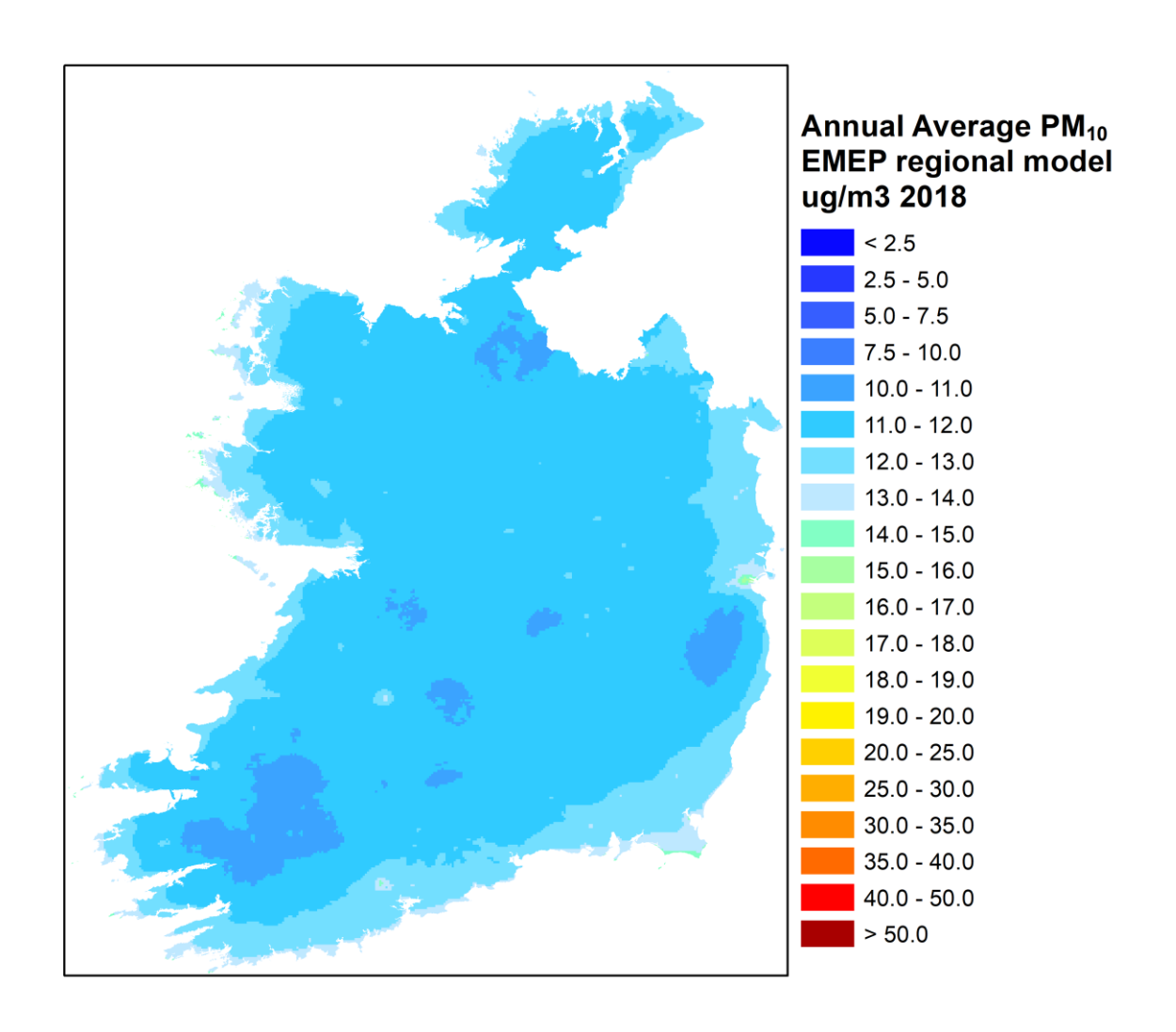


**Figure E.4** – Regional model (EMEP) annual average  $PM_{10}$  pollution map for 2018; transition to exceedance of AQSR limit (40  $\mu g/m^3$ ) shown in **bright red**.

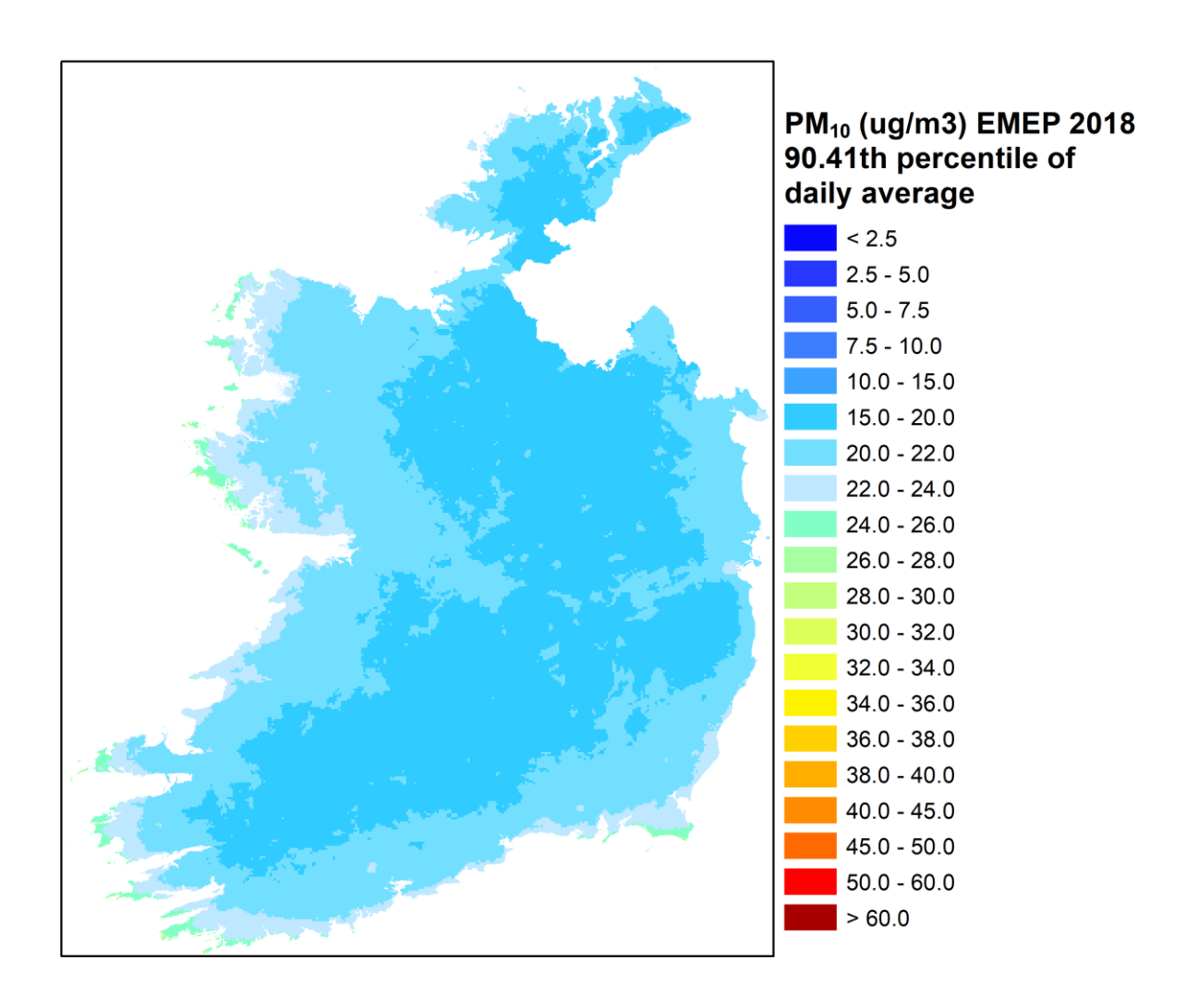


**Figure E.5** – Regional model (EMEP) 90.41 percentile daily  $PM_{10}$  pollution map for 2018; transition to exceedance of AQSR limit (50  $\mu$ g/m³) shown in **bright red**.

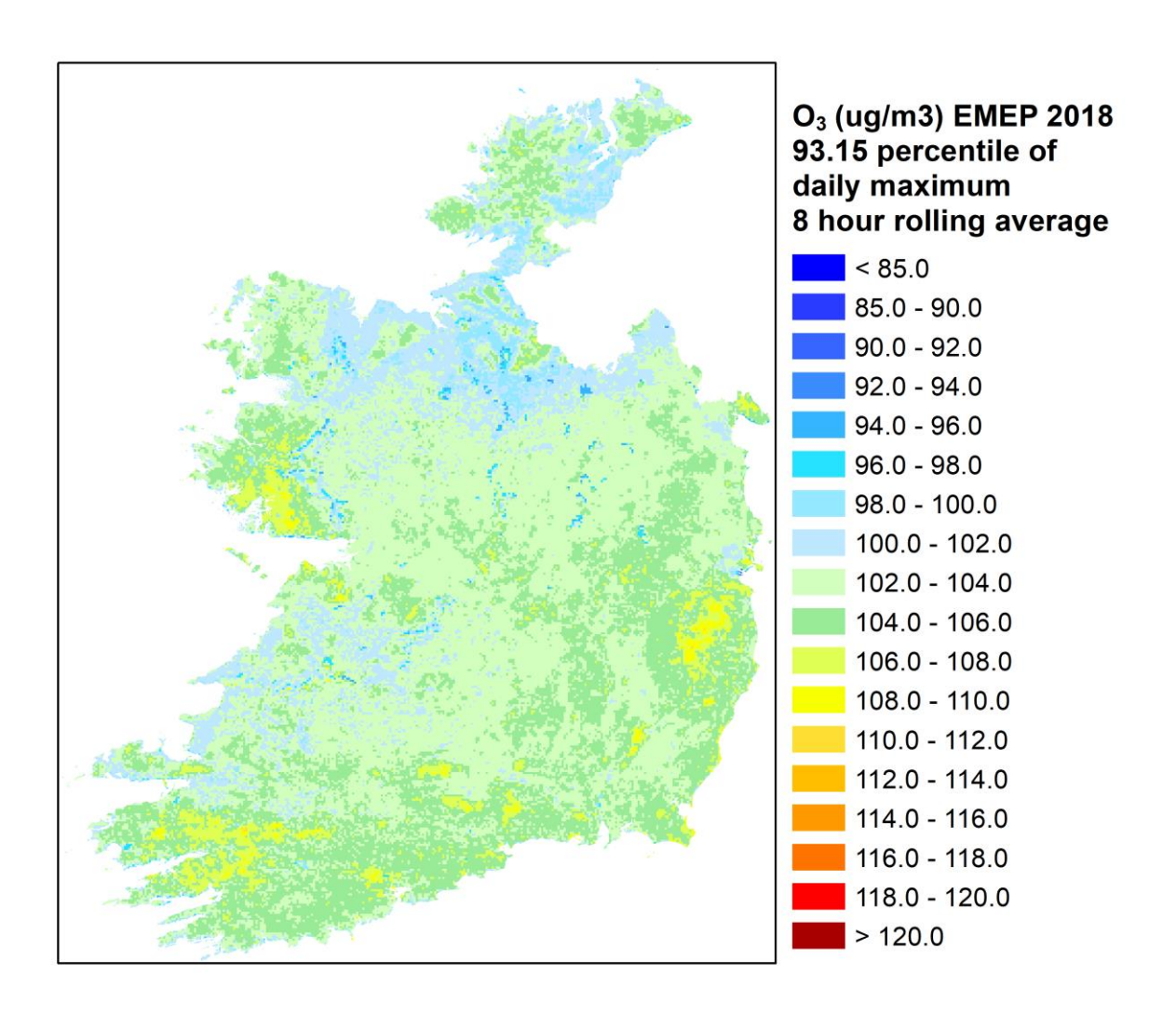


**Figure E.6** – Regional model (EMEP) 93.15<sup>th</sup> percentile of maximum daily 8-hour rolling  $O_3$  pollution map for 2018; transition to exceedance of AQSR target value (120  $\mu$ g/m³) shown in **dark** red.

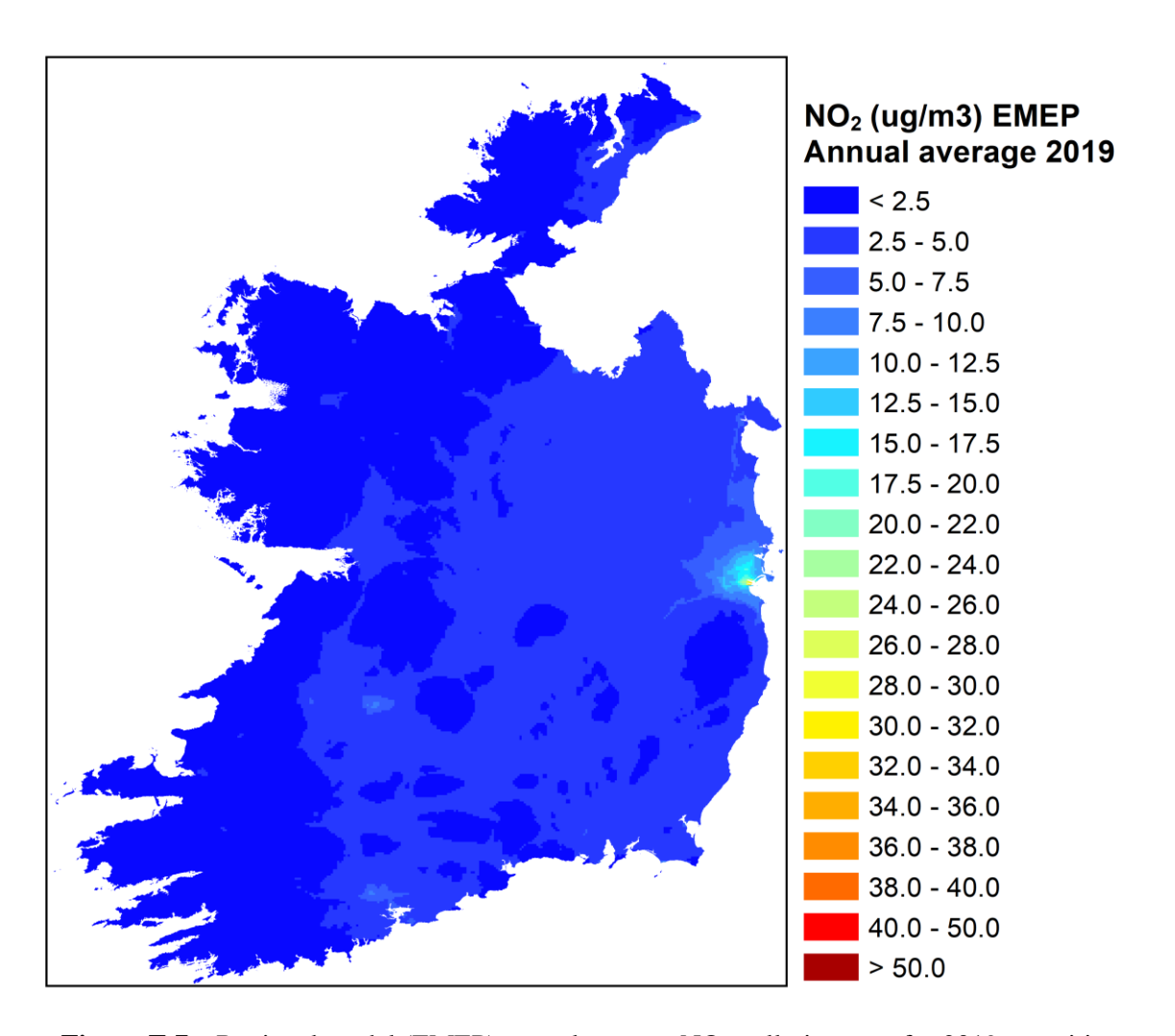


**Figure E.7** – Regional model (EMEP) annual average  $NO_2$  pollution map for 2019; transition to exceedance of AQSR limit (40  $\mu$ g/m³) shown in **bright red**.

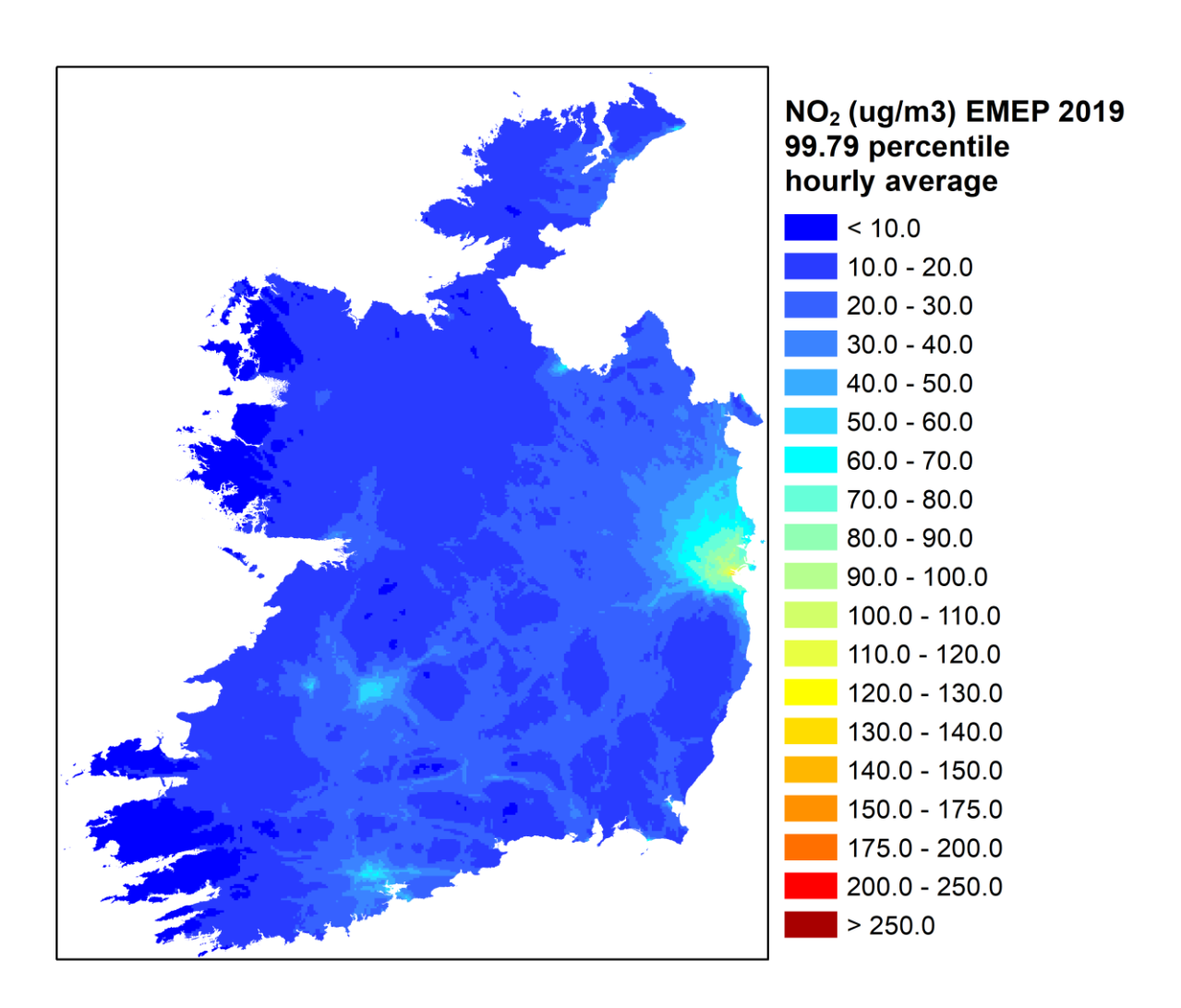


**Figure E.8** – Regional model (EMEP) 99.79<sup>th</sup> percentile hourly NO<sub>2</sub> pollution map for 2019; transition to exceedance of AQSR limit (200  $\mu$ g/m³) shown in **bright red**.

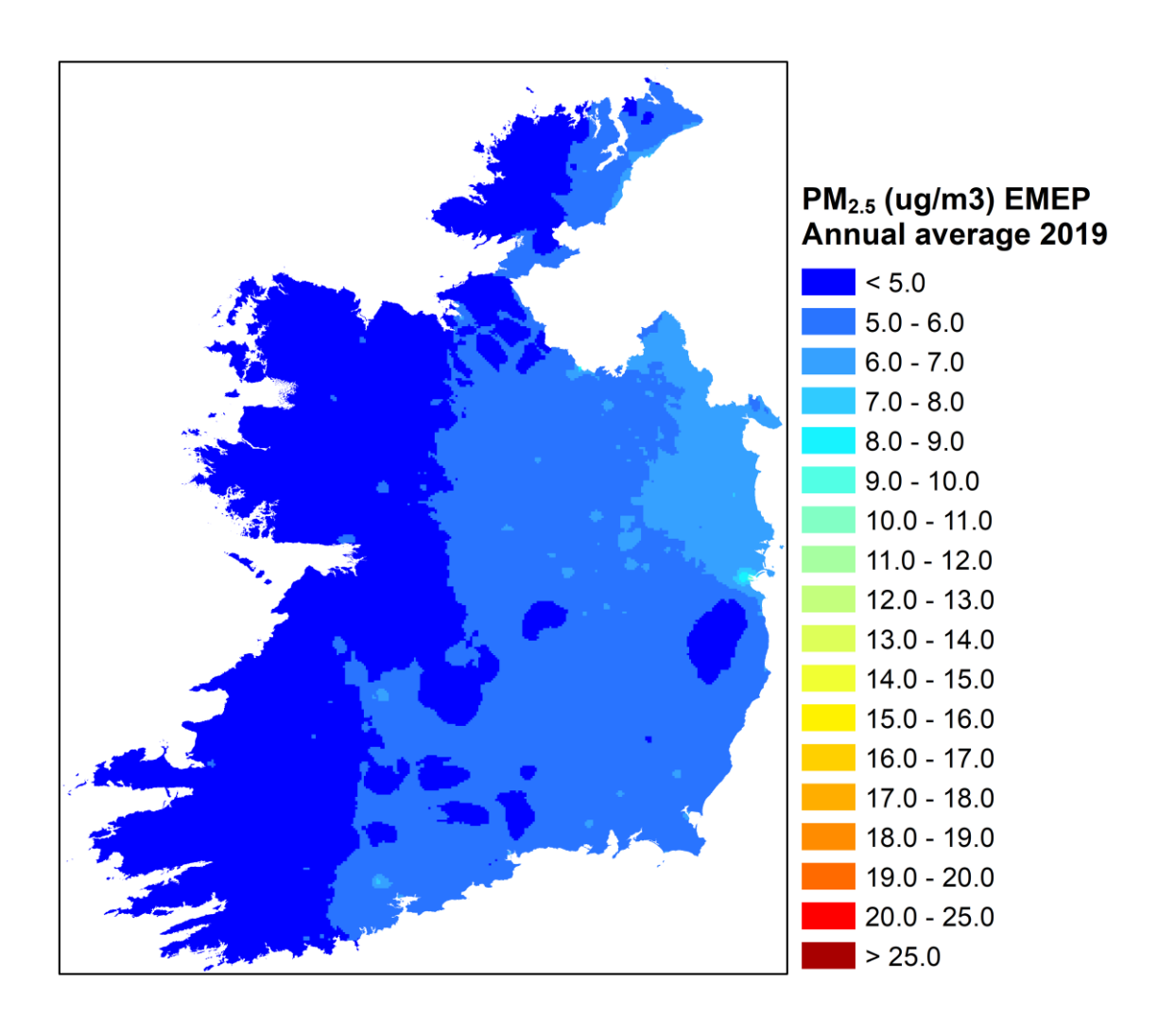


**Figure E.9** – Regional model (EMEP) annual average PM<sub>2.5</sub> pollution map for 2019; transition to exceedance of AQSR limit ( $20 \,\mu g/m^3$ ) shown in **bright red**; WHO guidelines transitions also shown as distinct contour levels (5,  $10 \,\mu g/m^3$ ).

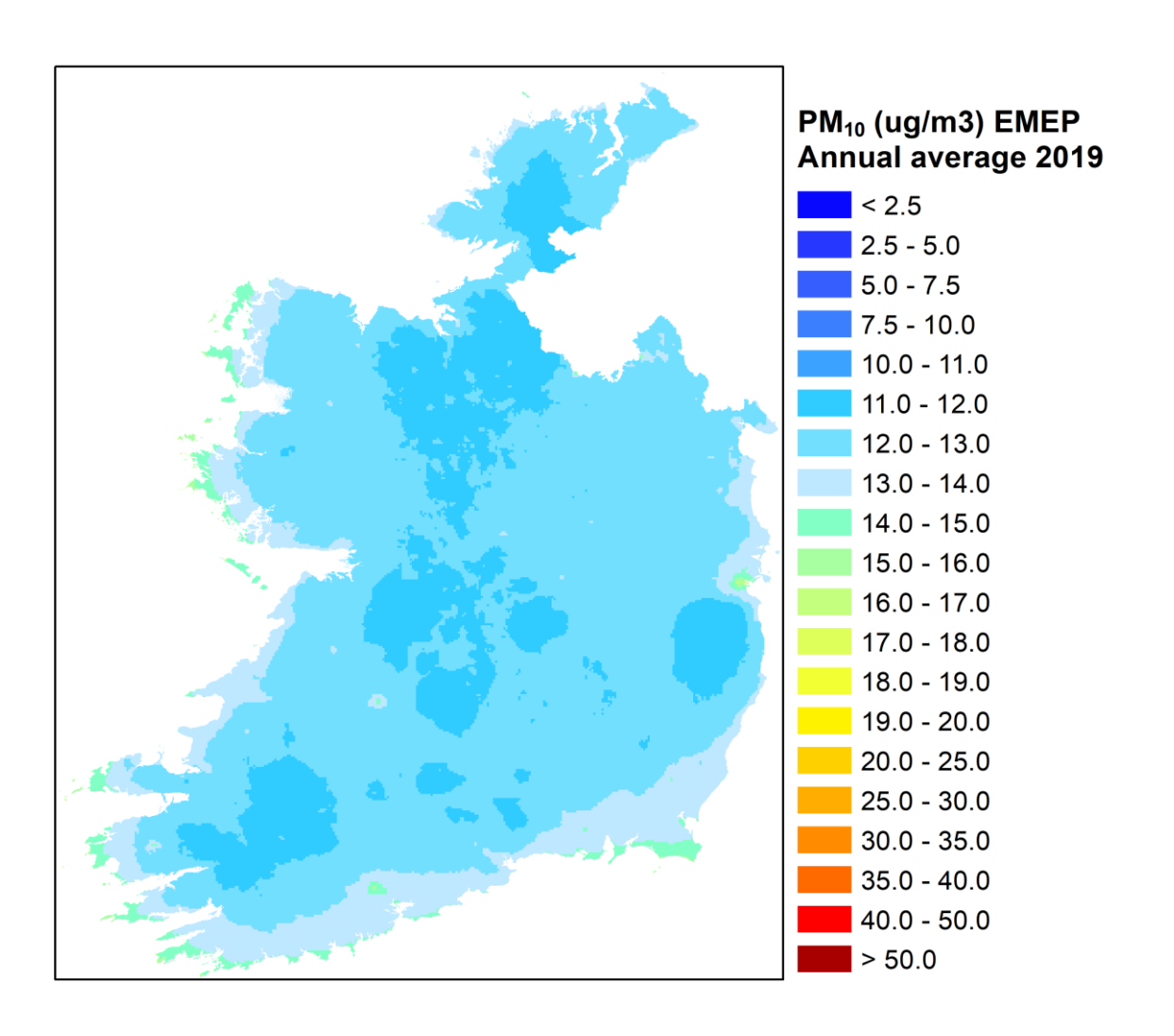


**Figure E.10** – Regional model (EMEP) annual average  $PM_{10}$  pollution map for 2019; transition to exceedance of AQSR limit (40  $\mu g/m^3$ ) shown in **bright red**.

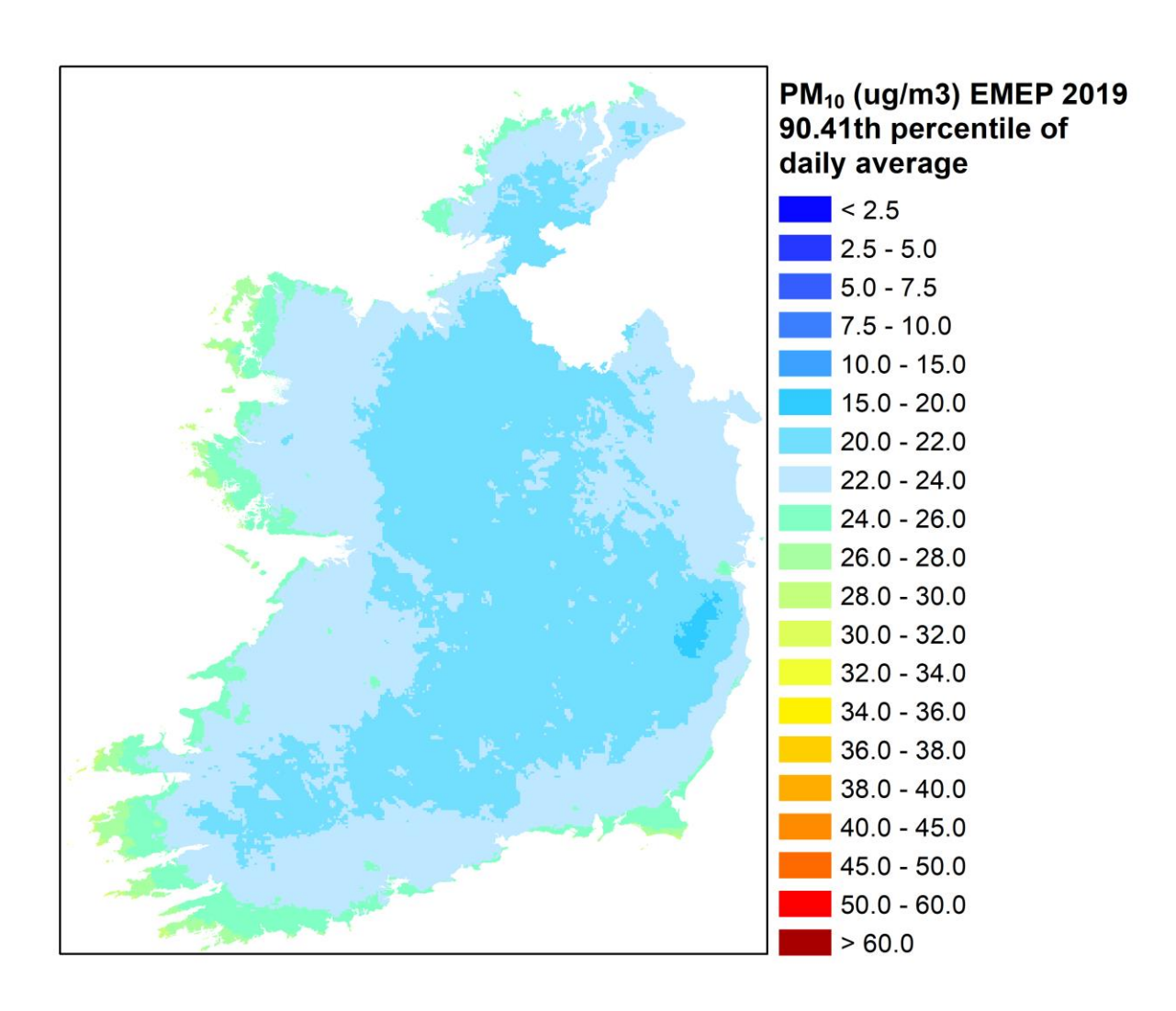
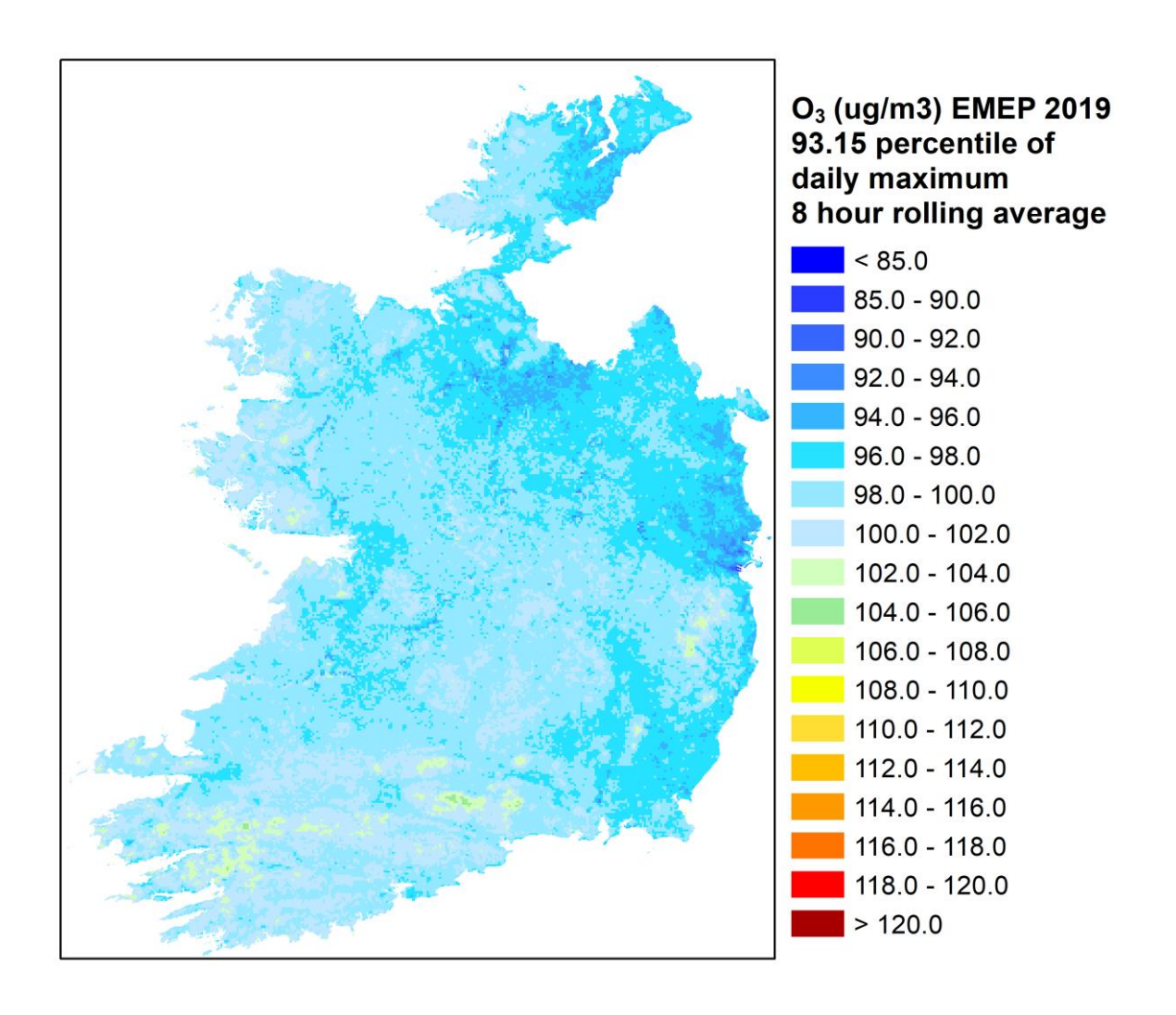
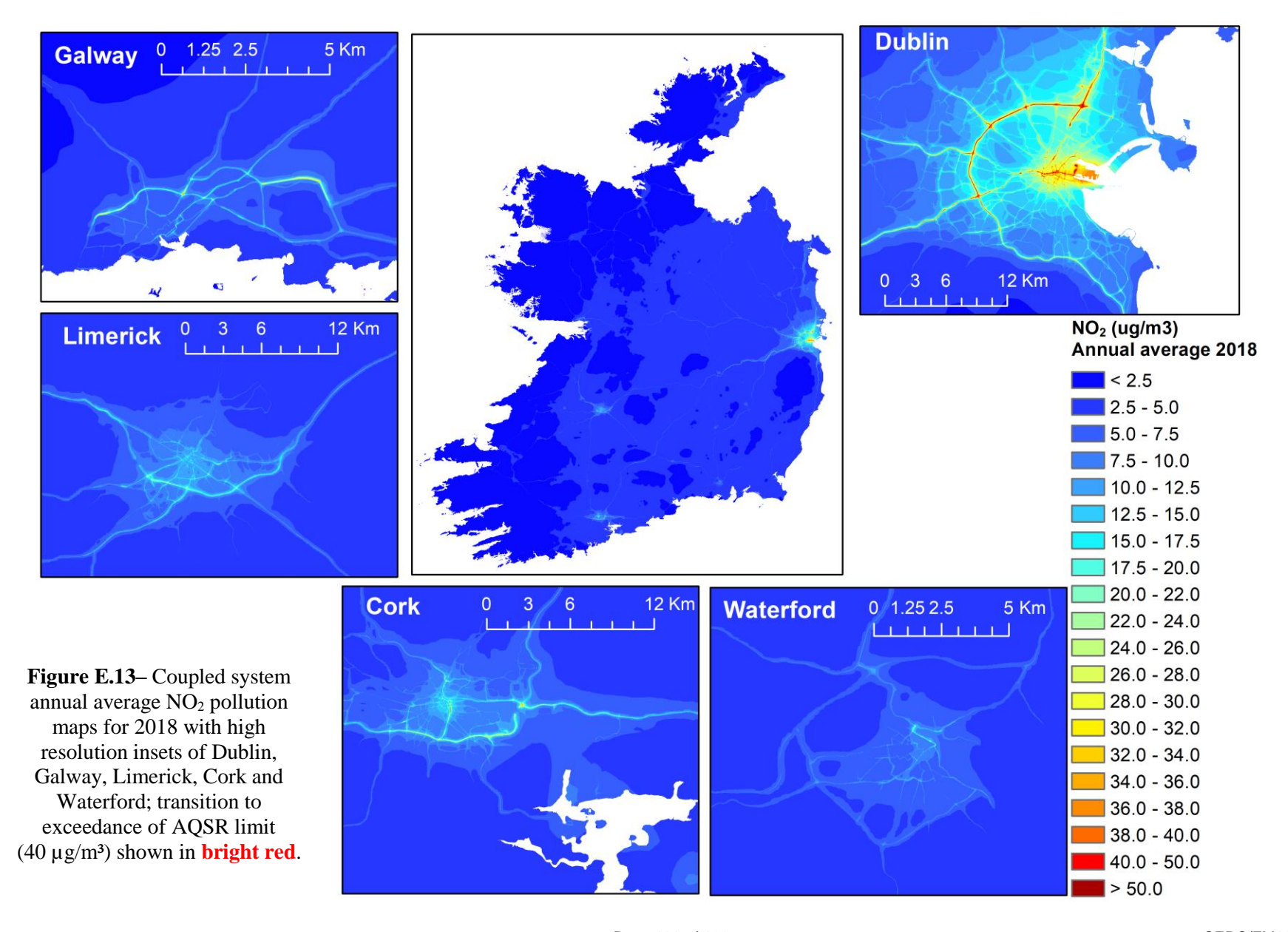


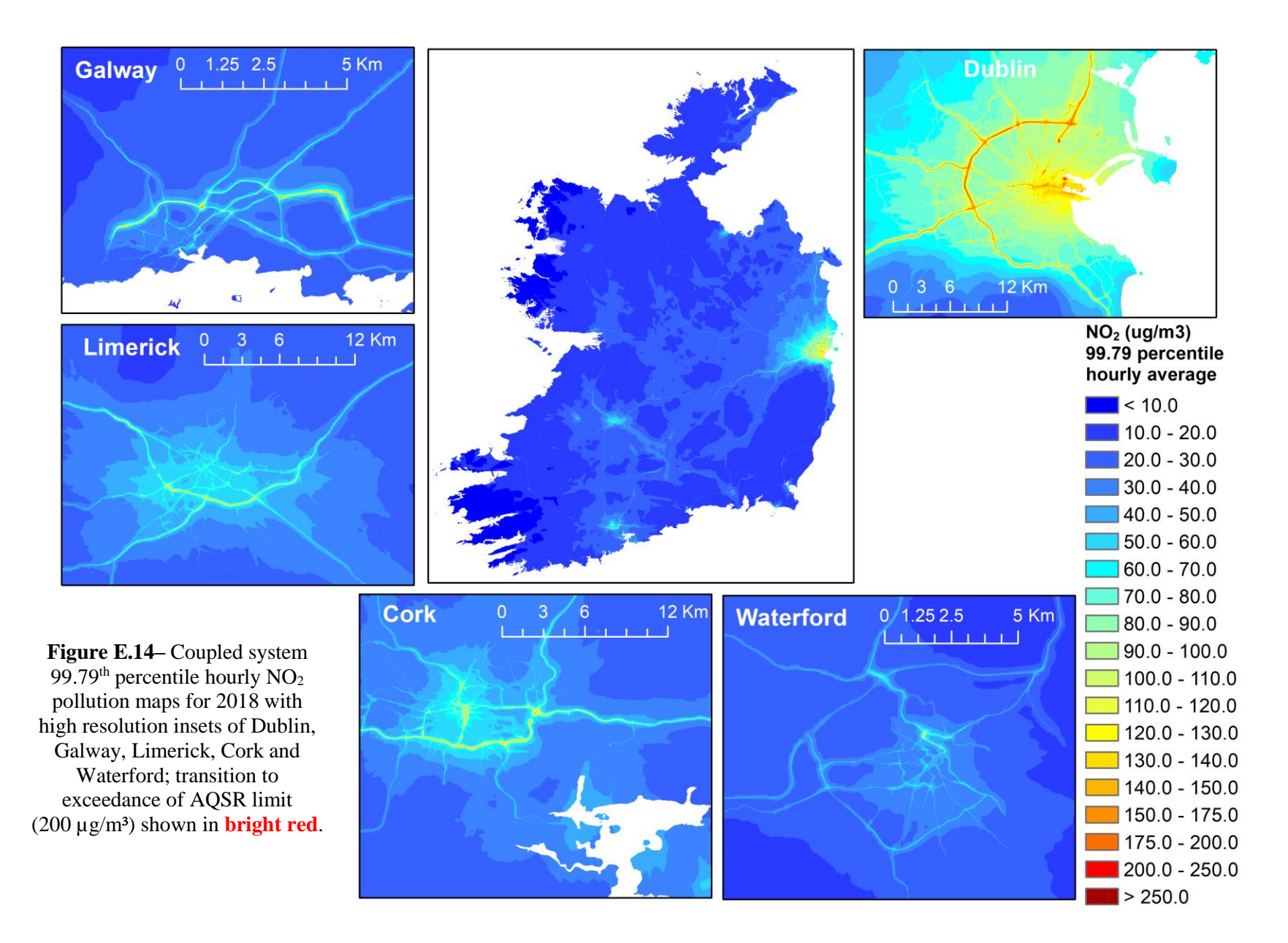
Figure E.11 – Regional model (EMEP) 90.41 percentile daily PM<sub>10</sub> pollution map for 2019; transition to exceedance of AQSR limit (50 μg/m³) shown in bright red.



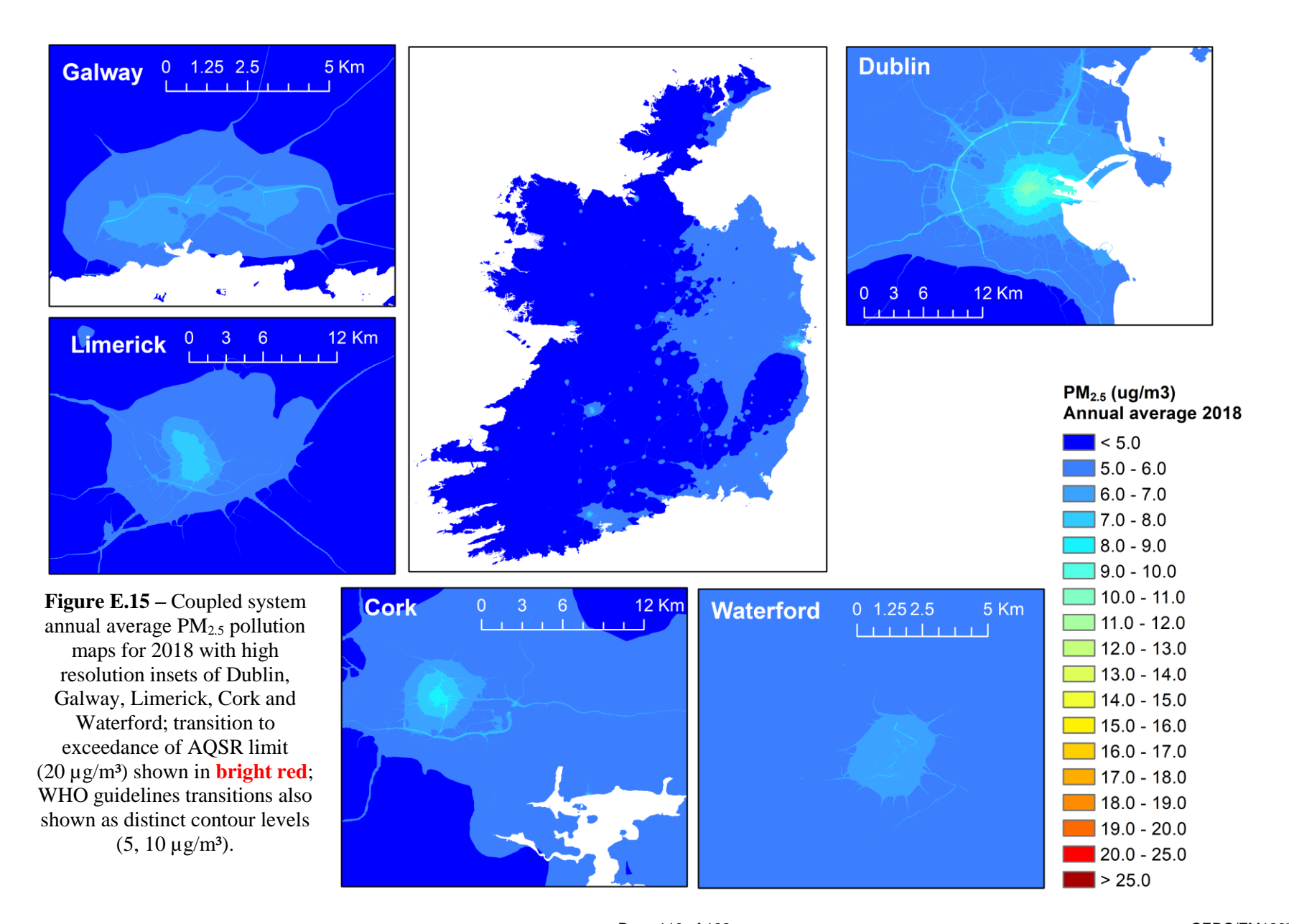
**Figure E.12** – Regional model (EMEP) 93.15th percentile of maximum daily 8-hour rolling  $O_3$  pollution map for 2019; transition to exceedance of AQSR target value (120  $\mu$ g/m³) shown in dark red.



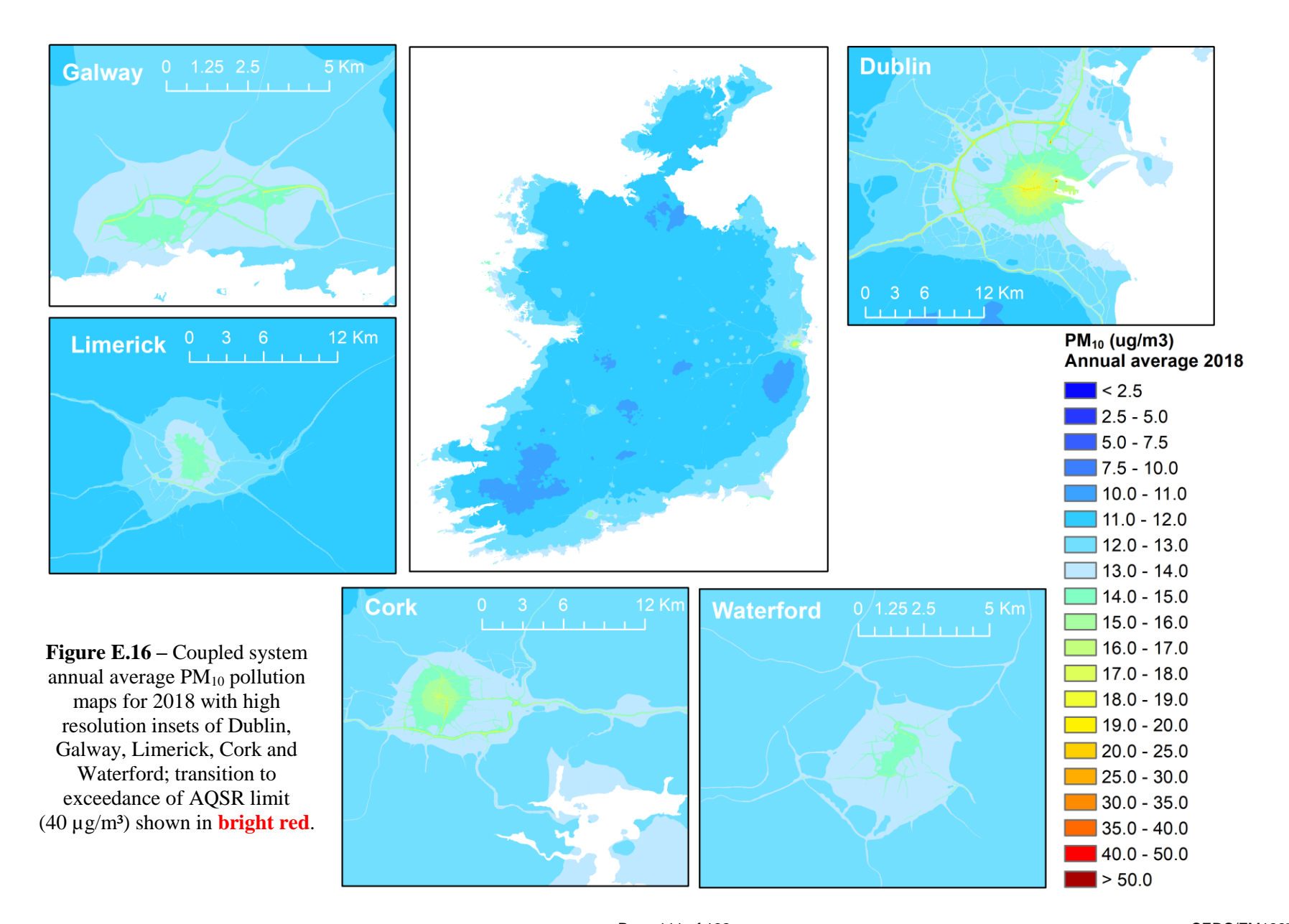
Page 108 of 132 CERC/FM1297



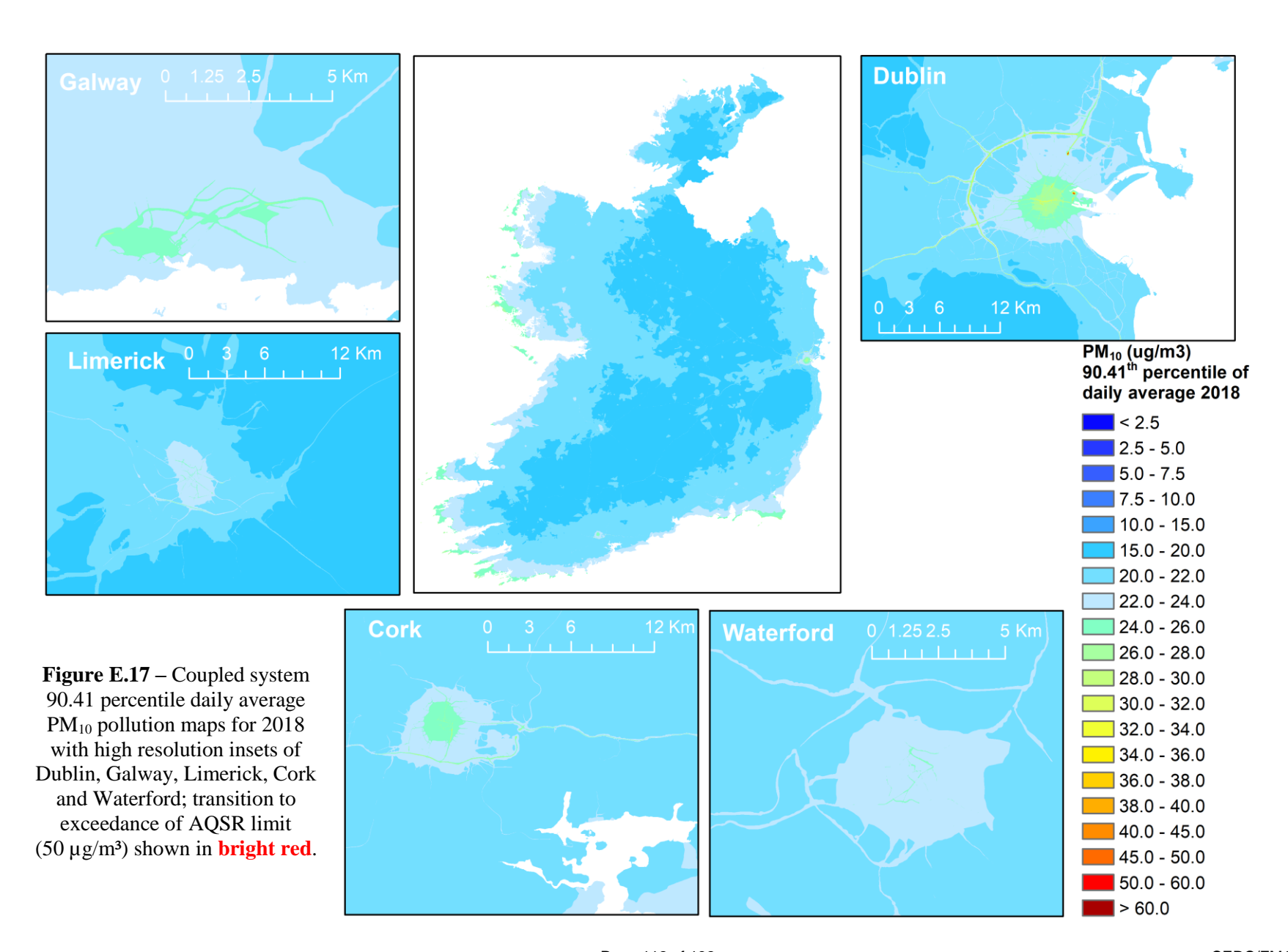
Page 109 of 132 CERC/FM1297



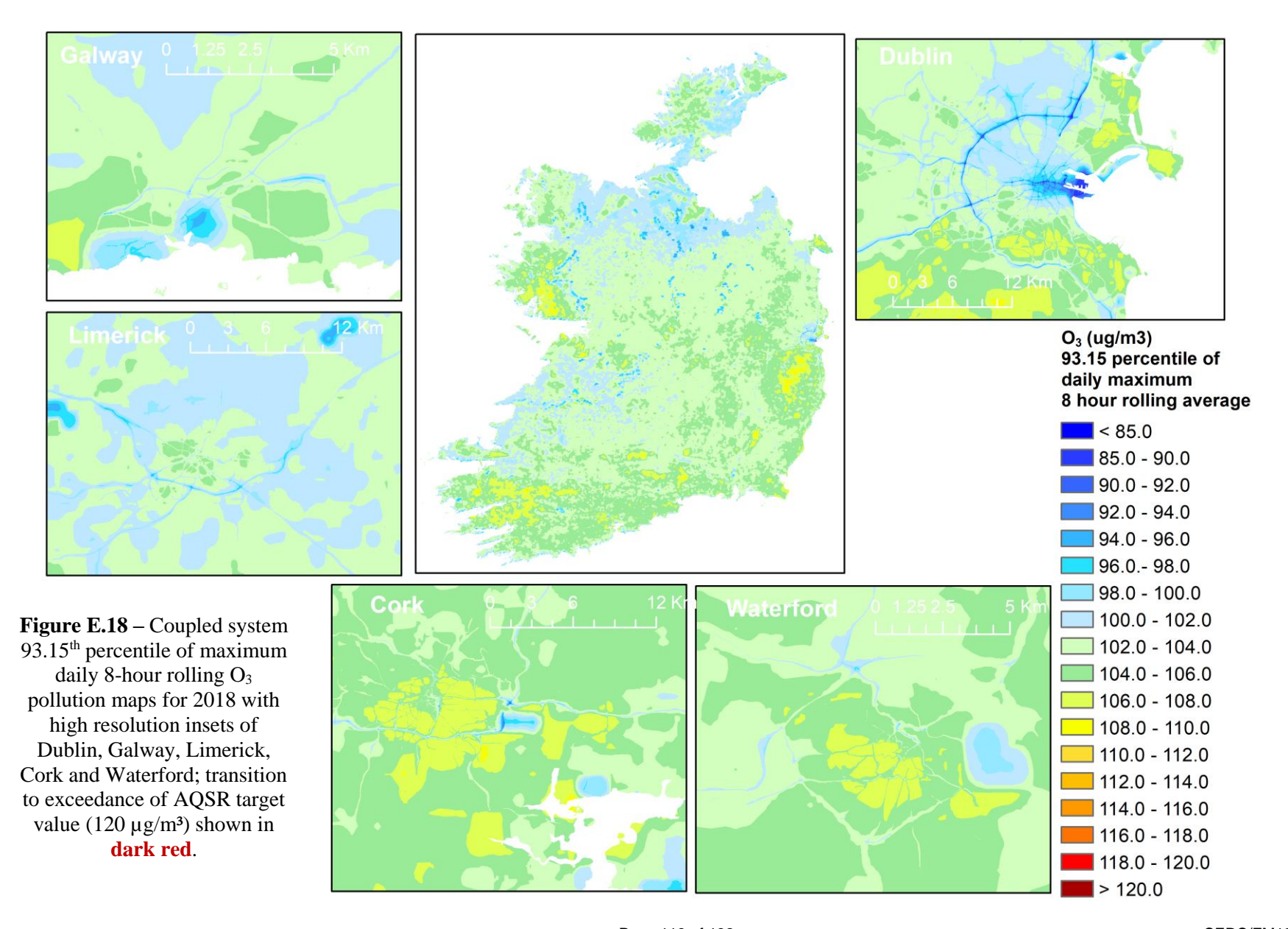
Page 110 of 132 CERC/FM1297



Page 111 of 132 CERC/FM1297



Page 112 of 132 CERC/FM1297



Page 113 of 132 CERC/FM1297



#### Appendix F Supplementary city model pollution maps

Figures F.1 to F.15 present high-resolution city plots of the coupled system annual average concentrations of  $NO_2$ ,  $PM_{2.5}$  and  $PM_{10}$  in 2019 for Dublin, Waterford, Limerick, Cork and Galway. Figures F.16 to F.23 present exceedance plots for  $NO_2$  in Dublin and Cork in 2018 and 2019, in which only the concentrations exceeding the AQSR limit of  $40 \mu g/m^3$  are shown.



**Figure F.1** – Coupled system annual average NO<sub>2</sub> city pollution map for 2019 of Dublin; transition to exceedance of AQSR limit (40 μg/m³) shown in **bright red**.

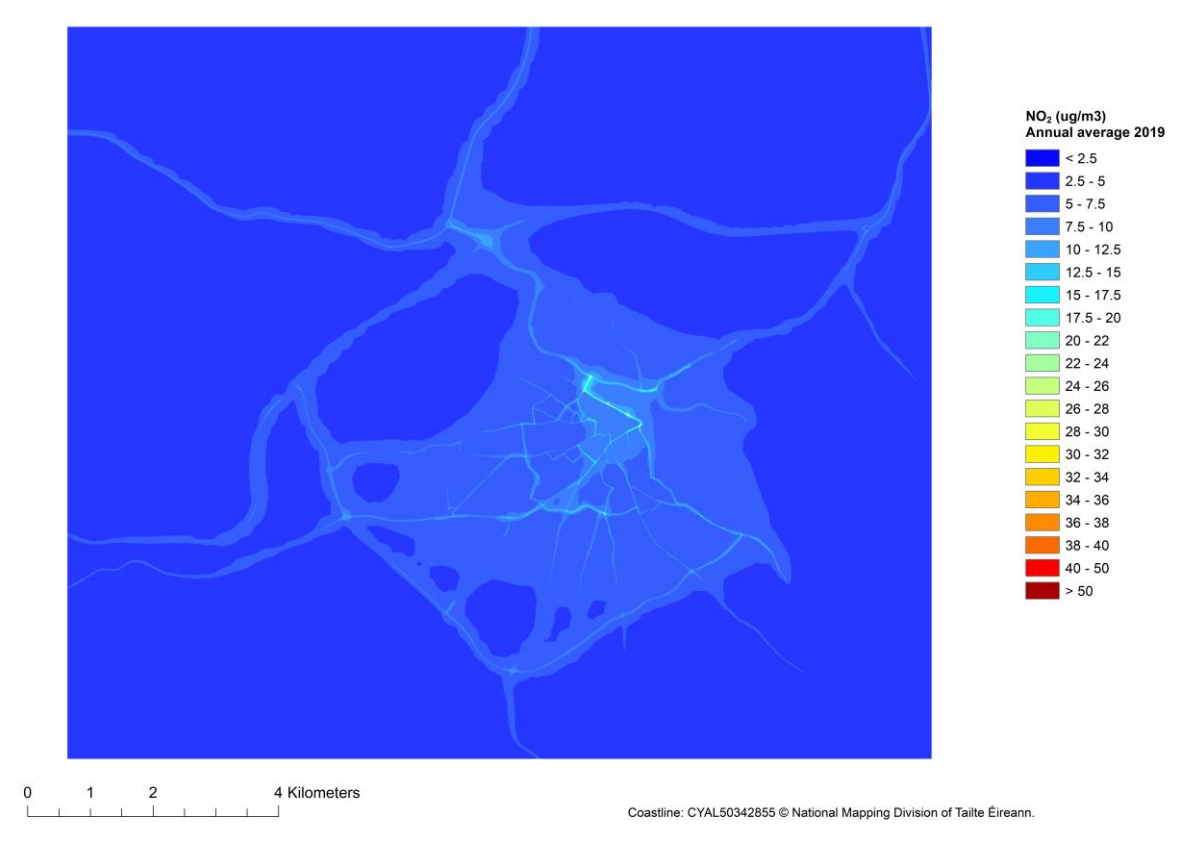


**Figure F.2** – Coupled system annual average NO<sub>2</sub> city pollution map for 2019 of Waterford; transition to exceedance of AQSR limit (40 μg/m³) shown in **bright red**.

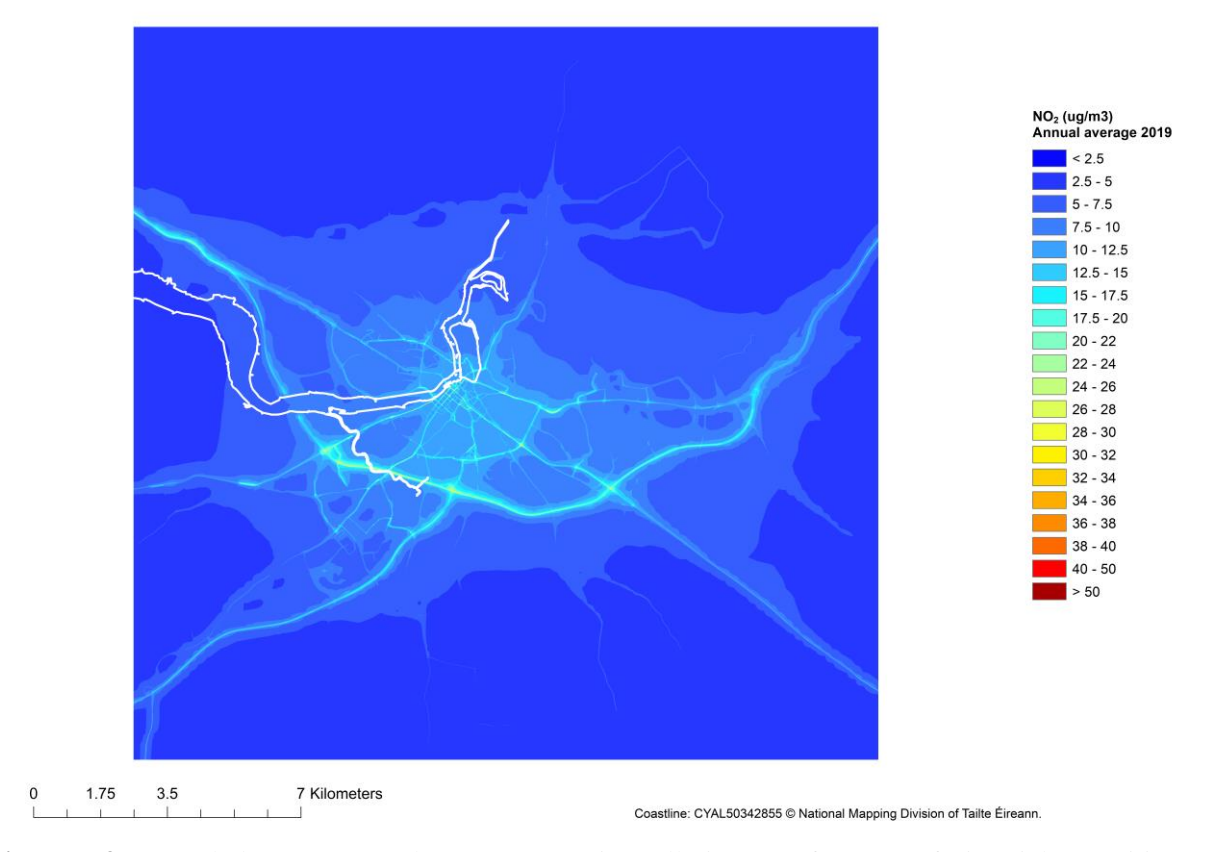


**Figure F.3** – Coupled system annual average NO<sub>2</sub> city pollution map for 2019 of Limerick; transition to exceedance of AQSR limit (40 μg/m³) shown in **bright red**.

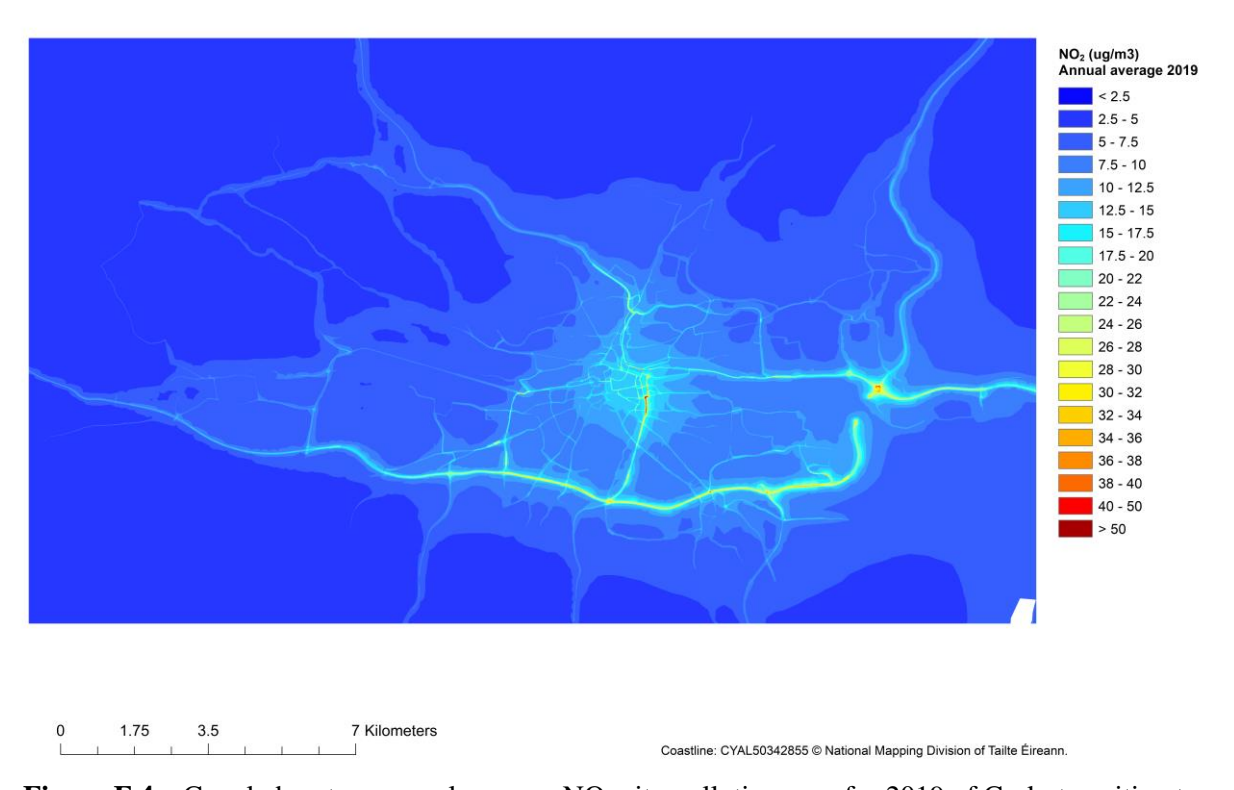


**Figure F.4** – Coupled system annual average  $NO_2$  city pollution map for 2019 of Cork; transition to exceedance of AQSR limit (40  $\mu$ g/m³) shown in **bright red**.

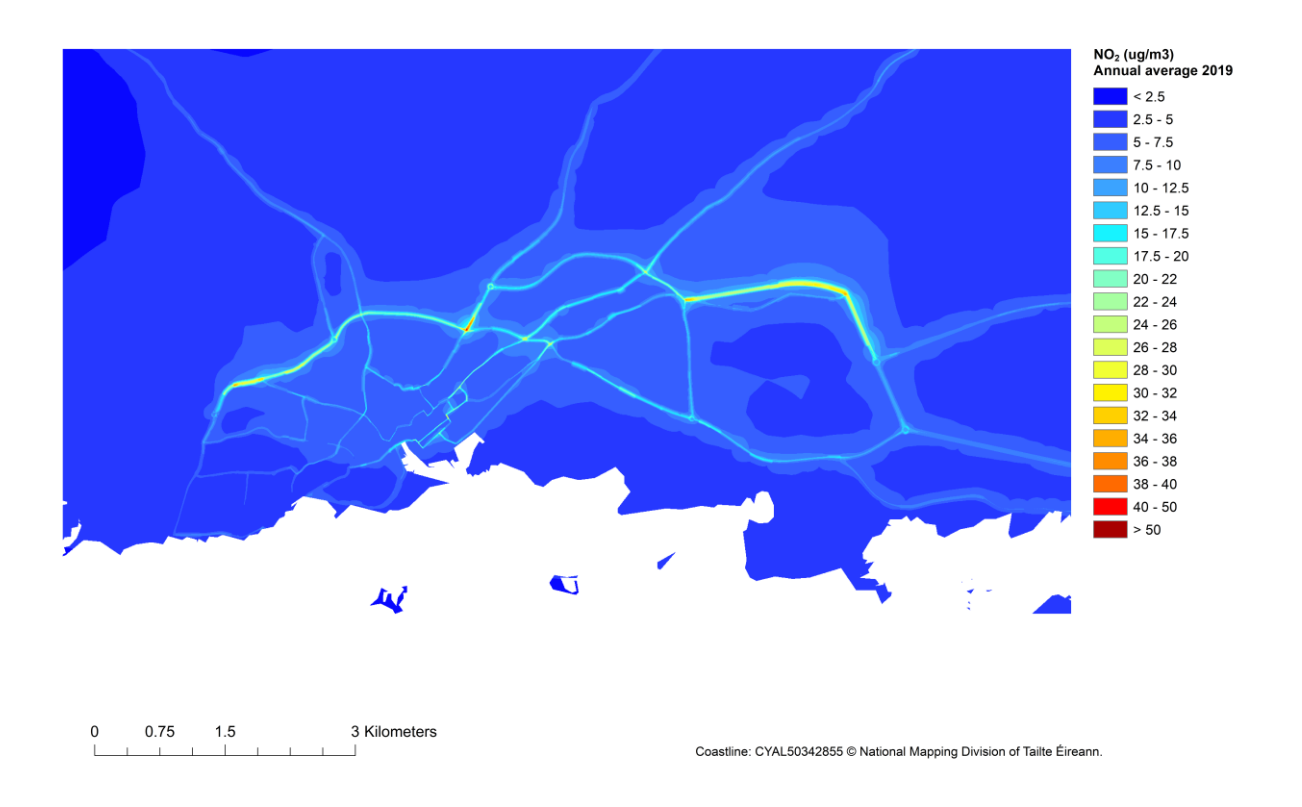


**Figure F.5** – Coupled system annual average  $NO_2$  city pollution map for 2019 of Galway; transition to exceedance of AQSR limit (40  $\mu$ g/m³) shown in **bright red**.

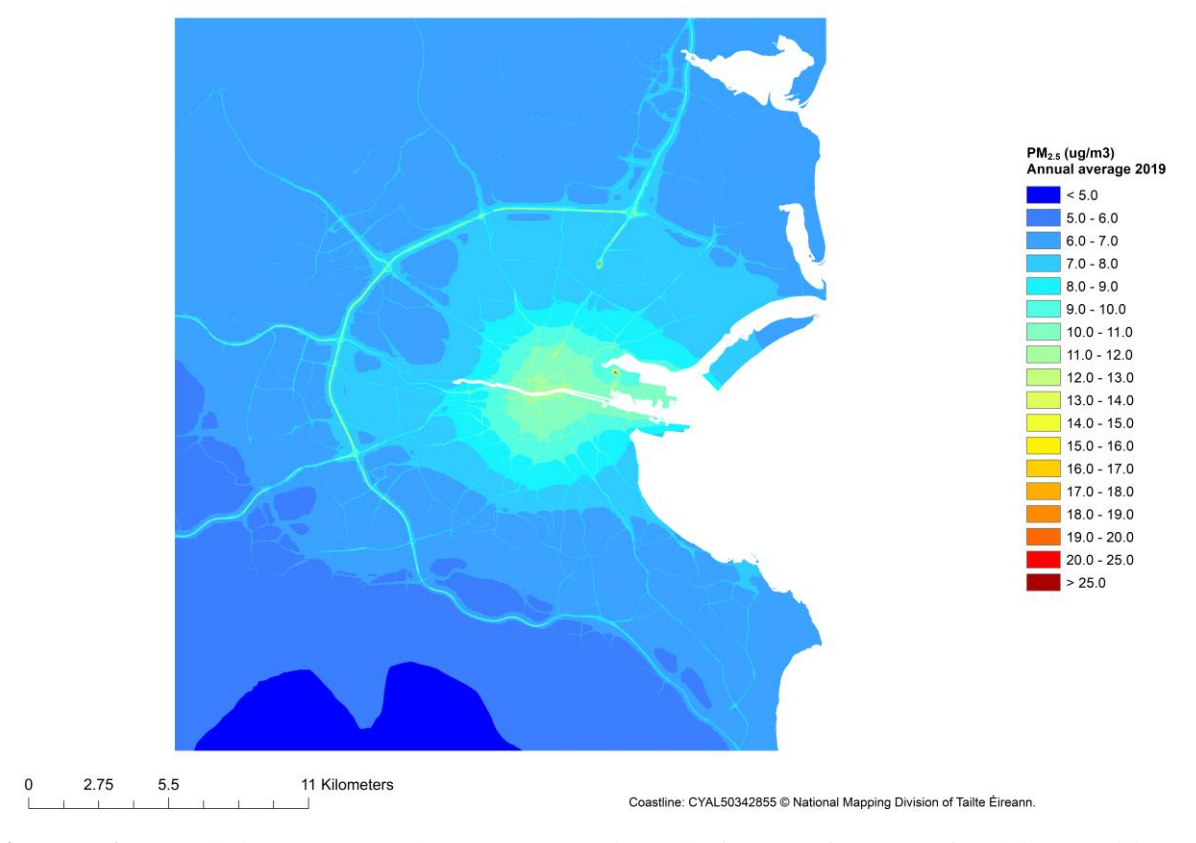


**Figure F.6** – Coupled system annual average PM<sub>2.5</sub> city pollution map for 2019 of Dublin; transition to exceedance of AQSR limit ( $20 \,\mu g/m^3$ ) shown in **bright red**; WHO guidelines transitions also shown as distinct contour levels (5,  $10 \,\mu g/m^3$ ).

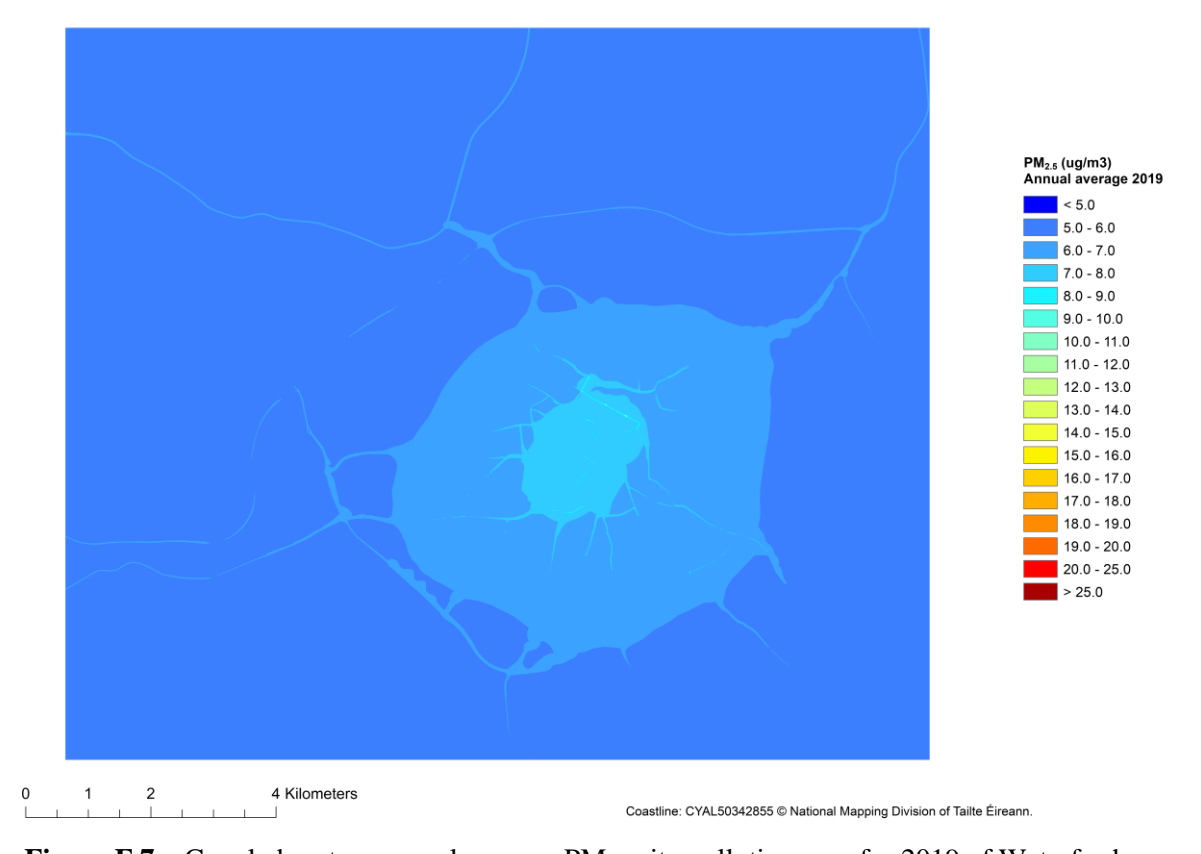


**Figure F.7** – Coupled system annual average  $PM_{2.5}$  city pollution map for 2019 of Waterford; transition to exceedance of AQSR limit (20  $\mu$ g/m³) shown in **bright red**; WHO guidelines transitions also shown as distinct contour levels (5, 10  $\mu$ g/m³).

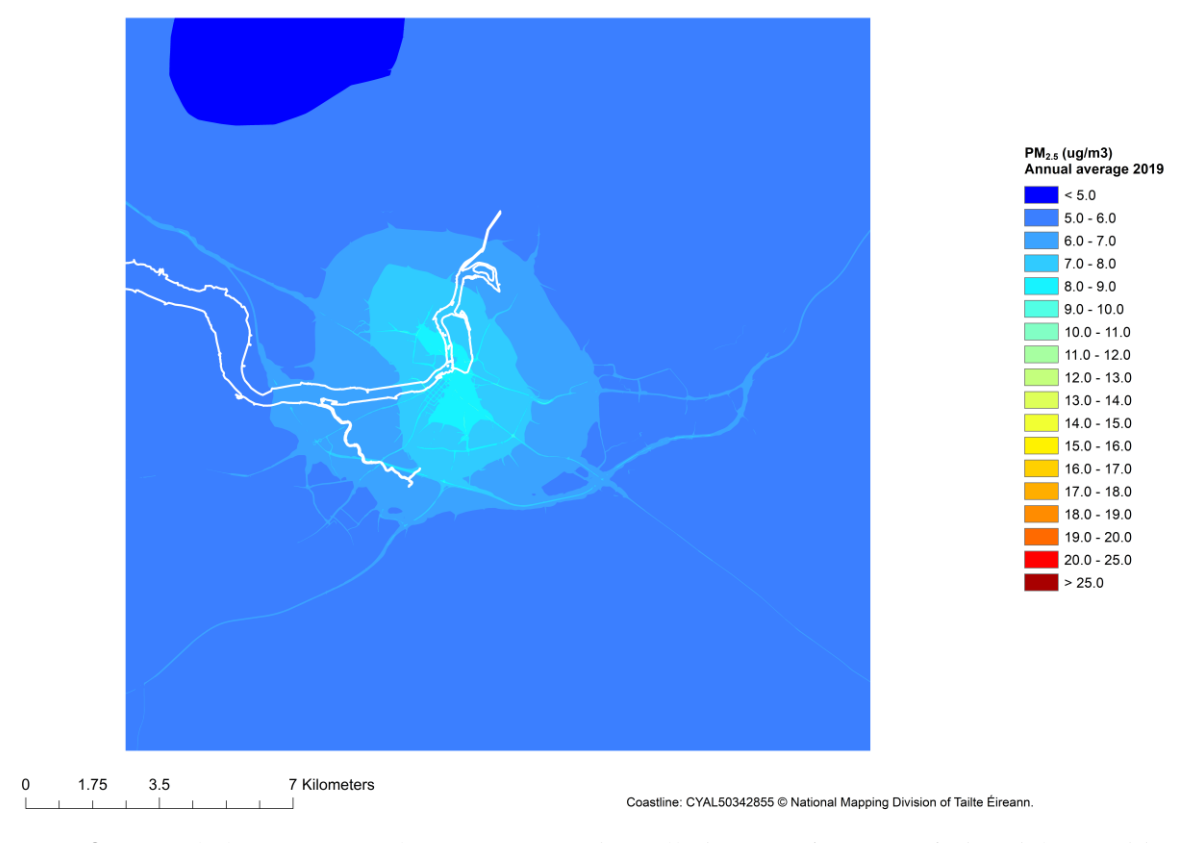


**Figure F.8** – Coupled system annual average  $PM_{2.5}$  city pollution map for 2019 of Limerick; transition to exceedance of AQSR limit (20  $\mu$ g/m³) shown in **bright red**; WHO guidelines transitions also shown as distinct contour levels (5, 10  $\mu$ g/m³).

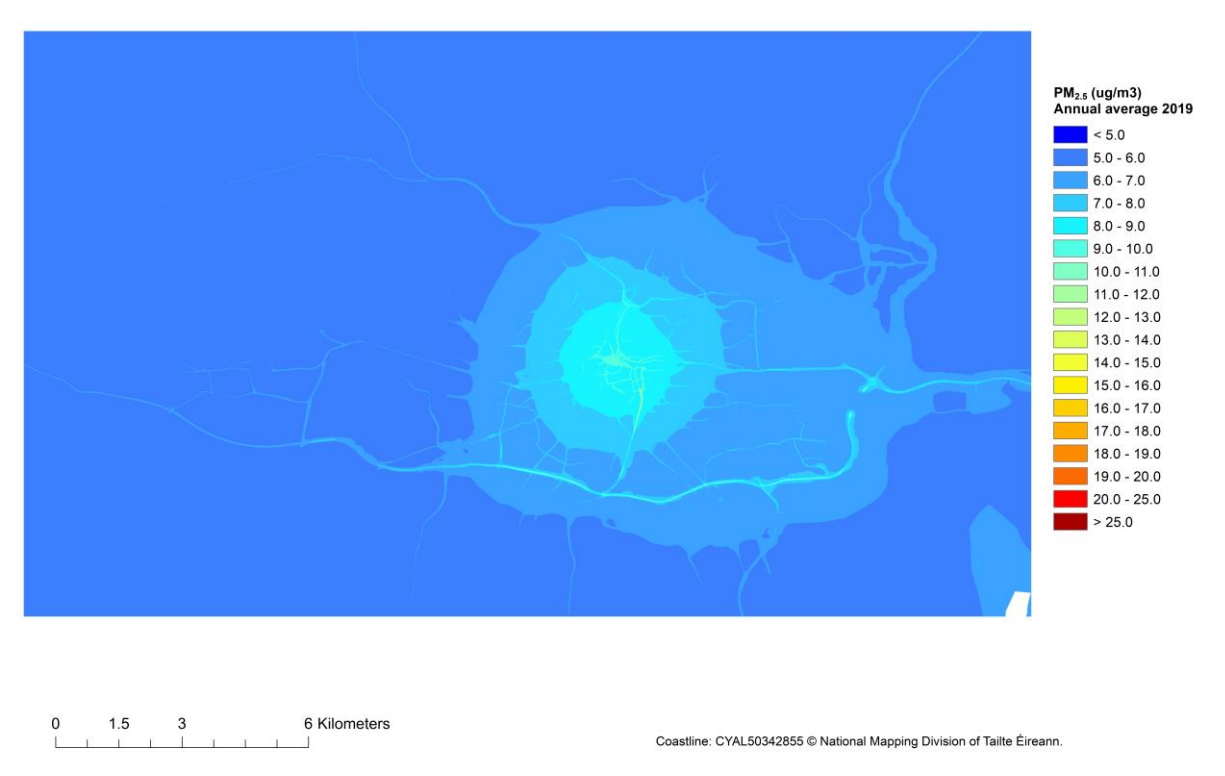


**Figure F.9** – Coupled system annual average PM<sub>2.5</sub> city pollution map for 2019 of Cork; transition to exceedance of AQSR limit (20  $\mu$ g/m³) shown in **bright red**; WHO guidelines transitions also shown as distinct contour levels (5, 10  $\mu$ g/m³).

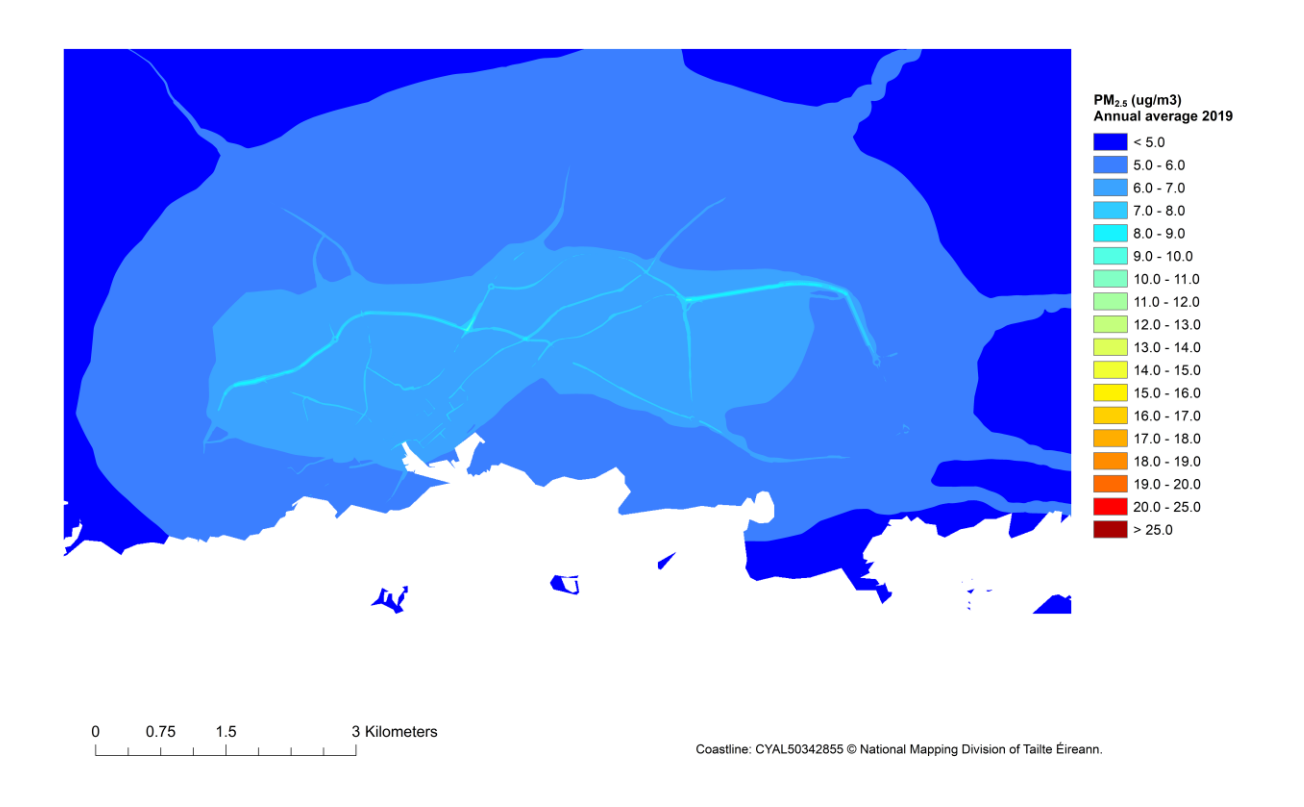


**Figure F.10** – Coupled system annual average  $PM_{2.5}$  city pollution map for 2019 of Galway; transition to exceedance of AQSR limit (20  $\mu$ g/m³) shown in **bright red**; WHO guidelines transitions also shown as distinct contour levels (5, 10  $\mu$ g/m³).

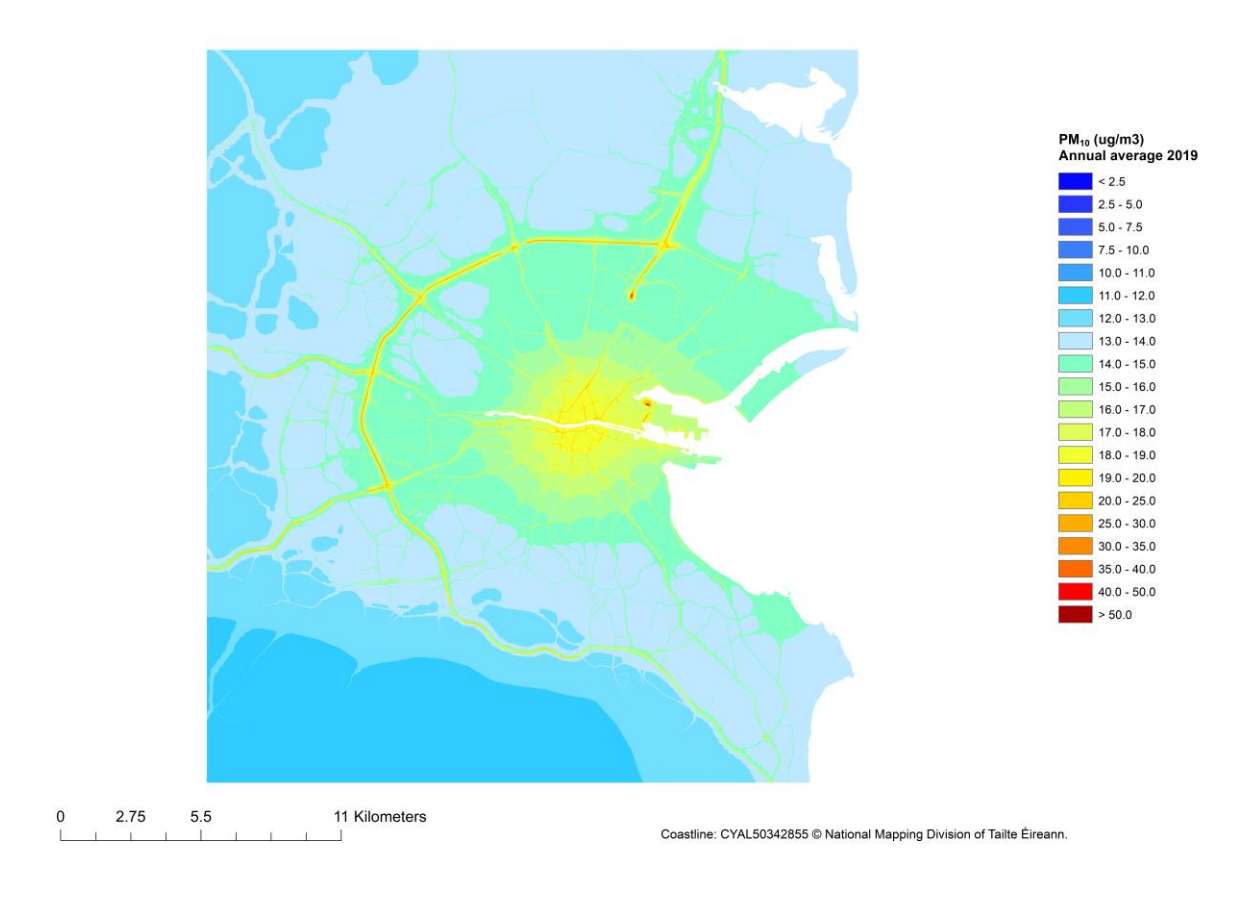


**Figure F.11** – Coupled system annual average  $PM_{10}$  city pollution map for 2019 of Dublin; transition to exceedance of AQSR limit (40  $\mu$ g/m³) shown in **bright red**.

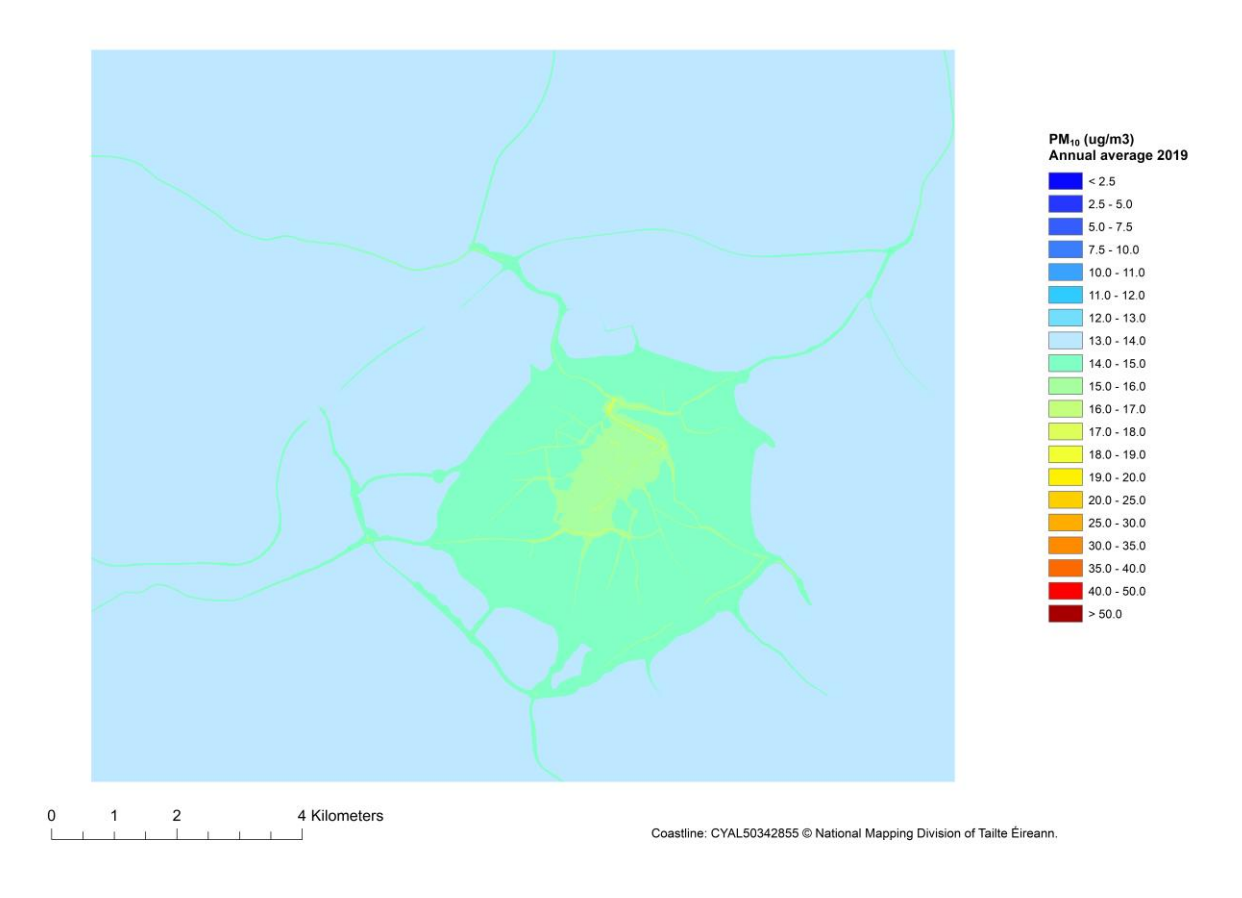


**Figure F.12** – Coupled system annual average  $PM_{10}$  city pollution map for 2019 of Waterford; transition to exceedance of AQSR limit (40  $\mu$ g/m³) shown in **bright red**.

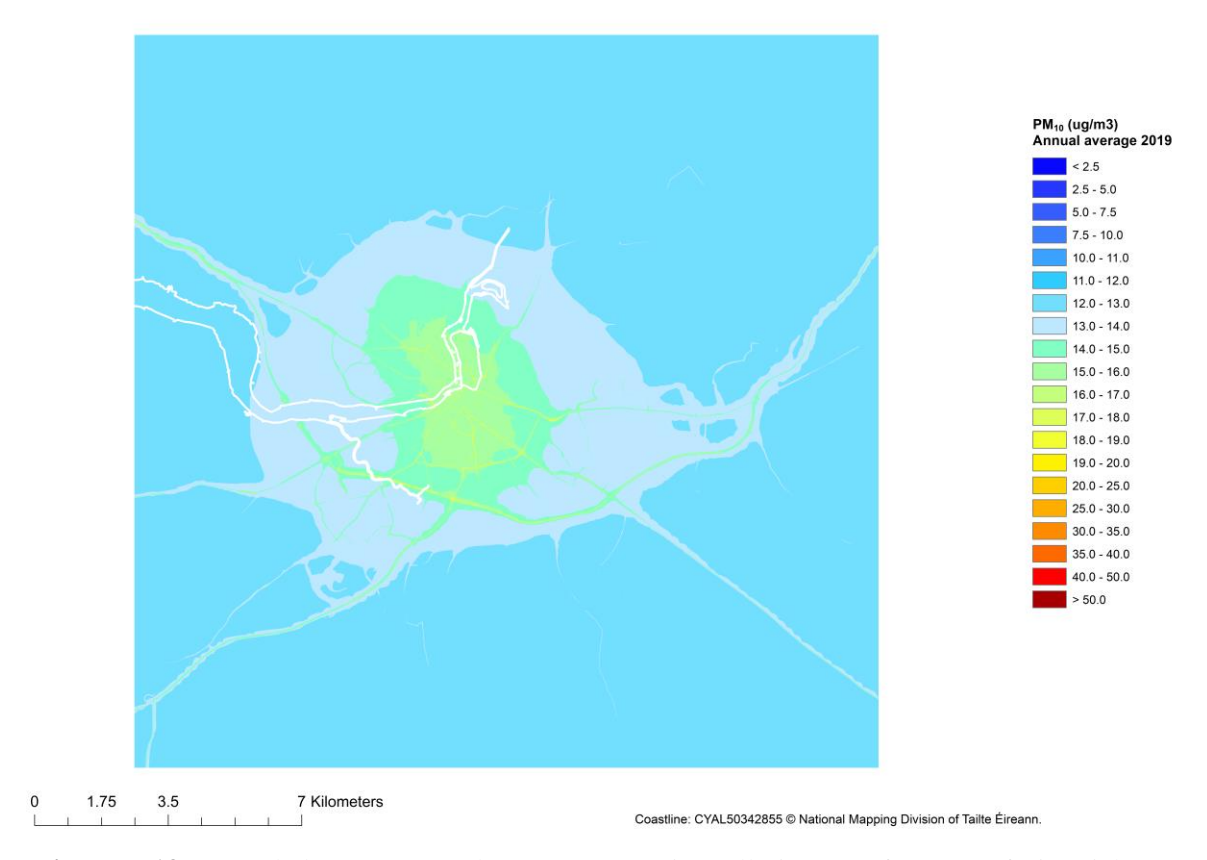


**Figure F.13** – Coupled system annual average PM<sub>10</sub> city pollution map for 2019 of Limerick; transition to exceedance of AQSR limit (40 μg/m³) shown in **bright red**.



**Figure F.14** – Coupled system annual average  $PM_{10}$  city pollution map for 2019 of Cork; transition to exceedance of AQSR limit (40  $\mu$ g/m³) shown in **bright red**.

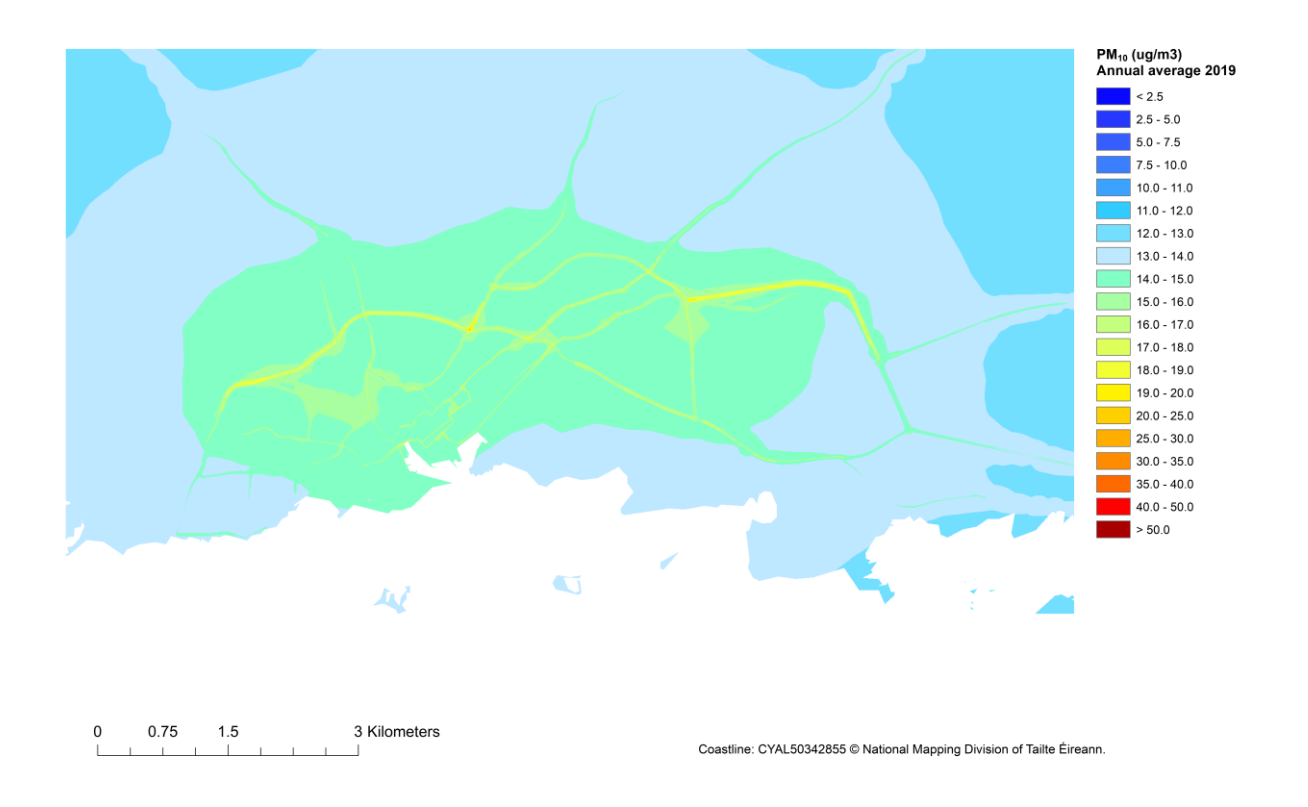
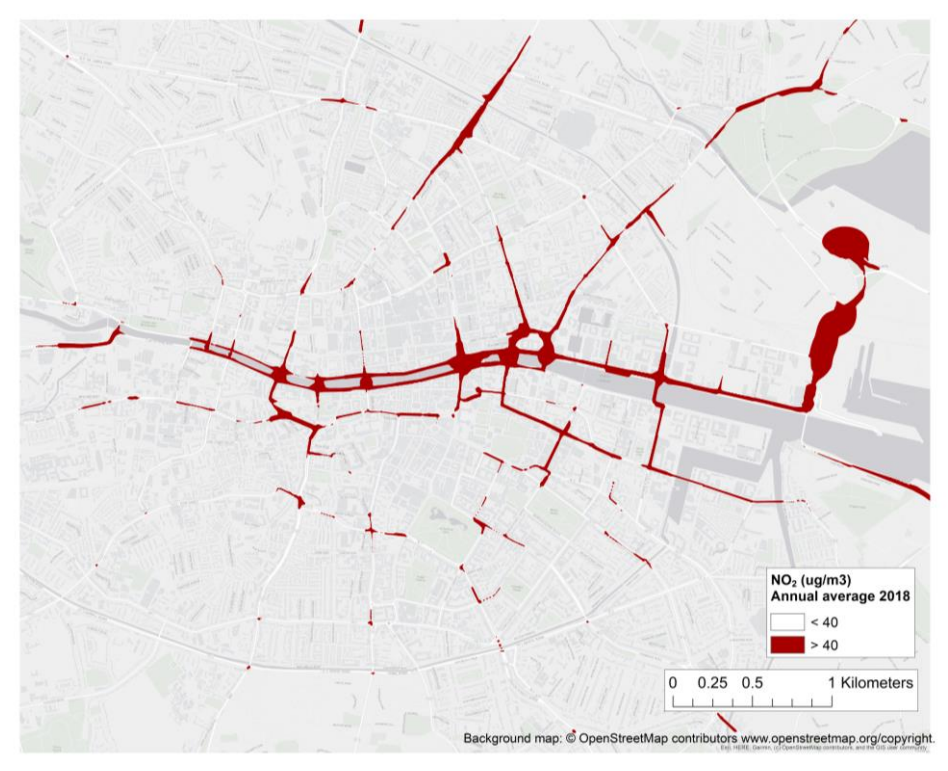


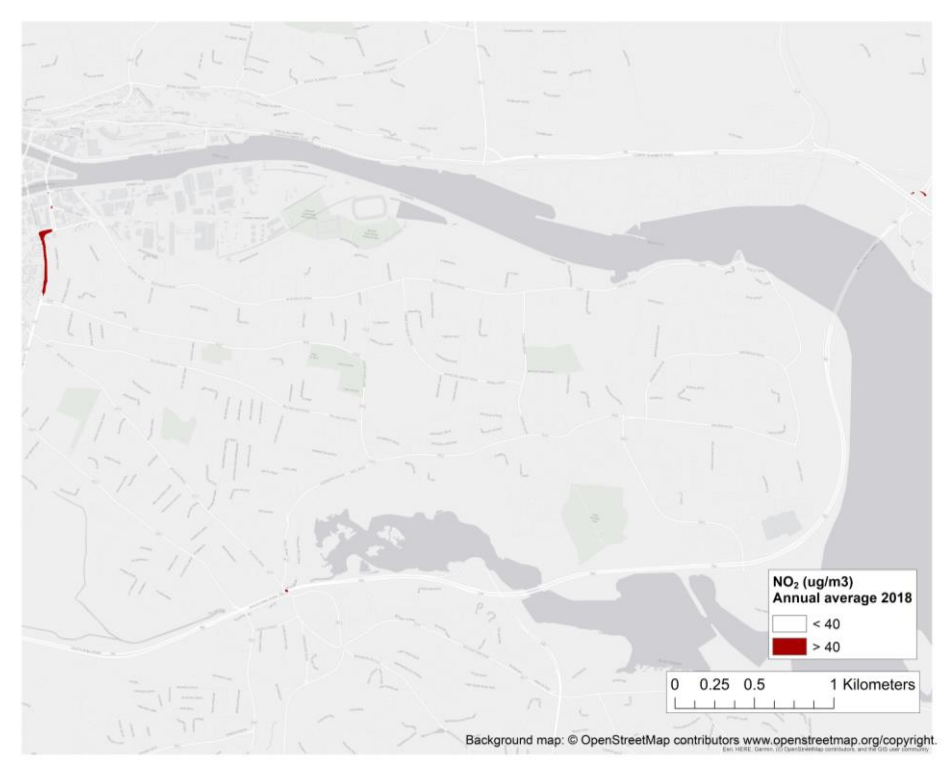
**Figure F.15** – Coupled system annual average  $PM_{10}$  city pollution map for 2019 of Galway; transition to exceedance of AQSR limit (40  $\mu$ g/m³) shown in **bright red**.



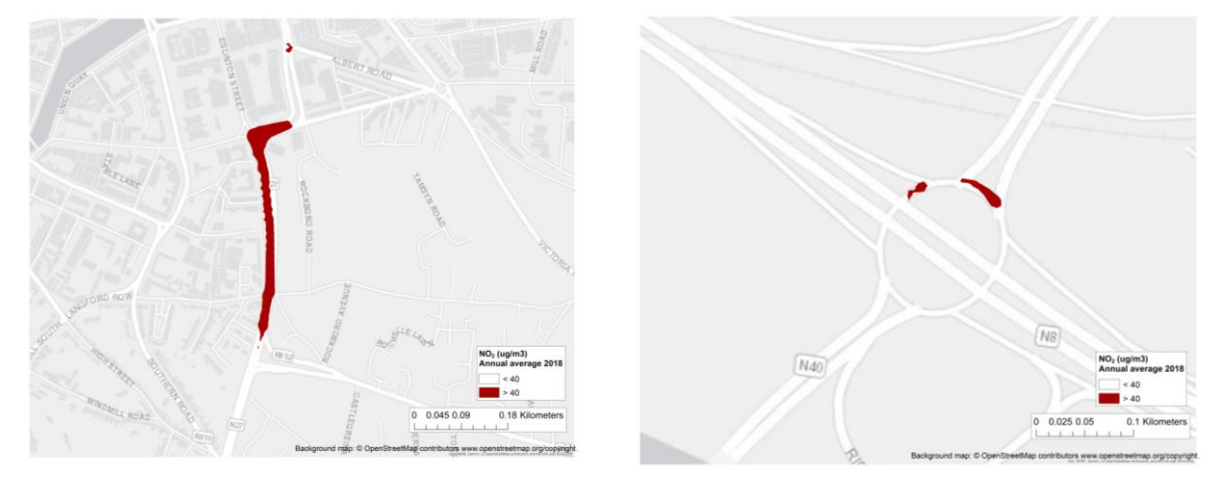
 $\begin{tabular}{ll} \textbf{Figure F.16}-Coupled system modelled exceedances of annual average NO$_2$ AQSR limit (40 $\mu g/m^3$) in Dublin for 2018. \end{tabular}$ 



 $\label{eq:Figure F.17} \textbf{Figure F.17} - \text{Coupled system modelled exceedances of annual average NO}_2 \ AQSR \ limit \ (40 \ \mu g/m^3) \\ \text{in central Dublin for 2018}.$ 



 $\begin{tabular}{ll} \textbf{Figure F.18}-Coupled system modelled exceedances of annual average NO$_2$ AQSR limit (40 $\mu g/m^3$) in Cork for 2018. \end{tabular}$ 



 $\begin{tabular}{ll} \textbf{Figure F.19}-Coupled system modelled exceedances of annual average $NO_2$ AQSR limit (40 $\mu g/m^3$) in central Cork locations for 2018. \end{tabular}$ 

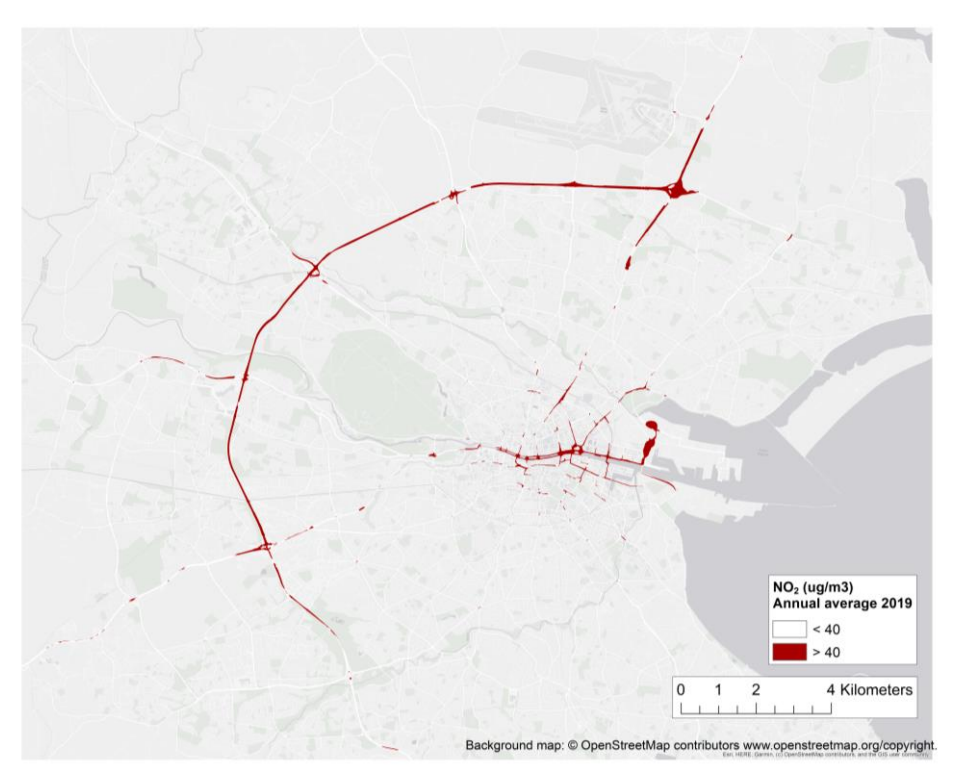
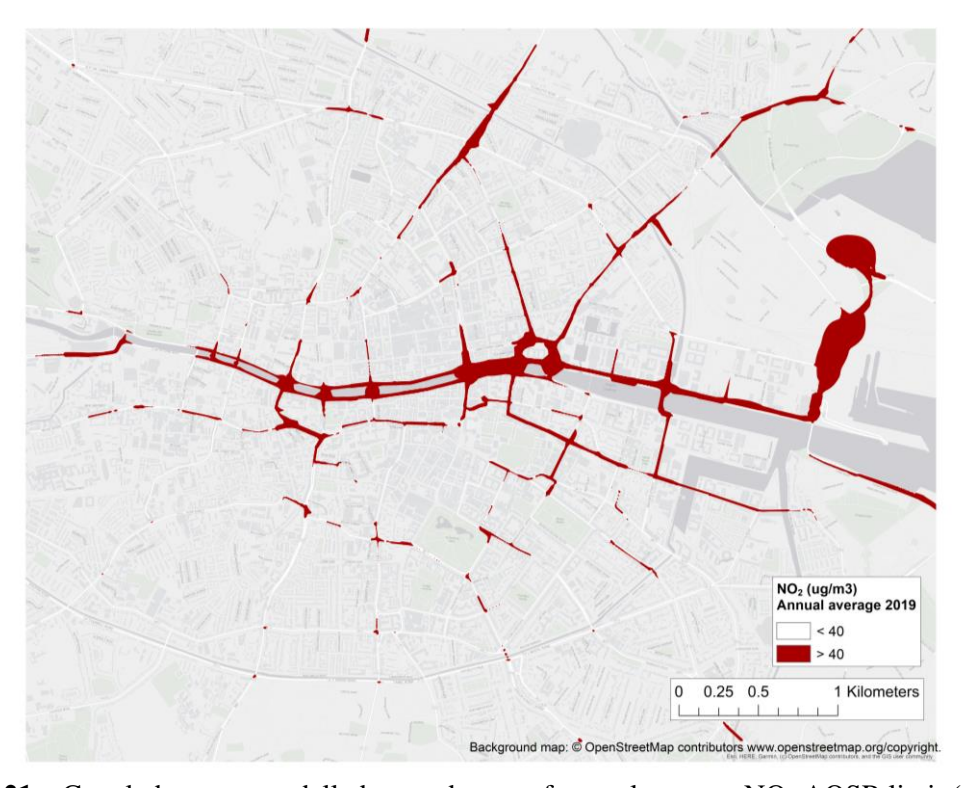
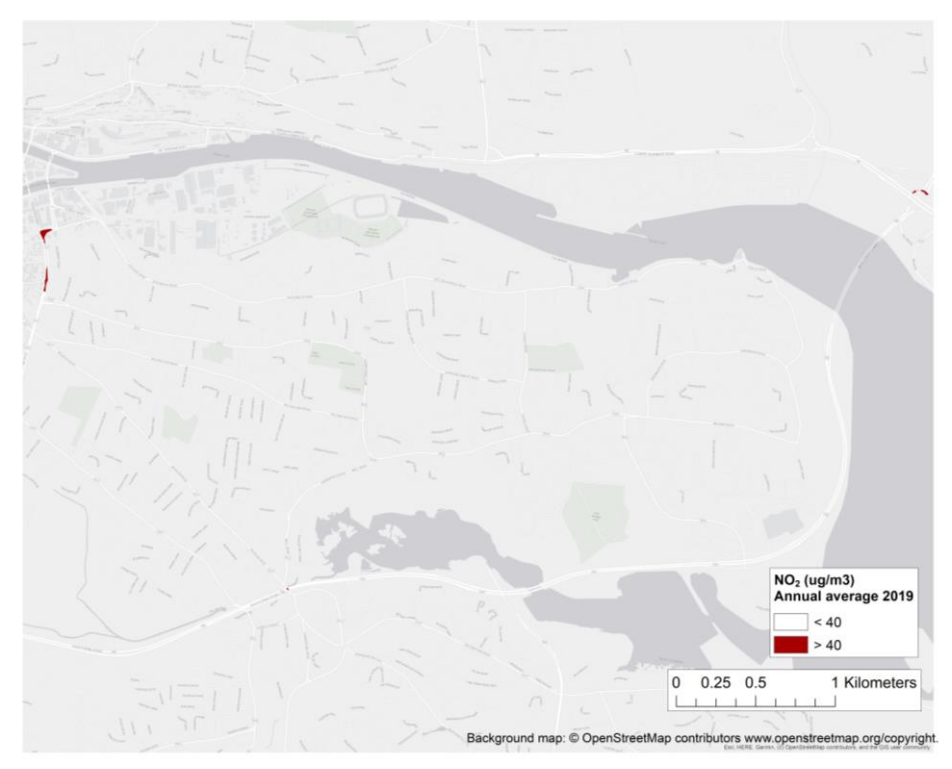


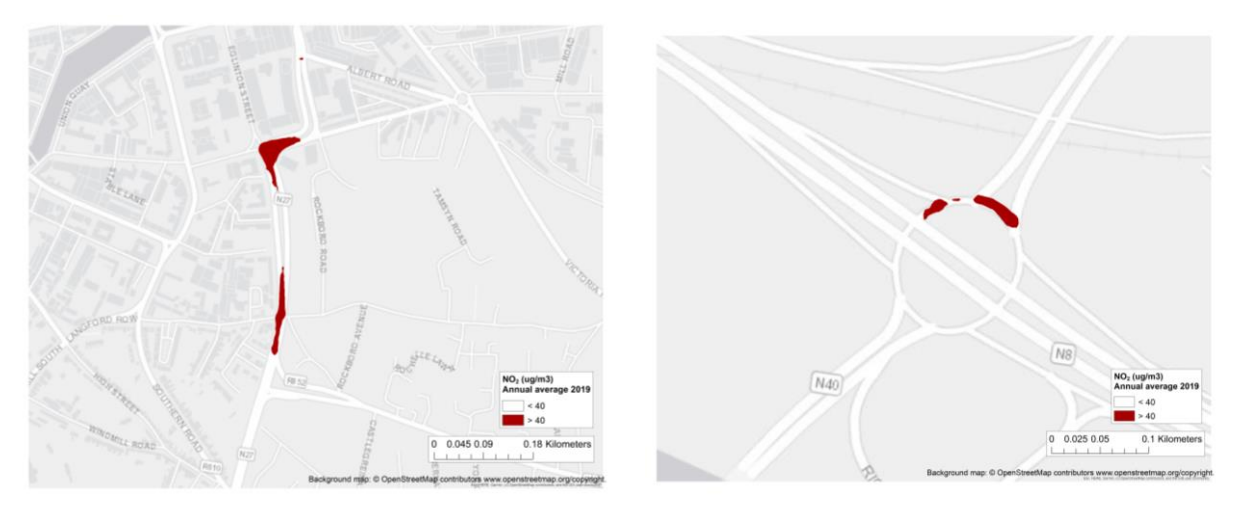
Figure F.20 – Coupled system modelled exceedances of annual average  $NO_2$  AQSR limit (40  $\mu g/m^3$ ) in Dublin for 2019.



 $\begin{tabular}{ll} \textbf{Figure F.21}-Coupled system modelled exceedances of annual average NO_2 AQSR limit (40 $\mu g/m^3$) in central Dublin for 2019. \end{tabular}$ 



 $\begin{tabular}{ll} \textbf{Figure F.22}-Coupled system modelled exceedances of annual average NO$_2$ AQSR limit (40 $\mu g/m^3$) in Cork for 2019. \end{tabular}$ 



 $\begin{tabular}{ll} \textbf{Figure F.23}-Coupled system modelled exceedances of annual average NO$_2$ AQSR limit (40 $\mu g/m^3$) in central Cork locations for 2019. \\ \end{tabular}$